



University of HUDDERSFIELD

University of Huddersfield Repository

Ngehnyuiy, Ngo Hansel

Characterisation of Bacterial Polysaccharides

Original Citation

Ngehnyuiy, Ngo Hansel (2020) Characterisation of Bacterial Polysaccharides. Doctoral thesis, University of Huddersfield.

This version is available at <http://eprints.hud.ac.uk/id/eprint/35297/>

The University Repository is a digital collection of the research output of the University, available on Open Access. Copyright and Moral Rights for the items on this site are retained by the individual author and/or other copyright owners. Users may access full items free of charge; copies of full text items generally can be reproduced, displayed or performed and given to third parties in any format or medium for personal research or study, educational or not-for-profit purposes without prior permission or charge, provided:

- The authors, title and full bibliographic details is credited in any copy;
- A hyperlink and/or URL is included for the original metadata page; and
- The content is not changed in any way.

For more information, including our policy and submission procedure, please contact the Repository Team at: E.mailbox@hud.ac.uk.

<http://eprints.hud.ac.uk/>

CHARACTERISATION OF BACTERIAL POLYSACCHARIDES

NGO HANSEL NGEHNYUIY, MSc



University of
HUDDERSFIELD

A thesis submitted to the University of Huddersfield in partial fulfilment of the requirements for the degree of Doctor of Philosophy

Department of Chemical and Biological Sciences

School of Applied Sciences

The University of Huddersfield

March 2020

ABSTRACT

A number Gram-positive bacterial strains including *Lactobacillus paracasei* DG, *Lactobacillus salivarius* CCUG44481 and *Bifidobacteria breve* 7017 have been known to possess probiotic properties which has led to their increasing use in commercial probiotic products. A range of exopolysaccharides (EPS) and capsular polysaccharides (CPS) produced by these number of probiotic Gram-positive bacteria were studied in an attempt to determine if the EPS contributed to the biological activity of these cultures. EPSs were isolated, purified and their structures determined. *Lactobacillus paracasei* DG generated an EPS and a CPS, which were similar. The ¹H-NMR spectrum indicated six anomeric signals confirming that the EPS contained six monosaccharides in their repeating units. The molecular weight determination indicated that a single polymer was produced with a narrow polydispersity. The combined GC-MS and HPAEC-PAD results confirmed that the structure was made up of L-rhamnose, D-galactose and D-N-acetylgalactosamine in a molar ratio 4:1:1. The nuclear magnetic resonance (NMR) as well as the linkage analysis indicated that the repeating unit contained 1,2-linked, 1,2,3-linked and 1,3-linked rhamnoses with a terminal hexose and an N-acetyl sugar. This analysis permitted the complete characterisation of the novel EPS structure. The results of this study allowed other research groups to determine the biological activity of the EPS with full knowledge that the immunotolerance observed was generated by a highly pure and well characterised polysaccharide.

The ¹H-NMR spectrum of the EPS recovered from *Lactobacillus salivarius* CCUG44481 identified three anomeric signals and these matched those observed in a commercial dextran. The NMR spectra suggested that the CCUG44481 strain produced a highly branched dextran than the commercial dextran with at least a third of the hexoses being present in the branches. The HPAEC-PAD and GC-MS results all gave a single glucose peak. The linkage analysis showed that the backbone was a repeating unit of α -(1,6)-linked glucose having multiple branches of 1,3-linked glucoses. The NMR spectra and the wet chemical analysis are all consistent with the EPS isolated from *L. salivarius* CCUG44481 being a highly branched dextran.

Two EPSs (S1 and S2) and two CPSs (C1 and C2) were isolated from *Bifidobacteria breve* 7017. NMR and chemical analysis of the S1 and C1 fractions were bacterial glycogen with a medium molecular weight. For the S2 fraction, ¹H-NMR spectrum indicated the presence of five anomeric peaks with one being identified as an impurity. The NMR spectra recorded for S2 changed with time and these corresponded to the slow loss of a ribitol like moiety on prolonged storage. The structure of the repeat unit of the S2 fraction was determined. The analysis of the C2 fraction identified two homoglycans: a β -D-(1,6)-galactofuranan and a β -D-(1,6)-glucan.

The characterisation of the EPS requires a time-consuming linkage analysis method. As part of this research an attempt was made to develop a more rapid method for linkage analysis using HPAEC-PAD. A range of variously substituted methyl glucose were separated: mono, di and tri-substituted glucoses could be separated. However, different isomers of either mono or di-substituted glucoses could not be separated. This then meant a HPAEC-PAD linkage method was unlikely to succeed.

ACKNOWLEDGEMENTS

Firstly, I would like to thank the Creator who is the Almighty and who has given me the strength and health to be able to complete my PhD studies.

My deepest sincere gratitude goes to my supervisor Prof. Andrew P. Laws who has been my mentor helping, assisting and guiding me throughout my research work. His encouragement, knowledge, constructive comments, suggestions and advice have been of great importance for me during this project.

I would like to thank Dr Neil McLay who ran the NMR experiments. I will also extend a great deal of thanks to Prof. Paul Humphreys and his microbiology team who have been of great assistance to me as I carried out the fermentations. I also thank Dr. Sohaib Sadiq for his help and assistance in the chromatography laboratory.

I would also like to thank my parents Mr and Mrs Ngo Pierre/Benedicta, siblings: Paul, Claire, Sherard and Delvin for their constant support and encouragement.

Special thanks from the bottom of my heart also goes to my fiancée Emmanuelle Se Se, who has also been supportive and encouraging during my research.

Lastly, I thank my fellow research colleagues who have also contributed in one way or the other for me to feel like a family throughout the research.

Abbreviations

AcO	Acetyl
ADP	Adenosine Diphosphate
ATP	Adenosine Triphosphate
<i>B.</i>	<i>Bifidobacteria</i>
CPS	Capsular Polysaccharide
CDM	Chemically Defined Medium
DMSO	Dimethyl Sulfoxide
d.p.	Degree of Polymerisation
D ₂ O	Deuterium Oxide
EPS	Exopolysaccharide
EPSs	Exopolysaccharides
<i>f</i>	Furanose
FDA	Food and Drug Administration
Gal	Galactose
GalNAc	<i>N</i> -acetyl-galactosamine
GlcNAc	<i>N</i> -acetyl-glucosamine
Glc	Glucose
GRAS	Generally Regarded As Safe
ICH	International Conference on Harmonisation
IUPAC	International Union of Pure and Applied Chemistry
JCM	Japanese Culture of Microorganisms
OH	Hydroxyl
LAB	Lactic Acid Bacteria
<i>L.</i>	<i>Lactobacillus</i>
LPS	Lipopolysaccharide
Me	Methyl
Mel	Methyl Iodide
MRD	Maximum Recovery Diluent
MRS	de Man, Rogosa and Sharpe Growth Media
NaOH	Sodium Hydroxide

OMe	Methoxy
<i>p</i>	Pyranose
PEP	Phosphoenolpyruvate
Rha	Rhamnose
TCA	Trichloroacetic Acid
TFA	Trifluoroacetic Acid

Experimental terms

1D	One-dimensional
2D	Two-dimensional
COSY	Correlated Spectroscopy
CZE	Capillary Zone Electrophoresis
DEPT	Distortionless Enhancement by Polarization Transfer
<i>dn/dc</i>	Refractive index increment
GC	Gas Chromatography
GC-MS	Gas Chromatography – Mass Spectrometry
HMBC	Heteronuclear Multiple Bond Correlation
HP-AEC-PAD	High Performance Anion Exchange Chromatography Pulsed Amperometric Detection
HPLC	High Pressure Liquid Chromatography
HSQC	Heteronuclear Single Quantum Coherence
HSQC-TOCSY	Heteronuclear Single Quantum Coherence – Total Correlation Spectroscopy
Hz	Hertz
IR	Infrared
LC	Liquid Chromatography
LC-MS	Liquid Chromatography Mass Spectrometer
M	Molar (mol/dm ³)
MALLS	Multi-Angle Laser Light Scattering
MS	Mass Spectrometer
<i>M_w</i>	Weight-average molecular weight
<i>M_n</i>	Number-average molecular weight

mV	Millivolt
NMR	Nuclear Magnetic Resonance
NOE	Nuclear Overhauser Effect/Enhancement
mg L ⁻¹	Milligrams per litre (equivalent to parts per million)
µg mL ⁻¹	Micrograms per millilitre (equivalent to parts per million)
ppm	parts per million
RI	Refractive Index
SEC	Size Exclusion Chromatography
TOCSY	Total Correlation Spectroscopy
UV	Ultraviolet

Table of contents

1.	Introduction	1
1.1.	Classification of Carbohydrates	2
1.1.1.	Monosaccharides	3
1.1.2.	Derivatives of Monomeric Sugar Units	7
1.1.3.	Disaccharides	9
1.1.4.	Oligosaccharides	10
1.1.5.	Polysaccharides.....	11
1.2.	Bacteria	13
1.2.1.	Bacterial Growth	15
1.2.2.	Bacterial Polysaccharides.....	17
1.3.	Probiotic Bacteria.....	18
1.3.1.	Lactic Acid Bacteria (LAB).....	19
1.3.2.	Lactobacillus species	20
1.3.3.	Importance of LAB in the Food Industry and Some Health Benefits	22
1.4.	Bifidobacteria.....	22
1.4.1.	Beneficial Effects of Bifidobacteria	24
1.5.	Capsular (CPS) and Exopolysaccharides (EPS).....	25
1.5.1.	Biosynthesis of Exopolysaccharides.....	25
1.5.2.	Production and Isolation of Exopolysaccharides	30
1.5.2.1.	Production of Exopolysaccharides (EPS).....	30
1.5.2.2.	Exopolysaccharide Isolation.....	32
1.6.	Exopolysaccharide Characterisation.....	33
1.6.1.	Determining the Purity of Polysaccharides and Analysis of Crude Fermentation Products.	33
1.7.	Classical Wet Chemical Analytical Methods	34
1.7.1.	Monomer Analysis of Carbohydrates by Gas Chromatography Mass Spectrometry (GC-MS).....	34
1.7.2.	High Performance Anion Exchange Chromatography with Pulsed-Amperometric Detection (HPAEC-PAD) Analysis of Carbohydrates	36
1.7.3.	Linkage Analysis	38
1.7.4.	Absolute Configuration Analysis of EPS	39
1.7.5.	Nuclear Magnetic Resonance (NMR) Analysis.....	40
1.7.6.	Solvent Choice for Dissolution of Polysaccharides	43
1.7.7.	Determination of average Molecular Weights (Mw) of EPS and CPS.....	44
1.8.	The Structures of the EPS Repeating Units from LAB	45
1.9.	The Structures of EPS Repeating Units from the <i>Bifidobacteria Species</i>	45

1.10.	Potential Rich Source of Methylated Glucose Molecule (Methylcyclodextrin).....	45
1.11.	Aims.....	47
2.	Materials and Methods.....	49
2.1.	General Reagents and Bacterial cultures.....	49
2.1.1.	Bacterial Media	49
2.1.2.	Bacterial Cultures and Bacterial Exopolysaccharides	49
2.2.	Preparation of the MRSc Agar	49
2.3.	Gram Staining.....	50
2.4.	Media for Use in Batch Fermentations	50
2.5.	MRS-c Broth Preparation	50
2.5.1.	Preparation of Broth Media Free of EPS-equivalent.....	50
2.5.2.	Chemically Defined Medium (CDM)	51
2.6.	Preparation of Dialysis Tubes.....	53
2.7.	Exopolysaccharide Isolation.....	53
2.7.1.	Exopolysaccharide Extraction from Broth Cultures	53
2.7.1.1.	Extraction of the Slime EPS (S1 and S2)	53
2.7.1.2.	Extraction of the Capsular EPS.....	54
2.8.	Exopolysaccharide Characterisation	55
2.8.1.	Quantification of the Solid Content	55
2.8.2.	Determining the Carbohydrate Content	55
2.8.3.	Structural Characterisation of EPS.....	55
2.8.3.1.	HPAEC-PAD	55
2.8.3.2.	GC-MS	56
2.8.3.3.	Nuclear Magnetic Resonance (NMR).....	56
2.8.3.4.	HP-SEC-MALLS.....	56
2.8.4.	Monomer Analysis of the Polysaccharides (EPS and CPS)	57
2.8.4.1.	Hydrolysis of the EPSs	58
2.8.4.2.	Reduction of the EPS.....	58
2.8.4.3.	Acetylation of the EPS.....	58
2.8.5.	Linkage Analysis of the EPSs	59
2.8.6.	Molecular Weight (Mw) Determination of the Isolated EPS	59
2.8.7.	Absolute Configuration of EPS	60
	Results and Discussion Sections	61
3.	Analysis and Structural Characterisation of the Novel EPS from <i>Lactobacillus paracasei</i> DG and <i>Lactobacillus Salivarius</i> CCUG44481	62
3.1.	Introduction	62

3.2.	Production and Isolation of Polysaccharides from <i>Lactobacillus paracasei</i> DG	67
3.2.1.	Molecular Weight Determination of <i>L. Paracasei</i> DG using HP-SEC-MALLS.....	73
3.2.2.	Monomers and Linkage Analysis of the Monosaccharides in the Repeating Unit Structure of <i>L. paracasei</i> DG.	75
3.2.2.1.	Monomers analysis of the <i>L. paracasei</i> DG polysaccharides using HPAEC-PAD and GC-MS	75
3.2.2.2.	Linkage Analysis of the <i>L. paracasei</i> DG Polysaccharides using the Methylated Alditol Acetate Method.....	79
3.2.2.3.	Absolute Configuration of the Polysaccharide of <i>L. paracasei</i> DG	83
3.2.3.	Usage of 1D and 2D-NMR in Determining the Sequence of the Monomers in the Repeated Units of <i>L. paracasei</i> DG	84
3.2.4.	Determination of Carbohydrate Content of Exopolysaccharide	89
3.3.	Conclusion.....	90
3.4.	Production and Isolation of <i>Lactobacillus Salivarius</i> CCUG44481.....	91
3.4.1.	Structural Characterisation of the Exopolysaccharides isolated from <i>L. Salivarius</i> CCUG44481	92
3.4.2.	Purity of the Exopolysaccharide from <i>L. salivarius</i> CCUG44481 by its Molecular Weight Determination using the HP-SEC-MALLS	93
3.4.3.	Monomers and Linkage Analysis of the Monosaccharides in the Repeating Unit Structure of <i>Lactobacillus salivarius</i> CCUG44481.....	94
3.4.3.1.	Monomers Analysis of the Exopolysaccharides Isolated from <i>Lactobacillus salivarius</i> CCUG44481 using HPAEC-PAD and GC-MS.....	94
3.4.3.2.	Linkage Analysis of the Exopolysaccharides Isolated from <i>Lactobacillus salivarius</i> CCUG44481.....	96
3.4.4.	Absolute Configuration of the Exopolysaccharide from <i>L. salivarius</i> CCUG44481	99
3.4.5.	NMR Analysis of the EPS from <i>L. salivarius</i> CCUG44481	100
3.4.6.	Analysis of the 2D-Homonuclear Spectra for the Commercial Dextran	104
3.4.7.	Analysis of the 2D-Homonuclear Spectra for the Dextran <i>from L. salivarius</i> CCUG44481.....	105
3.5.	Conclusion.....	108
4.	Attempt to Develop a robust and rapid method for Linkage Analysis using HPAEC-PAD and Employing partially Methylated Cyclodextrins as Model Substrates	110
4.1.	Introduction	110
4.2.	Monomer Analysis of Methylcyclodextrin and Separation of its Individual Sugar Units through a Carbon-Silica Column.	112
4.3.	Results.....	113
4.4.	Conclusion.....	126
5.	Production and Isolation of Polysaccharides that are Excreted or Presented at the Cell Surface of <i>B. breve</i> 7017.....	128

5.1.	Identifying Optimum Conditions for the Growth of <i>B. breve</i> JCM7017 in HBM Media.....	132
5.1.1.	Analysis of Polysaccharides Present in the S1-fraction; Attempted Recovery of Exopolysaccharides.....	137
5.1.2.	Analysis of Polysaccharides Present in the S2-fraction; Attempted Recovery of Exopolysaccharides.....	142
5.1.3.	Identification of the Resonance Position of the Protons and Carbons of the Monosaccharides (A to D) of the Repeat Unit.....	148
5.1.3.1.	Identification of the Monosaccharides and their Anomeric Configuration in S2-fraction of <i>B. breve</i> 7017.....	154
5.1.3.2.	Determination of the Linkage Pattern in the S2-fraction of <i>B. Breve</i> 7017.....	159
5.1.3.3.	Identifying other Components present in the S2-fraction of <i>B. Breve</i> 7017.....	163
5.1.3.4.	Analysis of the NMR Spectra Recorded for Material in the Dialysate.....	164
5.1.4.	Characterisation of the Polysaccharide Material Associated with the Cells: the C1 and C2-fractions.....	168
5.1.5.	Characterisation of the Polysaccharides Present in the C1-fraction from <i>B. Breve</i> 7017.....	169
5.1.5.1.	Monomers, Linkage, Absolute Configuration and SEC-MALLS Analysis of the C1 fraction from <i>B. breve</i> 7017.....	169
5.1.6.	Characterisation of the Polysaccharides Present in the C2-fraction from <i>B. breve</i> 7017.....	176
5.1.6.1.	SEC-MALLS, Monomers, linkage and Absolute Configuration Analysis for the C2 from <i>B. breve</i> 7017.....	176
5.1.6.2.	Use of 1D- and 2D-NMR to Determine the Structures of the Polysaccharides present in the C2-fraction from <i>B. breve</i> 7017.....	185
5.2.	Discussion.....	189
5.2.1.	The Identity of the Material Extracted from the Cells from <i>B. breve</i> 7017.....	189
5.2.2.	Identity of the Material Excreted into the Media by <i>B. Breve</i> 7017.....	192
5.3.	Conclusion.....	192
6.	Overall Conclusion and Future Work.....	194
References	198
Publications	208

LIST OF FIGURES

Figure 1.1: The 3 Carbon Sugars (trioses).....	4
Figure 1.1a: Epimers(sugars which differ in only 1 stereocentre highlighted in blue)	5
Figure 1.1b: Enantiomers(sugars which are mirror images to each other)	5
Figure 1.1c Diastereoisomers(sugars exact substituents on the chiral carbons but differ in their configuration).....	5
Figure 1.2a. The Two Cyclic Forms of D-glucose	6
Figure 1.2b. The Two Cyclic Forms of D-fructose	6
Figure 1.3. Neutral, Acidic, Amino, acyl, Phosphate and Sulphate Sugars.....	7
Figure 1.3a. D-Ribose and 2-Deoxy-D-ribose	8
Figure 1.4. The Two Chair forms of β -D-Glucopyranose	9
Figure 1.7. Structure of Cellulose	11
Figure 1.8 Structure of Xanthan Gum ³⁰	12
Figure 1.9. Cross section of Gram-positive bacteria cell wall (having a thicker peptidoglycan layer) and Gram-negative bacteria (having a thin peptidoglycan layer) [Images designed by McGraw-Hill companies Inc. (coloured image) & Ghuysen and Hackenbeck (1994) ³⁸ respectively].	14
Figure 1.10: Bacterial Growth Curve of a Culture as designed by the McGraw-Hill Companies Inc.	16
Figure 1.12. Hypothetical Biosynthetic Pathway for EPS as modelled by Hidalgo-Cantabrana <i>et al</i> (2014).....	28
Figure 1.13. Conventional Preparation of Alditol Acetates.....	34
Figure 1.14. HPAEC-PAD chromatogram profiles of standard monosaccharide mixture solution ¹⁹⁷ (a) NaOH concentration of 25.0mM. (b) NaOH concentration of 12.5mM. (Peak identity: A, Fucose: B, Rhamnose: C, Rhamnose: D, Galactose: E, Glucose: F, Mannose: G, Xylose: H, Fructose.....	38
Figure 1.15. Schematic Representation of Linkage Analysis	39
Figure 1.16. Newman Projection at top with Karplus Curve Demonstrating the Dihedral Angle-Coupling Relationship	41
Figure 1.17 Structure of a Methylcyclodextrin.....	46
Figure 2.1: Schematic Representation of the Extraction Procedure of the EPS and CPS.....	54
Figure 3.1. ¹ H-NMR Spectra for C1 and C2 Precipitated from <i>L. paracasei</i> DG Grown in MRS Broth from Batches 1, 2 and 3.....	69
Figure 3.2. ¹ H-NMR Spectra of the CPS (C2 top) and EPS (S2 middle) from <i>L. paracasei</i> DG as well as the S2 from HBM Control with no Bacteria (bottom).	70
Figure 3.3. ¹ H-NMR Spectra for C1 and C2 Precipitated from <i>L. paracasei</i> DG Grown in CDM Broth from Batches 7 and 8.....	72
Figure 3.4. ¹ H-NMR Spectrum of the CPS from <i>L. paracasei</i> DG	73
Figure 3.5. Chromatogram of the 1000 ppm Pullulan Standard with M_w of 800,000	74
Figure 3.6. SEC-MALLS Trace of the <i>L. paracasei</i> DG - Batch 2	75
Figure 3.6a. HPAEC-PAD chromatogram of the polysaccharide from <i>L. paracasei</i> DG compared with their various monomeric units identified (rhamnose, galactose,	

galactosamine and <i>N</i> -acetylgalactosamine) compared with standards (top right) for identification.....	76
Figure 3.7. Chromatogram for the Alditol Acetates of the Sugars obtained from the GCMS for Monomer Analysis of <i>L. paracasei</i> DG.	77
Figure 3.7a. Mass spectrum of Rhamnose in the Sample (<i>L. paracasei</i> DG) and its Fragmentation Pattern	78
Figure 3.7b. Mass spectrum of Galactose in the Sample (<i>L. paracasei</i> DG) and its Fragmentation Pattern	78
Figure 3.7c. Mass spectrum of <i>N</i> -acetylgalactosamine in the Sample (<i>L. paracasei</i> DG) and its Fragmentation Pattern	79
Figure 3.8. Chromatogram for the Methylated Alditol Acetates of the Sugars obtained from the GC-MS for Linkage Analysis of <i>L. paracasei</i> DG.....	80
Figure 3.8a. Mass Spectrum of 1,2,5-tri- <i>O</i> -acetyl-3,4-di- <i>O</i> -methyl-6-deoxyhexitol and its Fragmentation pattern which indicates it is a 1,2-linked Rhamnose.....	80
Figure 3.8b. Mass Spectrum of 1,3,5-tri- <i>O</i> -acetyl-3,4-di- <i>O</i> -methyl-6-deoxyhexitol and its Fragmentation Pattern which indicates it is a 1,3-linked Rhamnose.....	81
Figure 3.8c. Mass Spectrum of 1,5-di- <i>O</i> -acetyl-2,3,4,6-tetra- <i>O</i> -methyl-6-deoxyhexitol and its Fragmentation Pattern which indicates it is a Terminal Hexose (galactose).	81
Figure 3.8d. Mass Spectrum of 1,2,3,5-tetra- <i>O</i> -acetyl-4- <i>O</i> -methyl-6-deoxyhexitol and its Fragmentation Pattern which indicates it is a 1,2,3-linked Rhamnose.....	82
Figure 3.8e. Mass Spectrum of 1,3,5-tetra- <i>O</i> -acetyl-2-(acetylmethylamino)-2-deoxyl -4,6-di- <i>O</i> -methylhexitol and its Fragmentation Pattern which indicates it is a 1,3-linked 2- <i>N</i> -Acetylgalactosamine.....	82
Figure 3.9. The Chromatogram of the Distinct peaks of the Acetylated Butyl Polysaccharide of <i>L. paracasei</i> DG and the overlaying of these peaks with Standards of Acetylated Butyl ((S)-(+)-2-butanol) <i>L</i> -rhamnose, D-galactose and D- <i>N</i> -acetylgalactosamine.	83
Figure 3.9a. Standard structures of the Acetylated butyl ((S)-(+)-2-butanol) D-galactose, L-rhamnose and the D- <i>N</i> -acetylgalactosamine.	84
Figure 3.9b. Combination of a COSY Spectrum overlaid with a TOCSY Spectrum to identify the Position of the Ring protons. (Coupling of A to D, H1 to H6 and E, F H1 to H4; showed for illustration purposes)	86
Figure 3.9c. The Coupled ¹ H- ¹³ C-HSQC Spectrum Overlaid with ¹ H- ¹³ C-HSQC Decoupled	87
Figure 3.10. ¹ H- ¹ H-ROESY Spectrum Showing the Inter-residue NOES Identifying the Linkage in the Repeating unit of <i>L. paracasei</i> DG	88
Figure 3.11. Calibration Curve for the D-glucose Standard using the Dubois <i>et al</i> (1956) Test	89
Figure 3.12: ¹ H NMR Spectrum of EPS from <i>Lactobacillus salivarius</i> CCUG44481 in D ₂ O at 70 °C.....	93
Figure 3.13. SEC-MALLS trace of EPS from <i>Lactobacillus Salivarius</i> CCUG44481	94
Figure 3.14. HPAEC-PAD Chromatogram of <i>L. salivarius</i> CCUG44481 overlaid with Glucose and Galactose Standards.	95
Figure 3.15 . Chromatogram for the Alditol Acetates of the Sugars obtained from the GCMS for Monomer Analysis of <i>L. salivarius</i> CCUG44481.....	95

Figure 3.16. Chromatogram for the Methylated Alditol Acetates of the Sugars obtained from the GC-MS for Linkage Analysis of <i>L. salivarius</i> CCUG44481.....	96
Figure 3.16a. Mass spectrum of 1-deutrio-2,3,4,6-tetramethyl-1,5-di- <i>O</i> -acetylhexitol and its Fragmentation Pattern which Indicates it is a Terminal Hexose.....	97
Figure 3.16b. Mass Spectrum of 1-deuterio-2,4,6-trimethyl-1,3,5-tri- <i>O</i> -acetylhexitol and its Fragmentation Pattern which Indicates it is a 1,3-linked Hexose.....	97
Figure 3.16c. Mass spectrum of 1-deutrio-2,3,4-trimethyl-1,5,6-tri- <i>O</i> -acetylhexitol and its Fragmentation Pattern which Indicates it is a 1,6-linked Hexose.....	98
Figure 3.16d. Mass Spectrum of 1-deutrio-2,4-dimethyl-1,3,5,6-tetra- <i>O</i> -acetylhexitol and its Fragmentation Pattern which indicates it is a 1,3,6-linked Hexose.....	98
Figure 3.17. The Chromatogram of the Distinct Peaks of the Acetylated Butyl Polysaccharide of <i>L. salivarius</i> CCUG44481 and the Mass spectra of these Peaks matched with Standards D-Glucose in the Saved Library of Standards.	99
Figure 3.18. Structure of a Commercial Dextran.....	101
Figure 3.19. ¹ H-NMR Spectra from EPS of <i>L. salivarius</i> CCUG44481 (recorded at both room temperature and at 70 °C) and that for the Commercial Dextran at 70 °C.....	102
Figure 3.20. ¹³ C-DEPT 135 Spectrum for <i>L. salivarius</i> CCUG44481 indicating the C6-Methylene Signals	103
Figure 3.21. The ¹ H- ¹ H-COSY Spectrum of the Commercial Dextran indicating the Assigned Protons for the 1,6-linked Backbone.....	104
Figure 3.22. The ¹ H - ¹³ C- HSQC Spectrum of the Commercial Dextran indicating the Assigned Protons for the 1,6-linked Backbone.....	105
Figure 3.23. Overlaid COSY (black contours) and TOCSY (blue contours) Spectra of the Dextran EPS from <i>L. salivarius</i> CCUG44481.....	106
Figure 3.24. Overlaid ¹ H- ¹³ C-HSQC-Spectrum (black contours) of the EPS from <i>L. salivarius</i> CCUG44481 to that of the Commercial Dextran (blue contours).	107
Figure 4.1. HPAEC-PAD Traces of Methyl-β-Cyclodextrin after Hydrolysis.....	113
Figure 4.2. Gas Chromatogram of Methyl-β-cyclodextrin from GC-MS.....	114
Figure 4.3. Fragmentation Patterns of the 8 Peaks Analysed in Methyl-β-cyclodextrin	115
Figure 4.4. ¹ H-NMR Spectra of the Fractions obtained from 100% H ₂ O, 5% to 50% Methanol.	116
Figure 4.5. ¹ H-NMR Spectra of the Fractions obtained from 60% to 100% Methanol	117
Figure 4.6. HPAEC-PAD Traces for Fraction 1 (100% UPW).....	118
Figure 4.7. HPAEC-PAD Traces for Fraction 2 (5% Methanol)	118
Figure 4.8. HPAEC-PAD Traces for Fraction 3 (10% Methanol)	119
Figure 4.9. HPAEC-PAD Traces for Fraction 4 (20% Methanol)	120
Figure 4.10. HPAEC-PAD Traces for Fraction 5 (30% Methanol)	121
Figure 4.11. HPAEC-PAD Traces for Fraction 6 (40% Methanol)	122
Figure 4.12. ¹ H-NMR Spectrum for Fraction 6 (40% Methanol).....	122
Figure 4.13. ¹³ C DEPT 90 and 135 for the 40% Methanol fraction	124
Figure 4.14. ¹ H-NMR Spectrum for Fraction of 100% Methanol of the Second Run.	125
Figure 4.15. ¹ H-NMR Indicating the Two Sets of Three Methoxyl Groups.....	126
Figure 5.1. Growth Curve of <i>B. breve</i> 7017 at a 2h Interval Period with wavelength of 490nm	132

Figure 5.2. Graph of HBM Broth pH Recorded Containing the <i>B. breve</i> 7017 at same time during Growth Curve.	133
Figure 5.3. ¹ H-NMR Spectra for S2s of JCM Strains and Cork Strains of <i>B. breve</i> 7017	134
Figure 5.4. ¹ H-NMR Spectra for the C2s for <i>B. breve</i> 7017 (JCM, Cork and Mutant –ve EPS strains)	135
Figure 5.5. ¹ H-NMR Spectra for the C1s for <i>B. breve</i> 7017 obtained after Sonication.	136
Figure 5.6. ¹ H-NMR Spectra for the S2s (EPS) of <i>B. breve</i> 7017 Mutant Type compared with the Wild Type Strain.	137
Figure 5.7. ¹ H-NMR Spectra for the S1 for <i>B. breve</i> 7017 (in blue) compared with that of a Standard Starch (in red).....	138
Figure 5.8. SEC-MALLS trace of S1 from <i>B. breve</i> 7017 (Light scattering).....	139
Figure 5.9. HPAEC-PAD Chromatogram of the Polysaccharide (S1 fraction) from <i>B. breve</i> 7017 overlaid with glucose and galactose standards.....	139
Figure 5.10. Chromatogram and Mass Spectrometer for the Alditol Acetates of the Sugars obtained from the GCMS for Monomer Analysis of <i>B. breve</i> 7017.	140
Figure 5.11. Chromatogram and Mass Spectrometer for the Methylated Alditol Acetates of the Sugars obtained from the GCMS for Linkage Analysis of <i>B. breve</i> 7017 (S1).	141
Figure 5.12. ¹ H-NMR Spectra for the S2 of <i>B. breve</i> 7017.....	142
Figure 5.13. ¹ H - ¹³ C-HSQC Spectrum for S2 fraction of <i>B. breve</i> 7017	143
Figure 5.14. ¹ H-NMR Spectra for the S2s of <i>B. breve</i> 7017 for Batches 1 and 2 at the end of 12 weeks of their Transformation	144
Figure 5.15. The group of ¹ H - ¹³ C-HSQC Spectra for S2 fraction of <i>B. breve</i> 7017 indicating its Changes from when Freshly Extracted until Final Transformational Change after 12 weeks.	145
Figure 5.16. ¹ H-NMR Spectra for the S2s of <i>B. breve</i> 7017 for a Batch with the Impurity and Another Batch with Complete Absence of the Impurity.....	146
Figure 5.17. The Expanded Version of the ¹ H - ¹³ C-HSQC Spectra for S2 fraction of <i>B. breve</i> 7017 indicating its Changes in the Ring Protons from when Freshly Extracted until Final Transformational Change after 12 weeks	147
Figure 5.18. ¹ H- ¹ H-COSY Spectrum for S2 of <i>B. breve</i> 7017 after 12 Weeks of Transformation	148
Figure 5.19. ¹ H- ¹ H-TOCSY Spectrum for S2 of <i>B. breve</i> 7017 after 12 Weeks of Transformation	149
Figure 5.20. ¹ H - ¹³ C-HSQC Spectra for S2 fraction of <i>B. breve</i> 7017 indicating the 4 Unique Anomeric Protons of the 4 Monosaccharides (top spectra) and their Ring Protons (bottom expanded spectrum).	150
Figure 5.21. ¹ H - ¹³ C-HMBC Spectra for S2 fraction of <i>B. breve</i> 7017 indicating the Methyne Carbons for B4 and B5.	151
Figure 5.22. Combined ¹ H - ¹³ C-HSQC Spectrum and a ¹ H - ¹³ C-HSQC-TOCSY Spectrum for S2 Fraction of <i>B. breve</i> 7017 indicating the Final Methyne Signal for C5.	152
Figure 5.23. The coupled ¹ H- ¹³ C-HSQC Spectrum Overlaid with ¹ H- ¹³ C-HSQC Decoupled Spectrum S2 for <i>B. breve</i> 7017	154
Figure 5.24. SEC-MALLS Trace of S2 from <i>B. breve</i> 7017 (Light Scattering).....	155

Figure 5.25. HPAEC-PAD Chromatogram of the Polysaccharide (S2 fraction) from <i>B. breve</i> 7017	156
Figure 5.26. Chromatogram and Mass Spectrometer for the Alditol Acetates of the Sugars obtained from the GCMS for Monomer Analysis of <i>B. breve</i> 7017.	157
Figure 5.27. Chromatogram of the Absolute Configuration of S2 from <i>B. breve</i> 7017.....	158
Figure 5.28. Chromatogram and Mass Spectrometer for the Methylated Alditol Acetates of the Sugars obtained from the GCMS for Linkage Analysis of S2 from <i>B. breve</i> 7017....	159
Figure 5.29. MS of the 1,3-linkedglucosyl unit at 12.022 mins	160
Figure 5.30. MS of the 1,3-linkedglucosyl unit at 19.300 mins	160
Figure 5.31. MS of the 1,3-linkedglucosyl unit at 14.843 mins	161
Figure 5.32. MS of the 1,3-linkedglucosyl unit at 15.426 mins	161
Figure 5.33. ^1H - ^1H -ROESY Spectrum Showing the Inter-residue NOES identifying the Linkage in the Repeating Unit of <i>B. breve</i> 7017.	162
Figure 5.34. Combined ^1H - HMBC Spectrum and a ^1H - ^{13}C -HSQC Spectrum giving more Information for the Linkages.	163
Figure 5.35. Expanded Combined ^1H - COSY Spectrum and ^1H - TOCSY Spectrum indicating the Four Methyne Group Signals (Z, X, Y and S) and the Additional Methylene Proton Signals (R and U).	164
Figure 5.36. ^1H -NMR Spectrum of the Signals not Linked to the Anomeric Protons including the Lactic Acid (The Dialysate).....	165
Figure 5.37. The Edited ^1H - ^{13}C -HSQC Spectrum indicating the Six Unique Methyne Signals of the Dialysate of <i>B. breve</i> 7017.....	165
Figure 5.38. ^1H - ^1H -COSY Spectrum of the <i>B. breve</i> 7017 S2 Dialysate indicating Short Range Scalar Couplings between the Different Protons.	166
Figure 5.39. ^1H - ^1H -TOCSY Spectrum of the <i>B. breve</i> 7017 S2 Dialysate indicating the Additional Long Range Coupling between the Different Proton Resonances.	167
Figure 5.40. Fischer Projection indicating Positions of the Various Signals.	168
Figure 5.41. HPAEC-PAD Chromatography of C1 from <i>B. Breve</i> 7017 Overlaid with Glucose and Galactose Standards	170
Figure 5.42. Chromatogram for the Alditol Acetates from C1 of <i>B. breve</i> 7017 and its Mass Spectrometer.....	171
Figure 5.43. Chromatogram for the Methylated Alditol Acetates of the Sugars obtained from the GCMS for Linkage Analysis of C1 from <i>B. breve</i> 7017	172
Figure 5.44. The Mass Spec for the 1,4,6-link which is Branched in the Main C1 Polymeric Chain	173
Figure 5.45. Chromatogram and MS of the Absolute Configuration of C1 from <i>B. breve</i> 7017 and also an Overlaid Chromatogram with a Standard D-glucose (top-right)	173
Figure 5.46. ^1H -NMR for the C1 from <i>B. breve</i> 7017 of Two Different Batches Compared with that of a Standard Starch.....	174
Figure 5.47. Light Scattering of the C1 from <i>B. breve</i> 7017	175
Figure 5.48. Refractive Index of the C1 from <i>B. breve</i> 7017	175
Figure 5.49. Refractive Index of C2 from <i>B. breve</i> 7017.....	176
Figure 5.50. The UV of C2 from <i>B. breve</i> 7017	177

Figure 5.51. $^1\text{H-NMR}$ Spectra for the C2s from <i>B. breve</i> 7017 Wild Type (batches 1&2) and Mutant Type (-ve EPS)	178
Figure 5.52. HPAEC-PAD Chromatography of C2 from <i>B. breve</i> 7017.....	179
Figure 5.53. Chromatogram and Mass Spec for the Alditol Acetates of the Sugars obtained from the Monomer Analysis of C2 from <i>B. breve</i> 7017.....	180
Figure 5.56. Chromatogram for the Methylated Alditol Acetates of the Sugars obtained from the Linkage Analysis of C2 from <i>B. breve</i> 7017.	181
Figure 5.57. Mass Spec for 1,5-di- <i>O</i> -acetyl-2,3,4,6-tetra- <i>O</i> -methylhexitol (Terminal Hexopyranose).....	182
Figure 5.58. Mass Spec for 1,4-di- <i>O</i> -acetyl-2,3,5,6-tetra- <i>O</i> -methylhexitol (Terminal Hexofuranose)	182
Figure 5.59. Mass Spec for 1,4,5-tri- <i>O</i> -acetyl-2,3,6-tri- <i>O</i> -methylhexitol (1,4-linked-Hexopyranose or a 1,5-linked-hexofuranose)	183
Figure 5.60. Mass Spec for the second 1,4,5-tri- <i>O</i> -acetyl-2,3,6-tri- <i>O</i> -methylhexitol (1,4-linked-hexopyranose or a 1,5-linked-hexofuranose)	183
Figure 5.61. Mass Spec for 1,5,6-tri- <i>O</i> -acetyl-2,3,4-tri- <i>O</i> -methylhexitol (1,6-linked-hexofuranose).....	184
Figure 5.62. Mass Spec for 1,4,6-tri- <i>O</i> -acetyl-2,3,5-tri- <i>O</i> -methylhexitol (1,6-linked-hexopyranose)	184
Figure 5.63. Chromatogram and MS of the Absolute Configuration of C1 from <i>B. breve</i> 7017 and an Overlaid Chromatogram with a standard D-glucose (top-right).....	185
Figure 5.64. $^1\text{H-}^{13}\text{C}$ HSQC Spectrum for C2 of <i>B. breve</i> 7017.....	186
Figure 5.65. $^1\text{H-}^1\text{H-COSY}$ Spectrum for C2 of <i>B. breve</i> 7017	187
Figure 5.66. $^1\text{H-}^1\text{H-TOCSY}$ Spectrum for C2 of <i>B. breve</i> 7017	188

LIST OF TABLES

Table 1.1: The Main Classes of Carbohydrates.....	3
Table 1.2: Homopolysaccharide producing LAB.....	20
Table 1.3: Heteropolysaccharide producing LAB.....	20
Table 1.3: Some Common Carbohydrates with their Dissociation Constants in Water according to Rohrer (2012) ¹⁹⁴	37
Table 2.1: Composition of the HBM medium.....	51
Table 2.2: The Composition of the CDM.....	52
Table 2.3: Typical Chromatographic Conditions of HP-SEC-MALLS.....	57
Table 3.1: The EPS Structures of some existing LAB.....	63
Table 3.2: Amount of EPS and CPS for <i>L. Paracasei</i> DG.....	68
Table 3.3: Chemical shifts for C and H of the 6 sugars (A-F).....	85
Table 3.4: Results for the Carbohydrate Analysis of EPS from <i>L. paracasei</i> DG (Batch 4).....	90
Table 3.5: Results for the Carbohydrate Analysis of EPS from <i>L. salivarius</i> CCUG44481.....	108
Table 5.1: The EPS Structures from <i>Bifidobacteria species</i>	129
Table 5.2: Amount of EPS and CPS for <i>B. breve</i> JCM7017.....	134
Table 5.3: EPS yields of <i>B. breve</i> 7017 Cultured in HBM Broth.....	135
Table 5.4: Resonance Positions for the Hydrogens and Carbons.....	153
Table 5.5: Chemical Shifts of Monosaccharide Resonances.....	188

Publications

1. Balzaretto, S., Taverniti, V., Guglielmetti, S., Fiore, W., Minuzzo, M., Ngo, H., Ngere, J., Sadiq, S., Humphreys, P. and Laws, A. (2017) 'A novel rhamnose-rich hetero-exopolysaccharide isolated from *Lactobacillus paracasei* DG activates THP-1 human monocytic cells' *Applied and Environmental Microbiology* , 83 (2), pp. AEM.02702-16. ISSN 0099-2240.

Statement of contribution

In the above publication in 2017, we did the research work in collaboration with a team in Italy. Our contribution was on culturing the *Lactobacillus paracasei* DG using our developed Huddersfield broth medium (HBM) which was known to be free of any exopolysaccharide equivalence and then extracting the bacterial polysaccharide from the cell biomass and supernatant for characterisation. We were responsible for the chemical characterisation of this bacterial polysaccharide using the HPAEC-PAD, GC-MS, SEC-MALLS and NMR analysis methods. With all these methods, we were able to determine the structure of this extracted bacterial polysaccharide extracted and found it to be novel in comparison with all other isolates. We also extracted more of this pure bacterial polysaccharide and sent it to the Italian research team for them to carry out the identification of putative genetic clusters for exopolysaccharide biosynthesis and to investigate its immunomodulatory activity.

2. Alhudhud, M., Sadiq, S., Ngo, H.N., Hidalgo-Cantabrana, C., Ruas-Madiedo, P., Van Sinderen, D., Humphreys, P.N. and Laws, A.P., 2018. Extraction of the same novel homoglycan mixture from two different strains of *Bifidobacterium animalis* and three strains of *Bifidobacterium breve*. *Beneficial microbes*, 9(4), pp.663-674.

Statement of contribution

In this above publication in 2018, we cultured specifically the wild type *Bifidobacterium breve* 7017 as well as the mutant type *Bifidobacterium breve* 7017 (a non-EPS producer) in HBM media from where were separated the cell biomass from the supernatant. From the cell biomass, we extracted the capsular polysaccharide and from the supernatant we extracted the exopolysaccharides. We also used another

HBM media supplemented with an isotopically labelled D-glucose-1-¹³C for the culturing and extraction of the bacterial polysaccharides to prove that the carbon supplement is being synthesised *in situ* as the label was confirmed to incorporate into more than 95% of the anomeric carbons of each of these polysaccharides. We carried out characterisation of these extracted bacterial polysaccharides using the chemical analytical methods (HPAEC-PAD, GC-MS, SEC-MALLS and NMR analysis) to determine its chemical structure. We then did a comparison of the results obtained from the chemical analysis and the ¹H NMR profiles of the polysaccharides recovered the cells of wild and mutant type *Bifidobacterium breve* 7017 which were found to be similar to those from *B. animalis* subsp. *lactis* AD011 and A1dOxR, *B. breve* 7019 and *B. breve* 2258 under study in our research team.

Chapter 1

1. Introduction

Living organisms such as plants and animals usually have bacteria found associated with them and these are classified as either probiotics, commensals or pathogenic based on the influence that they exert to their living host organisation. Probiotics are organisms which have effects that are beneficial to the host organism and they have been generally referred to as “live microorganisms which when amounts are adequately administered, confer health effects which greatly benefits the host”^{1, 2}. The pathogenic bacteria are those with harmful effects such as inducing diseases to the host organisms which may result from their activities and/or the products which they release unto the host ³. Commensals are bacteria which have neither beneficial or harmful effect to the host ⁴.

For many centuries, probiotics have been widely used as part of traditional medicinal folklore but in relatively niche areas and they have only really been exploited commercially during the twentieth century. However, there is now an exponential growth in an interest in probiotics as exemplified by the fact that a market is expected to grow to provide \$46.55 billion in turnover value by 2020 ⁵. The proposed beneficial effects of probiotic bacteria to humans has seen them being included as dietary supplements mainly for improvement of the intestinal microbial balance⁶. Traditionally, probiotic bacteria have been utilized in producing a number of fermented foods e.g yoghurt, kefir grains and pickles. In both research and commercial development of probiotics, the majority of bacteria have come from a limited number of genera including *Lactobacillus spp* and the *Bifidobacterium spp*. These are the genera which have been given GRAS status (Generally Regarded as Safe) or the Qualified Presumption of Safety status in the US by the Food and Drug Administration (FDA) and in the EU by the European Food Safety Authority (EFSA) respectively^{5, 7}. It has become increasingly recognised that the consumption of specific strains of bacteria can provide health benefits and a number of theories exist which attempt to rationalise how these benefits are achieved⁸⁻¹¹. Recent research has suggested that the excretion of polysaccharides at or close to the surface of the bacteria known as capsular and exopolysaccharides are partially responsible for this biological activity^{5, 12, 13}. Unfortunately, not many of these carbohydrate-based materials have been isolated purified and characterised and, as such, very little is known

about the molecular processes by which these carbohydrates impart their biological activity. It is this issue which will be addressed in this thesis.

Generally, carbohydrates are some of the most abundant natural products on the earth and most have very important biological functions, the most significant being their use as sources of energy, as structural materials and as chemical messengers. Natural carbohydrates exist in many different forms including examples such as monosaccharides, disaccharides, oligosaccharides, polysaccharides or as derivatives often in combination with other biomacromolecules including lipids and proteins¹⁴. Monosaccharides are considered as the most basic building blocks and they can be generally defined as polyhydroxy-aldehydes or polyhydroxy-ketones which occur in an open chair or a heterocyclic ring form and they are frequently referred to as sugars^{15, 16}. Oligosaccharides and polysaccharides are formed from linking monosaccharides into chains (<10 = oligosaccharides, > 10 up to 1000s for polysaccharides). Polysaccharides are the most abundant polymeric materials in the biosphere, each year, approximately 4×10^{11} tons are biosynthesised by plants and bacteria¹⁷. Polysaccharides are made by a great variety of species (microbes, plants and animals) with the most common examples being the homoglycans that contain one type of monosaccharide *e.g* starch and cellulose which are composed entirely of glucose. The structural diversity of polysaccharides is very large and the natural world generates a large variety of polysaccharides with different monosaccharides and different linkages between monosaccharides and this is best illustrated by the different natural polymers of D-glucose which are produced: along with starch and cellulose, dextrans, levans and pullulans are also produced by bacteria and yeasts. Glycogen, starch and dextrans are all nutritional food reserves, which are broken down to monosaccharides units and then metabolised to yield energy for the respective individual species when needed. Cellulose, which is the most common organic compound on earth, is a structural polysaccharide found in plant cell walls and is composed of repeating chains of D-glucose monosaccharide¹⁴.

1.1. Classification of Carbohydrates

Historically, carbohydrates have been classified or grouped according to their molecular size, which is directly related to the number of monosaccharides/sugar units present and, especially when dealing with polysaccharides, this is frequently referred to as the degree of polymerisation (DP)¹⁸. In this work, carbohydrates will be classified as either monosaccharides

(DP1) disaccharides (DP2) oligosaccharides (DP3-DP10) or as polysaccharides (DP>10)¹⁸. It is worth noting that a slightly different classification is used by the food industry which divides carbohydrates into three main classes according to their DP as seen on table 1.1.

Table 1.1: The Main Classes of Carbohydrates

Class (DP)	Subgroup	Principal components
Sugars (1-2)	Monosaccharides	Fructose, glucose, galactose
	Disaccharides	Sucrose, lactose, maltose, trehalose
	Polyols (Sugar alcohols)	Sorbitol, mannitol, lactitol, xylitol, erythritol, isomalt, maltitol
Oligosaccharides (3-9) (Short-chain carbohydrates)	Maltooligosaccharides (α -glucans)	Maltodextrins
	Non- α -glucan oligosaccharide	Raffinose, stachyose, fructo and galacto-Oligosaccharides, polydextrose, inulin
Polysaccharides (≥ 10)	Starch (α -glucans)	Amylose, amylopectin modified starches
	Non-starch polysaccharides (NSPs)	Cellulose, hemicellulose, pectin, arabinoxylans, β -glucan, glucomannans, plant gums and mucillages, hydrocolloids

Degree of polymerization^{19, 20}

1.1.1. Monosaccharides

As stated earlier, monosaccharides are considered as one of the basic building blocks in carbohydrate chemistry, they are crystalline water-soluble compounds which are either aliphatic aldehydes or ketones and in addition to having a carbonyl group they have one or more hydroxyl groups. There are about twenty naturally occurring monosaccharide and approximately fifty that have been synthesised by man. The number of carbon atoms in a carbon chain is the basis of the classification of monosaccharides with monosaccharide of 3, 4, 5, 6, 7, 8, 9 and 10 carbon atoms being referred to as a triose, tetrose, pentose, hexose, heptose, octose, nanose and decose respectively. By far, the most abundant are the pentoses (containing 5 carbon atoms such as ribose and xylose) and the hexoses (containing 6 carbon atoms such as glucose, fructose galactose). Pentoses and hexoses are the main constituents of disaccharides (*e.g.* sucrose), oligosaccharides and polysaccharides (*e.g.* cellulose and starch)¹⁴. Monosaccharides cannot be further hydrolysed into simpler sugars and are frequently subcategorised as either aldoses or ketoses with examples being glyceraldehyde and dihydroxyacetone (3 carbon sugars) respectively (*Fig 1.1*). These two simplest aldo and keto sugars are isomers^{16, 21}.

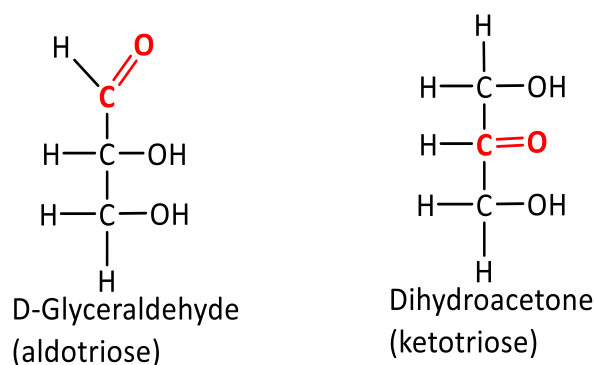


Figure 1.1: The 3 Carbon Sugars (trioses)

NB: The $\text{C}=\text{O}$ highlighted red is just to indicate the position of the functional group that differentiates these trioses.

In the natural environment, monosaccharides hexoses such as D-glucose (dextrose) and D-fructose are the most abundant¹⁶. The structures of these monosaccharides are often represented using Fischer projection formulae with the majority of the carbon atoms which form chiral centres have hydroxyl groups attached to them^{16, 22}. These chiral centres bring about the naturally existing sugar stereoisomers which are of biological significance given that the enzymes acting on sugars are stereospecific with preference shown to one stereoisomer than the other¹⁶. As a result of these monomeric sugar units having multiple stereocentres, there are several possible isomers, which include epimers (two sugars differing in configuration at only one stereocentre e.g D-mannose and D-glucose) *Fig 1.1a*, enantiomers (sugars with mirror images of each other which are non-superimposable e.g D- and L-glucose) *Fig 1.1b* and diastereoisomers (sugars having same exact substituents on the chiral carbons but differ in their configuration and are not mirror images of one another e.g D-altrose and D-glucose) *Fig 1.1c*^{16, 23}. Most monosaccharides studied usually have more than one chiral carbon atoms and are assigned an absolute configuration (D- and L-) which is determined by how the secondary group (-OH (hydroxyl)) at the highest numbered chiral centre is configured which in this case is at carbon atom 5 (C-5) for the D- and L-glucose^{16, 23, 24} (*Fig 1.1b*).

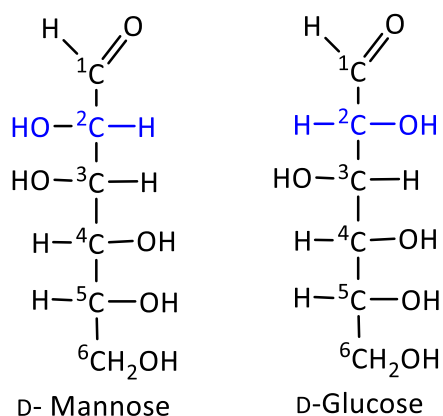


Figure 1.1a: Epimers(sugars which differ in only 1 stereocentre highlighted in blue)

NB: The H-C-OH highlighted in blue indicate the position at which they differ.

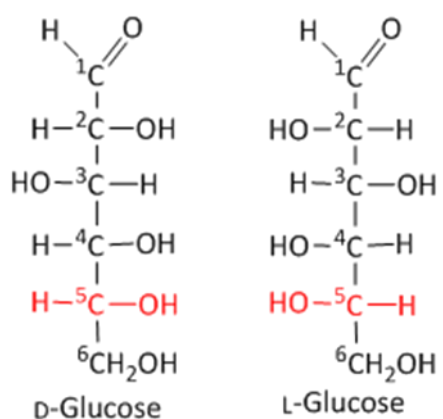


Figure 1.1b: Enantiomers(sugars which are mirror images to each other)

NB: H-C-OH highlighted in red indicates the pint at which they differ

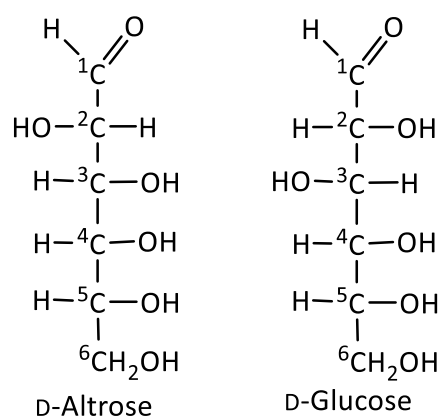


Figure 1.1c Diastereoisomers(sugars exact substituents on the chiral carbons but differ in their configuration)

The pentoses and hexoses can cyclize as either a five-membered ring (furanose) or a six-membered ring (pyranose)¹⁶. All monosaccharides having 5 or more carbon atoms occurs as cyclic rings in aqueous solutions where there is a formation of a covalent bond between the carbonyl group and a hydroxyl group found along the chain. There are a number of ways of representing cyclic sugars, one is using Howarth perspective formulas (*Fig 1.2a* and *Fig 1.2b*) and a second is to draw the sugars in 3D e.g. in chair conformations (*Fig 1.3*)¹⁶.

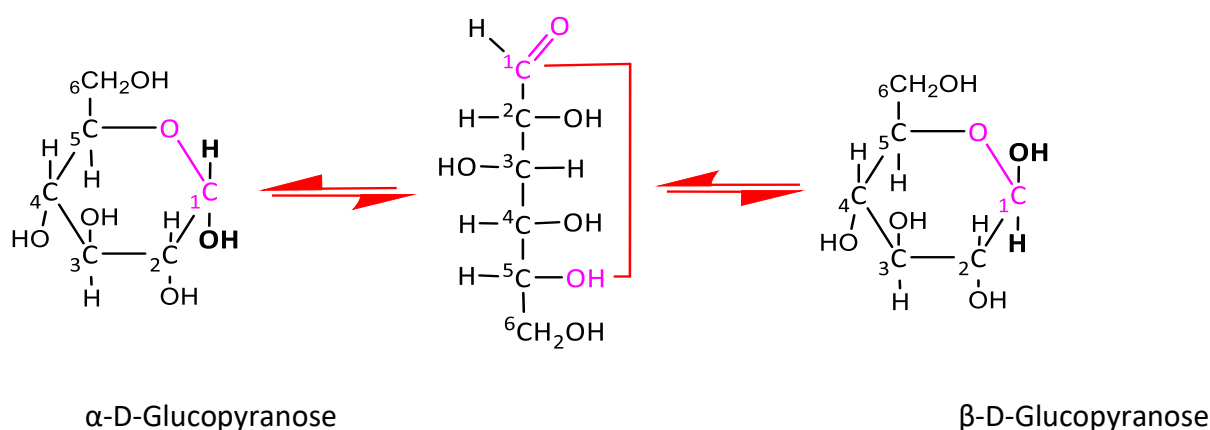


Figure 1.2a. The Two Cyclic Forms of D-glucose

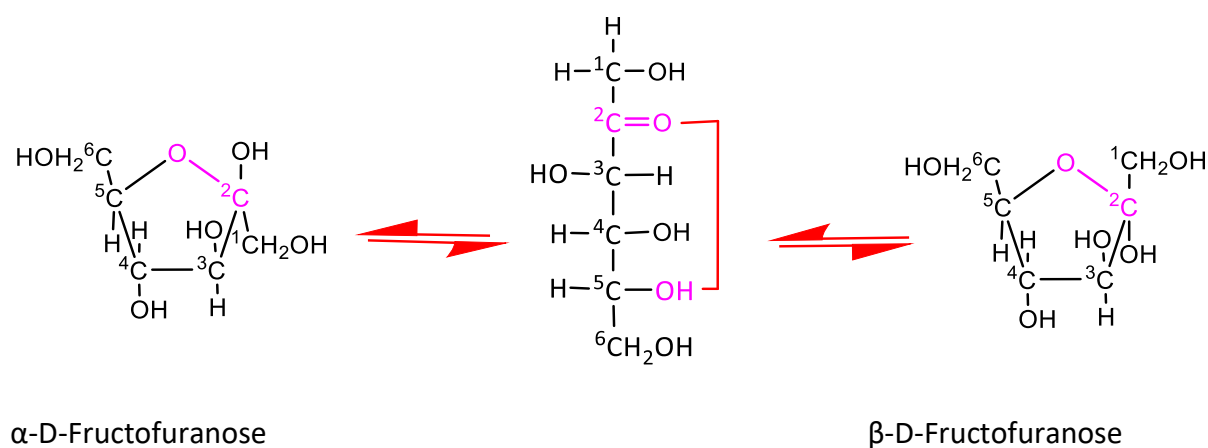


Figure 1.2b. The Two Cyclic Forms of D-fructose

NB: The O-, C=, OH all highlighted indicate the positions where cyclisation occurs.

Cyclisation to the pyranose or furanose conformation generates a new stereogenic centre and two stereoisomers known as α and β anomers^{16, 24}. When linear D-glucose and D-fructose cyclise, they form cyclic hemiacetal α/β -D-glucopyranose (*Fig 1.2a*) and cyclic hemiketal α/β -D-fructofuranose (*Fig 1.2b*) respectively^{16, 24}.

Monosaccharides are known to occur as neutral, acidic or amino sugars with some having non-sugar substituents (acyl groups such as acetyl or pyruvyl) as well as inorganic substituents (such as sulphate, phosphate groups) ²⁵ (Fig 1.3). Sugars which possess the amino and acidic groups account for their polyelectrolyte properties ²⁶.

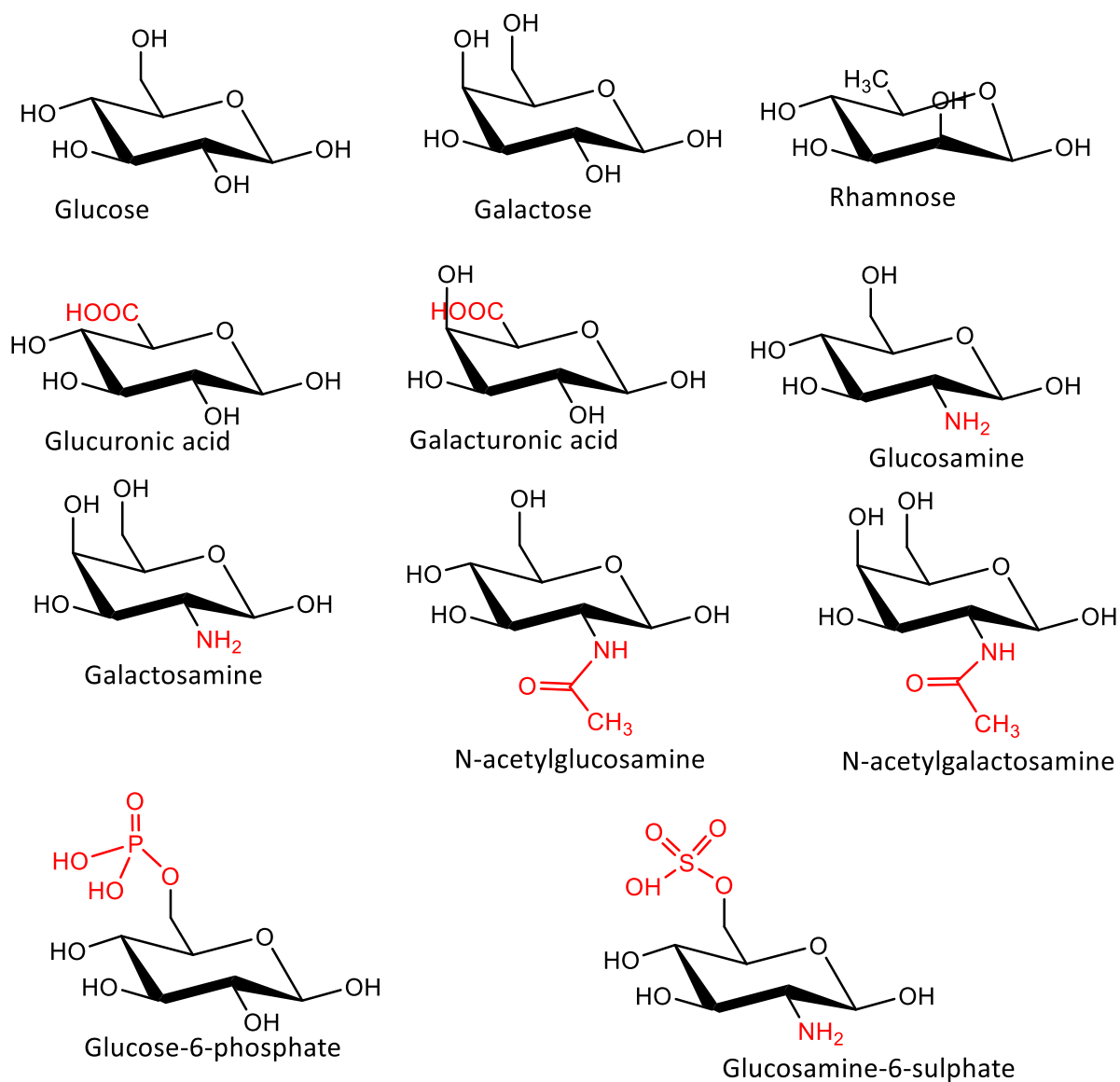


Figure 1.3. The various forms of sugars that exist: Neutral, Acidic, Amino, acyl, Phosphate and Sulphate Sugars

NB: All the functional groups from where the sugars derive their names are highlighted in red

1.1.2. Derivatives of Monomeric Sugar Units

A number of simple sugar derivatives exist in nature. During oxidation of an aldose, the aldehyde group can be converted into a carboxylic acid group which then produces an aldonic

acid (e.g gluconic acid). The oxidation of the carbon located at the end of the chain (C-6) or the primary alcohol of aldose produces a uronic acid (e.g glucuronic and galacturonic acids; *Fig 1.3*).

In the presence of a reducing agent such as sodium borohydride (NaBH_4), aldoses and ketoses are reduced to alditols (polyhydroxyl alcohols). Commonly encountered examples of alditols include sorbitol, mannitol, and xylitol.

The deoxy-sugars are those formed as a result of a hydroxyl group (OH) being replaced with a hydrogen atom (H) in the monomeric unit ^{16, 24, 27} (*Fig 1.3a*).

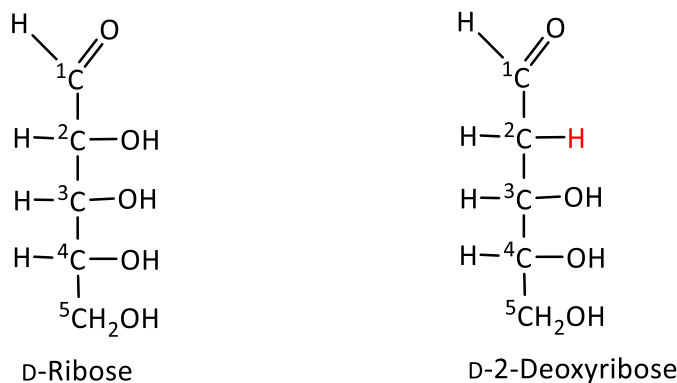


Figure 1.3a. D-Ribose and 2-Deoxy-D-ribose

The amino sugars (glucosamine and galactosamine) results from the replacement of the OH group with an amino group ($-\text{NH}_2$) at C-2 of the monosaccharide unit. This amino group can be acetylated resulting to an *N*-acetyl amino sugar (*N*-acetylglucosamine and *N*-acetylgalactosamine) *Fig 1.3*. Many structural polymers within microorganisms contain this glucosamine derivative (*N*-acetylglucosamine)¹⁶. Phosphorylated derivatives of sugars are often found as intermediates during the synthesis and metabolism of carbohydrates. A phosphate ester (glucose-6-phosphate; *Fig 1.3*) is a key intermediate in the biosynthesis of polysaccharides. Phosphate ester are being used by most organisms as the first metabolite during glucose oxidation to produce energy¹⁶.

The Howarth perspective formulae is the common form used in indicating the ring form of stereoisomers of single sugar units but it shows the ring as a planar structure hence not representing their true conformations accurately. As a result, the chair conformation is best used as it accurately provides the view of the substituents found at the axial and

equatorial positions²⁴ (Fig 1.4). Two possible chair conformations can be used but the one in which the equatorial positions are being occupied with the bulkiest ring substituents predominates^{24, 28} (Fig 1.4). Glucose is seen to be naturally abundant in nature and this could be as a result of its β -D-Glucopyranose form having all its non-H substituents occupying equatorial positions²⁴.

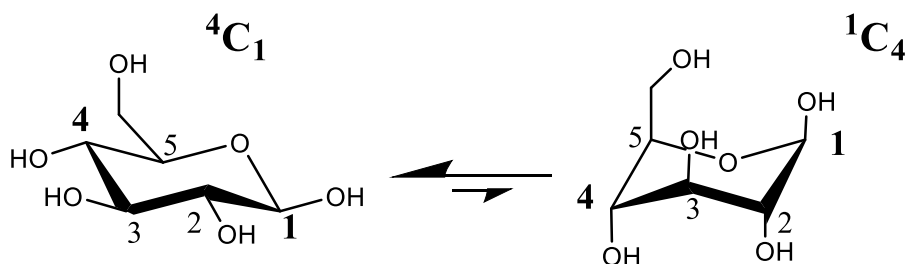


Figure 1.4. The Two Chair forms of β -D-Glucopyranose

It should be noted that the chair conformation is denoted as C during the description of the various pyranoid conformers²⁸ and a reference plane containing four of the six ring atoms must be selected so as to aid in designating the chair conformations as either 4C_1 or 1C_4 (Fig 1.4). Given that the O, C2, C3 and C5 atoms are chosen to be the reference plane, then the 4C_1 conformation is designated when the C4 is above and the C1 atom is below the reference plane. This is vice versa for the designation of the 1C_4 conformation.

1.1.3. Disaccharides

These are sugars made up of two monosaccharides units, which are covalently linked by an *O*-glycosidic bond resulting from the reaction between an OH group of one of the monomers and the anomeric carbon of the other monomer^{16, 24}. Hydrolysing these sugars using either acids or enzymes results in the breakage of this bond giving rise to the individual monosaccharides. Examples of disaccharides include lactose, sucrose, maltose, and trehalose. Generally, there exist different types of disaccharides, which are reducing and non-reducing sugars. This description of disaccharides is dependent on whether the anomeric carbons of one of the sugar molecule (which is at the end of the chain) is not involved in the glycosidic bond making it a reducing sugar but if it is involved then it is a non-reducing sugar. Consequently, lactose (β -D-galactopyranosyl-(1 \rightarrow 4)- β -D-glucopyranose; Fig 1.5a) is then a reducing sugar since the glucose unit possesses the free anomeric carbon whereas, sucrose (α -D-glucopyranosyl-(1 \leftrightarrow 2)- β -D-fructofuranoside; Fig 1.5b) is a non-reducing sugar as a

result of the anomeric carbon of the two sugars participating in the glycosidic linkage^{16, 23, 24}. Lactose naturally occurs in milk and when hydrolysed it breaks down into D-galactose and D-glucose. Sucrose is commonly known as table sugar, it is formed by plants and when hydrolysed it breaks down into D-glucose and D-fructose.

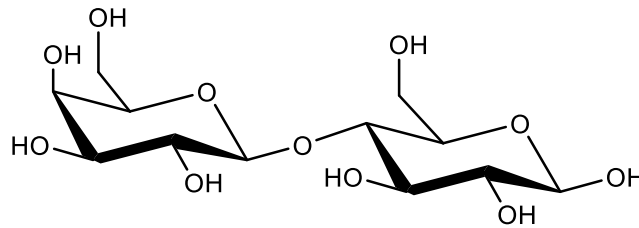


Figure 1.5a. β -D-galactopyranosyl-(1 \rightarrow 4)- β -D-glucopyranose

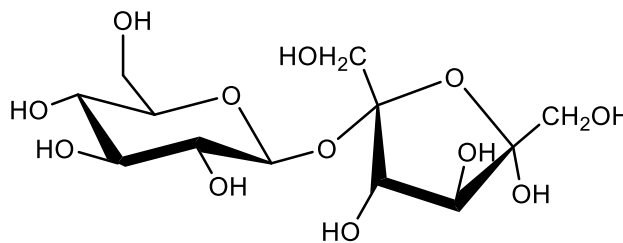


Figure 1.5b. α -D-glucopyranosyl-(1 \rightarrow 2)- β -D-fructofuranoside

1.1.4. Oligosaccharides

They are short-chain carbohydrates usually containing between 3 to 9 monomeric units covalently bonded to each other through O-glycosidic bonds and are of low molecular weight¹⁸. Depending on the number of monomer units linked together, they could be referred to as trisaccharides, tetrasaccharides and so on. Oligosaccharides containing the D-glucose, D-galactose and the D-fructose frequently occur in food e.g raffinose (*Fig 1.6*)

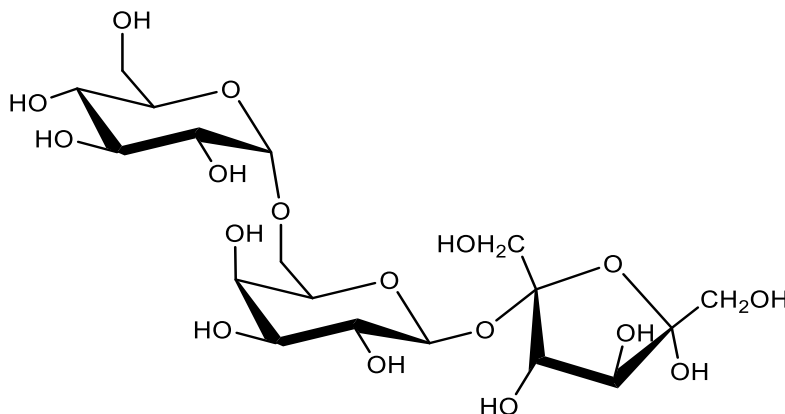


Figure 1.6. Raffinose

1.1.5. Polysaccharides

Most carbohydrates are generally produced as polysaccharides (glycans) and they frequently have high molecular weights consisting of many monomeric units linked together by glycosidic bonds^{14, 16, 24, 29}. Their structures are often seen to be linear although some chains may be branched. Common examples of polysaccharides of animal origin include glycogen, chitin and chitosan whereas those derived from plants include starch, cellulose, pectin and β -glucan. Some common microbial polysaccharides include pullulan, gellan, xanthan and dextran. The monomeric building units of the various polysaccharides brings about their distinct properties. Based on their monomeric building units, the classification of polysaccharides can be divided into two separate groups where those made up of the same monomeric units are referred to as homopolysaccharides (homoglycans e.g., starch, glycogen and cellulose which are formed from multiple glucose molecules linked together) whereas those made up of different types of monomeric units are referred to as heteropolysaccharides (heteroglycans e.g., xanthan gum, hyaluronic acid^{14, 16, 24}. The most abundant polysaccharide is cellulose which is a homopolysaccharide and is found in plants where it forms the major cell wall structural component. Cellulose is made up of multiple D-glucose units (*Fig 1.7*) which are all connected by a β -1,4-linkage¹⁴

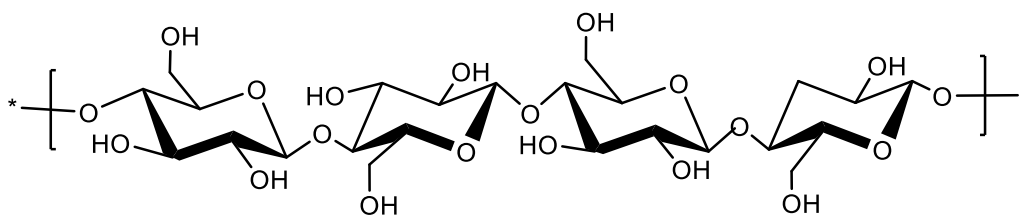


Figure 1.7. Structure of Cellulose

Xanthan is a heteropolysaccharide which is composed of more than one type of monomeric unit and is made up of β -D-glucopyranose as its backbone and having a trisaccharide made of glucuronic acid and two mannose molecules with one having an acetyl substituent at carbon 6 and the other having pyruvic acid at carbons 4 and 6 which is linked to every second β -D-glucopyranose unit³⁰ (*Fig 1.8*). Xanthan is mainly used in rheological modification when used as a food additive because of its importance in increasing viscosity. Xanthan is produced by the bacterium *Xanthomonas campestris*³¹

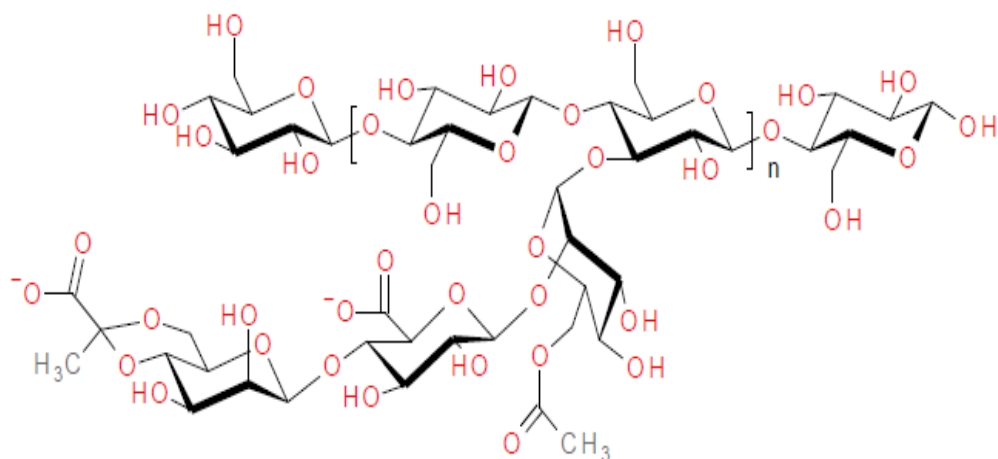


Figure 1.8 Structure of Xanthan Gum³⁰

In the work reported here we are concerned with polysaccharides produced by bacteria. A range polysaccharides are biosynthesised by bacteria³² at or close to the cell surface. During growth bacteria generate a class of polysaccharides which are released into the surroundings and which are not attached permanently to the bacterial cell wall and these are referred to as exopolysaccharides (EPS). They also produce a second class of polysaccharides which are known as capsular polysaccharides (CPS) which are attached to the bacterial cell surface. The substrates or substances as well as the growth conditions utilised by the bacteria determine the chemical constituents and the physical nature of the polysaccharides synthesised³³. The focus of this project will be to monitor the production, structure and characteristics of both the EPS and CPS biosynthesised by specific groups of Gram-positive bacteria.

1.2. Bacteria

Bacteria are single cell microorganisms known to exist in every habitat on earth such as in water, soil, deep down in the earth's crust, in organic matter as well as associated with the bodies of living organisms (plants and mammals)^{34, 35}. There exist about 40 million bacterial per gram of soil and typically about 1 million per millilitre of fresh water which all constitutes much of the world's biodiversity³⁶. These bacteria can either be spherical, spiral or rod-like in shape³⁷. Based on the structure of the cell wall, bacteria can be classified into two groups, which are Gram-positive and Gram-negative. A peptide-polysaccharide layer (peptidoglycan) is a strong protective unit found in almost all bacteria cell walls that is responsible in providing the shape and rigidity of the bacteria while at same time protecting its cell contents. In a bacterial cell, this peptidoglycan unit consists of alternating chains of a repeating disaccharide unit of *N*-acetylglucosamine (NAG or GlcNAc) and *N*-acetylmuramic acid (NAM) forming a mesh-like complex outside the plasma membrane³⁷. The two classes of bacteria can be differentiated based on the structure of their cell walls where the peptidoglycan unit of Gram-positive bacteria is approximately twenty times thicker than that of Gram-negative bacteria (*Fig 1.9*).

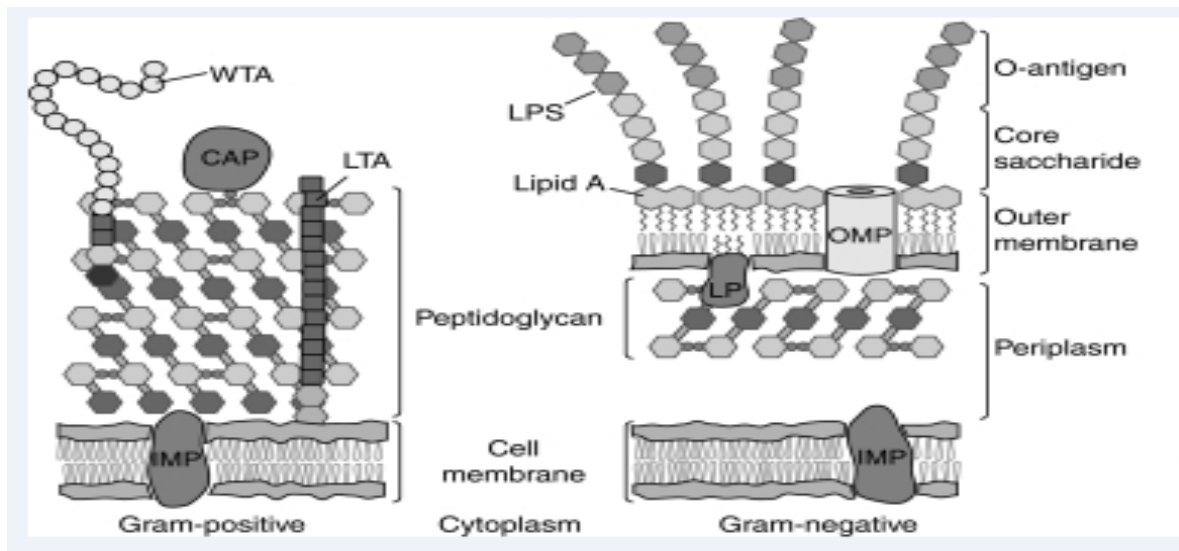
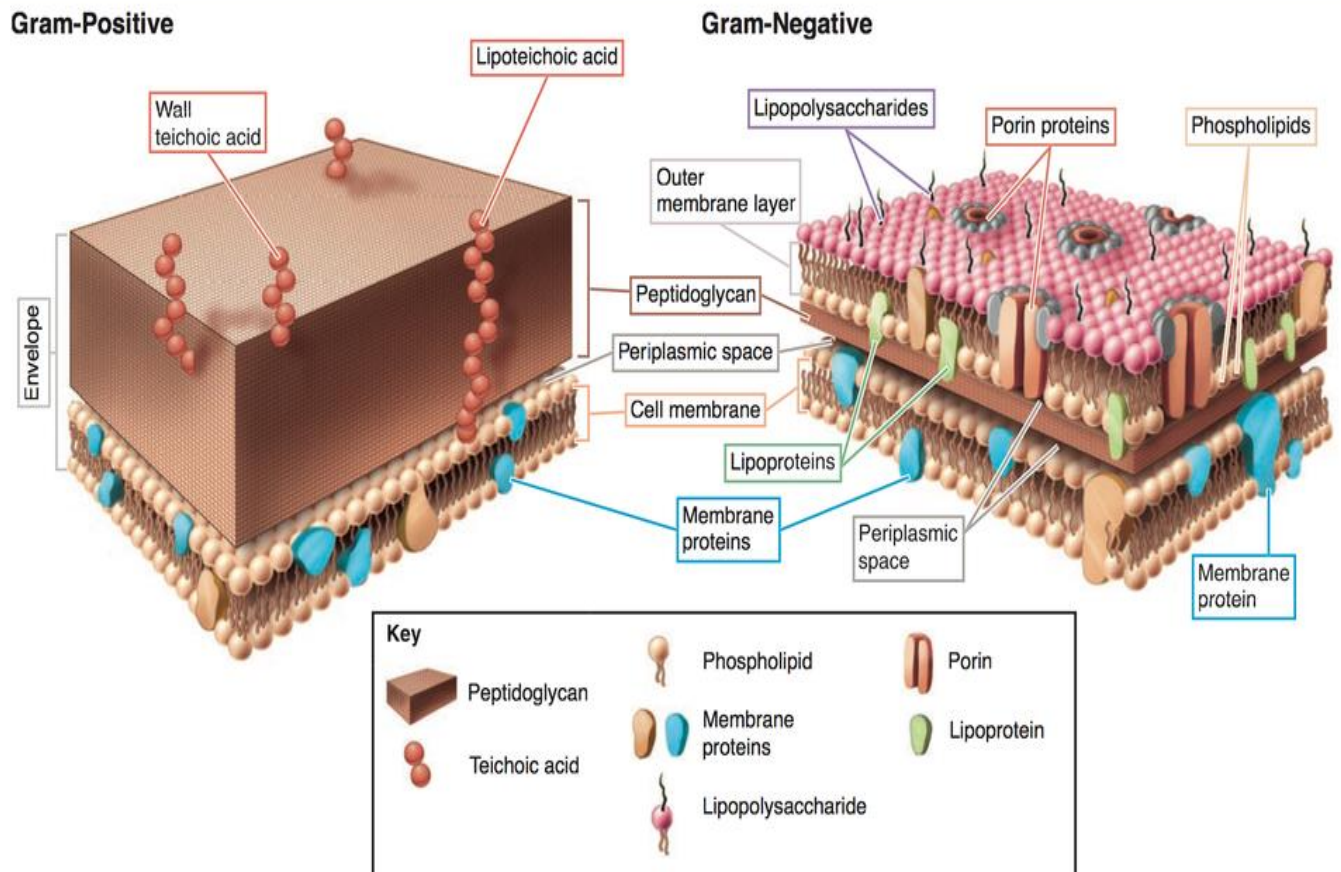


Figure 1.9. Cross section of Gram-positive bacteria cell wall (having a thicker peptidoglycan layer) and Gram-negative bacteria (having a thin peptidoglycan layer) [Images designed by McGraw-Hill companies Inc. (coloured image) & Ghuyssen and Hackenbeck (1994) ³⁸ respectively].

A number of structural elements are attached to peptidoglycan of Gram-positive bacteria including teichoic acids and lipoteichoic acids both of which are considered as polysaccharides, the former are covalently linked to the cell envelope whilst the latter are linked to a lipid³⁹ which is embedded in the cell membrane (*Fig 1.9*). The teichoic acids are responsible for the cell wall rigidity when it attracts cations like sodium and magnesium^{40, 41}. Added to the thin peptidoglycan layer in the cell structure of Gram-negative bacteria are the inner membrane (which contain the inner membrane proteins) and an outer membrane which contains lipopolysaccharides, porin proteins and phospholipids; *Fig 1.9*). The lipopolysaccharides (LPS: lipoglycan) are typical of Gram-negative bacteria and consist of a lipid, a core saccharide and an O-antigen (an oligosaccharide) all covalently linked together⁴²⁻⁴⁴. The LPS of Gram-negative bacteria is responsible in generating a very strong immune responses when in contact with a host with the O-antigen region playing the major role particularly as it is exposed outside the bacteria cell and easily recognised by antibodies of the host⁴⁵. The core saccharide, which is directly linked to the lipid is made of an oligosaccharide made of sugars like 3-deoxy-D-manno-oct-2-ulosonic acid and heptose though it can also contain non-carbohydrate substituents like amino-acids and phosphate⁴⁶. The lipid portion of the LPS in Gram-negative bacteria is the part responsible for toxicity. The LPS can also be involved in tricking the immune system especially for those bacterial strains having some parts of their LPS which are chemically similar to molecules of their host cell surface⁴⁷.

Gram staining was devised in 1884 by Christian Gram to classify bacteria according to their cell wall structures. Gram-positive bacteria retains the Gram stain (staining purple /blue) giving a positive result as a result of the thick peptidoglycan layer whereas the Gram-negative bacteria stains red/pink as result of its thin peptidoglycan layer^{48, 49}.

1.2.1. Bacterial Growth

Bacterial growth is associated with an increase in the number of bacterial cells within a given population and a bacterial growth curve can be used to illustrate growth trends with respect to time. After inoculating bacteria on to a fresh solid or liquid medium, the cell concentration can be measured periodically against time and a growth curve plotted which gives four distinct phases which are the lag, exponential, stationary and the death phases⁵⁰ *fig 1.10*.

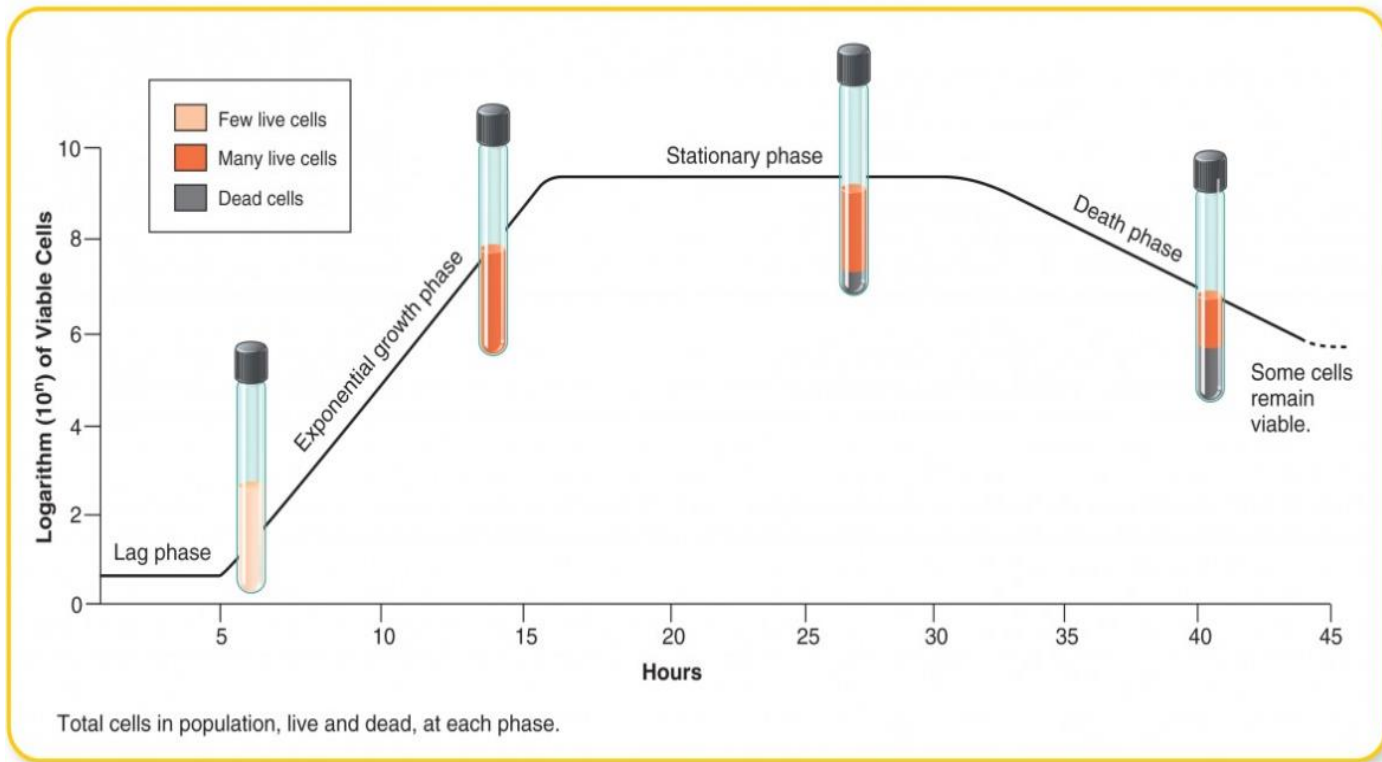


Figure 1.10: Bacterial Growth Curve of a Culture as designed by the McGraw-Hill Companies Inc.

When dormant bacteria are inoculated into a suitable medium, they switch into an active mode where they start consuming the required nutrients from the medium in preparation for reproduction. This is typically the lag phase where there is a tiny increase in the number of cells as they are still adapting to the new environment as well as taking time to synthesize essential nutrients. At this phase the number of new bacterial cells is equivalent to those dying hence bringing about the plateau region at the start of the growth curve. The duration of this phase could range from a few hours to days as a result of the type of bacterial species involved. The growth in cell number and volume starts increasing with regards to the availability of more nutrients for uptake.

The exponential phase starts at the end of the lag phase where the bacterial cells are actively dividing and doubling their population at a geometric rate. At this phase the increase in population and bacterial reproduction is at its maximum with factors such as temperature, pH, and culture medium constituents still controlling its rate of growth. When the required available nutrients have been completely used by the bacterial during growth and there is no

further increase or decrease in the bacterial cell numbers, it is called the stationary phase. During this phase cryptic growth occurs where the amount of bacteria cells that grow is equal to that amount that dies⁵¹. Toxic products are also generated at this phase, which builds up, and at the point where the cell production finally stops, then the death phase stage commences.

The death phase is the final phase where after all nutrients have been taken up then the bacteria, begin to die causing a decline in their cell number and volume. The rate at which the cells decline is exponential but in a much slower pattern as to that in the exponential phase. At this death phase there is a dramatic increase in the number of dying bacterial cells as well as some going into hibernation or dormant state in order to survive hence resulting in the decrease in the growth curve.

1.2.2. Bacterial Polysaccharides

Under appropriate conditions bacteria utilize activated monosaccharide substrate to produce a range of polysaccharides which have diverse structures and which have a range of molecular weights^{52, 53}. A wide range of biopolymers are produced by bacteria which possess varying chemical properties associated with specific biological functions and these can be either intracellular or extracellular^{54, 55}. The biopolymers presented at or close to the cell surface are often the first point of contact with other cellular structures and these are collectively referred to as extracellular polymeric substances. The extracellular polysaccharides are further classified with respect to where they are located in relation to the bacterial cell^{56, 57} as either exopolysaccharides or capsular polysaccharides with the polysaccharides often appearing as a mucoid type-layer coating cells. The mucoid material can be attached either covalently to the cell surface to form the CPS (capsular polysaccharides) or they could be separated completely from the cell surface to form EPS (exopolysaccharides)^{56, 58, 59} as mentioned earlier. However, often there are difficulties in clearly differentiating between the CPS and EPS especially in extraction and isolation scenarios where there is subsequent release of the CPS to the environment as well as scenarios where some EPS might still be linked to the cell surface during synthesis⁶⁰. Part of this current research work will be focused in determining the structures of the CPS and EPS found in the given Gram-positive bacteria which up to date, some published EPS and CPS structures of some bacteria have demonstrated similarities and vice versa. A large number of publications have suggested that

the EPS and CPS are biologically active (anticancer, antitumor and immunomodulatory properties) ⁶¹ which as a result is then responsible for their synthesis rather than any mechanical contribution they may make to the bacterial cell wall structure⁶². Unfortunately only a limited number of structures are known and it is not clear how the structure of an EPS or CPS contributes towards their biological activity⁶³. Many early studies on the structure of EPS mainly focused on those generated by Gram-negative bacteria because of an interest in understanding how they contribute to the pathogenicity of the bacteria. Whilst many of these earlier studies focused on pathogenic bacteria in the last decade the emphasis has shifted to study the polysaccharides secreted by probiotic bacteria which are mainly Gram-positive organisms including species such as lactic acid bacteria (LAB) and bifidobacteria ⁶⁴.

1.3. Probiotic Bacteria

As earlier mentioned, probiotics are known to manifest beneficial effects to their host effects and have been defined as “live microorganisms which when consumed adequately will provide health benefits to the host”^{1, 2}. With probiotics being supplemented into the diet nowadays to improve the intestinal microbial balance of the host⁶, they are still traditionally used in fermenting food products like yoghurt, cheese, milk and kefir grains⁶⁵. About 300 to 500 bacteria species inhabit the human intestines with 10 times more bacterial cells known to colonise the intestinal tract as compared to the human body cells⁶⁶. Immediately after birth the gut microflora is being colonised rapidly with a great variety of compositional patterns differing among individuals due to their age, illnesses, diet, antibiotic treatment and the adaptable strains⁶⁷. The presence of pathogenic bacterial species in the gut microflora as well as the probiotic species brings about much interest into understanding the functioning and implication of its role in terms of diseases and health.

It has been reviewed that specific probiotic strains of the genera *Bifidobacterium*, *Lactobacillus*, *Leuconostoc*, *Streptococcus*, *Bacillus*, *Enterococcus*, *Pediococcus* *Escherichia coli* have all demonstrated health benefit in their host (human microbiota) making them gain more attention nowadays with one of these benefits being the correction of dysbiosis from the consumption of these probiotics⁶⁸. Of all these genera, the majority of the probiotic bacteria under research are of the *Lactobacillus species* and *Bifodobacteria species* since they have the GRAS status and are going to be the probiotic bacteria under investigation and characterisation in this present study.

1.3.1. Lactic Acid Bacteria (LAB)

LAB are classified as Gram-positive non-spore forming bacteria which appear usually as rod-like or cocci in shape producing a major end-product (lactic acid) during the fermentation process where glucose is predominantly fermented to the lactate (lactic acid) ⁶⁹. They are anaerobes and can be found in the human digestive system although most of them are oxygen tolerant, growing and thriving whether in its absence and or presence and are dependent on complex nutrients and fermentable carbohydrates for active growth ⁷⁰. The fermentation process here, which brings about the lactic acid as the end product can occur through two pathways (the homolactic and heterolactic pathways). Bacteria species of the genera *Streptococcus*, *Lactococcus*, *Pediococcus*, *Enterococcus* as well as several *Lactobacillus* all generate energy needed for growth using the homolactic fermentation. This pathway is seen to be of great significance in the dairy sector where it is responsible for making sour milk, yoghurt, cheese and also other dairy goods ⁷¹. A wide range of these species are known to be used in preserving food and in fermenting meat products of various kinds ⁸. In this fermentation pathway, more than 95% of the end product (lactic acid) is produced from the sugar glucose.

Various *Lactobacillus* and *Leuconostoc* species can undergo heterolactic fermentation, with much importance laid on the latter especially during sauerkraut production and wine fermentation ^{72, 73}. Some strains of the former are also of particular importance in fermented milk used in the production of kefir drinks ⁷⁴. As opposed to homolactic fermentation, heterolactic fermentation results in the production of ethanol, carbon dioxide and lactic acid (lactate) which are the three catabolic outcomes of the pyruvate produced during glycolysis¹⁶.

As mentioned earlier, the polysaccharides of interest in this work are EPS and CPS and these can be classed into either being homopolysaccharides or heteropolysaccharides. When looking at the homopolysaccharides, those from different strains of LAB can be further subdivided into those having only glucose as its main building blocks (α -D-glucans, β -D-glucans) and those having only fructose as their building blocks (fructans) ³². The main homopolysaccharides produced by LAB have been compiled and are presented in table 1.2.

Table 1.2: Homopolysaccharide producing LAB

Subgroups	LAB Strains	Polysaccharide linkage units
α-D-glucans	<i>Leuconostoc mesenteroides</i> subsp. <i>Dextranicum</i> <i>Leuconostoc mesenteries</i> subsp. <i>mesenteroides</i>	α-1,6- linked D-glucose with usual branching at position 3, though may at times be at position 2 and 4 depending on the strain.
	<i>Streptococcus mutans</i> <i>Streptococcus sobrinus</i> <i>Leuconostoc mesenteries</i>	α-1,6-linked and α-1,3-linked D-glucose
β-D-glucans	<i>Pediococcus</i> spp. <i>Streptococcus</i> spp	β-1,3-linked D-glucose, with a branched β -1,2-Linkage
Fructans	<i>Streptococcus salivarius</i>	β-2,6-linked D-fructose with some branched β-1,2-linkage

As for heteropolysaccharide producing LAB species, they are grouped into either mesophilic or thermophilic strains depending on the temperature at which they grow best. Best growth for mesophilic strains ranges from 20 to 40 °C whilst thermophilic strain thrives best at temperatures higher than 40 °C and examples of these strains can be seen on table1.3.

Table 1.3: Heteropolysaccharide producing LAB

Subgroups	LAB Strains
Mesophilic strains	<i>Lactococcus lactis</i> subsp. <i>lactis</i> , <i>Lactococcus lactis</i> subsp. <i>cremoris</i> , <i>Lactobacillus casei</i> , <i>Lactobacillus sake</i> , <i>Lactobacillus rhamnosus</i>
Thermophilic strains	<i>Lactobacillus acidophilus</i> , <i>Lactobacillus delbrueckii</i> subsp. <i>bulgaricus</i> , <i>Lactobacillus helveticus</i> , <i>Streptococcus thermophilus</i>

Historically there has been considerable interest in the thermophilic strains as a result of the significant role played by their exopolysaccharides in the taste, texture and rheology of fermented products and milk drinks³².

1.3.2. *Lactobacillus* species

The genus *Lactobacillus* is known to be the most diverse of the LAB. The species predominantly found in dairy products include *Lactobacillus delbrueckii* ssp.

bulgaricus and *Lactobacillus helveticus*. Those which are common in the gastrointestinal tracts (GIT) in humans and animals *Lactobacillus acidophilus* and *Lactobacillus gasseri* and the species which are adaptable in various habitats include *L. plantarum*, *L. pentosus*, *L. brevis* and *L. paracasei*⁶⁹. This genus is a broad and heterogeneous group of Gram-positive bacteria which are essential as fermented include food starters in industrial applications and are also quite used as probiotics². For the LAB, lactic acid is the major end product for the fermentation process, as mentioned earlier, and as such they have historically been used in the fermentation and preservation of food and feeds^{70, 71}. *Lactobacillus paracasei* a strain of interest in the current work, is used extensively in dairy products as a starter culture as well as more recently in powder form as a probiotic. It is naturally found in the gut microbiota of humans and animals^{8, 73}. The ecological niches from where *L. paracasei* strains have been isolated include the human and animal gastrointestinal tracts and reproductive systems as well as in fermented products such as milk, cheese, sourdough bread starters and vegetables⁷². With probiotic effects being more strain-specific⁷⁴, the *L. paracasei* is frequently regarded as a preferred probiotic strain as it has beneficial technological properties and it has been reported to have health-promoting unique traits. *L. paracasei* DG and other strains of *L. paracasei*, which are specific, have been utilised as supplements in probiotic diets. Another strain of interest in this research is the *Lactobacillus salivarius* which has been reported to be isolated from various habitats such as the gastrointestinal tracts and oral cavity of humans, hamsters⁷⁵, swines,⁷⁶ birds (chicken)⁷⁷ as well as from human breast milk⁷⁸. This *L. salivarius* is a species of probiotic bacteria that has been found to exert therapeutic properties such as alleviation of irritable bowel syndrome⁷⁹, involved in the treatment of pancreatic necrosis, reversing the symptoms of atopic dermatitis in some children⁸⁰ as well as suppressing pathogenic bacteria hence promoting the host's well-being⁸¹.

Research has suggested that the consumption of these strains imparts health benefits. Health benefits which have been reported include improvement of ulcerative colitis⁸²; decreasing the side effects during eradication of *Helicobacter pylori*⁸³ and during treatment of bacteria overgrowth in the small intestines¹¹ as well as modulating Clostridiales in faeces and the level of butyrate in healthy individuals⁸⁴. Whilst these investigations have demonstrated the beneficial roles of Lactobacilli on the GIT and its microbiota^{84, 85} the molecular mechanisms by which the health benefits are achieved are unknown. However, both *in vivo* and *in vitro*

experiments have shown that the polysaccharides (capsular or exopolysaccharides) can play a part in generating health benefits such as stimulating the immune system^{9, 86}. These extracellular polysaccharides may also aid in attachment of probiotic bacteria to their surroundings where they can exert beneficial effects by alternative mechanisms including acting as a barrier to other pathogenic organisms^{87, 88}.

A wide range of health benefits have been associated with the consumption of probiotic and these include: anticancer⁸⁹, anti-hypercholesterolaemic (lowering levels of cholesterol in blood)^{90, 91}, antiulcer¹⁰ as well as immunocompetent effects^{92, 93}. Other health beneficial effects of LAB products include reduction of heart diseases, hypertension⁹⁴, hepatic encephalopathy⁹⁵, allergic reactions^{96, 97} and infection of the urogenital system⁹⁷.

1.3.3. Importance of LAB in the Food Industry and Some Health Benefits

In addition to the potential prebiotic effect of bacterial polysaccharides, their production is also of interest in food production where they can add texture to products and historically, LAB have been used in the food industry⁹⁸ for technological reasons. LAB used in the food industry include *Lactobacillus*, *Carnobacterium*, *Streptococcus*, *Aerococcus*, *Pediococcus*, *Lactococcus*, *Leuconostoc*, *Oenococcus*, *Weisella* and *Tetragenococcus*, with some capable of secreting EPS which is coupled with lactic acid production. These two traits are essential in the fermentation of dairy products like yoghurts, cheese and milk⁹⁹. EPS-producing bacteria are used when producing dairy products with an improvement of the viscosity and texture of yoghurts¹⁰⁰. Thermophilic LAB strains that produce slime generate products with increased viscosity and which are less vulnerable to syneresis (milk and yoghurts). The mesophilic LAB strains which are also slime-producing are also used in the production of fermented drinks¹⁰¹. During the production of cheese, especially that with a low-fat content, its rheological properties, visual appearance and flavour determines its quality and so introducing specific LAB as starter cultures can help maintain these properties¹⁰². According to Awad *et al* 2005¹⁰³, the EPS from *Lactobacillus lactis* spp. *cremoris* JFR1 was used as starter culture in the production of low-fat cheese with the rheological properties being maintained.

1.4. Bifidobacteria

In the 1900s Tissier discovered bifidobacteria in infant faeces by isolating a strange Y-shaped bacterium which he named *Bacillus bifidus*¹⁰⁴. Since the first discovery, more than 33 species of bifidobacteria have been determined belonging to the genus *Bifidobacterium* with 12

coming from the human gastrointestinal tract ¹⁰⁵ . In total more than 7000 different strains have being identified in various habitats ¹⁰⁴. The various habitats from which these *Bifidobacteria species* have been identified and recorded include the vagina, dental caries, sewage, human faeces and also the intestinal tracts of humans, animals and the honey bee¹⁰⁶. Those which are prevalent in the human intestinal tract include *B. longum*, *B. dentium*, *B. adolescentis*, *B. breve*, *B. pseudocatenulatum*, *B. catenulatum* and *B. angulatum* to name a few¹⁰⁷. Another strain also detected in the human gut is *B. animalis* subsp. *lactis* but this is known to originate from dairy products ¹⁰⁸.

Bifidobacteria are present in the microbiota of the intestinal tract of a wide variety of hosts ¹⁰⁹ and, like LAB, they are thought to manifest beneficial activities such as the reduction of intestinal disorders, modulation of the immune system, reduction of blood cholesterol as well as possessing anti-mutagenic and anti-carcinogenic ¹¹⁰ activity. Again it is believed that these bifidobacteria contain cell surface components, some of which are polysaccharides, which contribute to their biological activity ¹¹⁰.

The infant intestines are presumed to be sterile at birth but just after birth, there is rapid colonisation by bacteria such as the *Bifidobacterium infantis* subsp. *infantis*, *B. bifidum* and *B. breve* ¹⁰⁹. The *B. breve* is one of the bacteria, which will be used in this research as it is known to be one of the most useful probiotics in the human intestinal tract serving other regulatory and digestive functions as earlier mentioned in addition to its primary functions such sugar fermentation, lactic acid and acetic production. There has been of recent, a significant increase of interest to the *Bifidobacteria species* due to the health benefits they manifest while in the gut microbiota^{111, 112} where these researchers are particularly focusing on the interaction between the produced exopolysaccharides and the intestinal epithelial cell to bring about this biological activity^{113, 114}. Despite the benefits of this bacterial exopolysaccharides, very little exploitation has been carried out in regard to their structures. *Bifidobacteria species* are very sensitive to oxygen and are known to be very strict anaerobes ^{115, 116} which require complex growth medium hence bringing about the difficulties encountered in culturing these bacteria. This further gives one of the reasons why very few structures of these bacteria have been characterised and so there is a need to exploit more of these bacteria of the genus Bifidobacteria which in this work we will be

looking at the *Bifidobacteria breve*. Given that bacteria are known to produce polysaccharides which could be either loosely surrounding their cell wall or strongly attached to their cell wall, the hypothesis will be to show that this bacteria can secrete both of these polysaccharides in addition to determining their chemical structures.

There exist an association between Bifidobacteria and LAB and this is not surprising given that they both are found in the in same habitat such as the gastrointestinal tracts of animals and humans but they differ in various ways. The chromosomal G+C content (42-67%) of the Bifidobacteria is higher than those of LAB¹¹⁷. Another difference between these two is the different ways in which they ferment sugars; Bifidobacteria metabolise sugars using the “bifid shunt” (a unique metabolic pathway) to generate lactate and acetate as end products ¹¹⁸. Initially in this bifidobacterial heterolactic pathway, there is phosphorylation of two glucose sugar units to yield 2 fructose-6-phosphates. Despite these differences , there are similarities in the genes responsible for polysaccharide production especially in the eps-cluster in Bifidobacteria and those of LAB⁸ which also indicates the occurrence of two pathways for the EPS synthesis hence resulting to more than one polymer production¹¹⁹.

1.4.1. Beneficial Effects of Bifidobacteria

In the last decade, there has been a sharp increase in the development of fermented products such as milk and yoghurt using strains of bifidobacteria starter cultures which have the GRAS status^{120, 121}. It has also been suggested that bifidobacteria can survive in the gastrointestinal tract (GIT) in sufficient numbers¹²² as well as being able to adhere to the mucus lining of these tracts such that they can be considered probiotics¹²³. There are several health benefits which have been attributed to bifidobacteria found in the GIT and these include preventing diarrhoea which can be extremely dangerous to infants in developing and underdeveloped world¹²⁴, relieving lactose intolerance¹²⁵ and fighting against pathogenic bacteria as a result of their antimicrobial activities^{126, 127}. In addition to these, other health benefits assigned to bifidobacteria include their involvement in improving the immune system and stimulating antibody production ¹²⁸⁻¹³⁰. Their possession of properties which are anti-carcinogenic and anti-mutagenic are essential in cancer chemotherapy¹³¹. Much research has suggested that many of these health benefits have been associated with their ability to produce exopolysaccharides ^{12, 132}. The WHO/FAO uses all the above properties in order to choose, evaluate and classify the bacteria under study as being probiotics¹³³.

1.5. Capsular (CPS) and Exopolysaccharides (EPS)

As stated above, LAB and Bifidobacteria both have the capacity for the synthesis of EPS, which are secreted into their immediate surroundings. The terms 'ropy' or 'slime-forming' are often used to refer to EPS production while the term 'mucoïd' is often used to describe capsular extracellular polysaccharides¹³⁴. Both EPS and CPSs are made of repeated oligosaccharide units which are composed either of one type of monosaccharide (homopolysaccharide) or from a small number of different types of monosaccharides (heteropolysaccharides). The oligosaccharide units normally contain between three and eight monosaccharides with the monosaccharides being linked by a variety of different linkage types. The repeating units are synthesised at the cell membrane and then polymerised. EPS are then excreted whilst CPS are bonded to the peptidoglycan. The molecular weight, chemical structure, types of linkages of the polysaccharides will influence their functionality.

If the CPS and EPS are to be used in technological applications and as potential therapeutic agents, more information regarding the relationship between the structure and their function is needed

1.5.1. Biosynthesis of Exopolysaccharides

There are more than one biosynthetic pathway by which EPS and CPS can be synthesised. Polysaccharides can be synthesised extracellular using excreted enzymes and this is frequently the method that is employed by bacteria to produce homopolysaccharides (*Fig 1.11d*). In the extracellular synthetic pathway, the glycosyltransferase enzyme (sucrase) is used to synthesize the polysaccharides (homopolysaccharides)^{135, 136}.

A second approach is to build the polysaccharide at the cell membrane using intracellular enzymes and activated sugar donors. This route is used in the synthesis of the majority of heteropolysaccharides^{137, 138}. A variety of pathways can be used in the production of heteropolysaccharides including sequential or an *en bloc* mechanism: the *en bloc* mechanism is referred to as the Wzy-dependent pathway and the two sequential types are the ATP-binding ABC transporter-dependent pathway and synthase-dependent pathway (*Fig 11*).

In the Wzy-dependent pathway, the synthesis starts in the cytoplasm and can be broken into three distinct steps, which includes substrate uptake, the synthesis of activated sugar

precursors, the assembling of the repeat unit/polymer coupled to its transport to the surface of the bacteria (Fig 1.11).

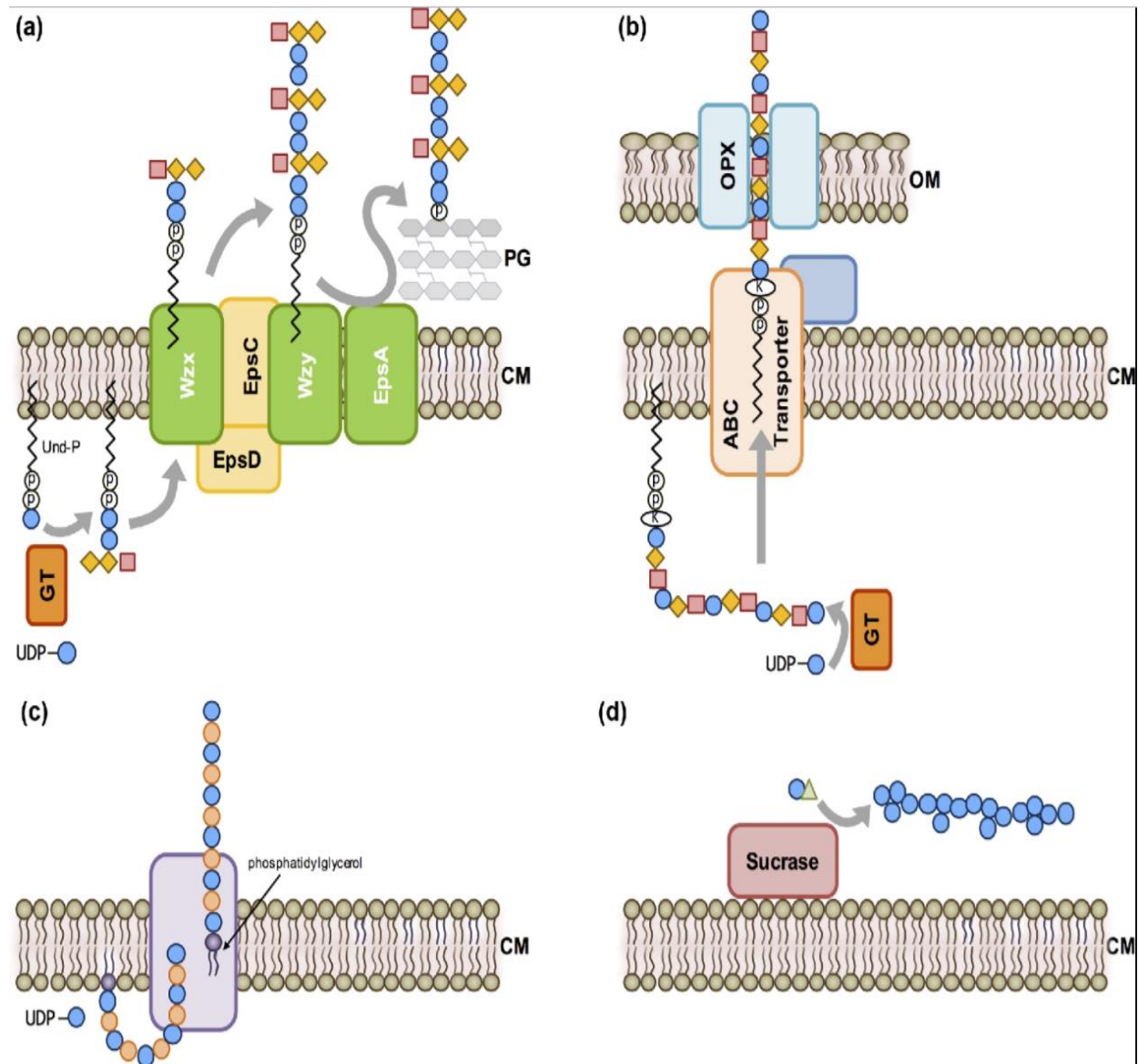


Figure 1.11. Bacterial Polysaccharides synthesis Pathways as modelled by Zeidan *et al* 2017¹³⁹ (a) the *en bloc* pathway (Wzy-dependent pathway) represented for Gram-positive bacteria. (b) ABC transporter-dependent pathway represented for Gram-negative bacteria. (c) Synthase-dependent pathway. (d) Extracellular synthesis pathway.

Keys for figure 1.11: Glucose (blue circle); galactose (yellow diamonds); rhamnose (pink squares); fructose (green triangle); cytoplasmic membrane (CM); outer membrane (OM);

peptidoglycan (PG); glycosyltransferase (GT); undecaprenylphosphate (Und-P); phosphate (P); poly-2-keto-3-deoxyoctulosonic acid linker (K).

Sugar uptake is the first step in the process of EPS biosynthesis. The substrate type determines the mechanism of its uptake (which can be through an active or passive transport system). One of the most common transport systems was described by Postma *et al* (1993)¹⁴⁰ who showed the phosphoenolpyruvate-sugar phosphotransferase system (PEP-PTS) to be a protein complex through which the substrate is actively transported into the bacterial cytoplasm. Once the substrate (e.g glucose) gets into the cytoplasm, a hexokinase enzyme converts the glucose into glucose-6-phosphate (Glc-6-P) through phosphorylation. Subsequently, a phosphoglucomutase (PGM) converts this Glu-6-P into glucose-1-phosphate (Glc-1-P) which is further catalysed by the enzyme uridine diphosphate-glucose pyrophosphorylase (UDP-Glc pyrophosphorylase) to produce the activated sugar nucleotide uridine diphosphate glucose (UDP-Glc) (*Fig 1.12*).

The next step is the formation of the basic repeat unit which is initiated when a phosphorylated isoprenoid alcohol (glycosyl carrier lipid) which is anchored in the cell membrane accepts the first activated sugar nucleotides which occurs under the influence of a priming glycosyl transferase enzymes (GTFs) found in the bacterial cell membrane (*Fig 1.12*). This leads to a sugar linked to the lipid anchor by a phosphodiester link and subsequently a range of GTFs sequential adds monosaccharides units until the repeating unit is formed on the inner face of the membrane.

The last step of the EPS biosynthesis that takes place in the cytoplasm involves the transport of the repeating unit across the membrane which is catalysed by a Wzx flippase and which is then polymerised by a Wzy polymerase (*Fig 1.11*).

As earlier mentioned after the synthesis of the polysaccharides in the cytoplasm of the bacteria, it is then exported to the outer environment of the cell through various mechanisms which will be discussed here. A sequential or an *en bloc* mechanism can be used in the production of bacterial polysaccharide by using one of these four different types which include the *en bloc* type (Wzy-dependent pathway, the two sequential types (the ATP-binding ABC transporter-dependent and synthase-dependent pathway) and then the extracellular synthesis using the enzyme sucrose¹³⁹ *Fig 1.11*.

In the sequential ATP-binding ABC transporter-dependent pathway the glycosyltransferases (GTs) plays a role in assembling the chain of polysaccharides linked to a poly-2-keto-3-deoxyoctulosonic acid in the inner membrane. The ABC transporters of the inner membrane and the periplasmic proteins of the OPX family in the outer membrane forms a complex efflux pump through which the completed polysaccharide is transported (*Fig 1.11b*).

In the sequential dependent pathway, the single synthase complex transportation and polymerization takes place from where the completed polysaccharide units are secreted across the membranes and the cell walls (*Fig 1.11b*).

From all the pathways listed above, two or more of them can take place in one bacterial species during the production of different polysaccharides molecules¹³⁹.

Until now, the Wzy-dependent pathway and the extracellular GT pathway have been described for polysaccharide production by lactic acid bacteria^{145, 146}. The extracellular GT

pathway is seen as the simplest biochemical route^{147, 148}. In contrast, the Wzy-dependent pathway used for biosynthesis of polysaccharides is seen as a complex process and one which is used to generate other cell wall polysaccharides¹⁴⁹ including CPS and EPS production in both Gram-negative and Gram-positive bacteria^{135, 136}. Generally, LAB use the Wzy-dependent pathway to produce exocellular polysaccharides that are made up of repeating monomeric units containing between 3 to 8 monosaccharides^{142, 143}. Galactose, rhamnose and glucose are the sugar moieties that are represented most often but the *N*-acetylglucosamine and *N*-acetylgalactosamine (acetylated sugars) are also present in some polysaccharides. In addition to this, there has been occasional presence of some sugar derivatives such as ribose, mannose, fucose, glucuronic acid and *N*-acetylmannosamine in the repeating units of the heteropolysaccharides of LAB¹⁵⁰⁻¹⁵².

The assembly and polymerisation occurring in the cell membrane have been mostly studied in pathogenic streptococci (especially in *S. pneumoniae* where capsules are synthesized) to show the steps involved in this biosynthetic pathway^{153, 154} but its characterisation in LAB is poor and few studies are described in the literature^{155, 156}.

1.5.2. Production and Isolation of Exopolysaccharides

EPS production capability varies widely according to the different bacteria and the EPS that are produced are known to possess different functions as well as structures^{55, 57}. The 'ropy' nature of the EPS is the initial test to determine the EPS producing ability of a bacterial strain which is performed by using an inoculation loop in extending a bacteria colony on a cultured plate and examining the formation of a long filament⁴⁹. In the case of where the bacteria are cultured in a liquid broth, its ropy nature can be revealed by the high flow resistance when pushed through serological pipettes and also by the formation of strands that are viscous when free fall occurs from the tip of the pipette¹⁵⁷.

1.5.2.1. Production of Exopolysaccharides (EPS)

Several bacteria have been found to secrete viscous polymers which are sticky to its external cell envelop known as the glycocalyx layer composed of the polysaccharides and peptides. This glycocalyx could be firmly or loosely attached to the cell wall forming a capsule layer or slim layer respectively¹⁵⁸. The production of extracellular substances of bacteria under certain conditions are for a purpose where in the case of pathogenic species these substances play a role in protecting them against the action of phagocytosis from host cell

response¹⁵⁹ though in some cases these extracellular substances contribute to their virulence¹⁶⁰. During biofilm formation, the glycocalyx is a very important component which aids the bacteria adhere to the immediate surroundings as well as to each other facilitating communication between them as they strive to survive⁶⁶. Biofilms are referred to as complex multicellular structures formed by bacteria which occur normally in four main stages (surface attachment, formation of microcolony, maturation of the biofilm and detachment of the bacteria which may invade new environment¹⁶¹⁻¹⁶³. Bacteria all covered with a biofilm exhibit a dormant growth phase thereby resisting the environmental stress exceptionally especially the effects of antibiotics¹⁶⁴. Vuong *et al* (2005)¹⁶⁰, reported the biofilms to play a major role in so many serious bacterial infections with the exopolysaccharides seen to be involved critically in the biofilm formation although with limited information regarding its biosynthesis. The bulk culture possibility of bacterial polysaccharides produced has made it gain a lot importance in the past years and despite the lack of clarity in regards to their physiological role, they are known to be very useful in processes such as pathogenicity, protection from harsh environments, formation of biofilm and quorum sensing^{165, 166}. Previous studies on bacterial EPSs of the common probiotic have indicated that the differences in their texturizing properties is responsible for their large structural diversity^{167, 168}. The adhering ability of the probiotics to the intestinal mucosa is one of its selection criteria which permits the intestinal tract to be colonized thereby competing with other microorganisms in mucoadhesion^{86, 169}.

Bacteria that generate homopolysaccharide can produce large amounts of material reaching tens of grams per litre. These tend to employ the enzyme dextran-sucrase and they also rely on sucrose being present in sufficient amounts with large yields being observed when optimal growth conditions are present. On the other hand, the heterosaccharide producing bacteria, including LAB and bifidobacteria, produce significantly smaller amounts of polysaccharides and the yields are normally ranging from 20 – 600 mg/L. The yields of heteropolysaccharides are also often influenced by the growth conditions used¹⁷⁰. Another factor which influences how much polysaccharide is produced is the period for incubation^{49, 134, 171}. A lot of research work, especially studies that have focused on improving conditions for growth, has been carried out to increase the yield of EPS with much of this work carried out on species such as *Streptococcus thermophilus* and *Lactobacillus delbrueckii* spp *bulgaricus*¹⁷²⁻¹⁷⁴. Bifidobacteria are strictly anaerobes, and as such, the EPS yield can be affected by the anaerobic conditions

¹⁷³. Generally, factors that have been found to affect yield of EPS include temperature, pH and oxygen concentration (growth conditions) as well as the media culture with its carbon source and other nutrients. There exist several media in which bacteria can be cultured such as MRS agar broth and CDM (chemically defined media) with all of them being supplemented with either one or a combination of various carbon sources including glucose, galactose, fructose, lactose and sucrose. The correct choice of media influences not only the amounts of EPS that is produced but also influences the analysis and quantification of the EPS. Analysis and quantification is frequently complicated by the inclusion of material as media components, which interfere with the analysis ⁴⁹. Bacterial growth and EPS synthesis require an optimal pH for the best yields of the EPS. During fermentation, the pH can be either controlled systematically through addition of base to maintain a constant level or the pH can be allowed to decrease on its own. EPS production seems to be growth associated with its maximum yield taking place during exponential growth and towards the end of this phase¹⁷⁵. It has been found that the longer fermentation periods have a negative impact on the amount of EPS produced and degradation of the EPS has been reported in the stationary and death phase. This degradation is suggested to be caused by the action of glycosyl-hydrolases as well as physiological changes of the cell environment ¹⁷⁶. There have been reports that when fermentation conditions are varied, specific strains of bacteria can generate two or more EPS with different molecular weights and with same or with different chemical composition ¹⁷⁷

1.5.2.2. Exopolysaccharide Isolation

During the synthesis of EPS, a full description of the content of the media used in the fermentation is essential for the determination of the methods required for its isolation and purification⁴⁹. The isolation process is also known to have an impact on the yield of EPS. A number of these established methods exist for extracting EPS and most start with the removal of proteins by either using the enzyme proteinase K or by precipitating proteins on addition of trichloroacetic acid ^{178, 179}. Once the culture media has been treated with either proteinase K or with TCA (14% w/v) the cells and precipitated proteins are removed by centrifugation. The carbohydrate present in solution are then precipitated by adding either acetone^{180, 181} or chilled absolute ethanol¹⁸²⁻¹⁸⁴ (more common now) and the solution is stored at 4 °C for 24 hours to recover maximum yields. The EPS recovered by centrifugation is reconstituted in a minimum amount of deionised water and the free monosaccharides are removed by dialysis

as well as the small proteins and salts that are still left. After dialysis, the solution is freeze-dried to give the solid EPS. The recovered polysaccharides can be further purified by either anion exchange or size exclusion chromatography if required.

1.6. Exopolysaccharide Characterisation.

The analytical methods used to determine the structures of the repeat unit of exopolysaccharides and capsular polysaccharides are very varied and include classical wet chemical methods that generate small molecules whose identity can be subsequently determined by GC-MS. These methods were originally developed in the 1950s and many have been continuously updated. The classical methods that are routinely applied to the characterisation of repeat unit structures include monomer analysis, linkage analysis and absolute sugar determination. In current research programmes, the data generated from GC-MS studies of small molecules is supplemented with the results generated from undertaking a range of 1D and 2D-NMR spectroscopy experiments. These give complementary data allowing the structures to be determined with a high degree of confidence.

1.6.1. Determining the Purity of Polysaccharides and Analysis of Crude Fermentation Products.

The extracts that are isolated from fermentations are frequently heterogeneous materials, so determining their content is important, and frequently this requires measurement of the amount of carbohydrates, proteins and nucleic acids that are present. Dubois *et al* (1956)¹⁸⁵ first reported the phenol-sulphuric assay test for determining the carbohydrate content of crude samples which is now the most common method used. The analysis in the Dubois method is dependent on the observation of furan derivatives formed from the reactions of carbohydrates reacting with strong acid under heat¹⁸⁶. When acidified phenol (5%) is added, a yellow complex is formed which are furan derivatives which absorb at 490 nm wavelength and is measured using a UV-Vis spectrophotometry^{185, 187}. A calibration curve for a range of concentrations of a sugar standard is constructed and used for the quantification of the carbohydrate content. This phenol-sulphuric assay only gives an approximate quantification of the carbohydrate present. The protein and nucleic acid content of the extracts recovered from fermentations can be determined by comparing the UV absorption of samples at 280 and 260 nm respectively—see section on SEC-MALLS that will be discussed later.

1.7. Classical Wet Chemical Analytical Methods

1.7.1. Monomer Analysis of Carbohydrates by Gas Chromatography Mass Spectrometry (GC-MS)

A number of different methods have been developed to determine the monosaccharide composition of polysaccharides but the procedure most commonly employed involves the preparation of alditol acetates. The alditol acetate method was originally introduced by Gunner *et al* (1961)¹⁸⁸ and has advantages over other derivatisation methods in that a single alditol acetate is formed for each monosaccharide. There has been continuous development and revision of the monomer analysis method over the years but that developed by Albersheim *et al* (1967)¹⁸⁹ and Blake *et al* (1970)¹⁹⁰ is the most commonly used modernised method (Fig. 1.13).

Other methods for the analysis of monomers including the formation of silyl ethers generate mixtures of anomers and this can lead to complex chromatograms if significant numbers of different types of monosaccharides are present. The alditol acetate method is a four step process which includes the acid catalysed hydrolysis of the polysaccharide to its constituent monosaccharides, the reduction of the aldose/ketoses to the corresponding alditols, the acetylation of the alditols to generate alditol acetates and finally, the analysis of the alditol acetates.

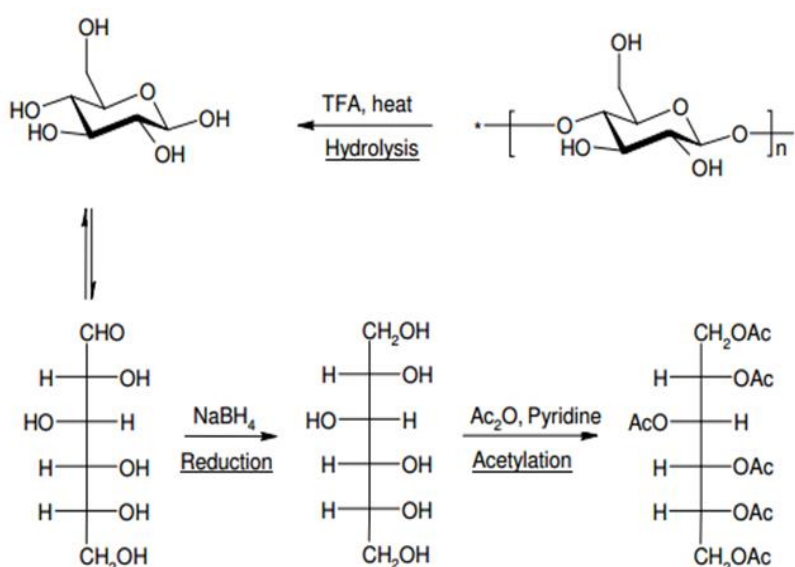


Figure 1.13. Conventional Preparation of Alditol Acetates

The first step in the process is the acid catalysed hydrolysis of the polysaccharides. Over the years, a lot of work has been done to optimise this step and this has been driven by the fact that the product monosaccharides are frequently unstable in acidic solution and degrade. In the past either hydrochloric acid ¹⁹¹ or sulphuric acid ¹⁹² were used as acids but both have their issues most notably with degradation of the sugars during the steps used to remove the acid. In our laboratories at the University of Huddersfield trifluoroacetic acid is used as the acid of choice as it is relatively volatile and can be removed without any neutralisation step being required and at relatively low temperatures (40 °C) without significant degradation of the monosaccharides. Trifluoroacetic acid was introduced by Fengel and Wegner(1979) ¹⁹³ for the rapid analysis of the monosaccharides present in wood pulp. The second step involves the reduction of the carbonyl group to generate an alditol and almost all research groups use sodium borohydride in aqueous solution to achieve this. Sodium borodeuteride is used at the University of Huddersfield as this makes it possible to identify the location of the carbonyl and allows the reducing end of symmetrical alditols, formed from some ketoses, to be determined. Once the reduction has been undertaken it is necessary to remove borate complexes formed during the reduction step. The borate complexes are removed by repeatedly adding methanol and acid and evaporating away any tetramethylborate that is formed. If this process is not undertaken, then the acetylation step that follows is slow or is totally inhibited. Unfortunately, the repeated evaporation takes a significant amount of time to complete. The final derivatisation step is to acetylate the alditol and this is normally achieved using acetic anhydride in the presence of a base catalyst, with sodium acetate and pyridine being popular choices. It is important to ensure that the sample is completely dry before the acetylation step is achieved however, if methylimidazole is used as a catalyst then the reaction can be performed with small amounts of water present¹⁹⁴. Once the alditol acetates are prepared, they can then be analysed by GC-MS and the different alditol acetates are relatively easy to separate on a capillary GC-column.

Whilst the alditol acetate method is a robust procedure for determination of neutral monosaccharides it does have to be performed carefully and, even then, it is not universally applicable. There are a number of issues with the method and these include: the need for additional derivatisation steps for acidic sugars, difficulties have been reported with the analysis of amino sugars, for polysaccharides decorated with alditols it is not possible to

differentiate between alditols generated from monosaccharides and the decoration, finally the process takes some considerable time to complete the four different steps.

1.7.2. High Performance Anion Exchange Chromatography with Pulsed-Amperometric Detection (HPAEC-PAD) Analysis of Carbohydrates

Rocklin and Pohl (1983)¹⁹⁵ first introduced the analysis of carbohydrates using the HPAEC-PAD where its applications and effectiveness have been reviewed in the works of Lee (1990)¹⁹⁶ and Cataldi *et al* (2000)¹⁹⁷. In the last couple of decades, the technique has increased in popularity and is now challenging the classical GC-MS experiments as the method of choice for determining the monosaccharide content of polysaccharides and this is especially true when only small amounts of material are available. At high pH (pHs above 13) most monosaccharides are partially ionised and the resulting anions can be separated using anion exchange chromatography. The degree of ionisation of a particular monosaccharide depends on the relative arrangement of hydroxyl groups within the molecules and this influences their dissociation constants (Table 1.3). The pKa examination of these listed neutral monosaccharides confirms the fact that they are weak acids¹⁹⁸. Monosaccharides, which are more acidic, are retained longer on an anion exchange column. A number of researchers have used HPAEC to separate complex mixtures of monosaccharides: Currie and Perry have used HPAEC¹⁹⁹ to separate neutral and acidic monosaccharides from plant cell walls and Cataldi *et al* (2000)¹⁹⁷ have used the same system to separate a range of monosaccharides including amino sugars. The advantage of the techniques is that a wide range of monosaccharides, including cationic and anionic sugars, can be analysed directly without the need for derivatisation steps. This reduces dramatically the time taken to determine the monomer composition of a polysaccharide. A second advantage of the techniques is that the anion chromatography can be coupled to a pulsed amperometric detector (PAD). In a pulsed amperometric detector the effluent from the column passes across the face of a gold electrode whose surface charge is continually changing. Redox active substrates can be oxidized or reduced on the surface of the working electrode and the current used in the redox process is used to monitor the concentration of an analyte. PAD detectors are especially sensitive for monosaccharides which can be reduced on the electrode surface and sub-ppm levels of monosaccharides can be detected²⁰⁰. Under standard conditions, individual monosaccharides can be base-line resolved using HPAEC (*Fig 1.14*). However, some care must

be taken in identifying the monosaccharides present by using only retention time data that is collected. Typically, sodium hydroxide (NaOH) is the mobile phase of choice and is used with either a gradient or an isocratic elution mode but when strong anions are present which require a mobile phase with a greater ionic strength before they elute, sodium acetate is added to the mobile phase with higher concentrations of sodium hydroxide. According to Xie *et al.* 2013²⁰¹ who investigated the separation of monosaccharides using varied concentrations on NaOH (2.5, 5.0, 7.5, 10.0, 12.5 and 25.0 mM) found that at higher concentrations of (25mM), the peaks eluted faster and were larger as compared with those of a lower concentration with 12.2mM NaOH giving the best resolution and highest efficiency in terms of separation (*Fig 1.14*). The retention times of analytes can vary considerably from day to day as carbonate impurities in either the analytes or in the mobile phases reduce the exchange capacity of the columns. For accurate results, it is necessary to frequently strip columns of strongly binding anions during regeneration steps.

Table1.3: Some Common Carbohydrates with their Dissociation Constants in Water according to Rohrer (2012)¹⁹⁸.

Sugars	pKa at 25 °C
Fructose	12.03
Mannose	12.08
Xylose	12.15
Glucose	12.28
Galactose	13.39
Dulcitol	13.43
Sorbitol	13.60
A-Methyl gluoside	13.71

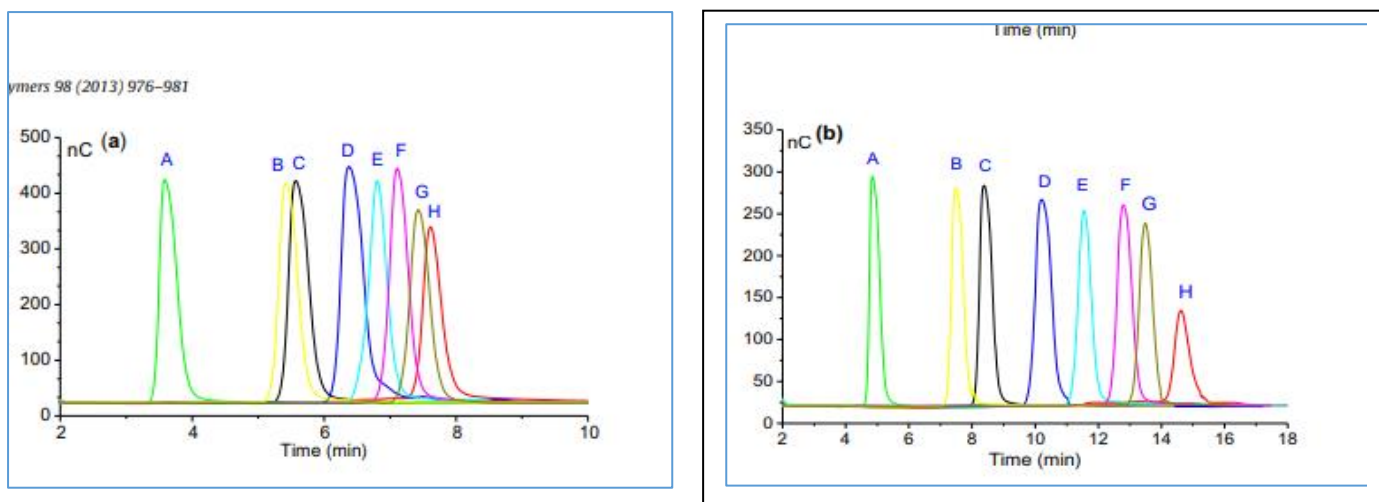


Figure 1.14. HPAEC-PAD chromatogram profiles of standard monosaccharide mixture solution²⁰¹ (a) NaOH concentration of 25.0mM. (b) NaOH concentration of 12.5mM. (Peak identity: A, Fucose: B, Rhamnose: C, Rhamnose: D, Galactose: E, Glucose: F, Mannose: G, Xylose: H, Fructose).

1.7.3. Linkage Analysis

Each monomer in a polysaccharide repeating unit can be linked differently to one another, this linkage pattern can be determined following the same procedures as for monomer analysis but prior to hydrolysis, there is the methylation of all the unsubstituted hydroxyl groups. Stellner *et al.* (1973)²⁰² developed the method which is commonly used in determining the type of linkage found in a polysaccharide repeating unit. Initially the methylation steps has been reviewed through several findings with the first being the works of Purdie and Irvine (1903)²⁰³ who treated polysaccharides in methanol with methyl iodide (MeI) and silver oxide to give the *O*-methylated polysaccharides. Denham and Woodhouse (1913)²⁰⁴ later revised this method by using the combination of dimethyl sulphate and sodium hydroxide to treat the carbohydrate in solution. In 1915, Howarth then employed the method, which involved the mixture of sodium hydroxide and methyl sulphate²⁰⁵. The above methods were used 50 years onwards with very little modifications to them until the development of the Hakomori method in 1964, where the per-*O*-methylated polysaccharides involved one step which was the addition of sodium methylsulphonyl carbanion solution containing dimethyl ions to a mixture of the MeI and the polysaccharide in dimethylsulfoxide (DMSO)²⁰⁶. All the above methods were being further revised and developed to avoid undermethylation²⁰⁷. The main purpose of this methylation step is ensuring all the free

hydroxyl groups of the carbohydrate (polysaccharides) are converted to methoxy groups before being hydrolysed. After hydrolysing the methylated polysaccharide using TFA into their monosaccharide units, the methylated monomer units are reduced to alditols using sodium borodeuteride (NaBD_4) and the resulting product is finally acetylated with acetic anhydride catalysed with pyridine (Fig 1.15).

The first procedure is often attributed to Hakamori²⁰⁶ whilst the latter was developed by Ciucani and Kerek²⁰⁸. The advantage of using solid sodium hydroxide in a heterogenous system is that any residual moisture present in the carbohydrate is absorbed by the hydroscopic base and doesn't interfere with the methylation step.

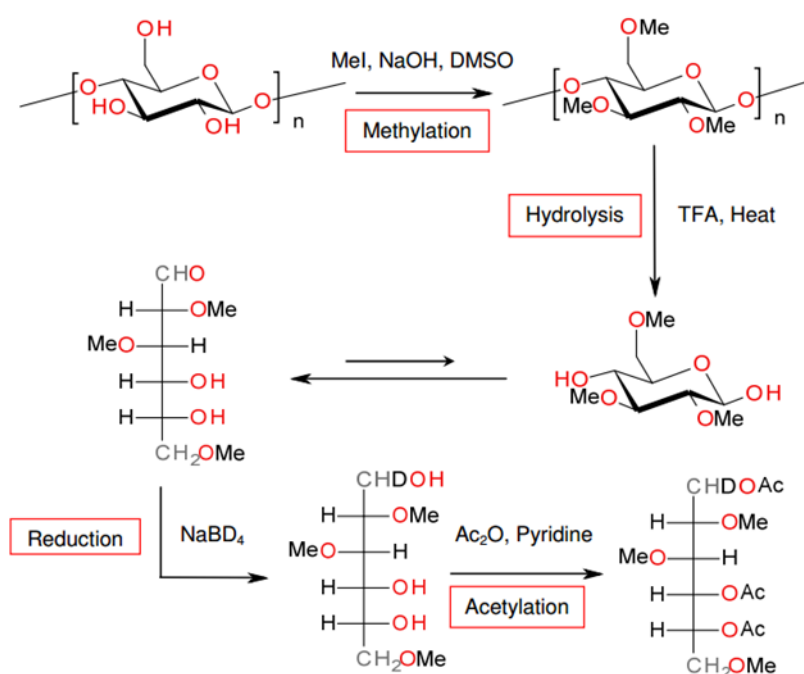


Figure 1.15. Schematic Representation of Linkage Analysis

The disadvantage of the method is that it is very time consuming and the large numbers of steps means that it is difficult to get reproducible results with sub-milligram quantities of polysaccharides.

1.7.4. Absolute Configuration Analysis of EPS

The method used to determine the absolute configuration of monosaccharides was introduced by Gerwig *et al.* (1978)²⁰⁹ and involves hydrolysis of the polysaccharide followed

by butanolization and acetylation using (S)-(+)-2-butanol to give the acetylated butyl glycosides as their α and β -anomers. The diastereoisomer formed because of the linkage between the secondary alcohol and the chiral centre of the glycosidic oxygen are separated by GC-MS. The steps involved will be further discussed later in the experimental section.

1.7.5. Nuclear Magnetic Resonance (NMR) Analysis

In polysaccharides, increasingly a lot of information about their structures is being determined through the use of NMR spectroscopy and the data generated is complimentary to that which is produced by the GC-MS methods described above. Information about the primary structure (the monosaccharides present), the secondary structure (how the monosaccharides are linked) and the tertiary structures (the 3D-arrangement of groups) of carbohydrate molecules can be determined using 1D and 2D NMR techniques²¹⁰. Both ^{13}C and ^1H -NMR are routinely used in characterising carbohydrates and less frequently other nuclei have also been employed including ^2H , ^{15}N , ^{17}O & ^{31}P ²¹¹⁻²¹³. The ^1H -NMR spectra obtained can be divided into three distinct regions: the anomeric region, the ring proton region and the reporter region. The anomeric region occurs between 4.4 to 5.5 ppm having the anomeric protons²¹⁴. The ring proton region located between 4.3 to 3.0 ppm contains the remaining protons of the ring. The reporter region below 3 ppm has signals, which identify the presence of deoxy-sugars, acetate groups, and pyruvate groups, all of which are found in polysaccharides. The anomeric signals are usually found in this lower field region distinct from the rest of the ring protons because of their location close to the electronegative oxygen, which has an electron withdrawing impact on this anomeric proton making it deshielded²¹⁵.

NMR spectroscopy was first used in determining the repeating unit structure of an EPS produced by *Streptococcus thermophilus* by Doco *et al* (1990)²¹⁶ which then paved the way for other researchers to use the 1D and 2D-NMR for structural determination of exopolysaccharides.

The most significant information that can be extracted from the anomeric region of the proton NMR is an indication of the number of monosaccharides in the repeat unit and their anomeric configuration. Normally, a pure polysaccharide will have single anomeric resonances for each of the different monosaccharides present and these frequently occur as broad singlets or as doublets with coupling to the neighbouring ring proton (H2), being visible

and they should have integrals with approximately whole number ratios. The anomeric configuration of sugars can be determined from the coupling constant i.e. the size of the 3J coupling constants of the anomeric proton $^3J_{1,2}$. The relationship between dihedral angle and $^3J_{1,2}$ coupling constants with values obtained from the Karplus curve as described by Tafazzoli and Ghiasi (2007)²¹⁷, applies that the $^3J_{1,2}$ coupling constant below 4 Hz corresponds to an α -anomeric configuration and when it is greater than 7.5 Hz a β -anomeric configuration is assigned. This rule is applicable only for monosaccharides which adopt the carbon 4C_1 chair conformation with the proton on the carbon 2 located in an axial position (Fig 1.16).

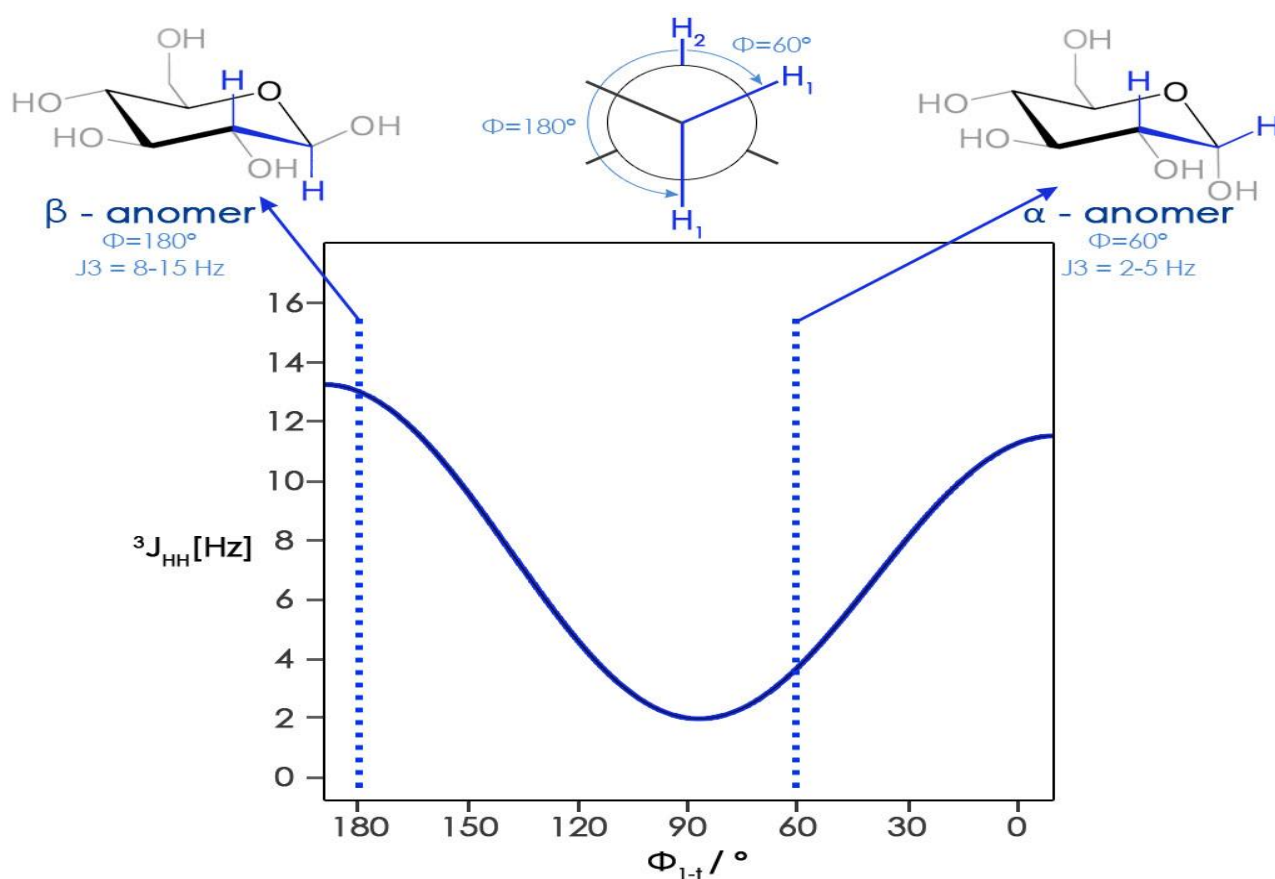


Figure 1.16. Newman Projection at top with Karplus Curve Demonstrating the Dihedral Angle-Coupling Relationship

Normally the ring proton region is congested and as such not much information can be extracted from this region of a $^1\text{H-NMR}$ spectrum. In contrast, the reporter region below 3 ppm gives significant information about the monosaccharides that are present and the decoration of these monosaccharides. The presence of sharp singlets integrating to multiples

of 3-protons centred around 2 ppm are normally associated with the presence of acetyl groups which can either be part of an N-Acetyl aminosugar or they are frequently present as substituents on the ring hydroxyl-groups. The presence of doublet peaks at approximately 1.5 ppm often identifies the presence of pyruvate decoration or lactate decoration of hydroxyl groups whilst doublets appearing at higher field, closer to 1.4-1.3 ppm, are indicative of the methyl groups of deoxy sugars rhamnose and fucose.

Additional information can be obtained from a carbon spectrum. The carbons present in a carbohydrate can have one, two or three hydrogen atoms (-CH, -CH₂ and -CH₃) attached which can be identified using by recording DEPT (Distortionless Enhancement by Polarization Transfer) spectra and specifically DEPT135 ¹³C-NMR experiment where the -CH₃ and -CH signals are seen to be positive peaks whereas the -CH₂ is a negative signal. The carbons C2-C5 usually have -CH and their signals generally occur between 65 to 85 ppm but if they have other substituents other than -OH such as amino or methyl groups, their signals will occur at a lower chemical shift. The location of the carbon C1 signals are generally between 95-105 ppm as a result of the electron withdrawing oxygen which are adjacent in the heterocyclic ring. In hexoses carbon C6 is a -CH₂, which generates a negative signal occurring between 60 to 70 ppm. In the case of any -CH₃ group present such as in a deoxy sugar such as rhamnose and fucose, the positive signal occurs at a lower ppm (20 ppm).

The 2D-NMR analysis in combination with 1D-NMR can be used to track the linkage between monosaccharides units, which then aids in determining the structure of the repeating oligosaccharide unit. Structural determination of these oligosaccharides repeating units of EPSs can be performed using the following 2D-experiments;

- 2D-COSY - Two Dimensional COrelated SpectroscopY; It is one which permits the proton resonances that are mutually coupled to be seen²¹⁸. This 2D is still one of the most sequences common used to date since it was first described in 1971 by Jeener²¹⁹.
- 2D-TOCSY - Two Dimensional Total COrelation SpectroscopY; It is quite similar to COSY, however, the observed cross peaks are not only for those mutually coupled but also between those with couplings which are connected in a chain²¹⁸.

- 2D–HSQC - Two Dimensional Heteronuclear Single Quantum Coherence (coupled and uncoupled); It is one where the correlations that exist between two different types of nuclei separated by a bond are detected. It is a highly sensitive 2D-NMR that can be used in a ^1H - ^{15}N system for protein NMR experiments as well as in ^1H - ^{13}C system²¹⁸.

- 2D–HMBC - Two Dimensional Heteronuclear Multiple Bond COrrrelation; It is one where the correlations between the different nuclei over ranges having about 2 to 4 bonds can be detected. This 2D-NMR is often used for quaternary and carbonyl carbons assignment.

- 2D–HSQC–TOCSY - Two Dimensional Heteronuclear Single Quantum Coherence Total COrrrelation Spectroscopy; This is a method which involves a combination of ^1H - ^{13}C HSQC with ^1H -TOCSY resulting to through-bond correlations between the ^1H attached to a ^{13}C and to those that are coupled. In other words, this is a 2D TOCSY being resolved into the carbon dimension and is very useful when identifying and distinguishing overlapping proton spectrum²¹⁸. The HSQC–TOCSY experiment is one which employs various isotropic mixing times in assigning the remotely positioned protons signals (such proton at position 6) from the ^1H ²²⁰.

- 2D–NOESY - Two Dimensional Nuclear Overhauser Enhancement Spectroscopy; This is a method which establishes the correlations for nuclei which are close in space regardless of if they are bonded to each other. The spectrum here has both cross and diagonal peaks similar to COSY but the cross peaks are for the spatially close nuclei rather than through the bond to each other²¹⁸.

- 2D–ROESY- Rotating-frame Overhauser Spectroscopy; This a method where the signals arising from protons close to each other through space can be determined which must not necessarily be bonded²¹⁸. ROESY can also be referred to "cross relaxation appropriate for minimolecules emulated by locked spins" ²²¹ and in addition, it can be used for both conformational and chemical exchange detection^{218, 221}.

1.7.6. Solvent Choice for Dissolution of Polysaccharides

Polysaccharides are often very poorly soluble in the various solvents used for NMR analysis and often deuterium oxide D_2O is the only solvent of choice. Despite being the solvent of choice, it contains a signal, which might hide important anomeric resonances, but this can be overcome by heating the sample at elevated temperatures of approximately $70\text{ }^\circ\text{C}$, which

then shifts the HOD signals of the D₂O to a clearer region exposing the important hidden signals. This elevated temperature can also increase the sample dissolve better into solution for better spectral resolution. Alternatively, modern NMR instruments use solvent signal suppression, but care should be used in case important anomeric resonances occur at the same frequency as that of water

1.7.7. Determination of average Molecular Weights (Mw) of EPS and CPS

Generally, the size of a polysaccharide is noted as its degree of polymerisation, which is related to its molecular weight as a multiple of the average molecular mass of its constituent monosaccharides. It has been recognised that the molecular weight of polysaccharides play an essential role in determining their functionality³².

Measurement of the molecular weight of a polysaccharide is not an easy task and the ease of the measurement depends on if the polysaccharide is monodispersed (each chain has a very similar molecular mass) or is polydispersed (a range of molecular masses). The EPS and CPS from Bifidobacteria and LAB are known to be polydispersed and as such usually have molecular weights ranging between 4.0×10^4 and 6.0×10^6 g/mol and until recently, it has always been difficult to determining their accurate molecular weights.

Traditionally Gel permeation chromatography (GPC) has been used to determine the *Mw* of polysaccharides and compares the retention time of polysaccharides with those of standards. More recently HP-SEC-MALLs (high performance size exclusion chromatography coupled with multi-angle laser light scattering) has been applied for determining the sizes and *Mw* of polysaccharides²²². The HP-SEC-MALLS works on the principle of separation according to the hydrodynamic volume just as was the case with the GPC. The molecular weight is determined by monitoring the light scattering at various angle the angular intensity of the scattering can be related to the average molecular mass. The advantage of the technique is that no reference material is needed. An additional advantage is the HPAEC system is often combined with a UV light detector which can be used to quantify nucleic acid and protein content of the material, these are used in combination with a differential refractive index detector which accurately determines the carbohydrate content of the material that is eluting from the size exclusion column²²³.

1.8. The Structures of the EPS Repeating Units from LAB

To date, the structures of the EPS and CPS from a large number of LAB have been reported and these have been collated in a number of reviews. Representative examples of the EPS produced by LAB will be seen in chapter 3 and these are included to demonstrate the diversity of the structures. Structures directly related to the cultures employed in this project will be considered and these will be collated at the start of the appropriate chapters. EPS and CPS produced by *L. paracasei* and *L. salivarius* will be covered in the introduction to chapter three whilst those from *Bifidobacteria species* will be discussed in the introduction to chapter 5. What is clear is that the repeating units of the polysaccharides that have already been characterised for Gram-positive bacteria are made up mainly of the neutral hexoses D-glucose, D-galactose and L-rhamnose. Occasionally the amino sugars, which can be *N*-acetylated such as D-*N*-acetylgalactosamine and D-*N*-acetylglucosamine appear. What is also clear is that a wide variety of structures are possible and a range of different decorations, including acetate, pyruvate, phosphate, are also present. In addition to hexoses, a number of polysaccharides contain alditols as part of their repeating units.

1.9. The Structures of EPS Repeating Units from the *Bifidobacteria Species*

The structure of EPS repeating units isolated from either the external environment of the cell (EPS) or from the cell wall (CPS) of Bifidobacteria have been reported with only a few fully characterised with some *in vitro* studies suggesting that specific EPSs do impart some key beneficial effects¹¹⁴. Most studies have been focused on the LAB polymers having the abilities in modulating the host immune system which is a characteristic common in some bifido-EPS but with only a few research works done as compared to that for LAB^{9, 114}. The characterised EPS structures have also been seen to comprise of the similar sugar units just like with the LAB strains such as D-glucose, D-galactose and L-rhamnose in addition to mannose, deoxytalose etc. The various reported structures of the Bifidobacteria will be seen in chapter 4.

1.10. Potential Rich Source of Methylated Glucose Molecule (Methylcyclodextrin)

It should be noted that monomer analysis by GC-MS and linkage analysis by GC-MS are accurate but time-consuming techniques and simple sugars can be efficiently separated and compared with reference standard monosaccharides used to identify and quantify monomers. Seeing that a simple method for linkage analysis has so far not been developed, our work we will explore the potential for using HPAEC-PAD and the separation of methylated

monomers for the linkage analysis. The commercially available methylcyclodextrin was found to best fit as a potential rich source of methylated glucose molecule to be used for this.

This methylcyclodextrin is a modified cyclodextrin which is obtained by the methylation of the parent cyclodextrin in which the methyl group could be found replacing the hydrogen of the hydroxyl (OH) groups in positions 2, 3, and 6 of the molecules (i.e. where ever the OH group is found, the -H is being replaced by a methyl group(-CH₃)). As seen in *fig 1.17* the -H groups of positions 2, 3 and 6 are partially replaced by -CH₃ groups.

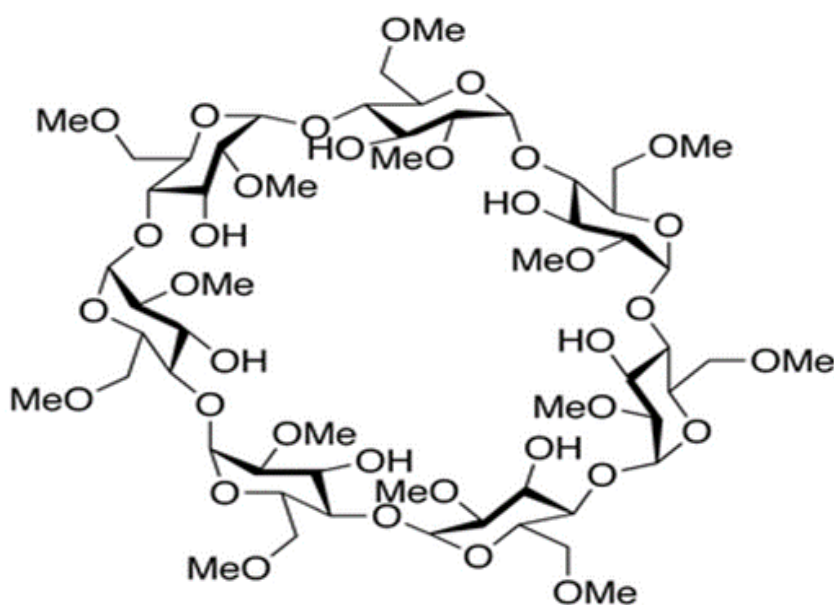


Figure 1.17 Structure of a Methylcyclodextrin

It was appreciated that this would require the development of a library of reference standards including variously methylated monomers

The rationale behind involving methylcyclodextrin in this research is that as a first attempt, it was suggested to see if various methylated glucose molecules could be prepared and if it was possible to separate these molecules and then use the HPAEC-PAD for linkage analysis.

1.11. Aims

Despite the fact that EPS from LAB and Bifidobacteria are thought to be responsible for biological activity, little is known about their structure. The focus of the work was to try to expand the number of known structures since there exist a wide diversity in this bacterial EPS structure among the different species as a result of the different monomeric units and glycosidic linkages in these repeating units²²⁴. The bacterial polysaccharides do have structural differences which has an effect on their functional characteristics host response regulation and colonization^{9, 225}. In determining the structures of these EPSs, the major techniques used included NMR, HPAEC-PAD, which were used for monomer analysis, GC-MS which was used for monomers, linkage and absolute configuration and the HP-SEC-MALLS which was used for molecular weight determination as well as the UV-Vis spectrometer which was used to determine the carbohydrate content of these bacterial polysaccharides. Research aims were as follows;

Several *in vitro* and *in vivo* studies have shown the surface polysaccharides (EPS and CPS) to play roles in both stimulating the immune system and displacing pathogenic organisms^{9, 86}. In order to understand the mechanism which brings about this probiotic activity, we undertook the process of isolating, purifying and characterising the surface polysaccharides produced. That said, our first aim was the extraction and characterisation of the EPS and CPS generated by *L. paracasei* DG cultured in MRS broth and from cultures grown in an EPS-equivalent free medium which is the Huddersfield Broth Medium (HBM) that has been reported to produce pure surface polysaccharides²²⁶. Added to this aim was to confirm the novel structure and review the yield variation from batch to batch.

Considering the fact that the production of EPS is a probiotic related trait, that for *Lactobacillus salivarius* has not been well explored and characterised as compared to the other commensal Lactobacilli²²⁷. A study on 33 strains of the genus Lactobacilli found that the isolate CCUG44481 which is of a bird origin produced EPS at dramatically higher levels than most other strains²²⁷. This now brings about the second aim which was to characterise the structure of the EPS generated by *Lactobacillus salivarius* CCUG44481 that was supplied by the research team in Cork and which has been reported to generate significant amount of exopolysaccharides as earlier stated.

With the cumbersome and lengthy nature of carrying out the linkage analysis in characterising these EPSs, we thought it wise to develop a faster and easier method given the fact that we wanted to determine the structures of a large number of EPS batches from the various probiotic bacteria. This led to the third aim which was to see if linkage analysis could be performed using HPAEC-PAD. This necessitated the synthesis and isolation of a range of methylated monomer standards derived from a model compound of cyclodextrin which was identified as a suitable substrate. The objective here was to separate the mono-, di- and tri-substituted methyl monomer units individually and then use them as reference standards.

The fourth aim was to determine the optimal growth conditions for culturing another probiotic *Bifidobacteria breve* 7017 and the conditions needed for the extraction of the EPS and CPS generated by *Bifidobacteria breve* 7017 of Huddersfield stock (JCM) purchased from Japanese Culture of microorganisms and Cork stock supplied from UCC (University College Cork). Additionally, further 1D and 2D-NMRs were performed to confirm that they are same bacteria species being analysed and a yield variation was also checked from one batch to the other of the extracted surface polysaccharides. A comparative study to see if there are any differences or similarities between the various EPS and CPS (S1, S2, C1 and C2) extracted from addition of 1 volume (for S1 and C1) and 2 volumes of chilled ethanol (S2 and C2) was carried out. Again, different carbon sources (glucose, galactose and lactose) were used in the HBM broth medium in order to see if there are any significant yield variation of the bacterial polysaccharide.

Chapter 2

2. Materials and Methods

2.1. General Reagents and Bacterial cultures

The general reagents used in all the experiments of this research were bought from Sigma-Aldrich Co. Ltd (Gillingham, Dorset, UK), Acros Organics which is under Thermo Fisher Scientific UK (Loughborough, Leicestershire, UK), Wilmad Labglass (Nantwich, Cheshire, UK), or Goss Scientific Instruments Ltd (Nantwich, Cheshire, UK) unless stated otherwise.

2.1.1. Bacterial Media

Casein-acid hydrolysate, Beef extract, dextrose (glucose), galactose, De Man-Rogosa-Sharpe (MRS) broth and Agar (were all purchased from LabM Ltd, Heywood, UK).

2.1.2. Bacterial Cultures and Bacterial Exopolysaccharides

Lactobacillus paracasei DG isolated from Enterolactis R Plus was a kind gift from Sofar S.p.A. in Italy, *Lactobacillus salavirus* CCUG44481 was obtained from the research group of Professor Paul O'Toole in University College of Cork (UCC), *Bifidobacteria breve* 7017 from the research group of Professor Douwe Van Sinderen still from UCC of the Republic of Ireland. We also purchased some more *B. breve* 7017 from Japanese Culture of Microorganisms (JCM).

2.2. Preparation of the MRSc Agar

MRS agar media (1L) was prepared by dispersing the powder (70.0g) in deionised water. The MRSc Agar is composed of peptone (1.0 %), beef extract (1.0 %), yeast extract (0.4 %), glucose (2.0 %), sodium acetate trihydrate (0.5 %), polysorbate 80 (also known as Tween 80 (0.1 %)), dipotassium hydrogen phosphate (0.2 %), triammonium citrate (0.2 %), magnesium sulfate heptahydrate (0.02 %), manganese sulfate tetrahydrate (0.005 %) and agar (1.0 %) with a pH adjusted to 6.2 at 25°C. Given that the bacteria under study are anaerobes, L-cysteine (0.05%) was added to the solution to achieve the anaerobic conditions favourable for their growth. The media was then sterilized by autoclaving at 121 °C for 15 mins, which was then cooled in a warm water bath (50 °C) followed by pouring on to petri dishes.

2.3. Gram Staining

After the 48h anaerobic growth of the isolates, a colony from the pure culture was collected with a sterile MRD and evenly spread on a microscopic glass slide. The smeared colony on the glass was then heat-fixed and following the developed method by Christian (1884)²²⁸, the Gram-staining dye was applied.

2.4. Media for Use in Batch Fermentations

2.5. MRS-c Broth Preparation

The MRS-c broth composed of all the ingredients mentioned in section 2.2 except the agar. In preparing 1L of MRS broth, 1L of deionised water was filled into a Schott bottle and the powder broth (55.0 g) was added and this was supplemented with L-cysteine (0.05%) to maintain its anaerobic condition. It was then autoclaved at 121 °C for 15 mins and kept in the cold room until needed.

2.5.1. Preparation of Broth Media Free of EPS-equivalent

Excellent growth of Bifidobacterium cultures can be supported by various media which include Tryptone Proteose peptone Yeast (TPPY) extract medium, reinforced clostridial medium, and De Man Rogosa and Sharpe (MRS) medium²²⁹⁻²³¹ but according to Gancel and Novel (1994)²³² all these media are known to have components containing polysaccharides i.e. EPS-equivalents (EPS-E) which will affect the quantification and characterisation of the EPS produced by the Bifidobacterium itself. A medium for culture growth, which is free of EPS-E, was developed by Alhudhud *et al* (2014)²²⁶ known as the Huddersfield Bifidobacteria Medium (HBM) and has previously been shown to permit culturing and EPS production of the *Bifidobacterium animalis ssp. Lactis* AD011 on a large scale.

In the present work, Reinforced Clostridial Medium (RCM) was chosen as the starting point for medium development. After identification of the essential elements, these were then either treated to remove the EPS-E or replaced with another material which is free of EPS-E. According to Alhudhud *et al* (2014)²²⁶, EPS-E are present in casein-acid hydrolysate (CAH) as well as in beef extract (BE), hence their treatment was essential in eliminating these interferences.

To remove EPS-E, a 20% w/v concentration of the BE and CAH were dissolved in deionised water and then autoclaved. The solution was left to cool to room temperature after which two and a half volumes of ethanol were added and the resulting suspension was left for

approximately 48 h at 4°C for the precipitation of the EPS-E. Centrifugation (25000G, 30 mins, 4° C) of the mixture was performed in order to obtain a clear supernatant from which the ethanol was distilled away. Another centrifugation was performed on the retained material before adding the rest of the media components which are listed in table 2.1.

Table 2.1: Composition of the HBM medium

Ingredients	Composition (g/L)
Treated Beef extract	10
Treated casein acid hydrolysate (TCAH)	10
Glucose	10
Yeast nitrogen base (YNB) with no amino acids	3
Sodium acetate	3
Sodium chloride	5
L-Cysteine-HCl	0.5

After the addition of the ingredients and the required volume attained by topping it up with deionised water, the entire HBM broth was then autoclaved for 15 mins at 121°C. The sterilized HBM was then transferred into the cold room and kept until when required.

In a similar manner another HBM broth was prepared but using galactose as a carbon source for the growth of the bacteria instead of the usual glucose.

2.5.2. Chemically Defined Medium (CDM)

This is a medium that was formulated by the research team in Italy, which we are in collaboration with. Seeing that the treatment process involved in making the HBM free of EPS-equivalent was time consuming, the CDM was then formulated as seen in the table 2.2. All the ingredients in solution were combined and then sterilized by autoclaving for 15 mins at 121°C. The sterilized solution was then stored for future use.

Table 2.2: The Composition of the CDM

Ingredients	Composition (g/l)
Solution. 1 (NH ₄) ₂ SO ₄ MgSO ₄ x 7H ₂ O MnSO ₄ x 4 H ₂ O	2 0.15 0.02
Solution. 2 Adenine Pyridoxal Nicotinic acid Ca ²⁺ -D-pantothenate Riboflavin Thiamine Vitamin B12 Biotin <i>p</i> -aminobenzoic acid Folic acid	0.005 0.002 0.001 0.001 0.001 0.001 0.000001 0.00001 0.000005 0.00001
Solution. 3* Guanine Xanthine Uracil	0.005 0.005 0.005
Solution. 4 K ₂ HPO ₄	4.56
Solution. 5 Sodium acetate Sodium citrate KH ₂ PO ₄ NaCl CaCl ₂	0.05 0.02 0.01 0.002 0.002
Solution. 6 Tween 80 Tween 20 Glycerol	1 1 1
Glucose	20
Casaminoacids	10

*1M NaOH was used as the solution and the pH was neutralized with the addition of 1M HCl.

2.6. Preparation of Dialysis Tubes

The cellulose membrane dialysis tube (12–14 kDa molecular mass cut-off) were prepared by initially running water on the tubes in a bowl for over 3-4 hours so as to get rid of the humectant (glycerol). The tube was then treated at 80°C with a Na₂S solution (0.3% w/v, sodium sulphide) for about a minute to wash away the sulphur compounds. The tube was next transferred into hot water of 60°C and stirred for 2 mins, then was moved into a solution of sulphuric acid (0.2% v/v) for 1 min and then finally rinsed with another portion of just hot water (60°C) to ensure no acid is left. Once complete the tubes are then stored at 4°C (cold room) in deionised water to be used when needed.

2.7. Exopolysaccharide Isolation

2.7.1. Exopolysaccharide Extraction from Broth Cultures

The bacteria of interest (*L. paracasei* DG and *B. breve* 7017) were taken from the -80 °C freezer and were inoculated from their respective microbanks on to petri dishes of MRS agar. After 3 days of growth, a loop full was inoculated into 20 ml bottles containing either MRS broth or HBM broth from which, after 18 to 24 h of growth, 1 ml was sub-cultured from each into another 20 ml of broth. This was done to get the most active bacteria ready to be cultured into a larger volume of broth (500 ml). From the second 20 ml after 18 to 24 h, 0.5% was then inoculated into a 500 ml of the MRS or HBM and these cultures were allowed to grow for 3 days. After 3 days of fermentation, the cells were then separated from the supernatant by centrifugation (10,000 G for 15 mins at 4°C).

2.7.1.1. Extraction of the Slime EPS (S1 and S2)

After centrifugation, 1 volume of chilled ethanol was added to the supernatant and left to precipitate for 2 days in the cold room giving rise to the EPS which was recovered by centrifugation (25,000 G, 4 °C, 30 mins) and labelled as S1. A second volume of chilled ethanol was added to the very supernatant, left for another 2 days to precipitate EPS which was then centrifuged again (25,000 G, 4 °C, 30 min) to yield S2. The S1 and S2 collected from the separate centrifugation was then dissolved in deionised water (25 to 30 ml) and dialysed changing the water 3 times daily in the cold room (4 °C). After 3 days of dialysis the EPSs (S1 and S2) were finally lyophilised (freeze-dried) (Modulyo 4K Freeze Dryer, Edwards, Northern Scientific, York, UK).

2.7.1.2. Extraction of the Capsular EPS

To the cells separated after centrifugation, NaOH (1 M in 200 ml solution) was added and left to stir overnight. The cells which had been treated with NaOH (1 M) were then centrifuged (10,000 G, 15 mins, 4°C) and the pellet discarded. One volume of chilled ethanol was added to the supernatant collected and the solution was left for 2 days to precipitate the CPS which was collected as C1. In addition, a second volume was added to this solution and left again for 2 days in the cold room to precipitate C2.

The C1 and C2 were all collected by centrifugation (25,000 G, 30 mins 4°C) *fig 1.19* and then dialysed. All the dialysed samples were then freeze-dried, weighed, dissolved in deuterium oxide (D₂O) and the proton NMR carried out for each of them. For some samples 2D-NMRs were also performed.

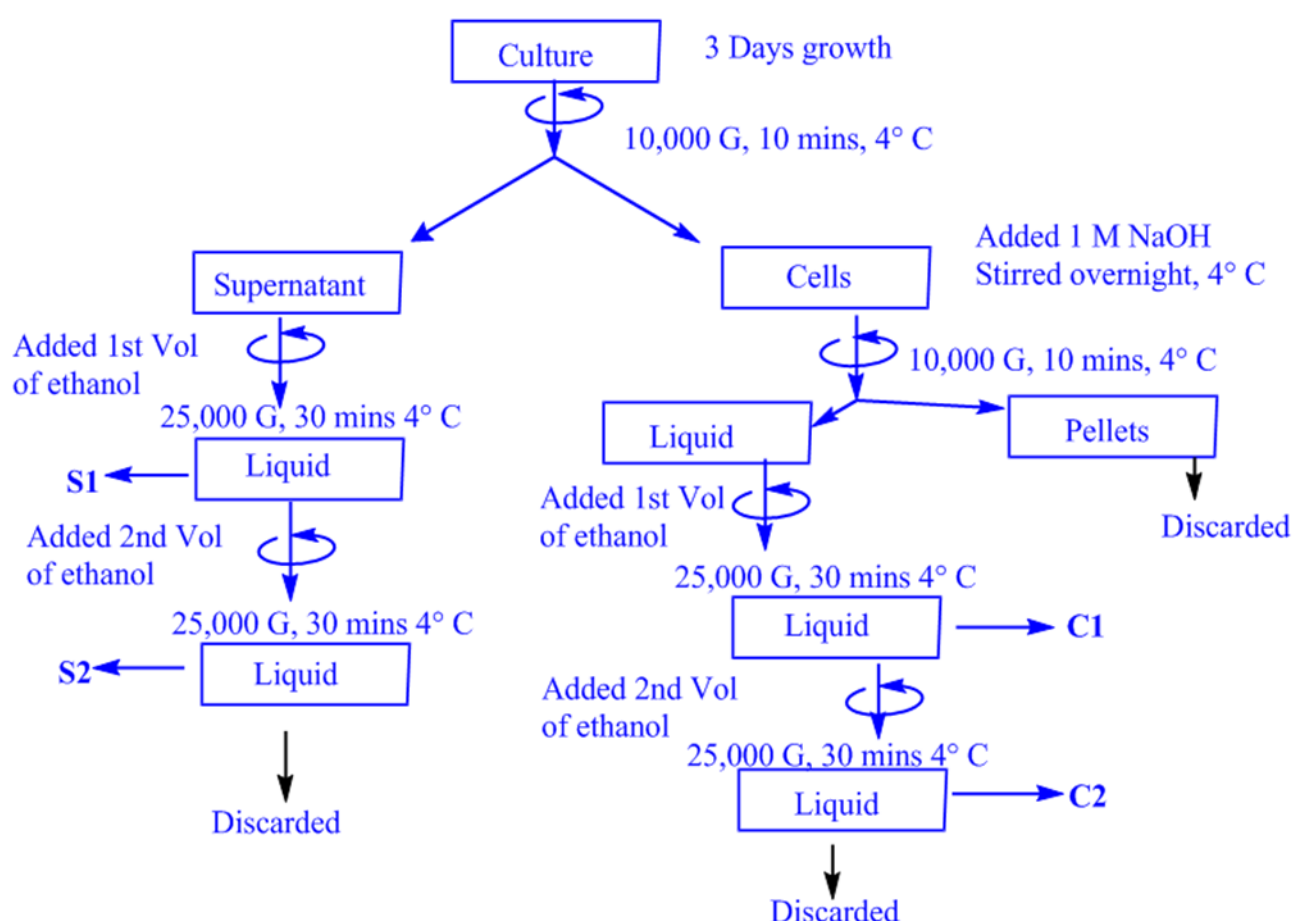


Figure 2.1: Schematic Representation of the Extraction Procedure of the EPS and CPS.

2.8. Exopolysaccharide Characterisation

2.8.1. Quantification of the Solid Content

The empty bottles (round or Schott) in which the dialysed samples are to be freeze-dried were first weighed before the samples were transferred. Once the transferred dialysed sample were completely freeze-dried, the entire bottle now containing the freeze-dried sample was again weighed and the difference in weight was recorded as the weight of the EPS.

2.8.2. Determining the Carbohydrate Content

The phenol sulphuric carbohydrate test by Dubois *et al* (1956)¹⁸⁵ was the method used to quantify the amount of carbohydrates in a crude EPS. The crude EPS was dissolved in deionised water (0.5ml, 0.25mg/L) and transferred into a high temperature resistant thick glass tube. A phenol solution (5%) was added closely followed by concentrated sulphuric acid (2.5 ml) with caution. The tubes were then kept in a water for 20 mins at 70 °C to ensure the completion of the reaction. Once the yellowish colouration was completely formed, the tubes were then let to cool for about 10 to 15 mins. The absorbance for each of these samples were recorded spectrophotometrically at a wavelength of 490 nm using deionised water as a blank. In addition, a calibration curve was generated from measuring the absorbance of six glucose standards with concentrations ranging between 10 and 300 µg/ml.

2.8.3. Structural Characterisation of EPS

There are several techniques and instrumentations used for the structural characterisation and analysis of the isolated EPS. These techniques are spectroscopic and chromatographic which in this study will include HPAEC-PAD, NMR and the GC-MS.

2.8.3.1. HPAEC-PAD

High performance anion exchange chromatography combined with pulsed amperometric detection (HPAEC-PAD) was performed on a Dionex ICS3000. The column used was a CarboPac PA20 (3×150 mm) analytical column with a particle size of 6 µm. The DP-Dual Pump System was used with a flow rate of 0.45ml/min and an injection volume of 25 µl. The solvents used were NaOH 200 mM (solvent A regenerant) and NaOH 10 mM (solvent B, which is the mobile phase). The Chromeleon system software was used to obtain data during the HPAEC-PAD analysis. Samples were eluted with a mobile phase containing 100% solvent B and in between runs the column was regenerated using 100% solvent A.

2.8.3.2. GC-MS

The gas chromatography mass spectrometry system (GC-MS) used included an Agilent 7683B series injector, a 7890A GC system, a 5975B inert XL EI/CI MSD autosampler. For the injection, the syringe size is 10 μ l with an injection volume set to be 1 μ l with a carrier gas flow rate of 1mL/min, an injection split ratio of 10:1 was used and also the heater set to be at a maximum temperature of 250 °C. The column used was of Agilent 190915-433: (60 to 325 °C: 30 m \times 250 μ m \times 0.25 μ m). The “monomers” and “Linkage analysis” method were set for analysis as will be seen section 2.8.4 and section 2.8.5 respectively.

2.8.3.3. Nuclear Magnetic Resonance (NMR)

All NMR spectra of the EPSs were run on a Bruker Avance AV500 500.13 MHz spectrum with an 11.7 Tesla Ultra ShieldTM magnet. All EPS samples were prepared in deuterium oxide (D₂O) and were recorded at 70 °C for the 500MHz NMR or at room temperature for the 400MHz NMR. A Bruker DPX400 400.13 MHz unshielded magnet or Bruker AVIII 400.13 MHz with a 9.1 Tesla AscendTM magnet was also used to record room temperature spectra. All one-dimensional NMR experiments (¹H and ¹³C DEPT 135) and two-dimensional NMR experiments (COSY, HMBC, HSQC, TOCSY, HSQC-TOCSY and NOESY) were run on different samples and standards of EPS.

2.8.3.4. HP-SEC-MALLS

This instrument consists of a combination of a Shimadzu HPLC system, which is comprised of an LC-20AD liquid chromatography system, a DGU-20 A₃ degasser and an SPD-20 A UV/Vis detector. Three aquagel-OH columns are connected in a sequence (table 2.3) and the detectors include a differential refractometer (Optilab-rEX, Wyatt technology, Santa Barbara, USA) and finally a MALLS detector (Dawn-EOS, Wyatt technology, Santa Barbara, USA). The chromatographic conditions as well as SEC-MALLS conditions are listed in table 2.3 that follows.

Table 2.3: Typical Chromatographic Conditions of HP-SEC-MALLS

Typical Chromatographic Conditions	
Instrument	Shimadzu HPLC System (Shimadzu, UK, Ltd)
Injector	Rheodyne 7125
Pump	LC - 20AD
3 columns used that were attached in series	
Column 1	PL aquagel - OH 40 15 μ m, 300 x 7.5 mm (used for separating low molecular weight EPS- 10,000-200,000 Da)
Column 2	PL aquagel - OH 50 15 μ m, 300 x 7.5 mm (used for separating medium molecular weight EPS- 50,000-600,000 Da)
Column3	PL aquagel - OH 60 15 μ m, 300 x 7.5 mm (used for separating high molecular weight EPS- 200,000->10,000,000 Da)
Guard Column	PL aquagel - OH Guard 15 μ m, 50 x 7.5 mm
Wavelength	280nm and 260nm
Mobile Phase	Ultrapure Water
Flow rate	0.7 mL / min
Injection volume	25.0 μ L
Pressure	450 psi
Run time	100 min.

2.8.4. Monomer Analysis of the Polysaccharides (EPS and CPS)

In determining the monomer composition of carbohydrate products, the following reactions were carried out. This process of monomer analysis is consisted of three steps (Hydrolysis, reduction and acetylation).

2.8.4.1. Hydrolysis of the EPSs

The samples (3 mg) were treated with trifluoroacetic acid (TFA, 2 ml, 2M) and then heated for 2 h at a temperature of 120 °C in a pressure tube. After cooling to room temperature, the pressure tube's cap was removed, and the solutions were then evaporated to dryness with a constant stream of nitrogen gas at 60 °C resulting to the monomers. The dried residue was reconstituted with ultrapure water (UPW, 3ml) and some portions used for HPAEC-PAD analysis.

2.8.4.2. Reduction of the EPS

Part of the reconstituted hydrolysed EPS in UPW was then reduced by adding NaBH₄ (10 mg). The pressure tubes were then sealed and heated at 40 °C for 2 h after which the solutions was evaporated to dryness under a constant stream of nitrogen at 60 °C. Glacial acetic acid (1ml) was then added to the dried residue and again evaporated to dryness under a constant stream of nitrogen at 60 °C. Methanol (1.5ml) was added and subsequently evaporated three times for the removal of the borate complex under a stream of nitrogen to give the sugar alditols.

2.8.4.3. Acetylation of the EPS

To the residues obtained from the reduction process, pyridine (2 ml) and acetic anhydride (2 ml) were added to the dried reduced sugar alditols and the solution heated for 2 h at 100 °C. After 2 h of heating the solution was then evaporated at 40 °C to dryness under a constant stream of nitrogen. The dried acetylated residue was then suspended in UPW (5 ml) and extracted 3 times with chloroform (5 ml). UPW (2ml) was again used to wash the organic (chloroform) layer collected and dried over anhydrous sodium sulphate for 30 mins to remove any water left over. The solution was then filtered, and the filtrates evaporated to dryness under a constant stream of nitrogen at 40 °C. Acetone (2 ml) was added to the dried acetylated residues, transferred to vials for analysis of the monomeric units by GC-MS.

For the monomer analysis, the HP-5 column (30m×250µm×0.25µm film) was used, for sample elution helium was employed as a carrier gas (9 psi, flow rate 1 mL/min) and a temperature gradient programme (start temperature of 150 °C, hold time of 4 min., and a final temperature of 250 °C reached via a rising gradient of 4 °C/min). During analysis, thermal decomposition of the amino-sugar was observed, so its final monomer ratio was obtained from integration of the NMR peak integrals for the respective anomeric and H₂-protons.

2.8.5. Linkage Analysis of the EPSs

This is a modified technique by Ciucanu and Caprita (2007)²³³ from the developed method by Ciucanu and Kerek (1984)²³⁴ and is also referred to as the partially methylated alditol acetate method. In determining the linkage pattern of the EPS, prior to hydrolysis, reduction and acetylation, a methylation step was carried out. Dimethyl sulfoxide (0.07 ml) was added to the EPS (3 mg) and the solution stirred until formation of a slurry mixture. Dried and crushed sodium hydroxide (70 mg) was added to the pressure tube with stirring along with methyl iodide (60 µl). This was allowed to stir for 30 mins and the resulting methylated EPS was then separated using a liquid/liquid extraction of ultrapure water (3 ml) and dichloromethane (3 ml) in a separating funnel at a ratio of 1:1. The organic layer was then washed 3 times with UPW (5 ml). The resulting liquid was then evaporated to dryness under a constant stream of nitrogen at 40 °C to give the methylated EPS, which was then hydrolysed, reduced and acetylated to give methylated alditol acetates. During the reduction process a NaBD is used. After the acetylation, the dried residue was reconstituted with acetone and analysed in the GC-MS using the linkage analysis method which ran for 45 mins. For this linkage analysis, the temperature programme used included a start temperature of 155 °C, hold time of 1 min, and final temperature of 195 °C reached via a rising gradient of 0.75 °C/min.

2.8.6. Molecular Weight (Mw) Determination of the Isolated EPS

This Mw was obtained by using the HP-SEC-MALLS. Approximately a 1000 ppm (1 mg/ ml) of the freeze-dried sample was dissolved in either 0.1M NaNO₃ or ultrapure water and stirred vigorously to ensure complete dissolution of the sample at room temperature. After stirring the sample was then filtered using a 22 µm filter and the filtered sample (100µl) was then injected into the SEC-MALLS system which had three Aquagel columns connected in sequence and the molecular weight obtained. HPLC pump (LC-20AD, Shimadzu, Milton Keynes, UK) was used at a flow rate of 0.7ml/min with 0.1M NaNO₃ as mobile phase to carry the sample through the system. The eluted sample was then passed through a series of detectors: a UV SPD-20A Shimadzu detector for protein identification, an OPTilab-rEX detector (a differential refractometer, Wyatt technology, Santa Barbara, USA) was used for the quantification of the EPS and then the Dawn-EOS, which is the MALLS detector with 16 incorporated photodetectors which detects the particle from different angles which permitted the determination of the molecular weight of every single peak. Each run was for 90 mins with a

refractive index increment (dn/dc) set at 0.147mL/g and then the Astra-6 software was used to process the data obtained.

2.8.7. Absolute Configuration of EPS

In determining the absolute configuration of the substituent monomeric repeating units of the EPSs by GC-MS analysis, the previously developed method by Gerwig *et al* (1978)²⁰⁹ was adapted into the new method which involved preparing the acetylated butyl glycosides to be analysed.

To the pressure tube containing TFA (2M), a sample of EPS (1 mg) was added and heated for 2h. After letting it cool down, the solution was then evaporated to dryness at 50 °C under a stream of nitrogen. Methanol (2 × 1 ml) was added to this dried hydrolysed residue and evaporated to dryness at 50°C under a stream of nitrogen. Re-*N*-acetylation was performed for EPSs known to possess amino sugars in their structure by addition of the acetic anhydride (125 µL) and kept at room temperature for 4 h. The solution was then evaporated to dryness. The dried residue was then dissolved in (S)-(+)-2-butanol (1 ml) followed by the addition of acetyl chloride (75 µL) and nitrogen gas bubbled into the solution for 30 secs and sealed. The sealed tube containing the mixture was then butanolized for 16 hours at 80 °C and then evaporated to dryness under a stream of nitrogen gas. Methanol (2× 1 ml) was added to the dried butanolized residue and evaporated to dryness. This dried residue was then acetylated by adding acetic anhydride (1 ml) and pyridine (1 ml) and heating for 1 h at 120 °C. After letting this solution cool down, it was then evaporated to dryness and toluene (2 × 1 ml) added and evaporated to dryness to give the acetylated butyl glycosides of the EPS. UPW (2 ml) was used to suspend this dried acetylated butyl glycosides and then extracted twice with ethyl acetate (2 ml). This extract containing the acetylated butyl glycosides was then evaporated and reconstituted with ethyl acetate and analysed by the GC-MS.

Results and Discussion Sections

3) Analysis and Structural Characterisation of the Novel EPS from *Lactobacillus*

4) Attempt to Develop a Robust and Rapid Method for Linkage Analysis Using HPAEC-PAD and Employing Partially Methylated Cyclodextrins as Model Substrates

5) Production and Isolation Polysaccharides that are Excreted or Presented at the Cell Surface of *B. breve* 7017

Chapter 3

3. Analysis and Structural Characterisation of the Novel EPS from *Lactobacillus paracasei* DG and *Lactobacillus Salivarius* CCUG44481

3.1. Introduction

In this section, emphasis will be on the production, isolation and characterisation of the various exocellular polysaccharide material secreted by two *Lactobacillus* strains (*L. paracasei* DG and *L. salivarius* CCUG44481). Both species are non-spore forming Gram-negative bacteria, where *L. paracasei* DG is an isolate from the human gut^{82, 84, 235} whereas *L. salivarius* is an isolate from an animal source (birds)^{227, 236}.

L. paracasei DG which have been included in a commercial probiotic product (Enterolactis®) is of interest in this study because *in-vivo* and *in-vitro* experiments have provided evidence for its probiotic properties but the structures for only a limited number of subspecies have been analysed.²³⁵ Despite these investigations, not much is known about the structure of exocellular polysaccharides and before our studies very little has been done in identifying the various monomeric units that make up the repeated unit of the exopolysaccharides. A research team in Italy with whom we are in collaboration has supplied the DG strain under study and they collaborate with the manufacturer of the commercial probiotic product (Enterolactis). It is necessary to undertake the identification of the polysaccharide molecule in *L. paracasei* DG to try and understand how the biological activity can be related to its structure. In this work three different media (MRS, HBM and CDM) were used to grow the bacteria *L. paracasei* DG and we at Huddersfield looked at how the composition of the media and the extraction process influenced the polysaccharides that were recovered from the fermentation broth and the cells. The work was done in close collaboration with Silvia Balzaretto and her team of the University of Milan who focused on isolating extracellular polysaccharides from the chemically defined media, its characterisation and measurement of its biological activity. In this thesis, we compare the yields and purity of different polysaccharide fractions recovered from *L. paracasei* DG when grown in MRS, HBM and CDM broths. Added to this, we also compare the yields and identity of the secreted material (exopolysaccharides) with material extracted from the surface of the cells (capsular polysaccharides). Representative examples of EPS producing LAB, which have been studied are listed below (table 3.1)

(IV)	Ac0.4 ↓ 2 β-D-Galp-(1→6)-β-D-Galf 1 ↓ 6	
→2)-α-L-Rhap-(1→2)-α-L-Galp-(1→3)-α-D-Galp-(1→3)-α-D-Galp-(1→3)-α-L-Rhap-(1→		
<i>Streptococcus thermophilus</i> OR901		241
<i>Streptococcus. thermophilus</i> Sts		242
(V)	-D-Galf 1 ↓ 6	
→2)-α-L-Rhap-(1→2)-α-L-Galp-(1→3)-α-D-Glcp-(1→3)-β-D-Galp-(1→3)-α-L-Rhap-(1→		
<i>Streptococcus thermophilus</i> Sti12		181
(VI)	Ac0.4 ↓ 2 -D-Galf 1 ↓ 6	
→4)-β-L-Glcp-(1→6)-β-L-Galp-(1→6)-α-D-Glcp-(1→3)-β-D-Galp-(1→3)-β-D-Galp-(1→3)-α-L-Rhap-(1→		
<i>Streptococcus thermophilus</i> EU20		243
C. EPS Structures from <i>Lactobacillus acidophilus</i>		
	β-D-GlcpNAc 1 ↓ 3	
→4)-β-L-Glcp-(1→4)-β-D-Glcp-(1→6)-α-D-Glcp-(1→4)-β-D-Galp-(1→		
<i>Lactobacillus acidophilus</i> LMG9433		177, 244
D. EPS Structures from <i>Streptococcus Macedonicus</i>		
β-D-Galf-(1→6)-β-D-Glcp-(1→6)-β-D-GlcpNAc 1 ↓ 3		
→4)-α-D-Glcp-(1→4)-β-D-Galp-(1→4)-β-D-Glcp-(1→		
<i>Streptococcus macedonicus</i> Sc136		245
E. EPS Structures from <i>Lactobacillus delbrueckii subsp. bulgaricus</i> (I-IV)		

(I)	$ \begin{array}{ccc} \beta\text{-D-Galp} & \alpha\text{-L-Rhap} & \beta\text{-D-Galp} \\ 1 & 1 & 1 \\ \downarrow & \downarrow & \downarrow \\ 4 & 3 & 3 \\ \rightarrow 3\text{-}\beta\text{-D-Glcp}\text{-}(1\rightarrow 3)\text{-}\beta\text{-D-Galp}\text{-}(1\rightarrow 4)\text{-}\alpha\text{-D-Galp}\text{-}(1\rightarrow 4)\text{-}\alpha\text{-D-Galp}\text{-}(1\rightarrow \end{array} $	246
<i>Lactobacillus delbrueckii</i> subsp. <i>bulgaricus</i> rr		
(II)	$ \begin{array}{c} \beta\text{-D-Galp}\text{-}(1\rightarrow 4)\text{-}\beta\text{-D-Glcp} \\ 1 \\ \downarrow \\ 6 \\ \rightarrow 4\text{-}\beta\text{-D-Galp}\text{-}(1\rightarrow 4)\text{-}\beta\text{-D-Glcp}\text{-}(1\rightarrow 4)\text{-}\alpha\text{-D-Glcp}\text{-}(1\rightarrow \end{array} $	240
<i>Lactobacillus delbrueckii</i> subsp. <i>bulgaricus</i> 291		
(III)	$ \begin{array}{c} \alpha\text{-L-Rhap} \\ 1 \\ \downarrow \\ 3 \\ \rightarrow 2\text{-}\alpha\text{-L-Rhap}\text{-}(1\rightarrow 4)\text{-}\alpha\text{-D-Glcp}\text{-}(1\rightarrow 3)\text{-}\beta\text{-L-Rhap}\text{-}(1\rightarrow 4)\text{-}\alpha\text{-D-Glcp}\text{-}(1\rightarrow \end{array} $	184
<i>Lactobacillus delbrueckii</i> subsp. <i>bulgaricus</i> EU23		
(IV)	$ \begin{array}{cc} \alpha\text{-D-Galp}\text{-}(1\rightarrow 3)\text{-}\alpha\text{-D-Glcp} & \alpha\text{-D-Glcp} \\ 1 & 1 \\ \downarrow & \downarrow \\ 3 & 6 \\ \rightarrow 4\text{-}\beta\text{-D-Glcp}\text{-}(1\rightarrow 3)\text{-}\alpha\text{-D-Galp}\text{-}(1\rightarrow \\ 2 \\ \uparrow \\ 1 \\ \beta\text{-D-Galp}\text{-}(1\rightarrow 4)\text{-}\beta\text{-D-Glcp} \end{array} $	247
<i>Lactobacillus delbrueckii</i> subsp. <i>bulgaricus</i> NCFB2074		
F. EPS Structures from <i>Lactobacillus rhamnosus</i> (I-II)		
(I)	$ \rightarrow 6\text{-}\alpha\text{-D-Galp}\text{-}(1\rightarrow 6)\text{-}\alpha\text{-D-Glcp}\text{-}(1\rightarrow 3)\text{-}\beta\text{-D-Galf}\text{-}(1\rightarrow 3)\text{-}\alpha\text{-D-Glcp}\text{-}(1\rightarrow 2)\text{-}\beta\text{-D-Galf}\text{-}(1\rightarrow $	248
<i>Lactobacillus rhamnosus</i> C83		
(II)	$ \begin{array}{c} \text{D-Galf} \\ 1 \\ \downarrow \\ 6 \\ \rightarrow 3\text{-}\alpha\text{-L-Rhap}\text{-}(1\rightarrow 3)\text{-}\alpha\text{-D-Galp}\text{-}(1\rightarrow 3)\text{-}\beta\text{-D-Galf}\text{-}(1\rightarrow 3)\text{-}\beta\text{-D-Galp}\text{-}(1\rightarrow 4)\text{-}\alpha\text{-D-GlcfNAc}\text{-}(1\rightarrow \end{array} $	249
<i>Lactobacillus rhamnosus</i> GG (ATCC 53103)		
G. EPS Structures from <i>Lactobacillus sakei</i>		

$sn\text{-glycerol-3-phosphate} \rightarrow 4)\text{-}\alpha\text{-L-Rhap}$ (Ac)0.85 \downarrow 2 $\rightarrow 3)\text{-}\beta\text{-L-Rhap-(1}\rightarrow 4)\text{-}\beta\text{-D-Glcp-(1}\rightarrow 4)\text{-}\alpha\text{-D-Glcp-(1}_$ \uparrow 1 $\beta\text{-D-Glcp}$	1 \downarrow 3 6 1	
<i>Lactobacillus sakei</i> 0-1		250
H. EPS Structures from <i>Lactobacillus helveticus</i> (I-VI)		
(I)	$\beta\text{-D-Galp-(1}\rightarrow 4)\text{-}\beta\text{-D-Glcp}$ 1 \downarrow 3 $\rightarrow 3)\text{-}\alpha\text{-D-Galp-(1}\rightarrow 3)\text{-}\alpha\text{-D-Glcp-(1}\rightarrow 3)\text{-}\beta\text{-D-Glcp-(1}\rightarrow 5)\text{-}\beta\text{-D-Galf-(1}\rightarrow$	
<i>Lactobacillus helveticus</i> TN-4		168
<i>Lactobacillus helveticus</i> Lh59		251
(II)	$\beta\text{-D-Galp-(1}\rightarrow 4)\text{-}\beta\text{-D-Glcp}$ 1 \downarrow 6 $\rightarrow 6)\text{-}\beta\text{-D-Glcp-(1}\rightarrow 3)\text{-}\beta\text{-D-Glcp-(1}\rightarrow 6)\text{-}\alpha\text{-D-GalpNAc-(1}\rightarrow 3)\text{-}\beta\text{-D-Galp-(1}\rightarrow$ 4 \uparrow 1 $\beta\text{-D-Galp}$	
<i>Lactobacillus helveticus</i> TY 1-2		252
(III)	$\beta\text{-D-Galp}$ 1 \downarrow 6 $\rightarrow 4)\text{-}\beta\text{-D-Glcp-(1}\rightarrow 6)\text{-}\beta\text{-D-Glcp-(1}\rightarrow 6)\text{-}\beta\text{-D-Galp-(1}\rightarrow 4)\text{-}\alpha\text{-D-Galp-(1}\rightarrow 3)\text{-}\beta\text{-D-Galp-(1}\rightarrow$	
<i>Lactobacillus helveticus</i> 2091		253
(IV)	$\beta\text{-D-Glcp}$ 1 \downarrow 3 $\rightarrow 3)\text{-}\beta\text{-D-Glcp-(1}\rightarrow 4)\text{-}\alpha\text{-D-Glcp-(1}\rightarrow 4)\text{-}\beta\text{-D-Galp-(1}\rightarrow 3)\text{-}\alpha\text{-D-Galp-(1}\rightarrow 2)\text{-}\alpha\text{-D-Glcp-(1}\rightarrow$	$\beta\text{-D-Glcp}$ 1 \downarrow 3
<i>Lactobacillus helveticus</i> Lb161		254
(V)		

$\beta\text{-D-Galp}$ 1 \downarrow 3 $\rightarrow 6)\text{-}\alpha\text{-D-Glcp}\text{-}(1\rightarrow 6)\text{-}\alpha\text{-D-Galp}\text{-}(1\rightarrow 6)\text{-}\alpha\text{-D-Glcp}\text{-}(1\rightarrow 3)\text{-}\beta\text{-D-Glcp}\text{-}(1\rightarrow 4)\text{-}\beta\text{-D-Glcp}\text{-}(1\rightarrow$	250
<i>Lactobacillus helveticus</i> NCDO 766	
(VI) $\beta\text{-D-Glcp}$ 1 \downarrow 6 $\beta\text{-D-Glcp}\text{-}(1\rightarrow 4)\text{-}\beta\text{-D-Glcp}$ 1 \downarrow 6 $\rightarrow 4)\text{-}\beta\text{-D-Galp}\text{-}(1\rightarrow 4)\text{-}\beta\text{-D-Glcp}\text{-}(1\rightarrow 4)\text{-}\alpha\text{-D-Glcp}\text{-}(1\rightarrow$	255
<i>Lactobacillus helveticus</i> K16	

3.2. Production and Isolation of Polysaccharides from *Lactobacillus paracasei* DG

The *L. paracasei* DG was cultured in MRS, HBM and CDM media. The HBM was used which according to Alhudhud *et al* (2014), it has no contaminating EPS-equivalents to interfere with materials extracted directly from the bacteria²²⁶. The CDM developed by the Italian team was also known to be free of EPS-equivalent and this was also used to see if this broth could favour production of pure polysaccharides. In isolating the polysaccharides for characterisation, it was essential to culture the *L. paracasei* DG in three different sets of media (MRS, HBM as well as the CDM) to see which of them is best suited for pure extraction of this polysaccharide. After 3 days of fermentation, the supernatant was separated from the cell biomass by centrifugation.

For the culture grown on MRS, the supernatant was collected from which the S1 and S2 fractions were precipitated (as described in section 2.7.1.1) and a ¹H-NMR spectrum was ran for these two fractions. These suggested that the major peaks were derived from the media components. The amount of material in the S1 fraction (from a 500ml batch) ranged between 30 to 40 mg whereas that for S2 ranged between 100 to 120mg (Table 3.2). Unfortunately, it is known that MRS broth contains EPS-equivalents that will interfere with the EPS from the bacteria, so no further analysis was performed on the S1 and S2 fractions. Our focus for this

fermentation was then applied to the cell biomass, which was then treated with NaOH (1M) (as described in section 2.7.1.2). A second set of polysaccharides (CPSs) were extracted as C1 and C2 fractions after addition of 1 volume and 2 volumes of absolute ethanol respectively to the NaOH extracts. The precipitated CPS were dialysed for 3 days, freeze-dried and then weighed. The identity of the CPS obtained from the NaOH treated cells was then checked by examining the proton NMR ($^1\text{H-NMR}$) spectrum (*Fig 3.1*).

Table 3.2 Amount of EPS and CPS for *L. Paracasei* DG

Batches	S1	S2	C1	C2
1 (MRS broth)	30.5mg/500ml	101.2mg/500ml	21.50 mg/500ml	15.40mg/500ml
2(MRS broth)	39.2mg/500ml	118.9mg/500ml	23.60mg/500ml	10.80mg/500ml
3(MRS broth)	discarded	Discarded	22.30mg/500ml	11.20mg/500ml
4(HBM broth)	< 2mg	26.28 mg/500ml	< 2mg	15.94 mg/500ml
5(HBM broth)	< 2mg	25.76 mg/500ml	< 2mg	11.45 mg/500ml
6(HBM broth)	< 2mg	22.60 mg/500ml	< 2mg	8.25mg/ 500ml
7(CDM broth)	-----	-----	23.75mg/500ml	14.61 mg/500ml
8(CDM broth)	-----	-----	23.70mg/500ml	11.20mg/500ml

The $^1\text{H-NMR}$ spectra recorded for C1 and C2 obtained from the *L. paracasei* DG grown in MRS broth indicated that the addition of 1 volume precipitated a relatively cleaner polysaccharide material the capsular polysaccharide (CPS) which were distinctively labelled as A, B, C, D, E and F as compared to that of second volume (*Fig 3.1*). The $^1\text{H-NMR}$ spectra for batches 1, 2 and 3 indicated that the addition of the second volume precipitated more impurities, which are the additional peaks in the anomeric region of the NMR spectra labelled as X. The C1 fraction was taken forward for further characterisation.

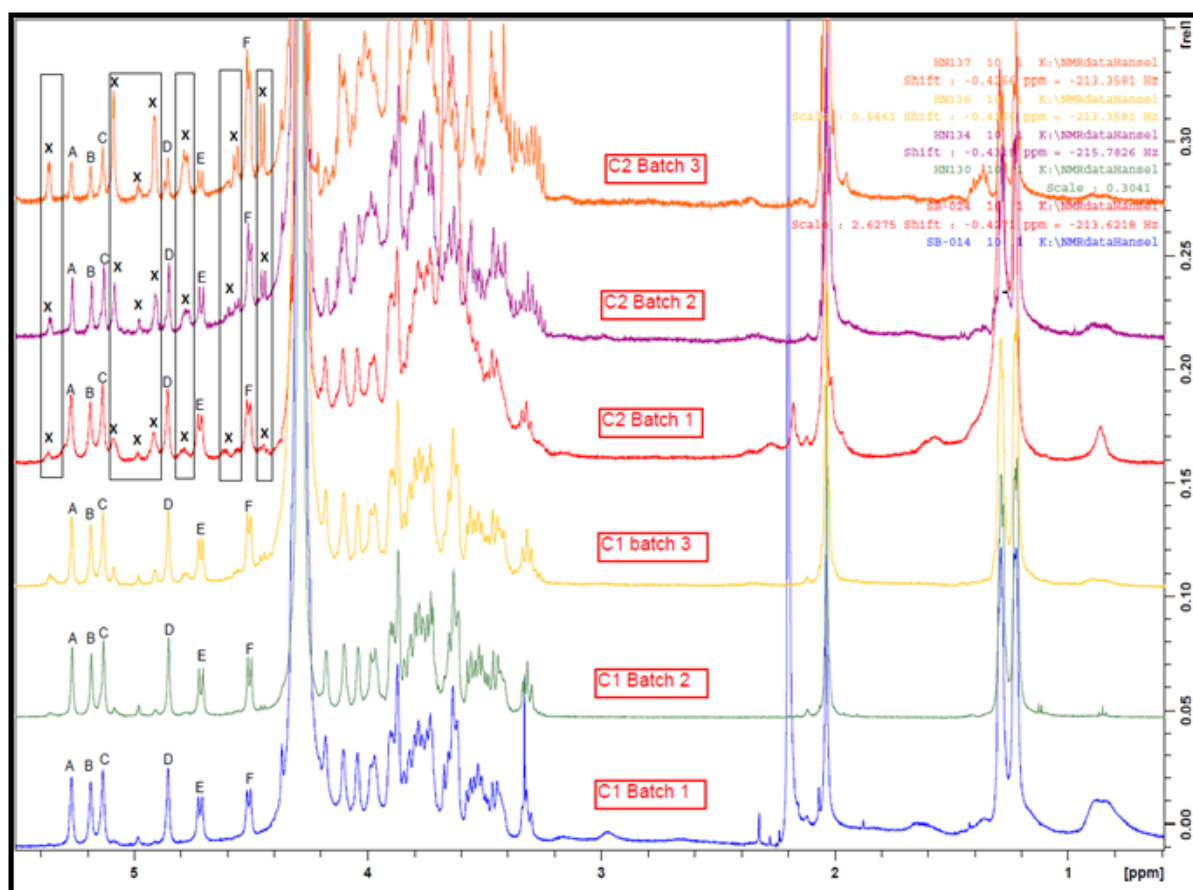


Figure 3.1. $^1\text{H-NMR}$ Spectra for C1 and C2 Precipitated from *L. paracasei* DG Grown in MRS Broth from Batches 1, 2 and 3

For the culture of *L. paracasei* DG grown on HBM, which is free of EPS-equivalents, the S2, and C2 fractions were isolated then dialysed, freeze-dried and weighed. The amount of EPS and CPS of *L. paracasei* DG produced varied from batch to batch (table 3.2). It was noted that the addition of one volume of absolute ethanol did not precipitate any significant amount of C1s and S1s in these batches but after the addition of the second volume, both S2 and C2 fractions were isolated (as seen in table 3.2).

The precipitates (S2 and C2) were found to contain polysaccharides with similar NMR profiles to the C1 fraction isolated from MRS but with a significant minor impurity. The cells obtained after separating the supernatant were treated with NaOH (1 M) as described in the case for cells extracted from the MRS broth to get the C2 (CPS). The $^1\text{H-NMR}$ spectra for the S2 and C2 fractions for *L. paracasei* DG cultured on the HBM as well as that for a control system for a

broth which had had no bacteria added (HBM control) were all processed in exactly the same way (Fig 3.2).

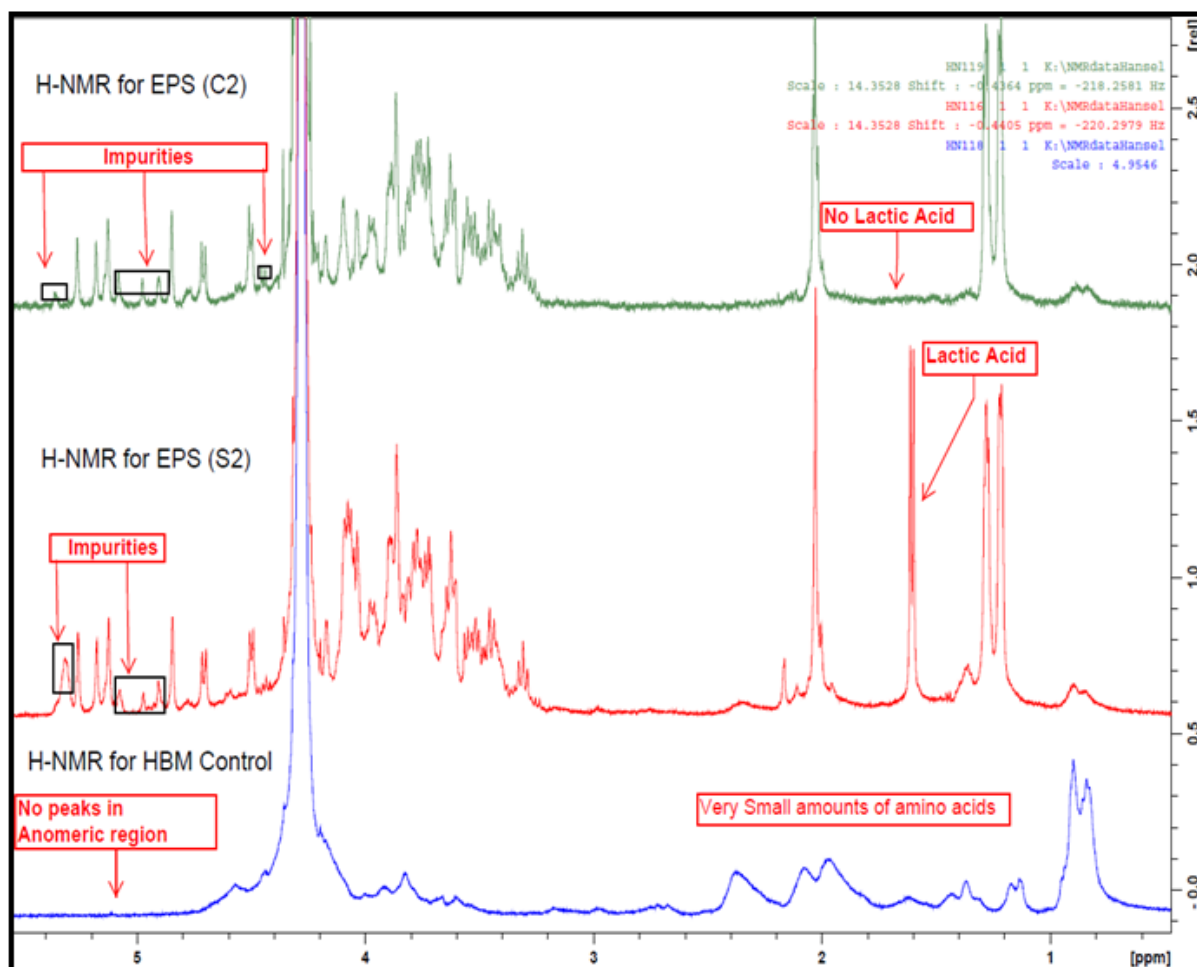


Figure 3.2. $^1\text{H-NMR}$ Spectra of the CPS (C2 top) and EPS (S2 middle) from *L. paracasei* DG as well as the S2 from HBM Control with no Bacteria (bottom).

Looking at these $^1\text{H-NMR}$ spectra in Fig 3.2 (for the control, EPS and CPS of the DG), it is clear that the only significant difference between the C2 and S2 materials is in the level of the lactic acid peak. This lactic acid peak results from the fact that this *L. paracasei* DG is a lactic acid producing bacteria and this suggests that the dialysis process might have not effectively removed the lactic acid completely. The absence of peaks in the anomeric region for the control medium confirms the fact that the HBM used for the polysaccharide extraction process is free of EPS-equivalent although it shows presence of small amounts of amino acids probably coming from the medium, which does not interfere with the polysaccharide characterisation. Inspection of the minor peaks in the $^1\text{H-NMR}$ spectra for both S2 and C2

fractions suggests that a second but minor polysaccharide is also extracted along with the main components.

The CDM broth was also used to grow a culture of *L. paracasei* DG but its growth was visually slower than those witnessed with MRS and the HBM broths. The visual growth rate was based on the length of time it took for the broth to become cloudy indicating bacteria growth. The CDM broth was known to be free of EPS-equivalence as neither beef extract nor casein were used and it was easier to prepare, as none of the ingredients required any treatment as was the case with HBM. After the growth of the bacteria, the supernatant and the cells were separated and both S and C fractions extracted accordingly. After the addition of one volume of chilled absolute ethanol and subsequent addition of the second volume to the supernatant, no precipitate was extracted and consequently no S1 nor S2 fractions could be collected. The separated cells were then treated with NaOH (1M) and the C1 and C2 fractions extracted (batches 7 and 8). The proton NMR for these CPSs (C1 and C2 fractions) were recorded (*Fig 3.3*). The C1 fractions (batch 7 and 8) showed very weak signals in contrast to the C2 fractions which showed strong peaks indicating the 6 anomeric signals as expected. The latter result is quite surprising given that the amount of C1 fractions extracted were significantly higher compared to those of the C2 fraction (table 3.2)

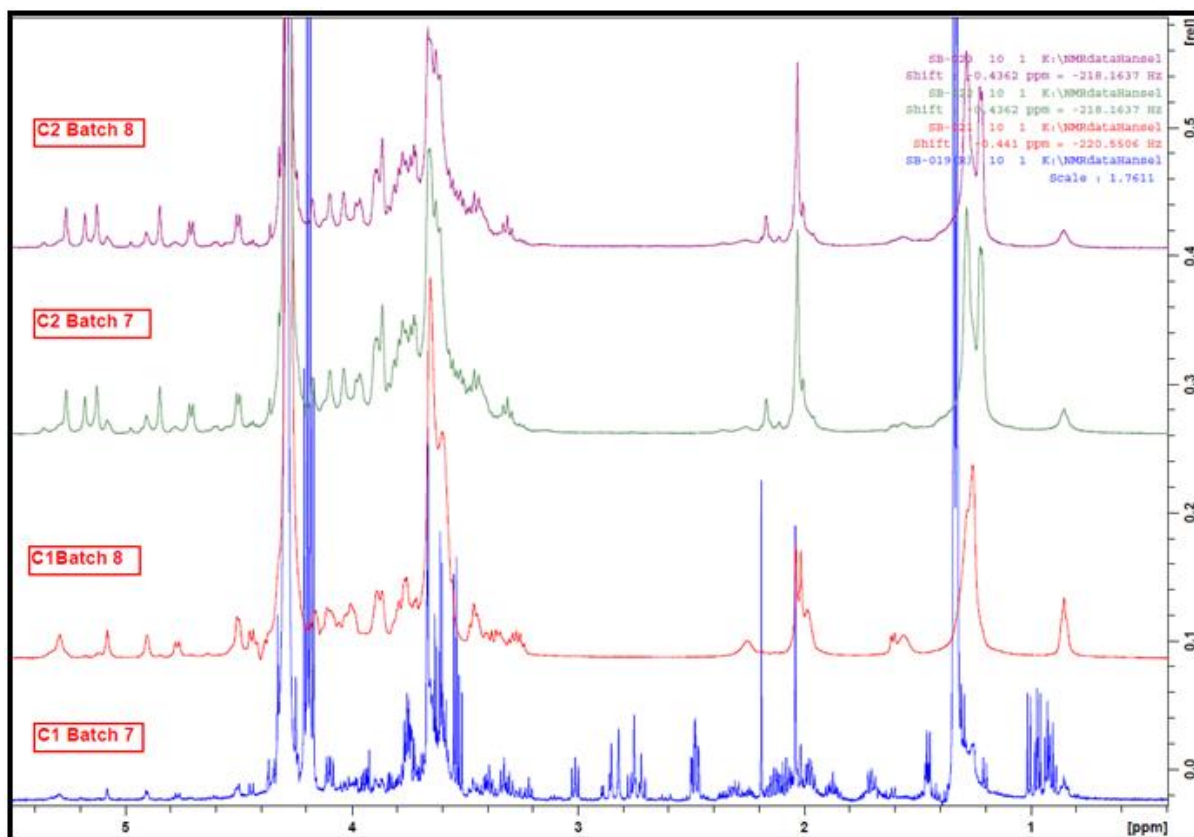


Figure 3.3. ^1H -NMR Spectra for C1 and C2 Precipitated from *L. paracasei* DG Grown in CDM Broth from Batches 7 and 8

From the three different media, the fractions that contained the cleanest polysaccharide sample was the C1 fraction extracted from the bacteria grown in MRS broth and this was then used to determine polysaccharide structure (*Fig 3.4*)

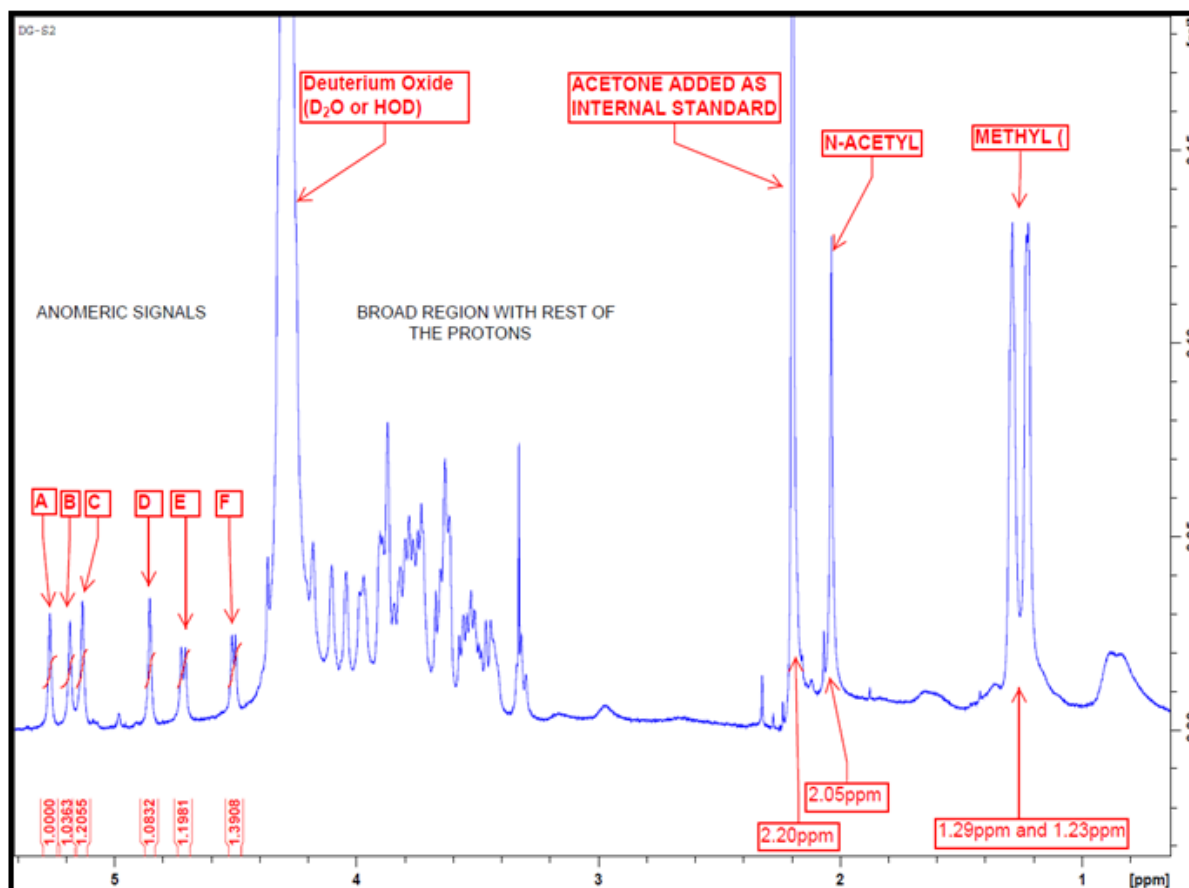


Figure 3.4. $^1\text{H-NMR}$ Spectrum of the CPS from *L. paracasei* DG

In the $^1\text{H-NMR}$, there are six anomeric signals in the low field region of the spectrum (Fig 3.4, A-F) with each of these signals having approximately the same peak integrals when taking into consideration the error within the experiments. These six anomeric signals indicated that the CPS (C2) has a repeating unit which contains six monosaccharides linked together to form the polysaccharide chain. Signals A to D which displayed a single peak implied they were alpha (α) anomeric sugar units whereas signals E and F which were doublet peaks implied they were beta (β) sugar units. Acetone (0.1 μl) was added to the sample as an internal standard which is a peak at a chemical shift of 2.20 ppm in D_2O (Fig 3.4). Also, a single resonance is visible at a chemical shift of 2.05 ppm which indicates that an *N*-acetylhexosamine is present and in addition the 2 sets of overlapping doublets at 1.29 ppm and 1.23 ppm which integrate to 6 protons indicates the presence of four 6-deoxyhexoses in the repeat unit.

3.2.1. Molecular Weight Determination of *L. Paracasei* DG using HP-SEC-MALLS

Firstly, the accuracy of the of the instrument HP-SEC-MALLS was verified using pullulan a standard homopolysaccharide material having a known molecular weight and low

polydispersity which consist mainly of glucose units. The pullulan standard used in this experiment is known to have the molecular weight of $800,000 \text{ gmol}^{-1}$ with a value of 1.23 for polydispersity and 0.148 mL g^{-1} for dn/dc as described in literature²⁵⁶. When a 1000 ppm solution of a pullulan standard was ran on the HP-SEC-MALLS at a flow rate 0.7 ml/min using NaNO_3 (0.1 M) as the mobile phase, the single peak was eluted (Fig 3.5) having a molecular weight (M_w) of 807600 gmol^{-1} with a polydispersity (M_w/M_n) of 1.07 confirming the accuracy of the instrument. This showed the capability of the HP-SEC-MALLS in determining the accurate and precise molecular weights of neutral polysaccharides.

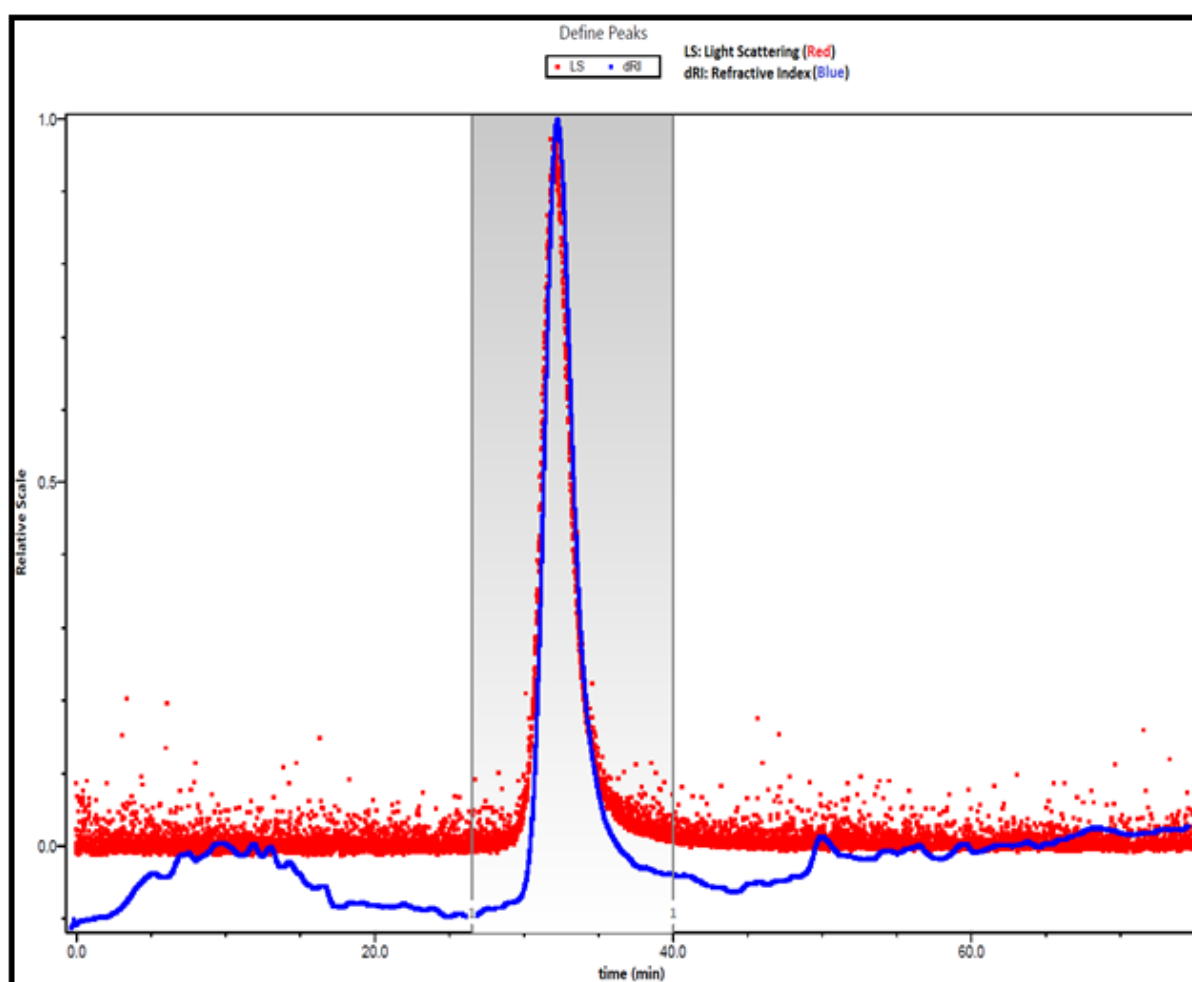


Figure 3.5. Chromatogram of the 1000 ppm Pullulan Standard with M_w of 800,000

With the accuracy and precision of the SEC-MALLS being confirmed with standard pullulan, the C1 for batch 2 of the *L. paracasei* DG was analysed. A single peak was eluted for the light scattering (Fig 3.6) having a M_w of $2.98 \times 10^5 \text{ gmol}^{-1}$ (298000 gmol^{-1}) and a narrow polydispersity of 1.03. When observing the refractive index, it gives 2 peaks in blue (Fig 3.6)

with the second peak having a M_w of $4.69 \times 10^4 \text{ gmol}^{-1}$ (46900 gmol^{-1}) and a narrow polydispersity of 1.20. This SEC-MALLS trace for the DG strain shows that the EPS is composed of a high molecular weight (HMw) and a medium molecular weight (MMw) material. No traces of the UV indicate that no proteins are present in the extracts, which confirms its purity. The fluctuations which occur in the yields of the polysaccharides between batches is as a result of the instability in the production of the polysaccharide production as well as the length of time taken for the fermentation process ²⁵⁷.

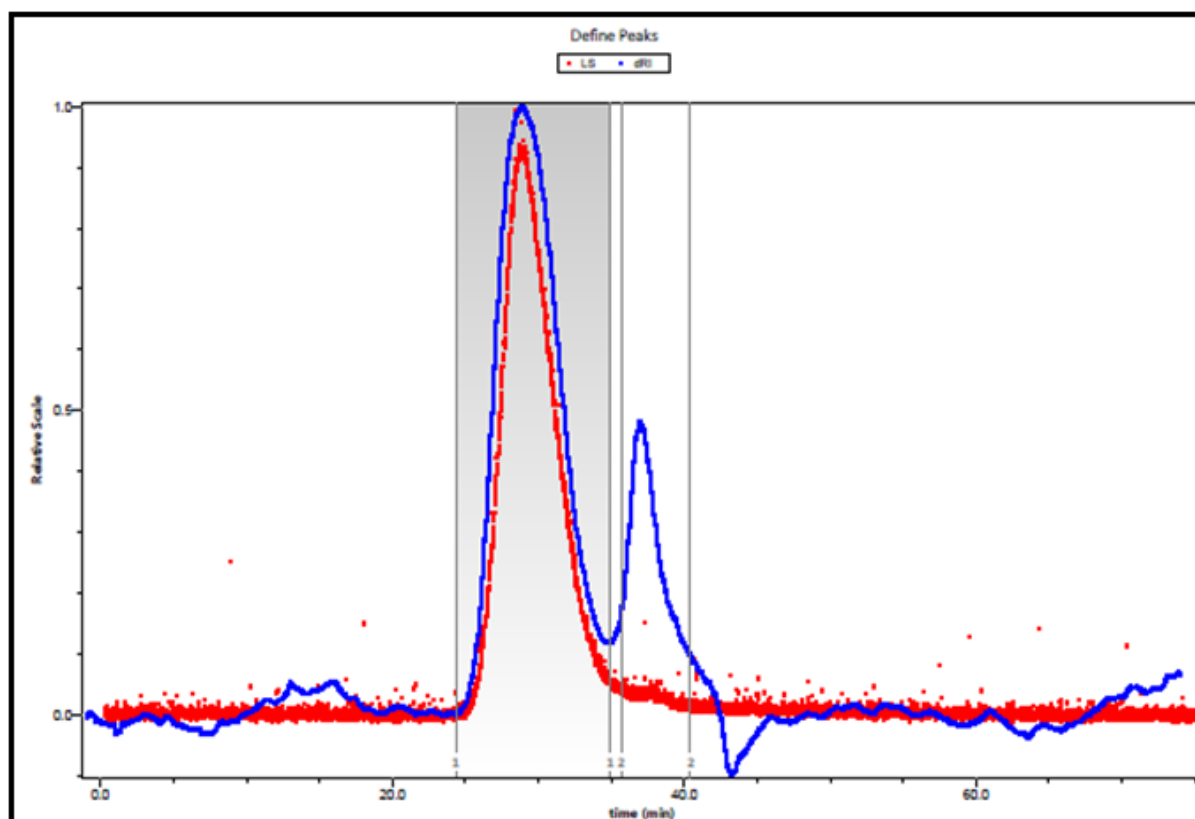


Figure 3.6. SEC-MALLS Trace of the *L. paracasei* DG - Batch 2

3.2.2. Monomers and Linkage Analysis of the Monosaccharides in the Repeating Unit Structure of *L. paracasei* DG.

3.2.2.1. Monomers analysis of the *L. paracasei* DG polysaccharides using HPAEC-PAD and GC-MS

During monomer analysis, after hydrolysis of the polysaccharide as described in section 2.8.4.1 the results from the HPAEC-PAD analysis gave three distinct peaks, which

corresponded to rhamnose, galactose and galactosamine, and a tiny peak corresponding to the *N*-acetylgalactosamine (Fig 3.6a). These peaks were matched according to their standards and considering their retention times for the individual peaks using an overlaid chromatogram of all the standards involved (included in Fig 3.6a at top right).

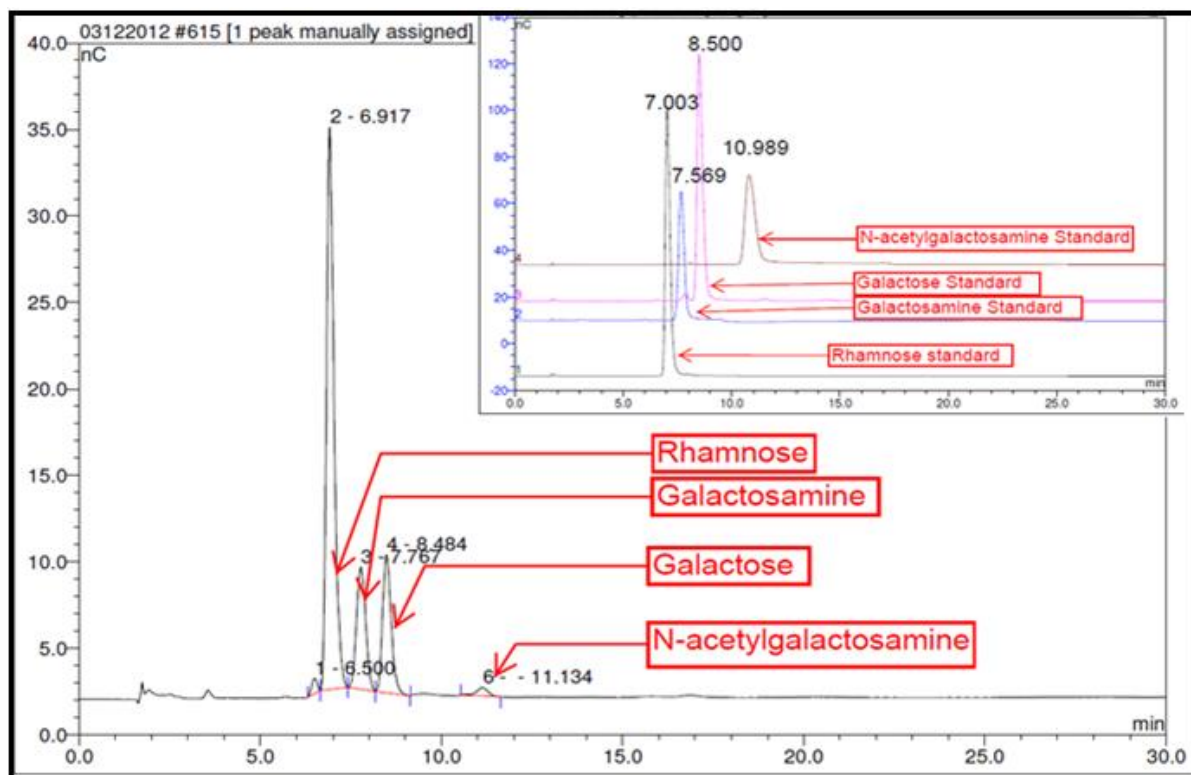


Figure 3.6a. HPAEC-PAD chromatogram of the polysaccharide from *L. paracasei* DG compared with their various monomeric units identified (rhamnose, galactose, galactosamine and *N*-acetylgalactosamine) compared with standards (top right) for identification.

The tiny traces of the *N*-acetyl-galactosamine and the presence of the galactosamine indicates that the monomer could definitely be the *N*-acetylgalactosamine, whose acetyl group drops off after hydrolysis to become the galactosamine. The *N*-acetylgalactosamine will be confirmed in the GC-MS results that follows as well as in the 2D NMR data analysis. The GC-MS results showed the presence of rhamnose, galactose and *N*-acetylgalactosamine in the repeating unit (Fig 3.7) which, will be further confirmed with the 2D-NMR analysis.

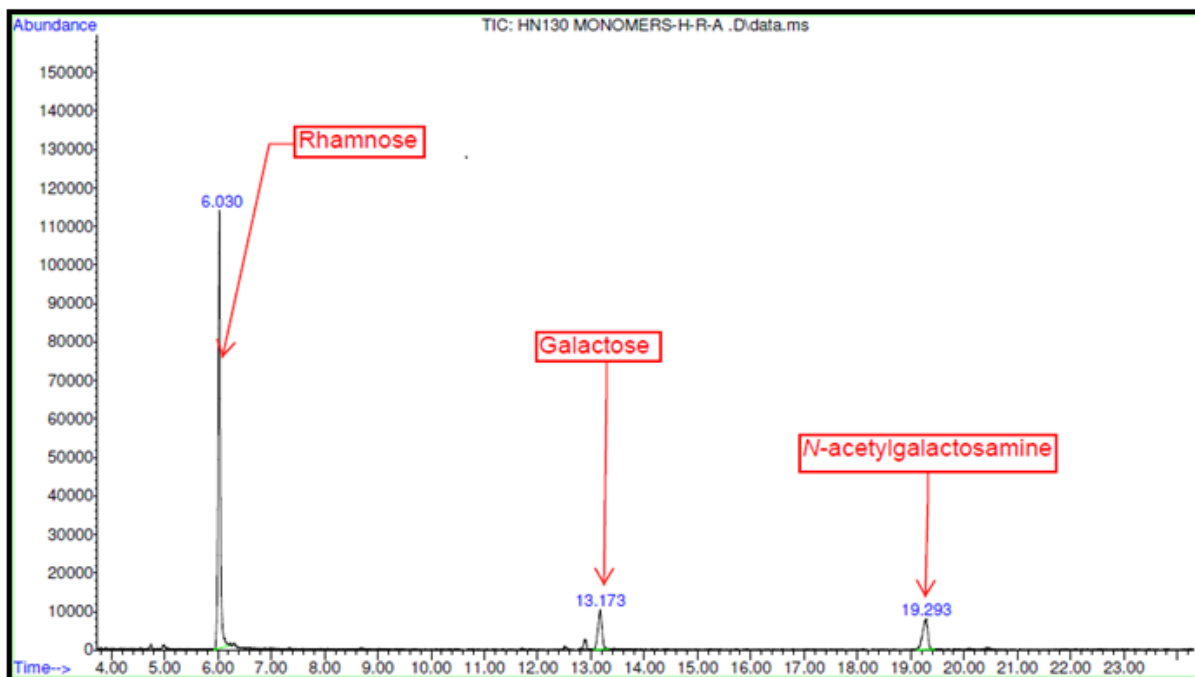


Figure 3.7. Chromatogram for the Alditol Acetates of the Sugars obtained from the GCMS for Monomer Analysis of *L. paracsei* DG.

The mass spectra of these peaks (Figs 3.7a, 3.7b and 3.7c) were used to identify the presence of 1,2,3,4,5-penta-*O*-acetyl-L-rhamitol, 1,2,3,4,5,6-hexa-*O*-acetyl-d-hexitol (galactose) and 2-acetyl-*N*-amino-1,3,4,5,6-penta-*O*-acetyl-2-deoxy-d-hexitol (*N*-acetylgalactosamine) in the ratio 4:1:1. The retention times and mass spectra of the commercially available standards of these various sugars were obtained from the GC-MS (using the alditol acetate method) to further confirm these sugar units previously identified with the HPAEC-PAD analysis. The mass spectra of these sugar units were also confirmed with those found in literature (Biermann and McGinnis, 1989)²⁰⁷.

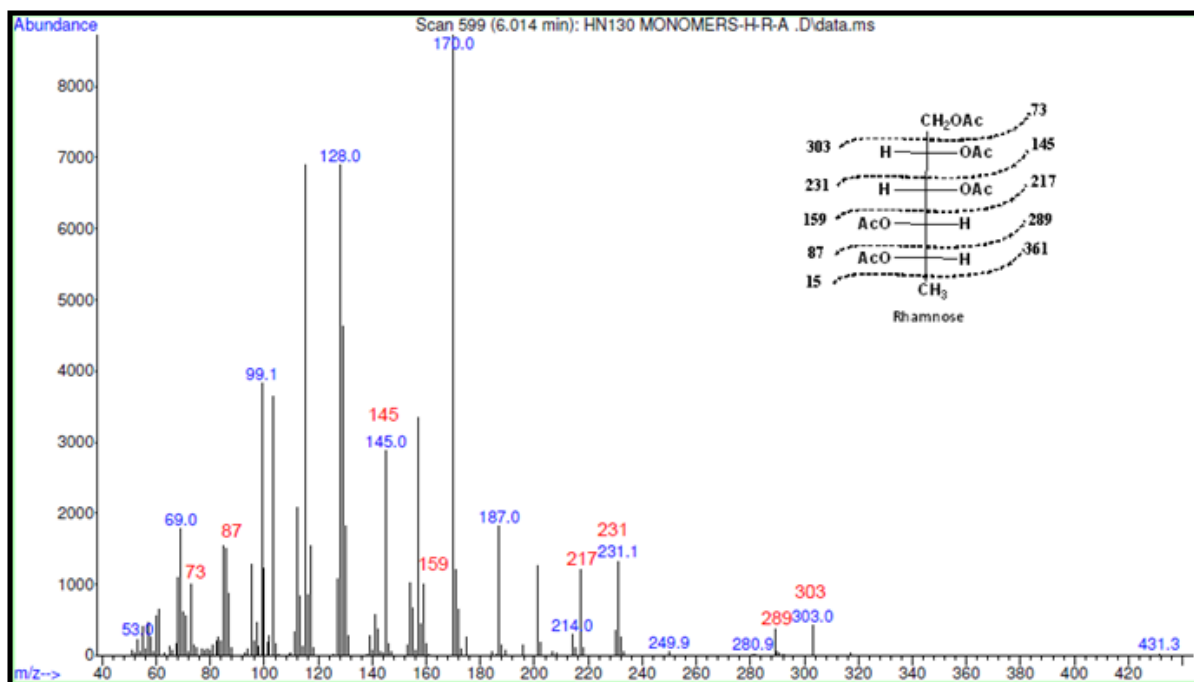


Figure 3.7a. Mass spectrum of Rhamnose in the Sample (*L. paracasei* DG) and its Fragmentation Pattern

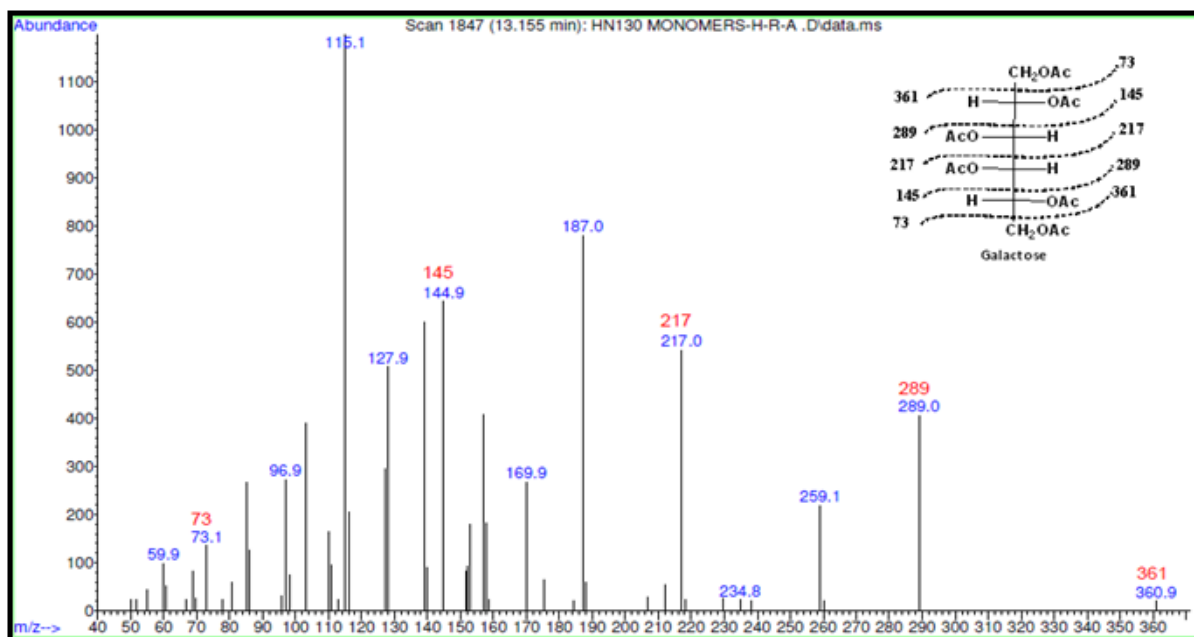


Figure 3.7b. Mass spectrum of Galactose in the Sample (*L. paracasei* DG) and its Fragmentation Pattern

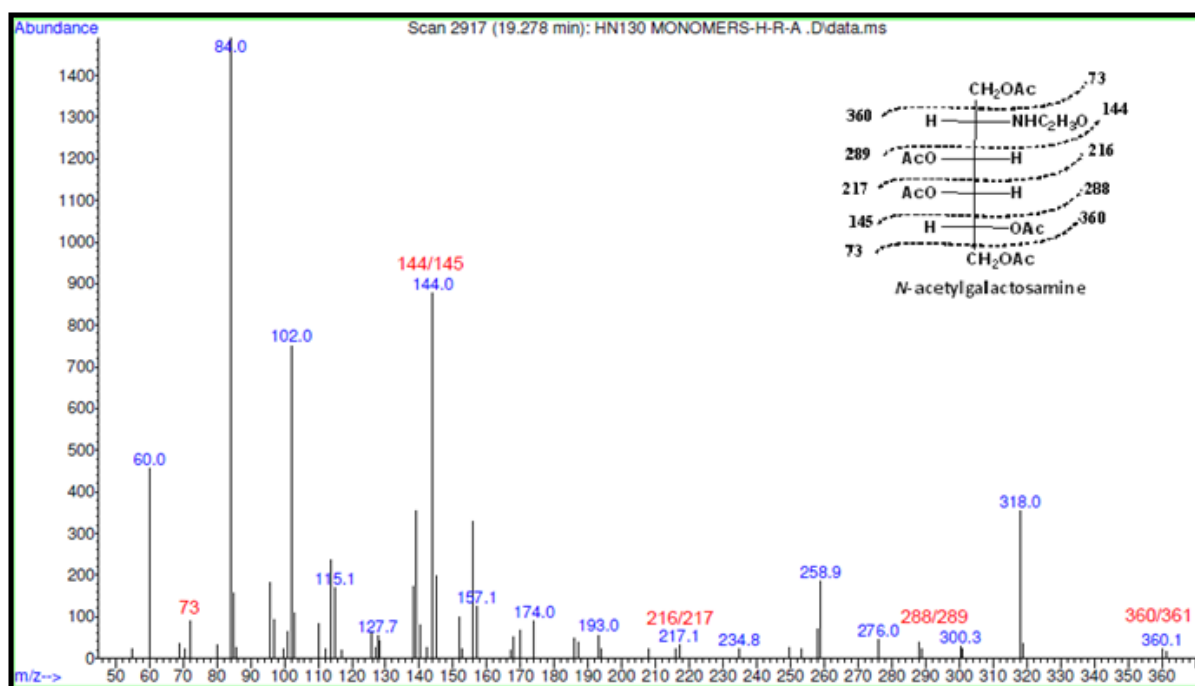


Figure 3.7c. Mass spectrum of *N*-acetylgalactosamine in the Sample (*L. paracasei* DG) and its Fragmentation Pattern

3.2.2.2. Linkage Analysis of the *L. paracasei* DG Polysaccharides using the Methylated Alditol Acetate Method.

The linkage analysis generated the methylated alditol acetates which include a 1,5-di-*O*-acetyl-2,3,4,6-tetra-*O*-methylhexitol which confirms the terminal hexose (galactose) sugar, a 1,3,5-tri-*O*-acetyl-2-acetyl-*N*-amino-4,6-*O*-dimethyl-2-deoxyhexitol which confirms the 1,3-linked pyranose *N*-acetylhexosamine, two 1,2,5-tri-*O*-acetyl-3,4-di-*O*-methyl-6-deoxyhexitol which confirms two of the 6-deoxysugars to be 1,3-linked monomers, a 1,3,5-tri-*O*-acetyl-2,4-di-*O*-methyl-6-deoxyhexitol which confirms the 1,2-linked deoxysugar and finally a 1,2,3,5-tetra-*O*-acetyl-4-*O*-methylhexitol which confirms the 1,2,3-linked deoxysugar that forms a bridging point in the repeating unit. This linkage is confirmed by comparing the mass spectra of the peaks obtained from linkage analysis to those found in the literature ¹⁹⁴as well as its fragmentation patterns (*Fig 3.8a to Fig 3.8e*). The GC trace for the linkage analysis (*Fig 3.8*) shows five distinct peaks which is then followed by their MS (*Fig 3.8a –Fig 3.8e*)

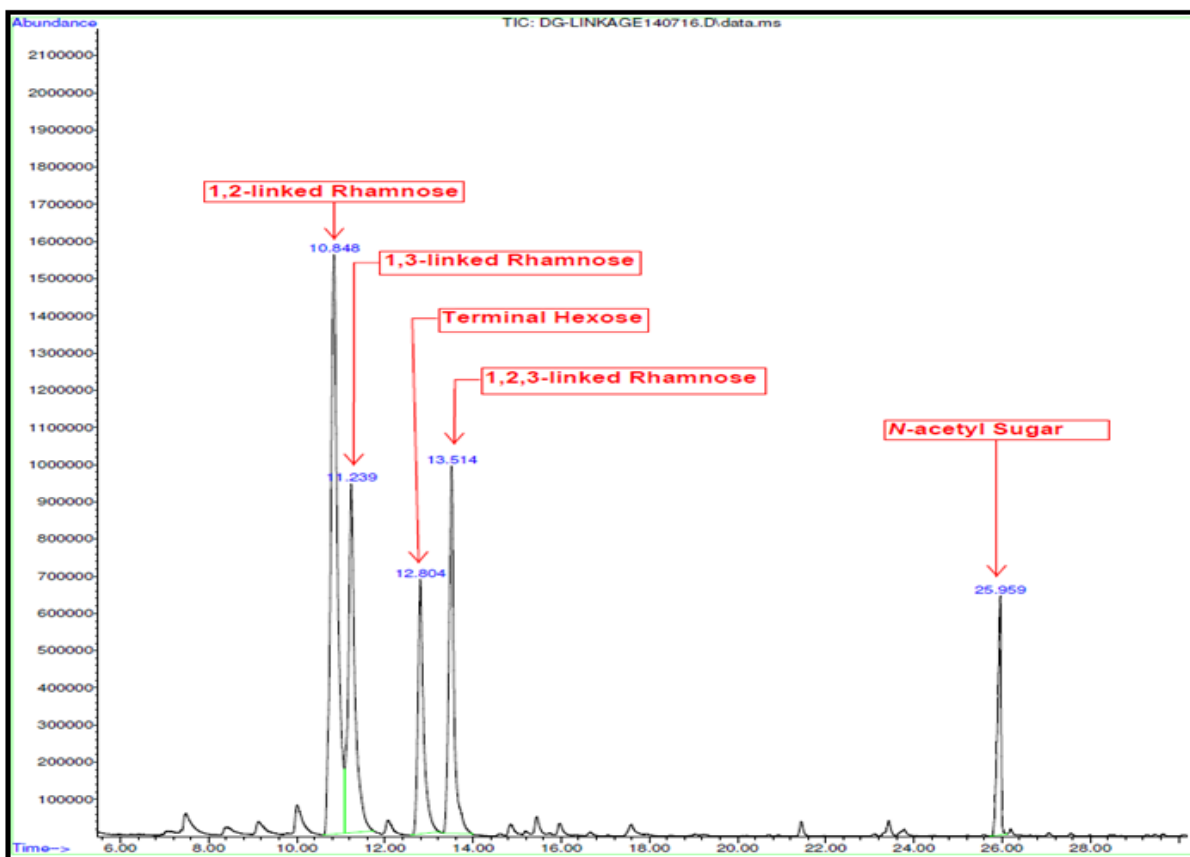


Figure 3.8. Chromatogram for the Methylated Alditol Acetates of the Sugars obtained from the GC-MS for Linkage Analysis of *L. paracasei* DG

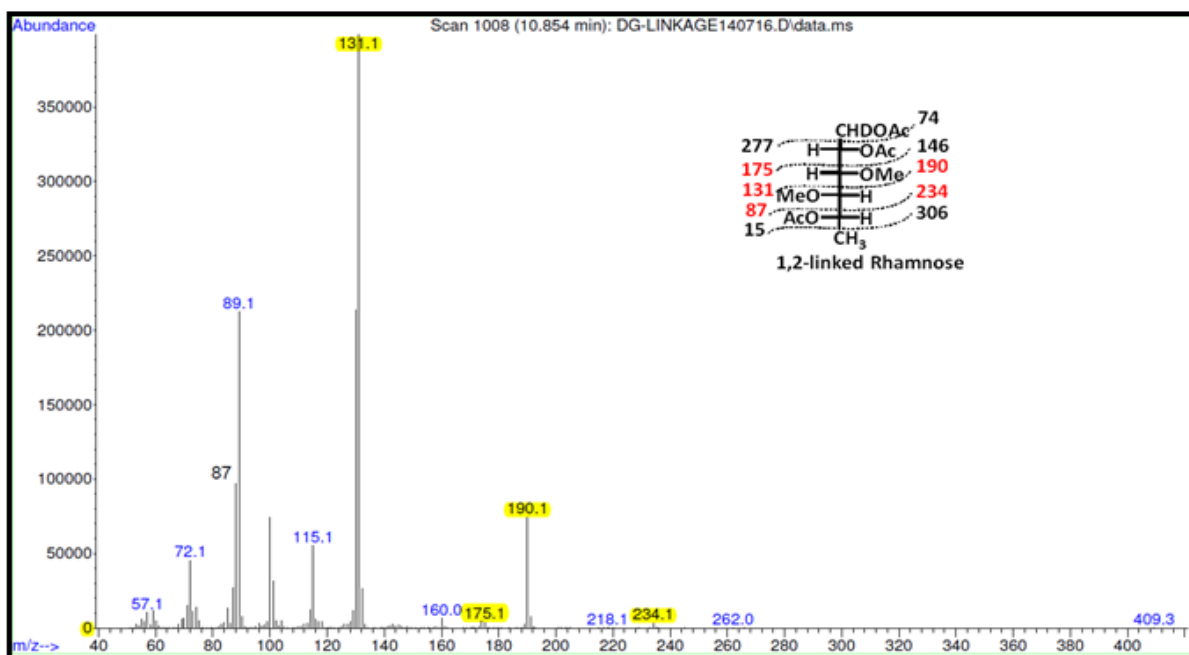


Figure 3.8a. Mass Spectrum of 1,2,5-tri-*O*-acetyl-3,4-di-*O*-methyl-6-deoxyhexitol and its Fragmentation pattern which indicates it is a 1,2-linked Rhamnose.

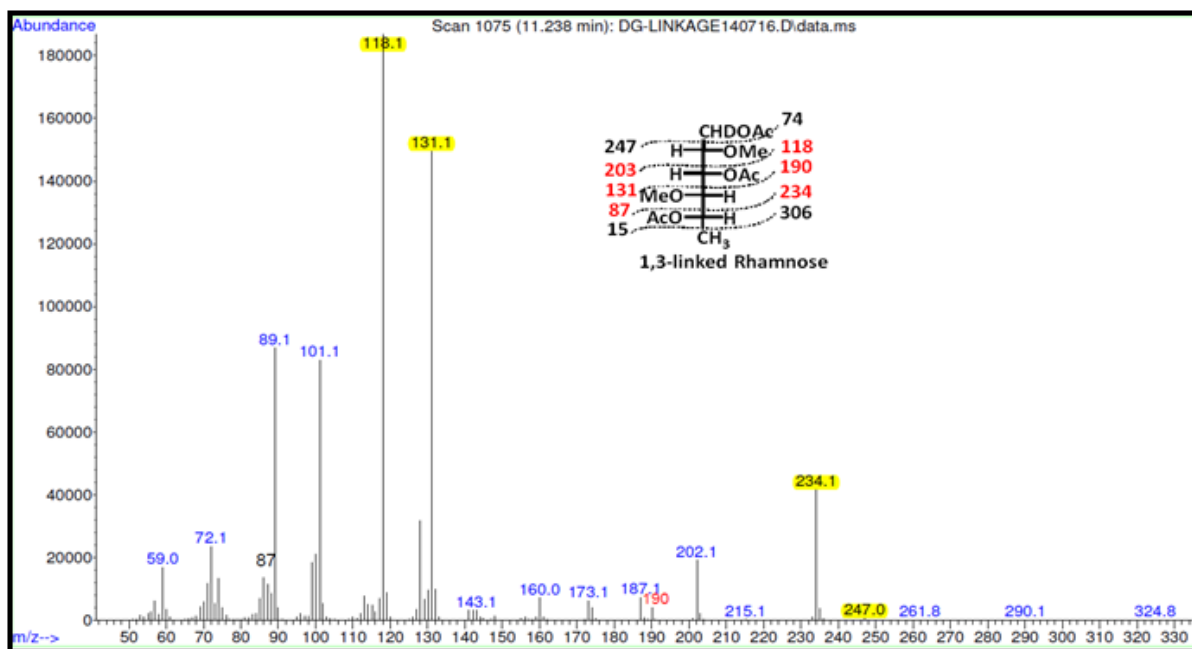


Figure 3.8b. Mass Spectrum of 1,3,5-tri-*O*-acetyl-3,4-di-*O*-methyl-6-deoxyhexitol and its Fragmentation Pattern which indicates it is a 1,3-linked Rhamnose.

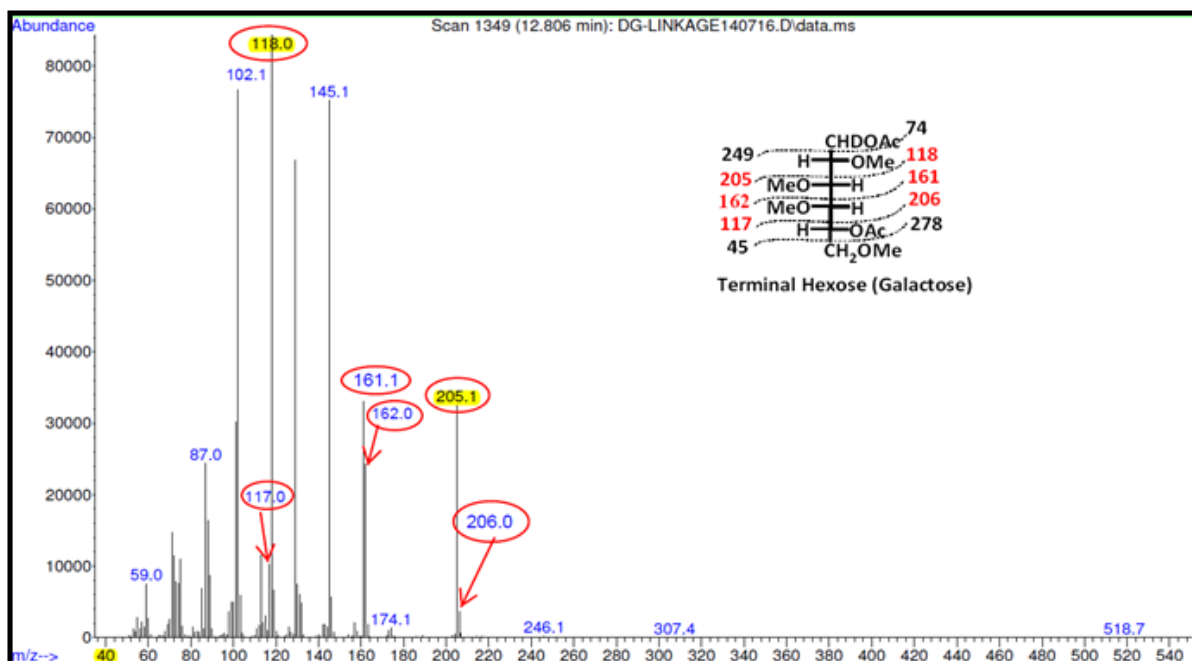


Figure 3.8c. Mass Spectrum of 1,5-di-*O*-acetyl-2,3,4,6-tetra-*O*-methyl-6-deoxyhexitol and its Fragmentation Pattern which indicates it is a Terminal Hexose (galactose).

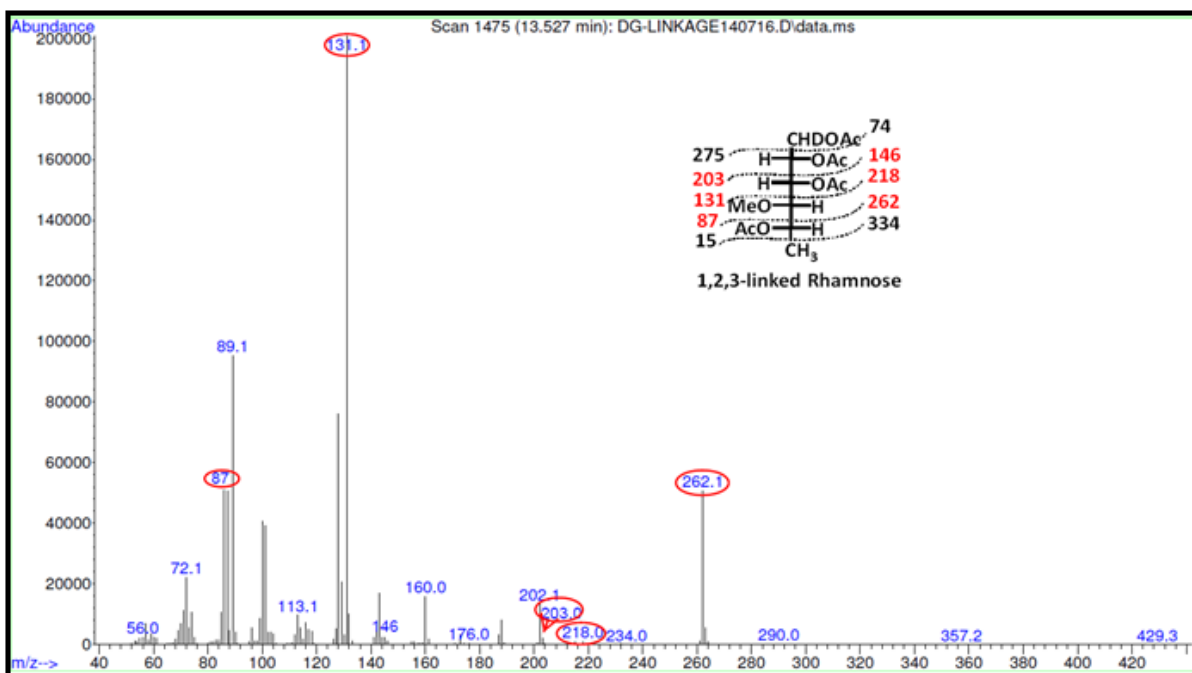


Figure 3.8d. Mass Spectrum of 1,2,3,5-tetra-*O*-acetyl-4-*O*-methyl-6-deoxyhexitol and its Fragmentation Pattern which indicates it is a 1,2,3-linked Rhamnose

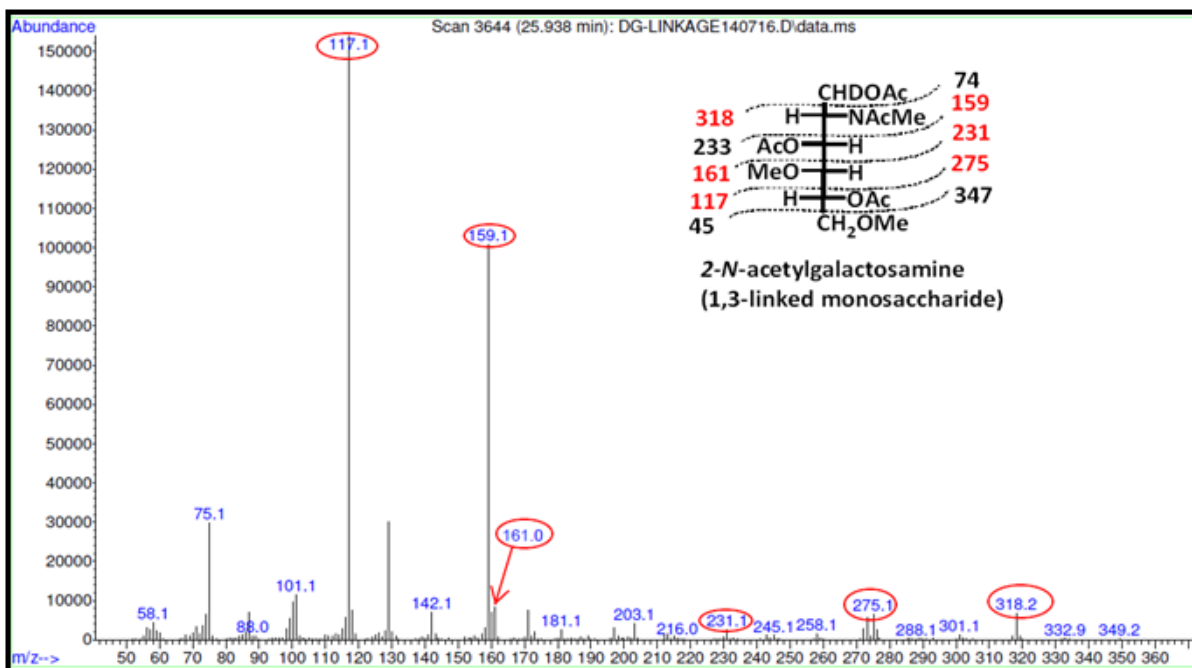


Figure 3.8e. Mass Spectrum of 1,3,5-tetra-*O*-acetyl-2-(acetylmethylamino)-2-deoxy-4,6-di-*O*-methylhexitol and its Fragmentation Pattern which indicates it is a 1,3-linked 2-*N*-Acetylgalactosamine.

3.2.2.3. Absolute Configuration of the Polysaccharide of *L. paracasei* DG

After the preparation of the acetylated butyl glycosides as described in section 2.8.7, the absolute configuration of the various substituent monomeric units in the polysaccharide isolated from *L. paracasei* DG were determined using the GC-MS. The identification of all the bacterial polysaccharides up to date have always shown the rhamnose to have the L-configuration given that they naturally occur in this configuration whereas the other neutral sugars such as the glucose, galactose and the amino sugars have always expressed their D-configurations. Despite these, it is still necessary for the absolute configuration of the various monomeric substituents to be determined for the full communication and validation of the repeated unit structure. The chromatogram showed several distinct peaks (Fig 3.9) from which their identification was determined by comparing them with acetylated butyl ((S)-(+)-butanol) standards of L-rhamnose, D-galactose, and D-N-acetylgalactosamine (Fig 3.9a).

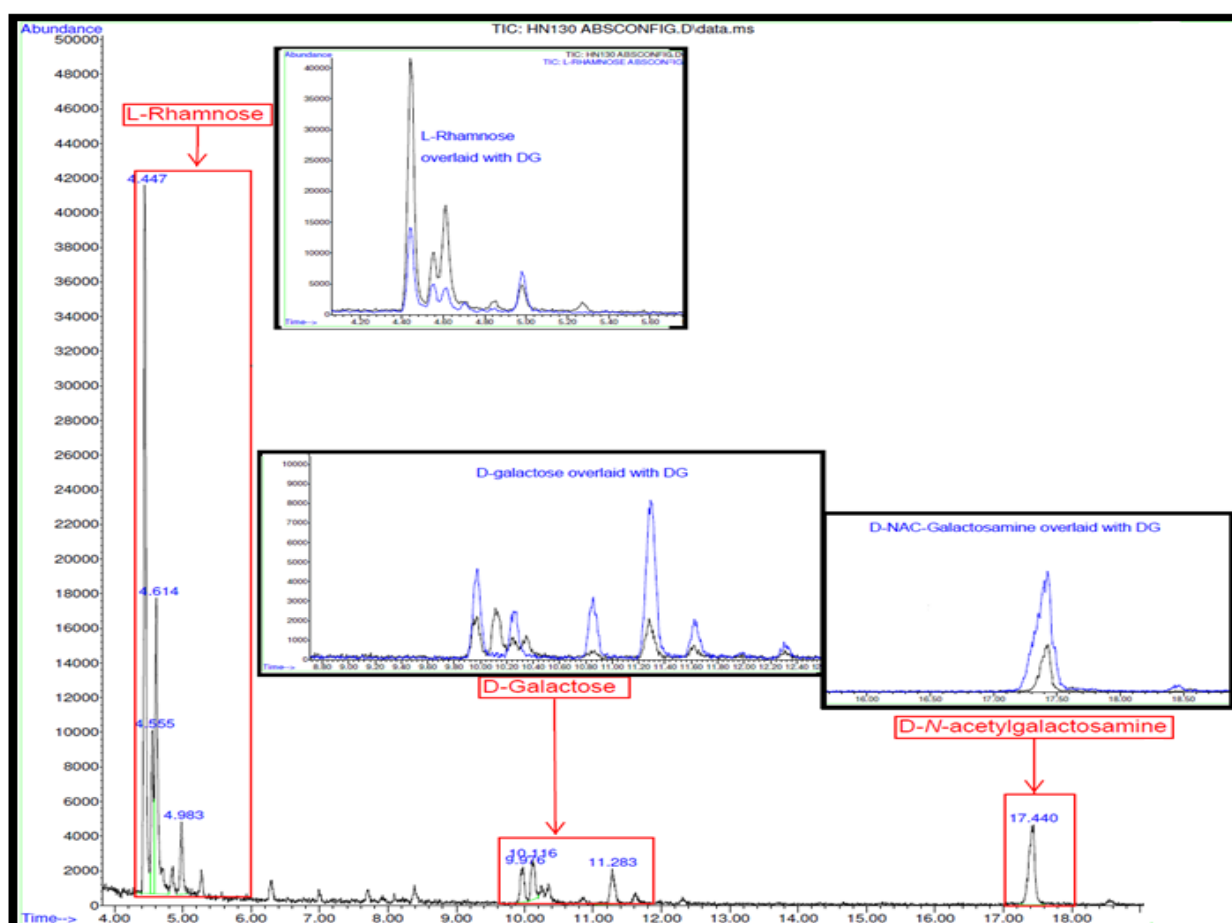


Figure 3.9. The Chromatogram of the Distinct peaks of the Acetylated Butyl Polysaccharide of *L. paracasei* DG and the overlaying of these peaks with Standards of Acetylated Butyl ((S)-(+)-2-butanol) *L-rhamnose*, *D-galactose* and *D-N-acetylgalactosamine*.

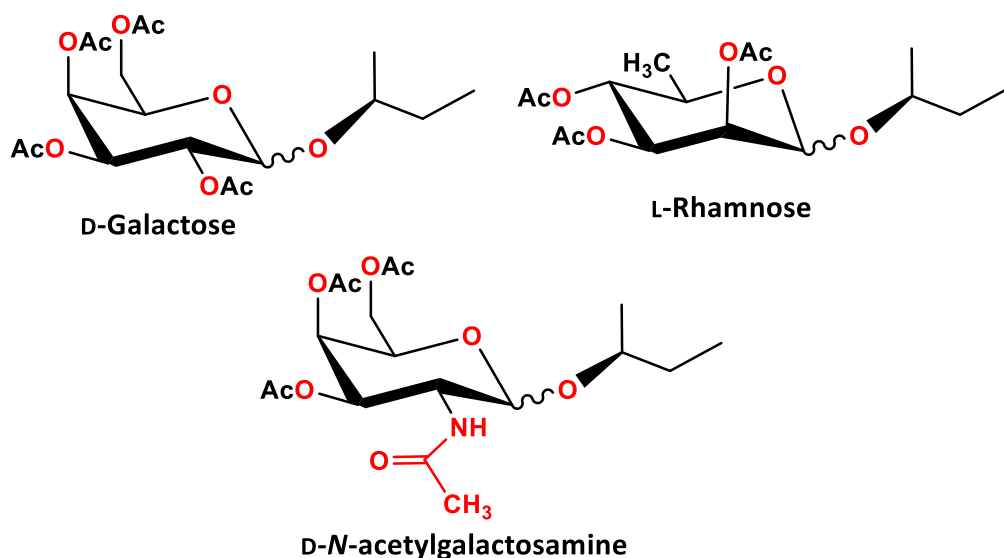


Figure 3.9a. Standard structures of the Acetylated butyl ((S)-(+)-2-butanol) D-galactose, L-rhamnose and the D-N-acetylgalactosamine.

As the (S)-(+)-2-butanol bonds to α and β anomers of the monomeric unit, two peaks are generated for each of these monomers which can be seen for the absolute configuration of *L. paracasei* DG (Fig 3.9). These sets of peaks are overlaid with the various acetylated butyl standards (Fig 3.9) as well as comparing their mass spectra with those of already stored standards in the library to confirm their absolute configurations. After converting the monomeric units to their 2-butyl glycoside epimers, all the rhamnose were confirmed to be of L-absolute configuration whereas those for galactose and N-acetylgalactosamine were confirmed to be of D-absolute configuration.

3.2.3. Usage of 1D and 2D-NMR in Determining the Sequence of the Monomers in the Repeated Units of *L. paracasei* DG

A series of the 1D and 2D-NMRs were used to obtain the chemical shifts of each of the protons and carbons found in the repeat unit and these are listed in table 3.3. Using a combination of ^1H - ^1H COSY (blue contours in Fig 3.9b) and ^1H - ^1H TOCSY (red contours in Fig 3.9b), the scalar coupling within the individual sugars were tracked from the anomeric protons listed in decreasing order of chemical shifts and labelled **A** to **F** (Fig 3.4). The positions of the protons in the rhamnose sugars (A, B, C and D) have their H1 to H6 identified as well as the H1 to H4 of the galactose and N-acetylgalactosamine monomers in (Fig 3.9b) and their chemical shifts listed in table 3.3.

Table 3.3: Chemical shifts for C and H of the 6 sugars (A-F)

Position	A	B	C	D	E	F
H1	5.30	5.21	5.15	4.87	4.72	4.53
C1	102.6	102.2	102.4	102.5	103.5	106.0
H2	4.21	4.07	4.13	3.90	4.11	3.59
C2	79.8	79.6	80.3	71.63	57.1	3.99
H3	4.01	3.91	3.86	3.79	3.65	3.60
C3	78.2	72.0	71.3	79.5	83.1	76.51
H4	3.67	3.49	3.35	3.55	3.54	3.93
C4	70.4	73.6	73.7	72.9	72.6	70.1
H5	3.82	3.77	3.66	4.02	3.45	3.53
C5	70.6	70.6	73.8	70.5	77.3	70.0
H6	1.32	1.32	1.25	1.25	3.91/3.75	3.75
C6	18.6	18.1	18.0	17.9	62.4	62.3

The points of linkages for rhamnose in this polymeric sugar units were identified by inspecting the carbon chemical shifts of their ring carbons and identifying those carbons with chemical shifts that have moved towards low field positions (above 78ppm highlighted in red in the table above) in comparison with those usually associated with unsubstituted ring positions (which for rhamnose is less than 74). This identified **A** as a 2,3-linked rhamnose (C2 =79.8 ppm, C3=78.2 ppm), **B** as a 2-linked rhamnose (C2 = 79.6 ppm), **C** as a 2-linked rhamnose (C2=80.3 ppm) and **D** as a 3-linked rhamnose (C3= 79.5 ppm). The linkage for *N*-acetylgalactosamine was already identified as a 1,3-linked through the linkage analysis as earlier seen in the linkage section (*Fig 3.8e*) which is again confirmed by the high chemical shift of **E** (C3=83.1ppm). Finally, for **F**, the chemical shifts for the carbons confirms are all high fields (less than 78ppm) which suggests that it is a terminal galactose sugar.

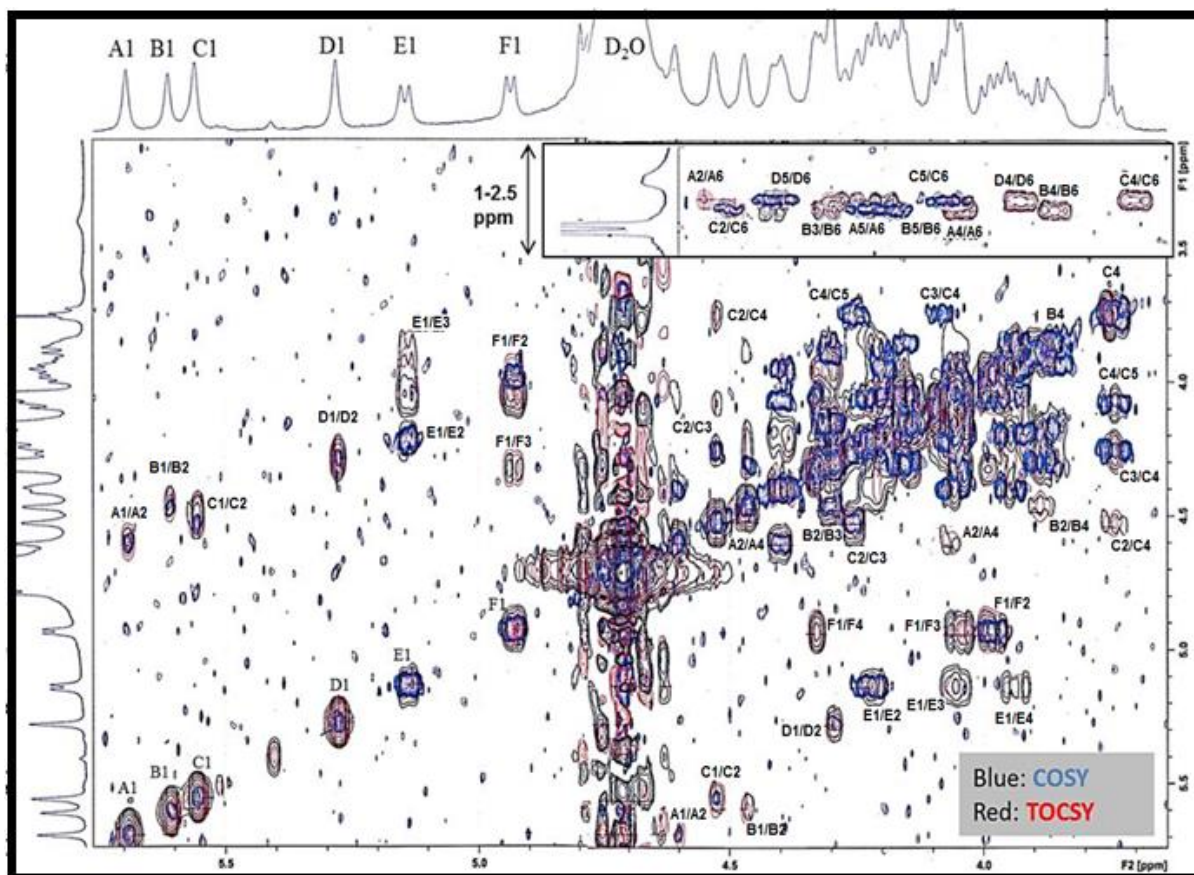


Figure 3.9b. Combination of a COSY Spectrum overlaid with a TOCSY Spectrum to identify the Position of the Ring protons. (Coupling of A to D, H1 to H6 and E, F H1 to H4; showed for illustration purposes)

In order to determine the configuration (α and β) of the monomeric sugar units, the $^1J_{C1-H1}$ coupling constants were measured which were visible on the coupled HSQC spectrum (labelled blue) overlaid with a decoupled HSQC (labelled red) (Fig 3.9c).

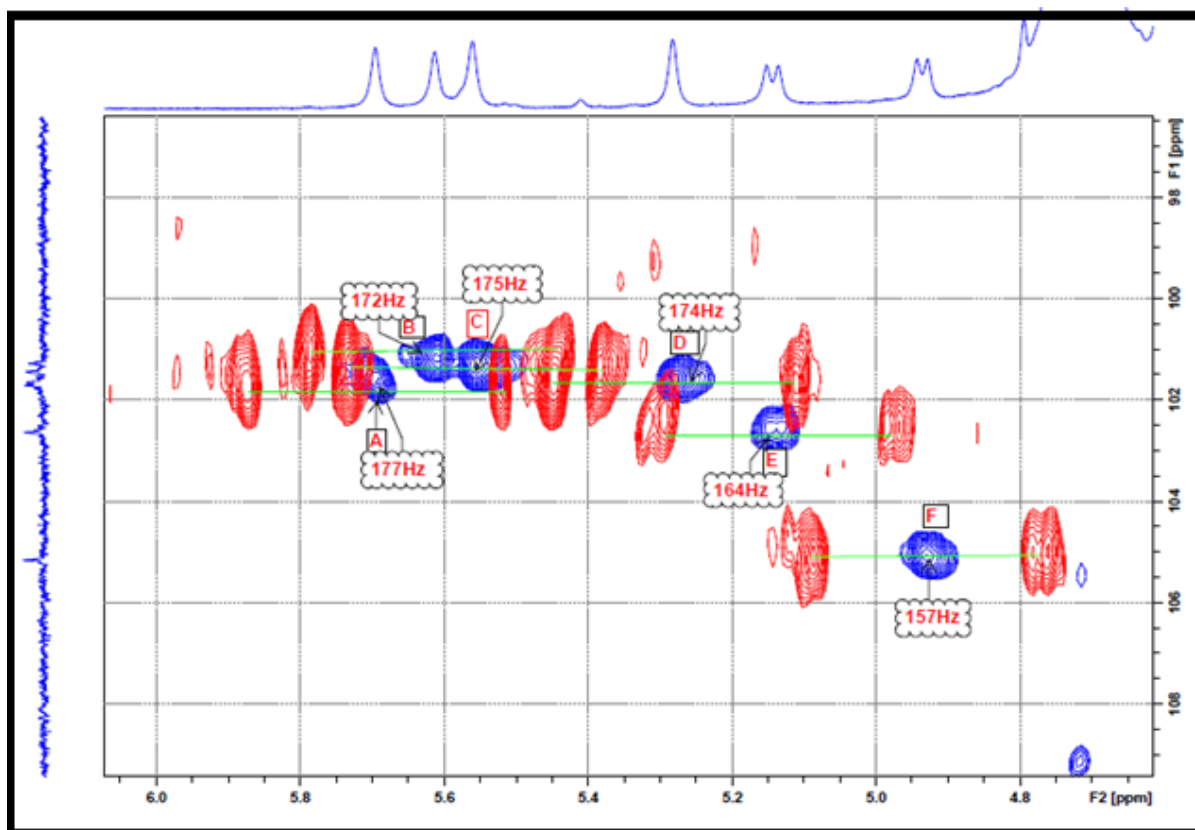


Figure 3.9c. The Coupled ^1H - ^{13}C -HSQC Spectrum Overlaid with ^1H - ^{13}C -HSQC Decoupled

Residues **A** to **D** had $^1J_{\text{C1-H1}}$ coupling constants of **A** (177 Hz), **B** (172 Hz), **C** (175 Hz) and **D** (174 Hz) which are greater than 170 Hz hence indicating that the rhamnose residues are alpha-linked whilst the size of the $^1J_{\text{C1-H1}}$ coupling constants in **E** (164 Hz) and **F** (157 Hz) implies that the *N*-acetylgalactosamine and the terminal galactose are beta-linked monomers.

The sequence of the repeating sugar units was finally established through inspection of both the ^1H - ^{13}C -HMBC spectrum (not shown) and a ^1H - ^1H -ROESY spectrum (Fig 3.10). On the ROESY spectrum inter-residue NOEs were observed between **A**-H1 & **D**-H3 confirming the **A**(1-3)**D** linkage; between **B**-H1 and **A**-H3 identifying that **B** is linked to the three position of **A**; between **C**-H1 & **B**-H2 confirming the **C**(1-2)**B** linkage; between **D**-H1 & **E**-H3 identifying a **D**(1-3)**E** linkage; between **E**-H1 & **C**-H2 identifying the **E**(1-2)**C** linkage and also between **F**-H1 & **A**-H2 confirming the **F**(1-2)**A** linkage.

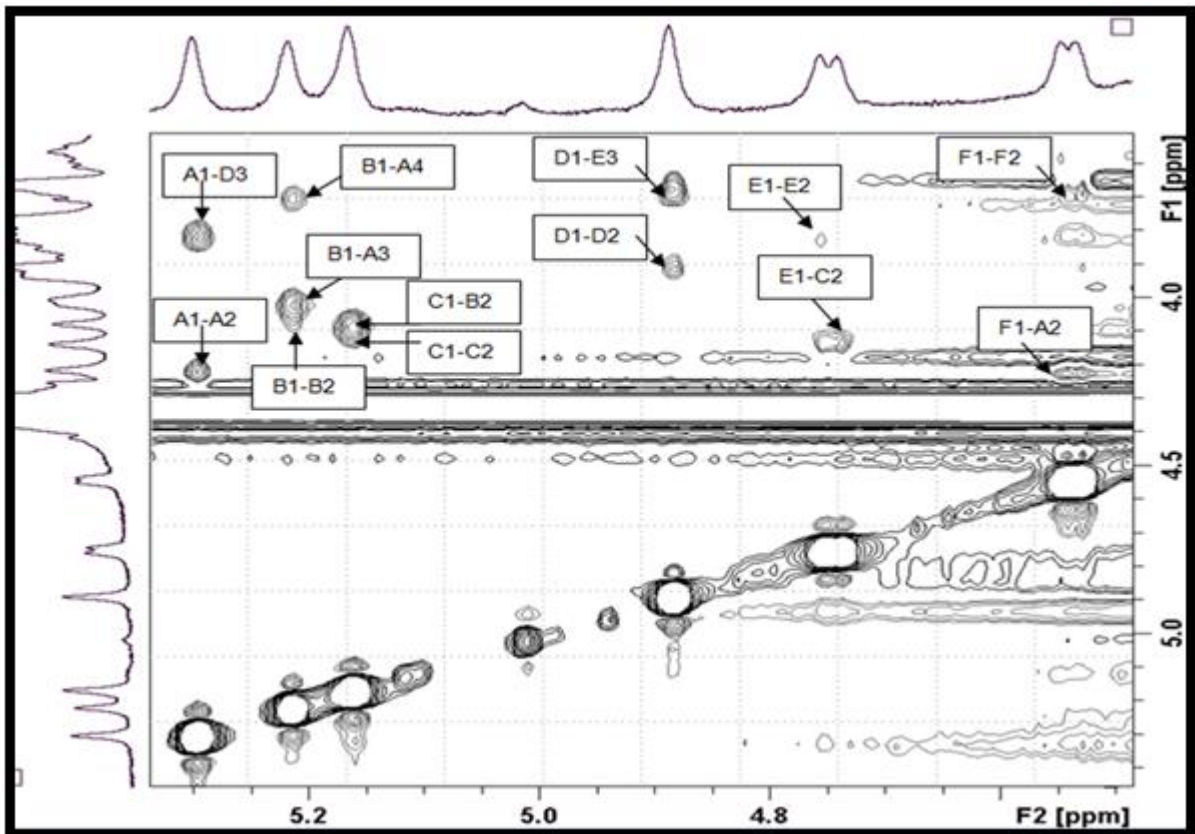
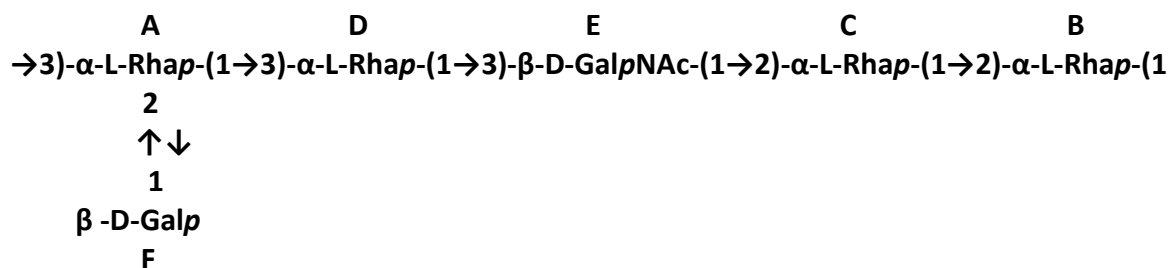


Figure 3.10. ^1H - ^1H -ROESY Spectrum Showing the Inter-residue NOES Identifying the Linkage in the Repeating unit of *L. paracasei* DG

Combining the results of the chemical and NMR analysis of the EPS isolated from the *L. paracasei* DG confirms that the EPS is a novel heteropolysaccharide having a repeated unit structure as follows:



L. paracasei DG is present in commercial probiotic products as Enterolactis® (trade name) and has been used for a number of years. Previously, the consumption of *L. paracasei* DG had been noted to provide health benefits such as maintaining remission of symptomatic uncomplicated diverticulosis, reducing the inflammation in mild colitis²⁵⁸ as well as the side effects associated with therapies targeted at *Helicobacter pylori* eradication⁸³ and after antibacterial treatment of small intestinal bacterial overgrowth^{11,83}. This novel repeated unit

structure and those of other bacteria used in a range of probiotic products are noted to be rich in rhamnose content in its polymeric back-bone²³⁵. This repeated unit structure is different from those previously published from other species of *L. paracasei* as well as those of a range of lactic acid bacteria.

3.2.4. Determination of Carbohydrate Content of Exopolysaccharide

After lyophilising the dialysed isolated polysaccharides (EPS) from the various strains (*L. paracasei* DG, the Dubois *et al*¹⁸⁵ test as described in section 2.8.2 was performed on their S2s particularly. As earlier mentioned in section 1.6.1, this Dubois' method is being widely used in determining the carbohydrate concentration in samples and has been reported to be cost effective¹⁸⁷. The higher the amount of sugar present the higher the intensity of colouration formed. A series of D-glucose standards (0 ppm, 20 ppm, 40 ppm, 60 ppm, 80 ppm and 100 ppm) were used to evaluate the amount of carbohydrate content found in the EPS and a calibration curve plotted against their absorbance readings (*Fig 3.11*). Studies have revealed that the complex developed from the reaction of the phenol-sulphuric assay has a maximum absorbance observed at 490nm¹⁸⁷ and that is why we use this wavelength in this experiment.

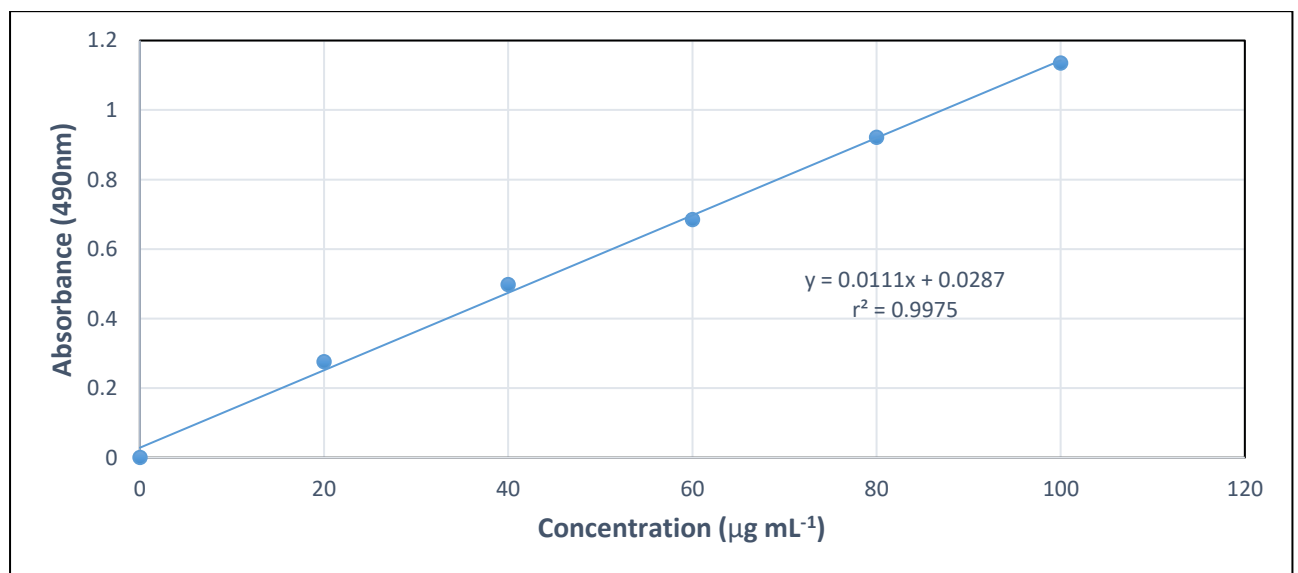


Figure 3.11. Calibration Curve for the D-glucose Standard using the Dubois *et al* (1956) Test

A satisfactory correlation ($r^2 = 0.9975$) from the trendline is shown for the concentration of the D-glucose standards. There is a significant slight positive bias from the trendline, but it does not have any effect on the EPS sample since their concentrations are expected to be

towards the top end of the curve. The carbohydrate content was calculated using the equation of the trendline and the results shown in table 3.4.

Table 3.4: Results for the Carbohydrate Analysis of EPS from *L. paracasei* DG (Batch 4)

Bacteria species/batch	Absorbance at 490nm	Calculated amount ($\mu\text{g mL}^{-1}$)	Carbohydrates %w/w
<i>L. paracasei</i> DG (Batch 4, S2)	0.5325 \pm 0.005	491.13	49.11

In each of the batches the amount of carbohydrates produced is below expectation, which matches the findings of Tuiner *et al* (1999)²⁵⁹, who also proved a low carbohydrate content even after purification of the exopolysaccharide isolated from *Lactococcus lactis* subsp. *Cremoris*. The results indicated the presence of other substances like proteins, inorganic material and water. The carbohydrate content indicates that the EPS produced is a mixture with other materials possibly coming from within the cell, the extraction process is known to sometimes lyse the cell releasing more materials into the surroundings. Some of the materials could have been obtained from the broth used for its culturing.

3.3. Conclusion

In general, using probiotic in modulating the host immune response looks promising in preventing and managing inflammatory conditions of the gut mucosa. With this promising strategy, it is of great importance to identify the cell surface components mediating the interaction between the probiotic and its host cell which triggers the probiotic effect. Thanks to our collaborative partners in Italy, the genomic analysis of *L. paracasei* DG revealed two potential genes clusters coding for EPS biosynthesis which prompted us to further investigate biologically and characterise the polysaccharide produced. After extracting and purifying the surface polysaccharides of the DG strain, the chromatographic and NMR spectroscopic methods were used to characterise its novel repeating unit structure. It was observed that the polysaccharide obtained as C1 upon addition of 1 volume of NaOH (1M) to the *L. paracasei* DG grown in MRS broth eluted distinctively clean peaks for the ¹H-NMR spectra. The subsequent addition of the second volume precipitated some impurities which appeared as additional peaks on the ¹H-NMR spectra of C2. When the HBM broth was used for culturing *L. paracasei* DG, significant polysaccharides were extracted only for the S2 and C2 which

showed a similar $^1\text{H-NMR}$ spectrum to that of C1 extracted from cells grown in MRS broth though with minute impurities. Using the CDM broth in culturing this *L. paracasei* DG indicated a slower visual growth as it took almost 48 to become cloudy when compared to the usual 18 to 24 hours growth when cultured in MRS and HBM broths.

The $^1\text{H-NMR}$ spectra of this *L. paracasei* DG had six anomeric signals which indicated that the isolated polysaccharide was made of repeating units of six monosaccharides linked together forming the chain. Results from the SEC-MALLS indicated that the isolated polysaccharide was made up both a high molecular weight and a medium molecular weight with no UV traces of protein confirming its purity. The monomers and linkage analysis using HPAEC-PAD and GC-MS identified the sugars in the repeating unit to be rhamnose, galactose and *N*-acetylgalactosamine in the ratio 4:1:1 which was further confirmed by the 2D NMRS including their linkage and absolute configurations. The combined chemical and NMR analysis of this isolated polysaccharides from *L. paracasei* DG confirmed it to be a novel rhamnose-rich heteropolysaccharide when compared with previous findings. This repeating unit structure of *L. paracasei* DG reported here is different to those of the previously published *Lactobacillus casei* groups²⁶⁰⁻²⁶⁶ as well as those from a range of LAB^{32, 267}. In collaboration with our Italian team, the immunological characterisation of the isolated polysaccharide was found to display immuno-stimulatory abilities through gene expression enhancement of the proinflammatory cytokines (chemokine expression). Our study here provided novel information that the *L. paracasei* DG produced a rhamnose-rich heteropolysaccharide which is unique having immunocompetent properties making it a molecule with potential applications in pharmaceutical and nutraceutical companies.

3.4. Production and Isolation of *Lactobacillus salivarius* CCUG44481

As earlier mentioned, not much of the EPS produced has been well characterised and explored for *L. salivarius* when compared to other commensal lactobacilli. The *L. salivarius* CCUG44481 (from a bird isolate) is another strain which is of interest in this present study that has been rarely studied. Previous research show very little has been done in regards to probiotics of bird origin with the most recent being the poultry derived isolate (*Lactobacillus johnsonii* F19785)²²⁴. This isolate has been investigated for its probiotic activity in competing and controlling the impact of the pathogen *Clostridium perfringens* which causes human food poisoning as well as economic loss in the poultry industry (necrotic enteritis)^{224, 268}. Some

researchers have shown that the structural differences of bacterial polysaccharide have an impact in their functioning in terms of colonizing and regulating the host immune response^{9, 225, 269}. That said, the functional properties of the EPS may be obtained through identifying the primary structure of the bacterial polysaccharides isolated from *Lactobacillus salivarius* CCUG44481 since they are presumed to possess similar probiotic activity to *Lactobacillus johnsonii* F19785 like adhering to the tissue culture and the GIT of the bird, out-competing the pathogenic bacteria. In collaboration with the research team from UCC (University College Cork), samples of polysaccharides from this CCUG44481 strain which had been reported to be a significant EPS producer was available. According to Raftis *et al.* (2011)²²⁷, this strain was seen to have dramatic high production levels of EPS compared to the other *L. salivarius* strains under investigation. It has previously been reported that the *L. salivarius* strain CCUG44481 is capable of producing significant amounts of an exopolysaccharide when using sucrose as a carbon feed²²⁷. A sample of the EPS was supplied by Prof. Paul O'Toole's group at University College Cork (UCC) extracted from the HBM broth which is free of EPS-equivalence as described in section 2.7.1.1. This EPS was recovered as S2 after the addition of 2 volumes of chilled absolute ethanol which yielded about 52mg/L and we at the University of Huddersfield recorded a series of NMR spectra for the sample which included 1D and 2D-NMRs (COSY, TOCSY, HSQC and HMBC). These NMR results were then combined with the results from several chemical analyses (monomer, linkage analysis and absolute sugar determination) in an attempt to characterise the structures of the EPS.

3.4.1. Structural Characterisation of the Exopolysaccharides isolated from *L. salivarius* CCUG44481

Determining the monomeric repeated units found in the EPS produced by the CCUG44481 strain, 1D and 2D NMR analysis were performed alongside the molecular weight determination using HP-SEC-MALLS for initial observation. From the ¹H NMR analysis, the integrated results indicated that there were three anomeric protons (designated as A-B/C, Fig 3.12).

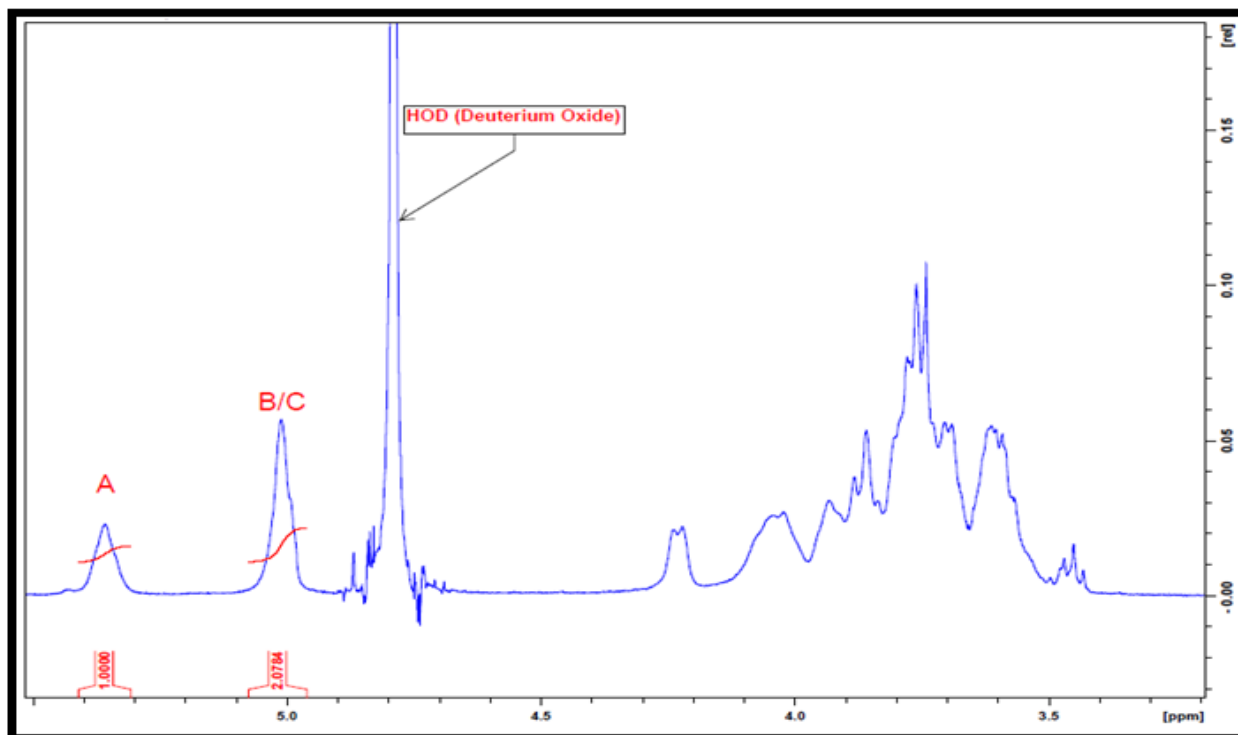


Figure 3.12: ^1H NMR Spectrum of EPS from *Lactobacillus salivarius* CCUG44481 in D_2O at 70 $^\circ\text{C}$

3.4.2. Purity of the Exopolysaccharide from *L. salivarius* CCUG44481 by its Molecular Weight Determination using the HP-SEC-MALLS

In the first experiments, the purity of the polysaccharide was examined using size exclusion chromatography and monitoring the elution of peaks using a multi-angle light scattering detector in combination with a concentration dependent differential refractometer and a UV-detector. The sample eluted as a single narrow peak (*Fig 3.13*) which had a weight average molecular mass of $11.2 \times 10^6 \text{ g mol}^{-1}$ and the sample had a polydispersity of 1.06, which suggested that the sample had a narrow distribution of molecular masses. No peaks were visible in the UV-trace and the sample was free of proteins and nucleic acid contaminants.

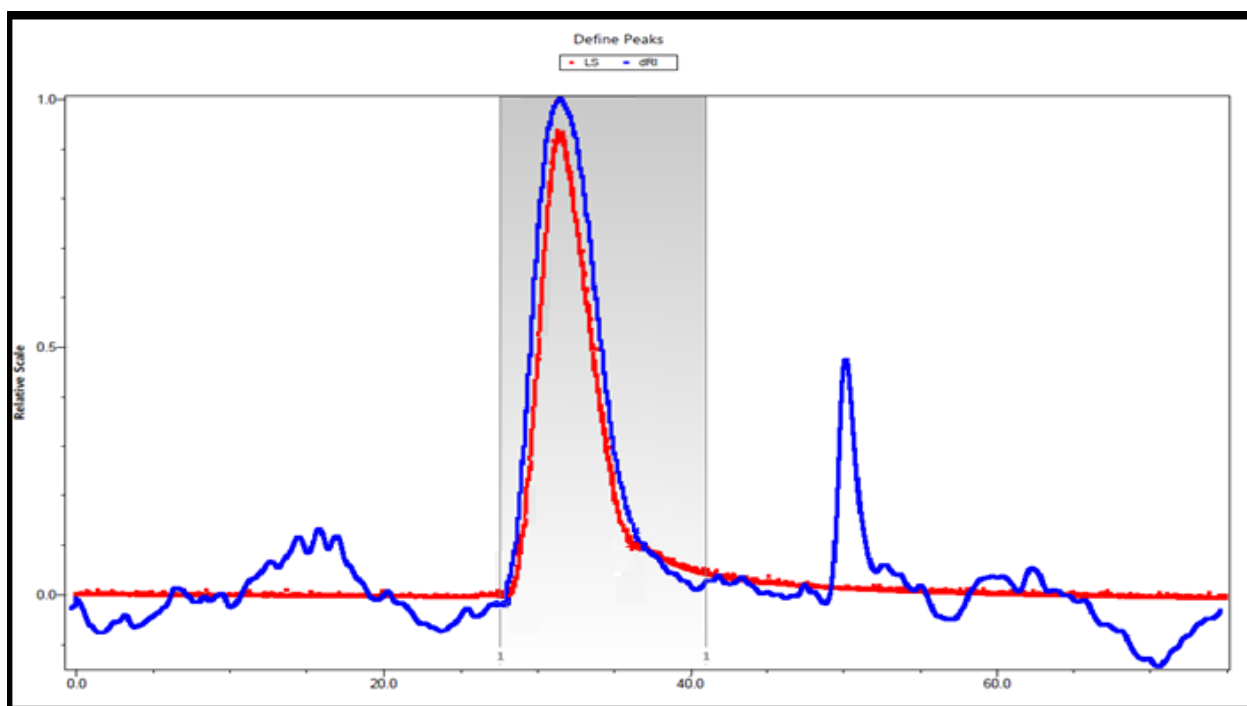


Figure 3.13. SEC-MALLS trace of EPS from *Lactobacillus Salivarius* CCUG44481

3.4.3. Monomers and Linkage Analysis of the Monosaccharides in the Repeating Unit Structure of *Lactobacillus salivarius* CCUG44481.

3.4.3.1. Monomers Analysis of the Exopolysaccharides Isolated from *Lactobacillus salivarius* CCUG44481 using HPAEC-PAD and GC-MS

After hydrolysis as described in section 2.8.4.1 of this isolated polysaccharide, a 50ppm solution was prepared and monomer analysis was attempted using the HPAEC-PAD. The HPAEC-PAD chromatograph (*Fig 3.14*) had a single peak, which eluted at the same time as a glucose reference standard suggesting that the EPS was a homoglycan, a glucan. The hydrolysed sample was further reduced and acetylated as described in sections 2.8.4.2 and 2.8.4.3 respectively for the alditol acetate method. For the GC-MS analysis, the chromatograph included a single peak which had exactly the same retention time as that of a 1,2,3,4,6-penta-*O*-acetylglucitol and the corresponding mass spectrum was consistent with the starting monosaccharide being glucose (*Fig 3.15*).

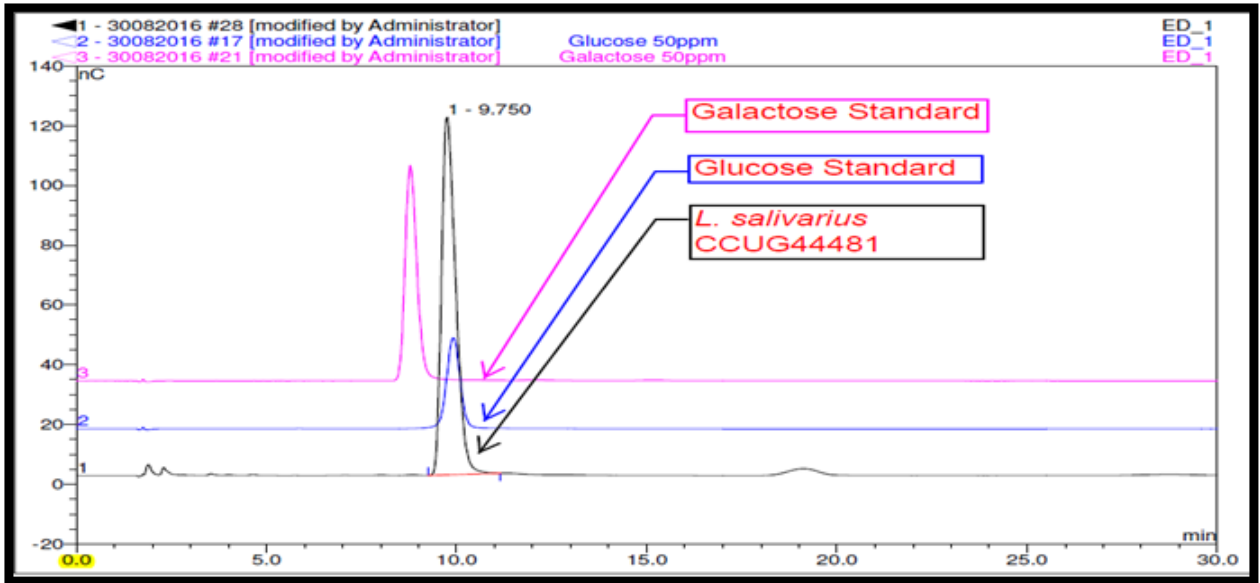


Figure 3.14. HPAEC-PAD Chromatogram of *L. salivarius* CCUG44481 overlaid with Glucose and Galactose Standards.

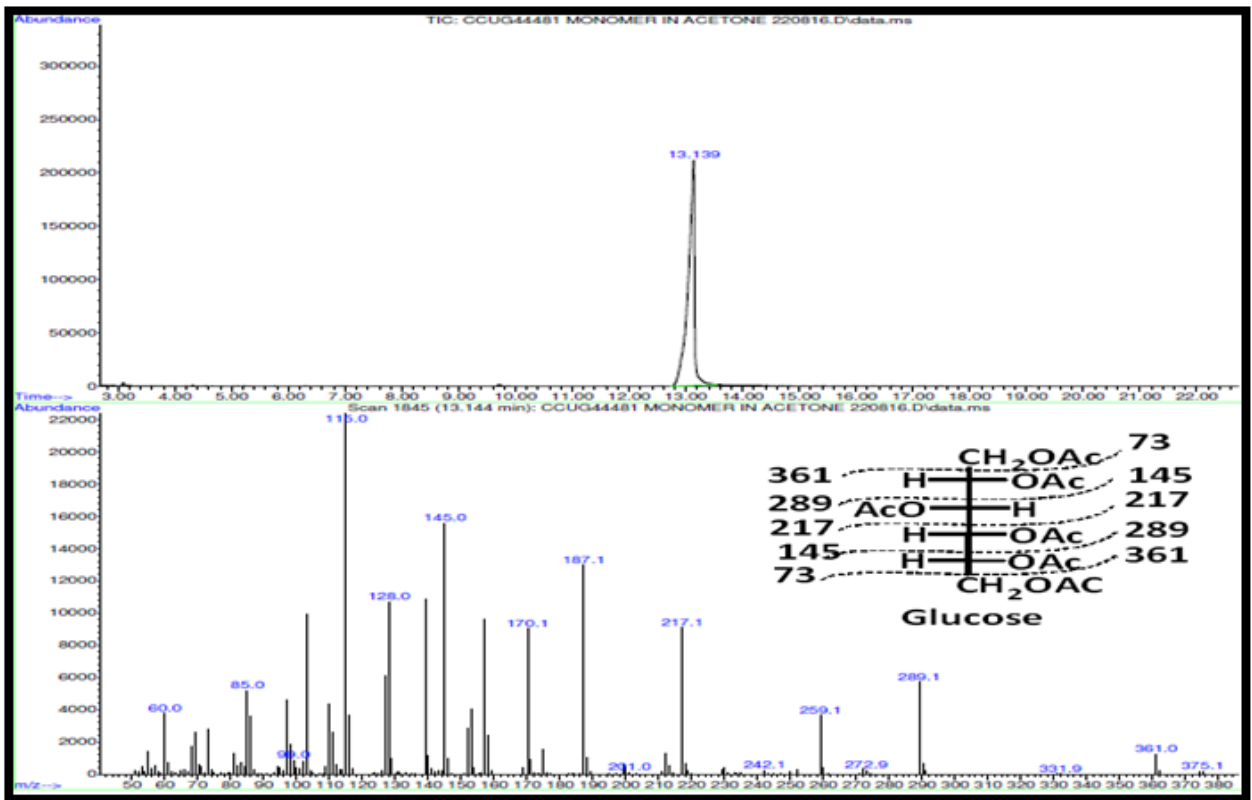


Figure 3.15 . Chromatogram for the Alditol Acetates of the Sugars obtained from the GCMS for Monomer Analysis of *L. salivarius* CCUG44481.

3.4.3.2. Linkage Analysis of the Exopolysaccharides Isolated from *Lactobacillus salivarius* CCUG44481

Analysis of the linkages in the EPS using the method described in section 2.8.5 gave rise to a chromatograph containing four peaks (Fig 3.16) and the MS (Figs 3.16a, 3.16b, 3.16c and 3.16d) confirmed that these were: 1-deutrio-2,3,4,6-tetramethyl-1,5-di-*O*-acetylhexitol derived from a terminal hexose; 1-deuterio-2,4,6-trimethyl-1,3,5-tri-*O*-acetylhexitol which is consistent with a 1,3-linked hexose; 1-deutrio-2,3,4-trimethyl-1,5,6-tri-*O*-acetylhexitol derived from a 1,6-linked hexose and the fourth peak was a 1-deutrio-2,4-dimethyl-1,3,5,6-tetra-*O*-acetylhexitol derived from a 1,3,6-linked hexose.

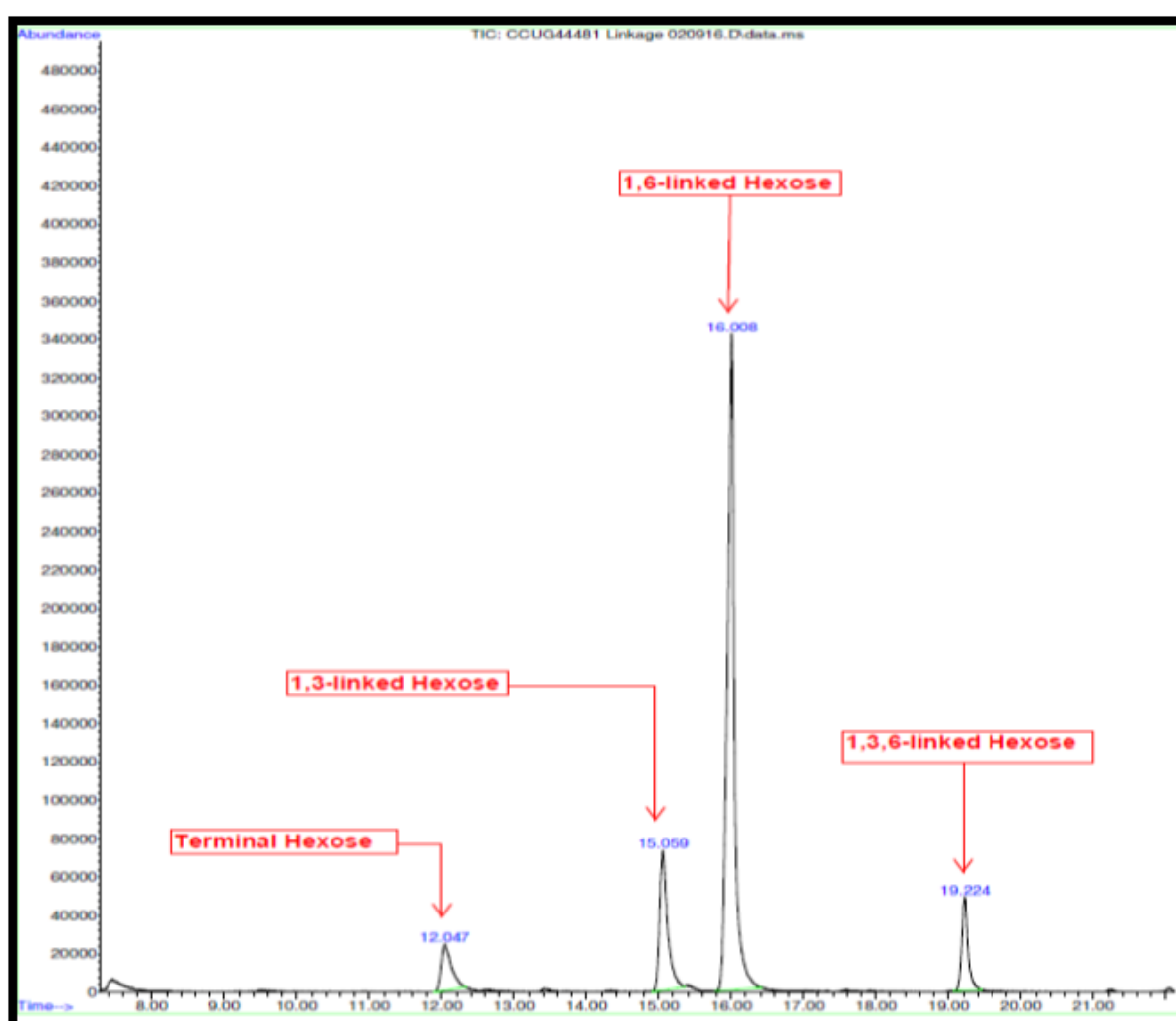


Figure 3.16. Chromatogram for the Methylated Alditol Acetates of the Sugars obtained from the GC-MS for Linkage Analysis of *L. salivarius* CCUG44481

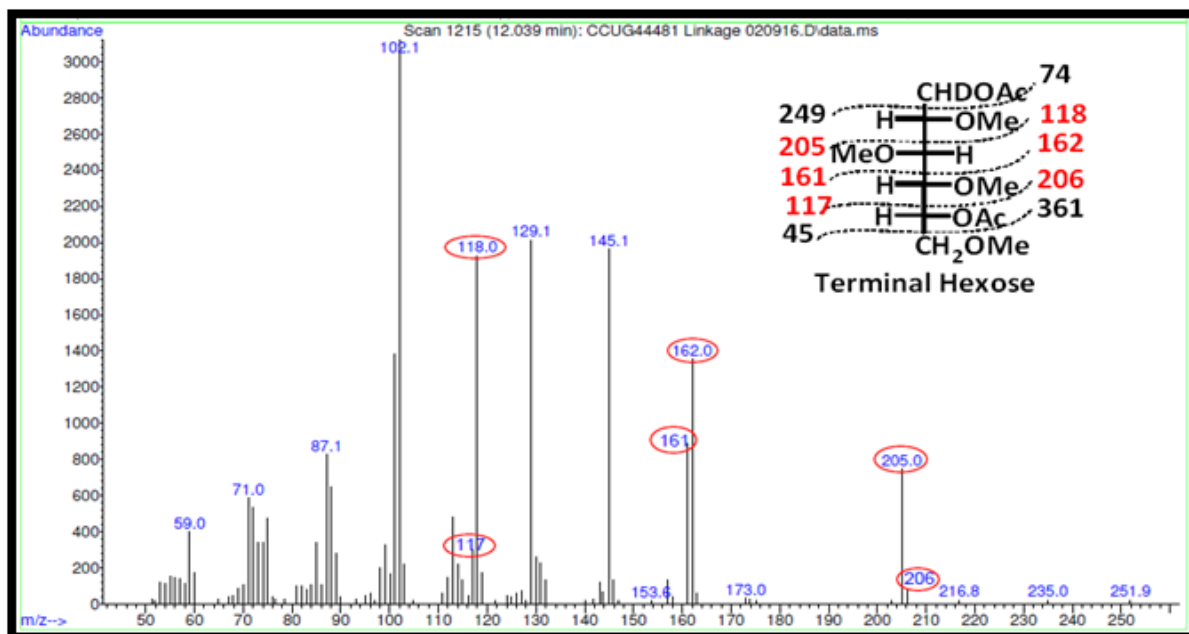


Figure 3.16a. Mass spectrum of 1-deutrio-2,3,4,6-tetramethyl-1,5-di-*O*-acetylhexitol and its Fragmentation Pattern which Indicates it is a Terminal Hexose.

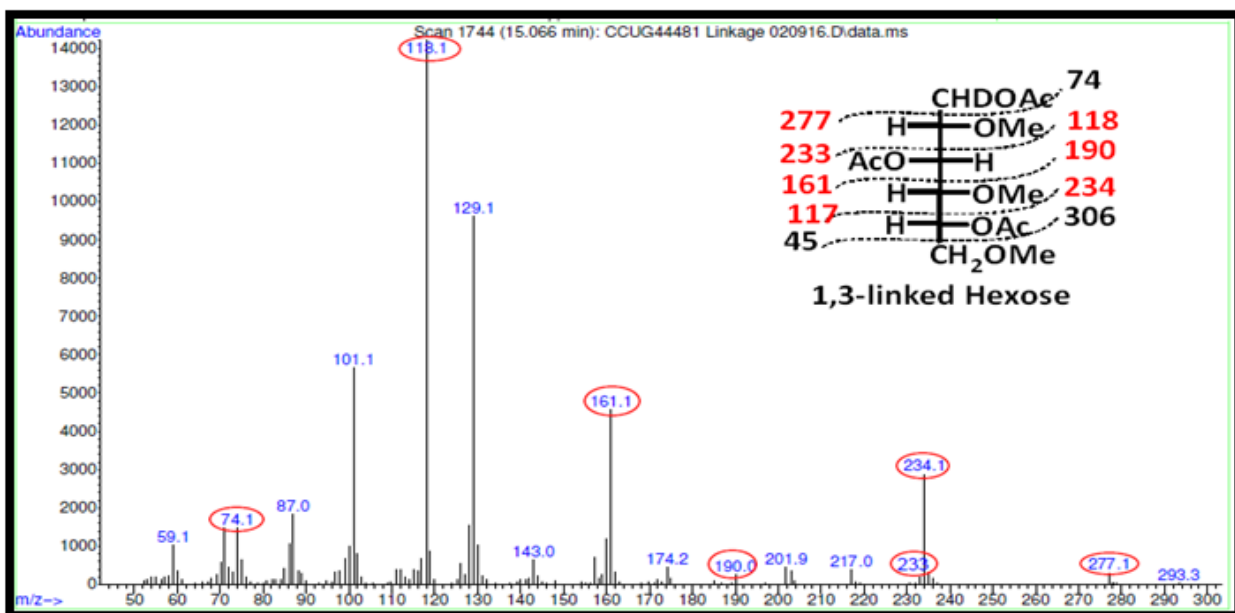


Figure 3.16b. Mass Spectrum of 1-deuterio-2,4,6-trimethyl-1,3,5-tri-*O*-acetylhexitol and its Fragmentation Pattern which Indicates it is a 1,3-linked Hexose.

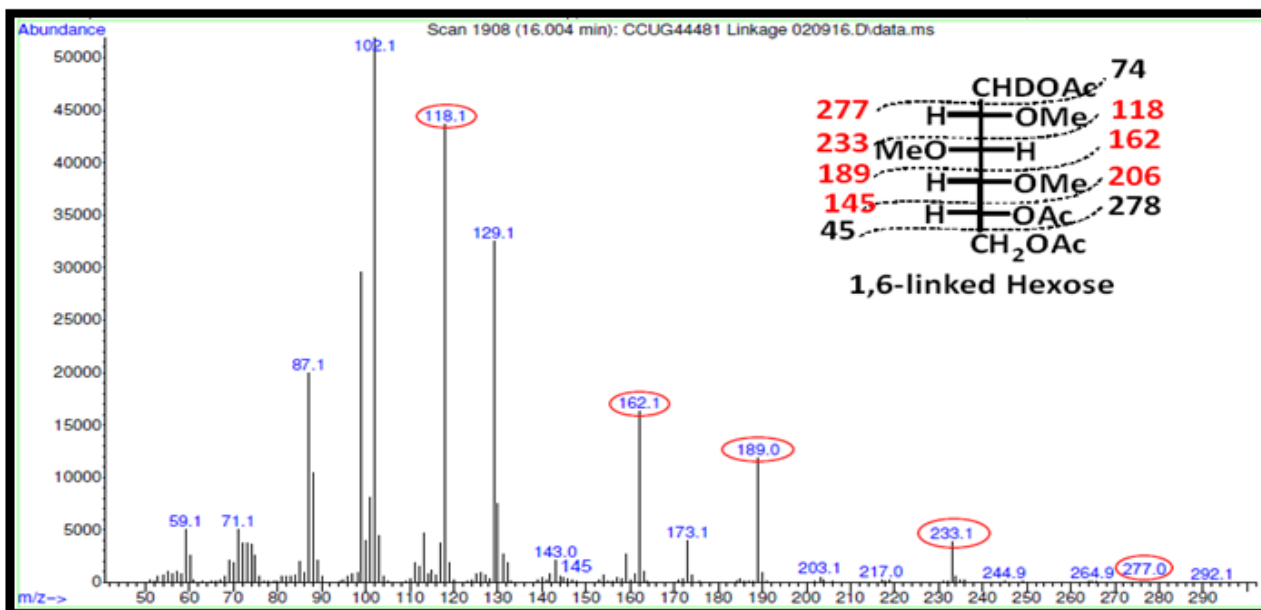


Figure 3.16c. Mass spectrum of 1-deutrio-2,3,4-trimethyl-1,5,6-tri-*O*-acetylhexitol and its Fragmentation Pattern which Indicates it is a 1,6-linked Hexose.

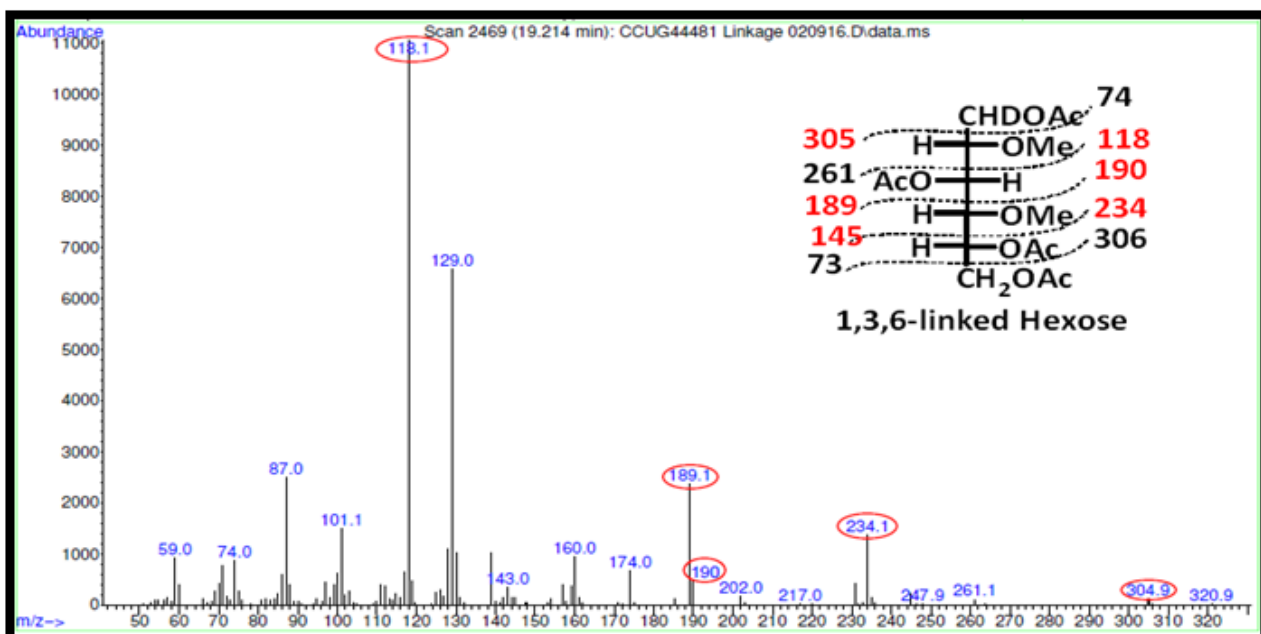


Figure 3.16d. Mass Spectrum of 1-deutrio-2,4-dimethyl-1,3,5,6-tetra-*O*-acetylhexitol and its Fragmentation Pattern which indicates it is a 1,3,6-linked Hexose.

3.4.4. Absolute Configuration of the Exopolysaccharide from *L. salivarius* CCUG44481

Absolute sugar analysis using the method described in section 2.8.7 confirmed that the EPS was composed of D-glucose. The chromatogram of this exopolysaccharide indicated two peaks (Fig 3.17) as expected since it is made of a glucose unit. This D-glucose was further confirmed when the mass spectra of the two eluted peaks matched perfectly with a standard stored mass spectrum of a D-glucose in the saved library of standard mass spectra of various sugars.

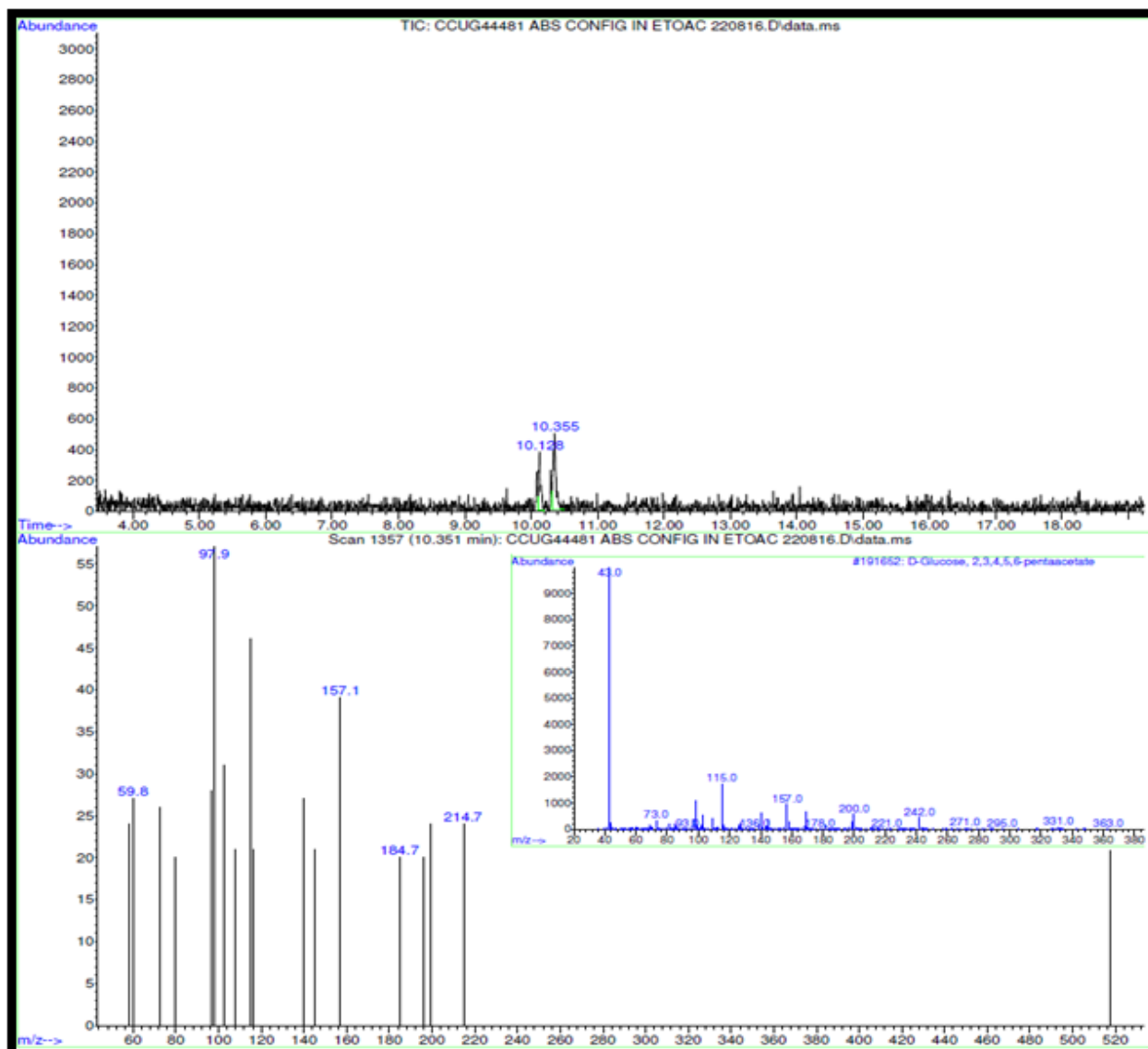


Figure 3.17. The Chromatogram of the Distinct Peaks of the Acetylated Butyl Polysaccharide of *L. salivarius* CCUG44481 and the Mass spectra of these Peaks matched with Standards D-Glucose in the Saved Library of Standards.

In conclusion the results of the wet chemical analysis suggested that the EPS was likely a highly branched dextran.

3.4.5. NMR Analysis of the EPS from *L. salivarius* CCUG44481

It is known that bacteria can synthesise several different types of dextrans which has also been reported to be produced by LAB as an extracellular bacterial polysaccharide^{270, 271}. This extracellular bacterial polysaccharide (dextran and its derivatives) produced by this LAB have been used in the medical industries (for an antithrombotic effect, in intravenous fluids), food industries (particularly in bakery products such as sourdough fermentation) as well as in cosmetics (as a moisturizer and thickener having anti-inflammatory effects on the skin)²⁷⁰⁻²⁷². The most common structural motif of a dextran is a backbone of repeating α -(1,6)-linked glucose residues²⁷². Where bacterial dextran differ from one another is in their branches, which can contain various linkage types and varying lengths of branches which according to Jean *et al* (1954)²⁷⁰ depends very much on the subspecies. For the majority of dextrans branching begins at the 3-position of the anhydroglucose residues of the main chain (*Fig 3.18*). Whilst a wide variety of different branches have been identified, the first to be studied by high-field NMR were those containing either single terminal alpha-linked glucoses, alpha-linked isomaltose, branches with multiple α -(1,6)-linked glucoses or branches with single or multiple α -(1,3)-linked glucoses.

In order to confirm that the EPS produced by *L. salivarius* CCUG44481 was a dextran and to determine more details about the type of branching present a series of 1D and 2D-NMR spectra were recorded and these were compared to NMR spectra recorded for a commercial dextran with an average molecular mass of 270K Da which was purchased from the Aldrich chemical company.

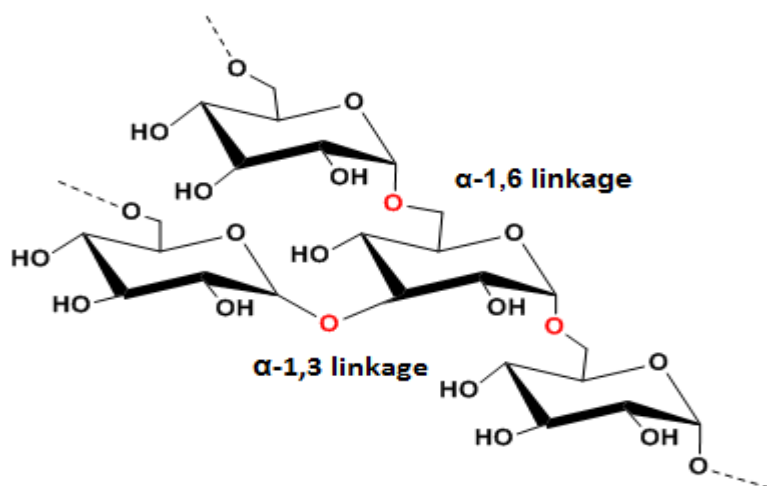


Figure 3.18. Structure of a Commercial Dextran.

The proton NMRs from the EPS of *L. salivarius* CCUG44481 (recorded at both room temperature and at 70 °C and for the commercial dextran sample show a number of similarities in the anomeric region (4.5-5.5 ppm) whilst at the same time there are a number of distinct differences at the periphery of the ring-proton region (4.3-3.3 ppm) (Fig 3.19). In the anomeric region both spectra show two broad sets of anomeric proton resonances: the first signal close to 5.3 ppm and a second up-field signal close to 5.0 ppm. In the spectra for CCUG44481 EPS the anomeric resonances are broad, and this may well be due to the high viscosity of the NMR sample which is frequently observed for very high molecular weight EPSs. Attempts to reduce the viscosity by heating the sample to 70 °C had little, if any, positive effects on the resolution of the spectrum. Walker *et al* (1990)²⁷³ have previously reported the high-field proton NMR spectra of a number of dextrans where they found similar anomeric resonances with the downfield signal being assigned to the anomeric proton of the (1,3)-linked glucoses attached as branches and the up-field signal was assigned to the anomeric protons of the main chain (1,6)-linked glucoses.

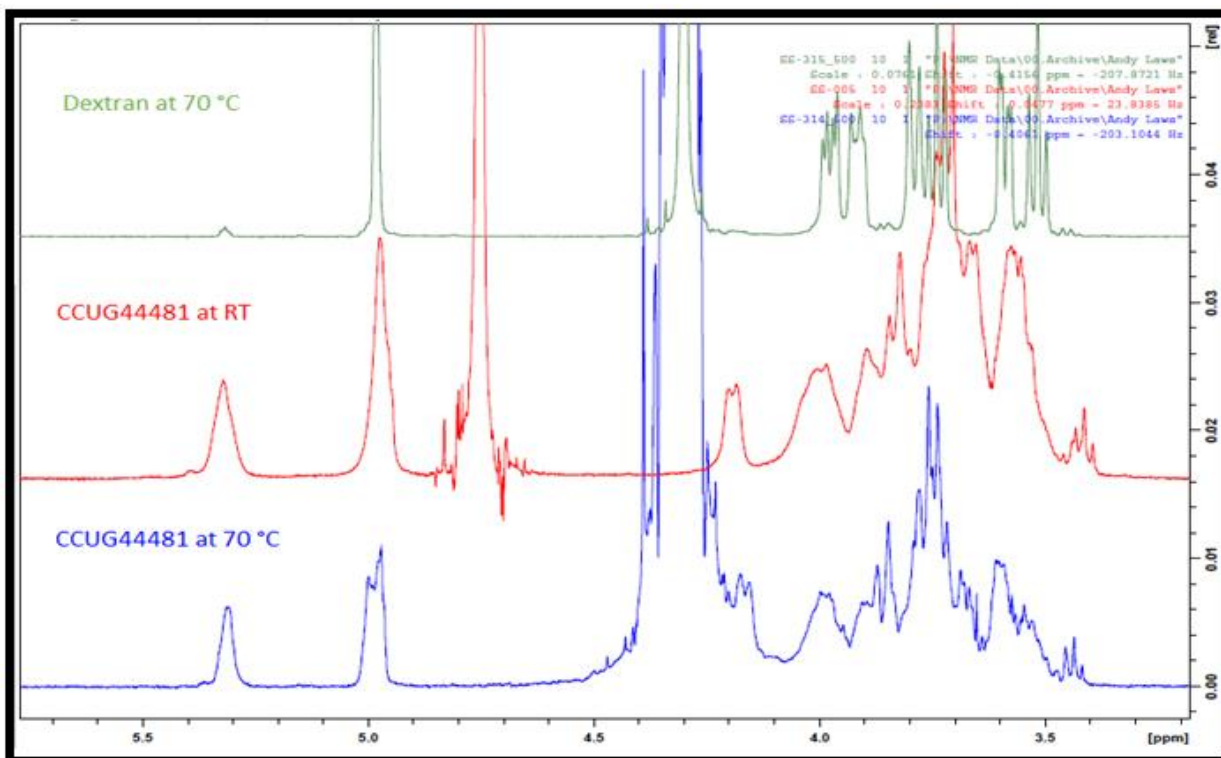


Figure 3.19. ^1H -NMR Spectra from EPS of *L. salivarius* CCUG44481 (recorded at both room temperature and at $70\text{ }^\circ\text{C}$) and that for the Commercial Dextran at $70\text{ }^\circ\text{C}$.

In the EPS the resonance at 5.0 ppm is clearly derived from two overlapping anomeric proton resonances and this has previously been observed by Walker *et al* (1990)²⁷³ who attributed the different resonances to 1,6 linkages involved directly at the point of branching (1,3,6-linked hexoses) and the 1,6 linkages not involved in branching (1,6-linked hexoses). Integration of the 5.3 ppm resonance and that of the 5.0 ppm resonance and comparison of the ratio of the two signals suggest that in the commercial dextran there is a relatively small number of hexoses involved in branches (ratio 3.5:100) whereas in the EPS produced by *L. salivarius* CCUG44481 the down-field anomeric resonance is much larger (ratio 49:100) and this suggests that the EPS is a highly branched dextran with at least one third of the hexoses being present in branches. A ^{13}C -DEPT 135° spectrum was recorded for the *L. salivarius* CCUG44481, the resonances were also broad which is consistent with a random location of the branches within the backbone (Fig 3.20).

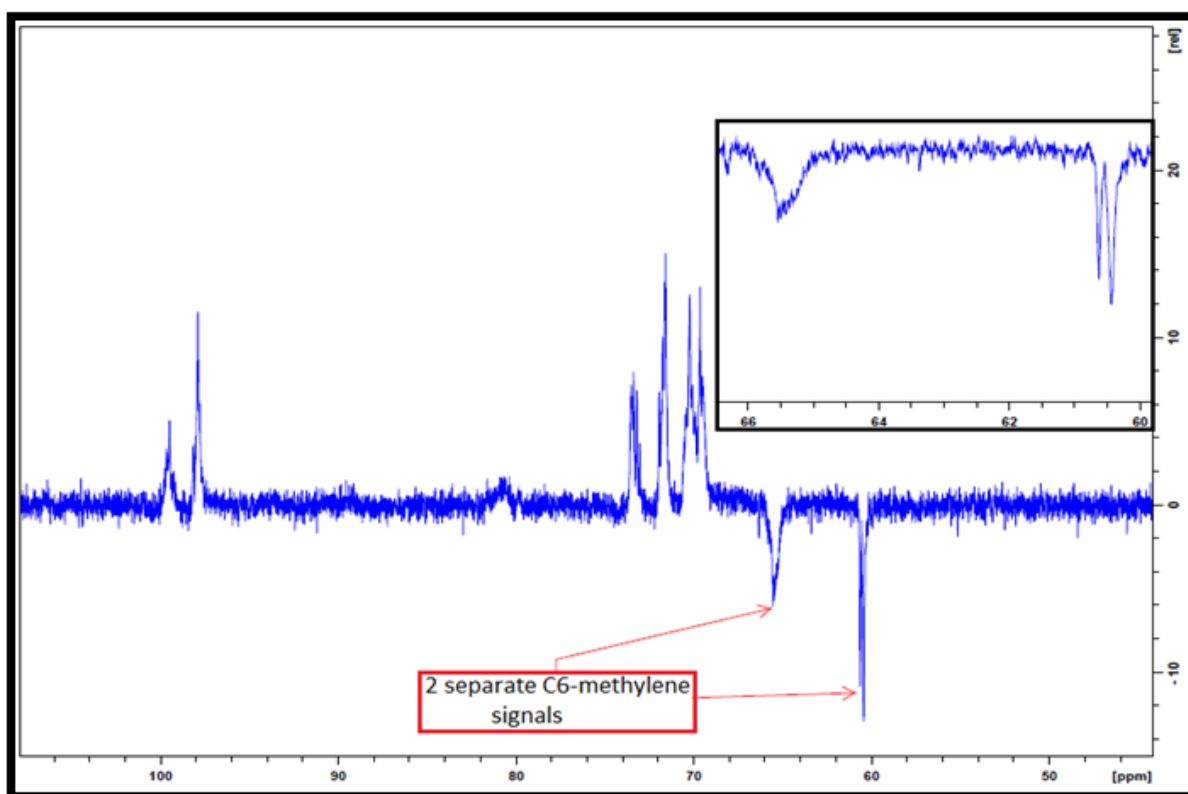


Figure 3.20. ^{13}C -DEPT 135 Spectrum for *L. salivarius* CCUG44481 indicating the C6-Methylene Signals

Two separate broad C6-methylene signals are visible, one at 61.3 ppm and the second at 66.34 ppm. The high-field signal is indicative of a C-6, which is not part of a glycosidic bond whilst the low field signal is where a C6-carbon forming part of a glycosidic bond would be expected as reported by Bock and Pedersen (1974)²⁷⁴. If the region of the spectra containing the methylene protons is expanded (inset in Fig 3.20), it is clear both the high field and low field methylene signals correspond to more than one resonance. This observation is consistent with the results of the linkage analysis which identified the presence of 1,3-linked and terminal hexoses which would be expected to have their C6-resonances close to 60 ppm and also 1,6- and 1,3,6-linked hexoses which would be expected to have their C6-resonances shifted to lower field (66 ppm).

In order to determine if any further information about the structure of the *L. salivarius* CCUG44481 dextran could be determined by NMR, a series of 2D-NMR spectra were recorded including homonuclear ^1H - ^1H -COSY and ^1H - ^1H -TOCSY spectra and a heteronuclear ^1H - ^{13}C -

HSQC spectrum. Again, in order to aid the interpretation of the spectra, a COSY and HSQC spectrum were recorded for the commercial dextran standard.

3.4.6. Analysis of the 2D-Homonuclear Spectra for the Commercial Dextran

In order to simplify the interpretation of the spectra of the EPS it was decided to run 2D-spectra for the commercial dextran sample, which is known to be primarily composed of 1,6-linked glucoses residues^{273, 275, 276}. A full assignment of each of the protons for the main chain 1,6-linked backbone was achieved from inspection of a COSY spectrum (Fig 3.21).

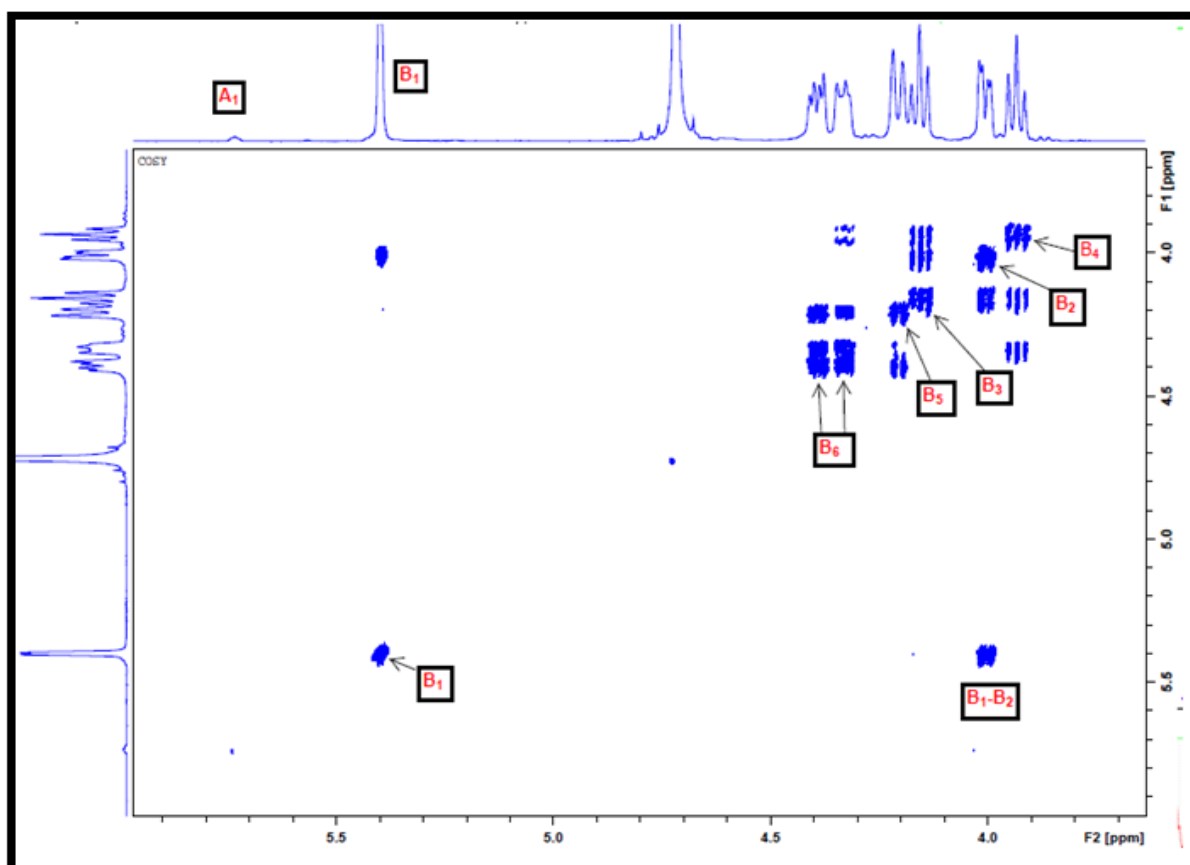


Figure 3.21. The ^1H - ^1H -COSY Spectrum of the Commercial Dextran indicating the Assigned Protons for the 1,6-linked Backbone

The corresponding carbon resonances were identified from inspection of the HSQC spectrum (Fig 3.22).

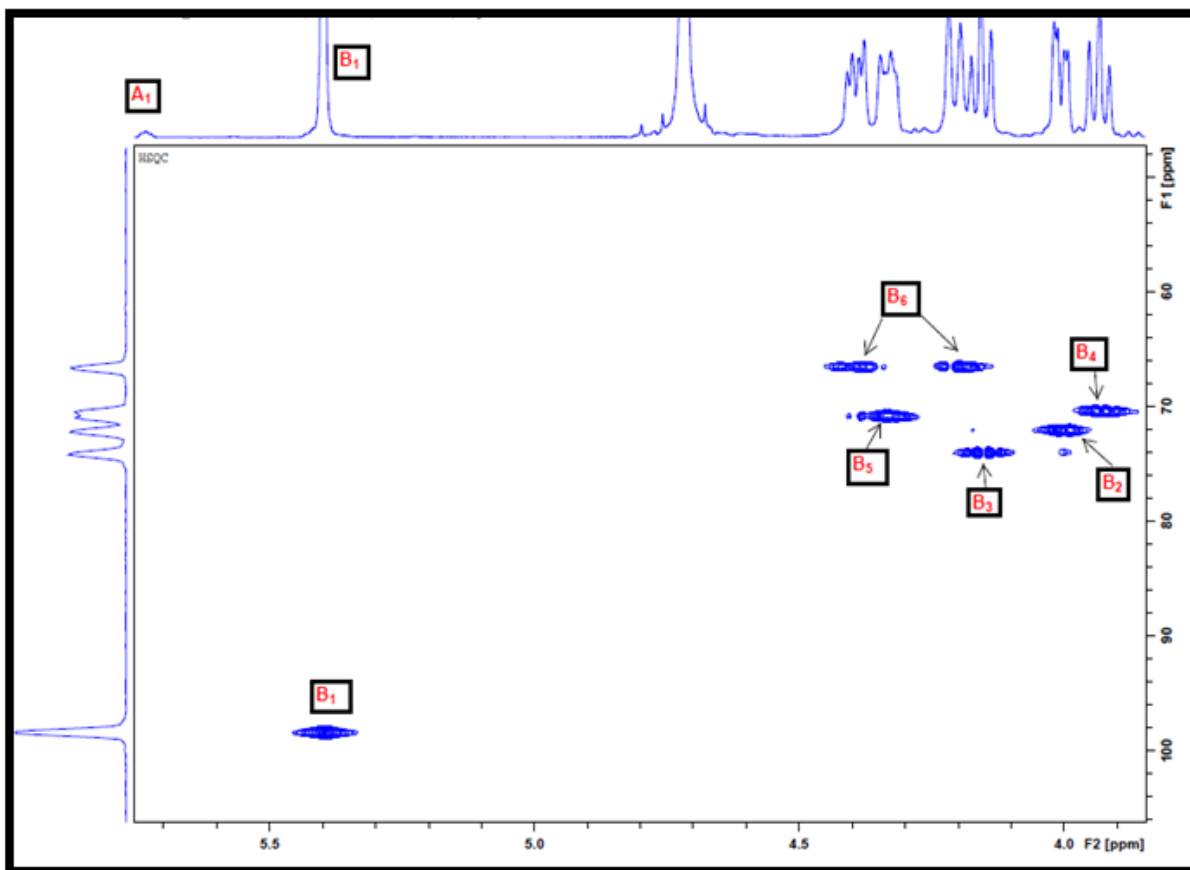


Figure 3.22. The ^1H - ^{13}C - HSQC Spectrum of the Commercial Dextran indicating the Assigned Protons for the 1,6-linked Backbone.

3.4.7. Analysis of the 2D-Homonuclear Spectra for the Dextran from *L. salivarius* CCUG44481.

As was stated at the start of this chapter, that linkage analysis for the dextran from *L. salivarius* CCUG44481 identified the presence of terminal glucoses, 1,3-linked glucoses, 1,6-linked glucoses and 1,3,6-linked glucoses. Walker *et al*²⁷³ in their 1990 publication have published spectra of a range of dextrans where they have reported the location of the anomeric protons of the differently linked monosaccharides and from which it is possible to extract their chemical shifts and these are: 5.31 ppm (1,3-linked glucose), 5.29 ppm (terminal glucose), 4.97 (1,3,6-linked glucose) and 4.95 ppm (1,6-linked glucose). It is worth noting however, a survey of anomeric sugars in EPSs suggests that the average chemical shift for an α -linked terminal glucose is closer to 5.0 ppm and is located at 4.81 ppm in methyl α -D-glucopyranoside²⁷⁷ whilst that for a sugar with an α -3-link is rarely below 5.1 ppm (it is possible that the assignment in Walker's work for these two sugars has been inverted). To aid the assignment of the 2D-spectra the four potential anomeric resonances have been assigned

labels A to D based on their proposed chemical shifts: A for the highest chemical shift and D for the lowest chemical shift.

On the COSY spectrum recorded for the EPS (Fig 3.23- Black contours) it was not possible to identify two distinct diagonal peaks for each of the broad anomeric resonances and this was because A1 & B1 overlap as do C1 & D1. However, for the up-field pair (C and D) the two cross-peaks are well resolved and this allows the position of the H2-H4 for C and D to be identified on the TOCSY spectrum (Fig 3.23- Blue contours).

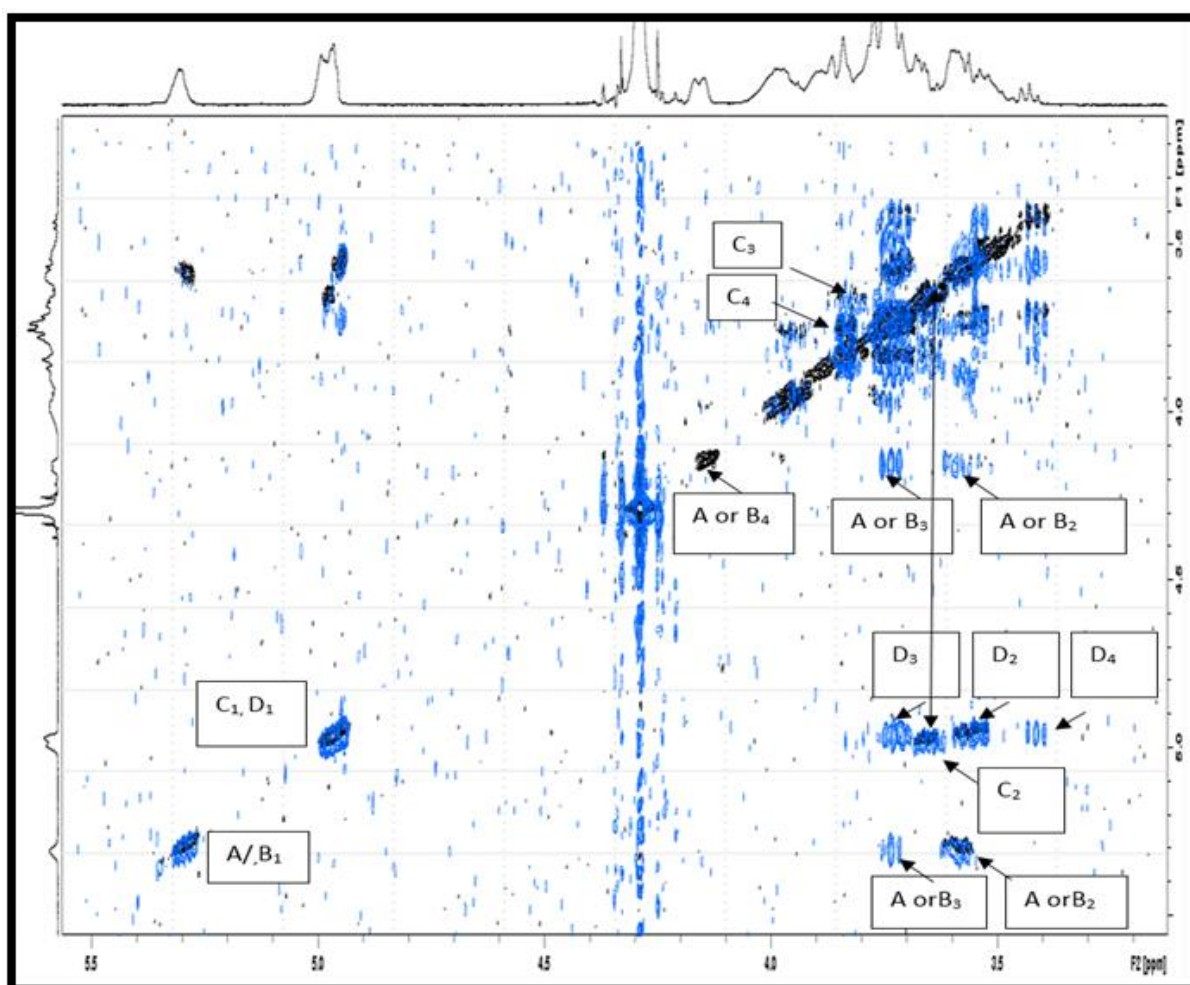


Figure 3.23. Overlaid COSY (black contours) and TOCSY (blue contours) Spectra of the Dextran EPS from *L. salivarius* CCUG44481

The position of the most significant carbons was determined by locating the corresponding cross peaks derived from their respective protons on a ¹H-¹³C-HSQC-spectrum (Fig 3.24 -black contours) and by reference to the HSQC spectrum of the commercial dextran (Fig 3.24-blue contours).

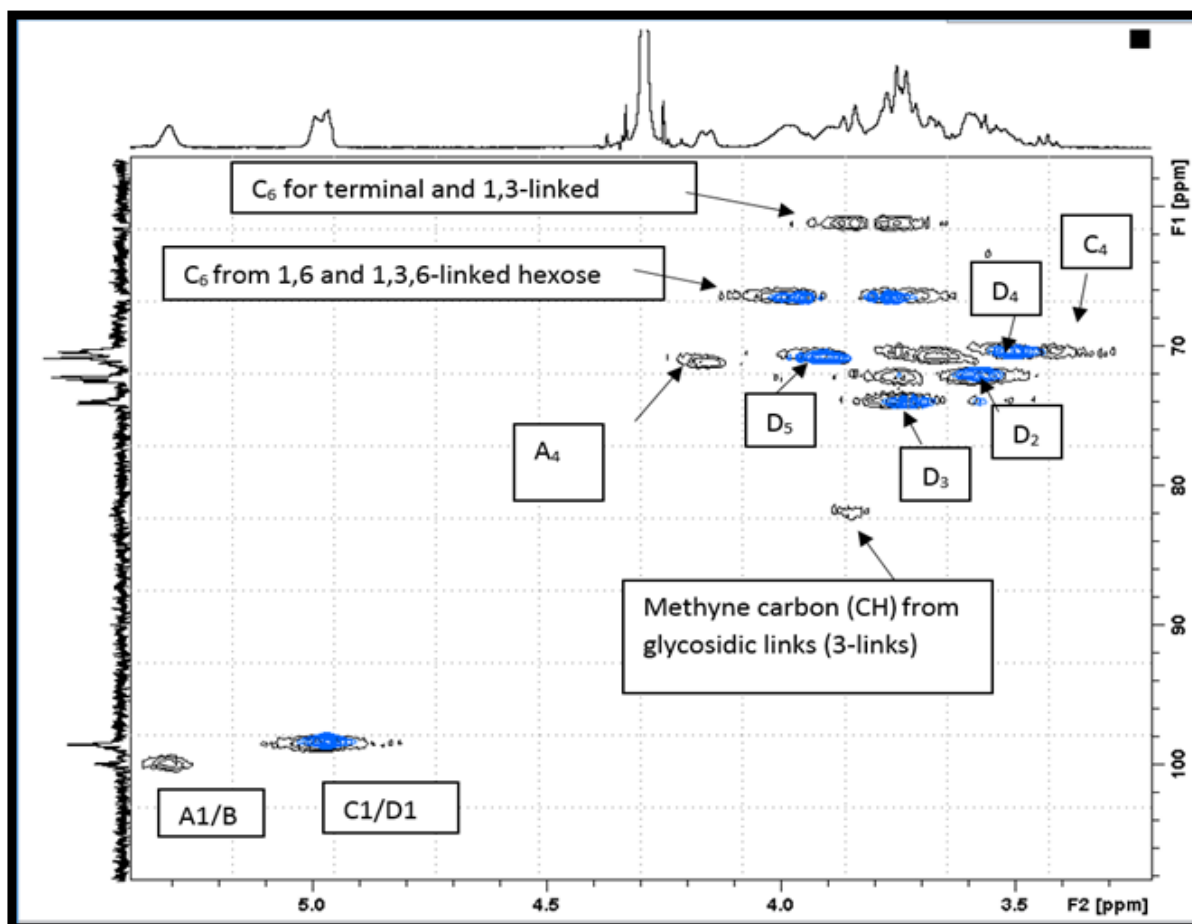


Figure 3.24. Overlaid ^1H - ^{13}C -HSQC-Spectrum (black contours) of the EPS from *L. salivarius* CCUG44481 to that of the Commercial Dextran (blue contours).

3.4.8. Determination of Carbohydrate Content of Exopolysaccharide Isolated from *L. salivarius* CCUG44481

The dialysed isolated polysaccharides (EPS) from *L. salivarius* CCUG44481 was freeze-dried and the Dubois *et al*(1956)¹⁸⁵ test as described in section 2.8.2 was carried out. The higher the amount of sugar present the higher the intensity of colouration formed. A calibration curve was plotted for a series of D-glucose standards (0 ppm, 20 ppm, 40 ppm, 60 ppm, 80 ppm and 100 ppm) against their absorbance (*Fig 3.11*) which was then used to evaluate the amount of carbohydrate content found in the EPS.

A satisfactory correlation ($r^2 = 0.9975$) from the trendline is shown for the concentration of the D-glucose standards. There is a significant slight positive bias from the trendline, but it does not have any effect on the EPS sample since their concentrations are expected to be towards the top end of the curve. The carbohydrate content was calculated using the equation of the trendline and the results shown in table 3.5.

Table 3.5: Results for the Carbohydrate Analysis of EPS from *L. salivarius* CCUG44481

Bacteria species/batch	Absorbance at 490nm	Calculated amount ($\mu\text{g mL}^{-1}$)	Carbohydrates %w/w
<i>L. salivarius</i> CCUG44481 DG (S2)	0.854 \pm 0.009	743.52	74.35

The findings of Tuiner *et al* (1999)²⁵⁹ showed that amount of carbohydrates produced was below expectation which was the case here. In addition, they also proved a low carbohydrate content even after purification of the exopolysaccharide isolated from *Lactococcus lactis* subsp. *Cremoris*. The results suggested that there could be some indication of other substances like proteins, inorganic material and water present. The carbohydrate content indicates that the EPS produced is a mixture with other materials possibly coming from within the cell. The extraction process is known to sometimes lyse the cell releasing more materials into the surroundings. Some of the materials could have been obtained from the broth used for its culturing.

3.5. Conclusion

In this present study, the EPS that was isolated from *L. salivarius* CCUG44481 was investigated since it was from a bird origin and was reported to produce significantly higher amounts the released EPS when compared with other strains²²⁷. Until recent not much has been done in characterising the EPS produced from form the *L. salivarius* when compared to the other commensal Lactobacilli. The EPS from the *L. salivarius* CCUG44481 was analysed by both chromatographic methods and NMR spectroscopy to determine the underlying components that make up its structure. The ¹H-NMR spectra for the supplied S2 of the strain CCUG44481 indicated the presence of three anomeric signals and the results obtained from the SEC-MALLS suggested the bacterial EPS to have a high molecular weight with a narrow distribution of molecular masses. Comparing the ¹H-NMR profile of the isolated EPS from the CCUG44481 strain to that of a commercially available dextran was a match confirming the EPS to be a dextran unit but with much more branches. The monomer analysis using the HPAEC-PAD and GC-MS indicated a single peak which was confirmed to be D-glucose implying the EPS to be a homopolysaccharide. The linkage analysis produced four peaks which were confirmed to be terminal hexose, 1,3-linked, 1,6-linked and 1,3,6-linked hexoses. In conclusion, it is evident

that the NMR spectra and the wet chemical analysis are all consistent with the EPS isolated from *L. salivarius* CCUG44481 being a highly branched dextran. The majority of 1,6-links observed in the linkage analysis and the very close overlap of the corresponding contours on the HSQC spectrum of the commercial dextran resonances (blue) with a set of those present in the *L. salivarius* CCUG44481 spectrum (black contours) supports the proposition that the main chain is 1,6-linked as has been reported by previous researchers²⁷⁰⁻²⁷². The observation of a single branching point in the linkage analysis (1,3,6-linkedhexose) and the observation of anomeric resonances at 5.3 ppm is consistent with branching from the 3-position of hexoses in the main chain. Information about the number of branches can be estimated from the number of terminal glucose residues in the linkage analysis; the number of terminal sugars must match the number of branching points and the percentage areas observed in the GC-chromatographs are reasonably close (this assumes similar response factors for the corresponding methylated alditol acetates). The highly branched nature of this characterised dextran EPS from *L. salivarius* CCUG44481 is unique in comparison to other making it a novel structure in addition to the probiotic being of a bird origin.

Chapter 4

4. Attempt to Develop a Robust and Rapid Method for Linkage Analysis using HPAEC-PAD and Employing Partially Methylated Cyclodextrin as Model Substrates

4.1. Introduction

In the two previous chapters linkage analysis was used to determine the substitution pattern of the monosaccharides present in either the EPS or CPS, which were isolated from bacterial sources. The process is cumbersome and a reasonable amount of skill is required to complete the four steps needed to undertake the classical linkage method^{206, 208}. As was stated in the introduction, the method used for linkage analysis in the laboratories at the University of Huddersfield was the permethylation procedure introduced by Ciucanu and Kerek (1984)^{208, 233, 234} in which solid sodium hydroxide is employed as a base and methyl iodide as the electrophile. The methylated polysaccharides are subsequently hydrolysed, reduced with sodium borodeuteride and the methylated alditols acetylated with acetic anhydride and pyridine. Unfortunately, the base catalysed acetylation step that is used in both monomer and linkage analysis is inhibited by the borate salts produced during the reduction step and it was necessary to remove the borate by repeated addition of methanol and evaporation of volatile borate esters. The process normally takes a minimum of two days to complete and requires very small quantities of polysaccharide. In 2013, Mischnick *et al*²⁷⁸ undertook a critical re-investigation of the method and modified the procedure to use an acid catalysed acetylation reaction to overcome problems with borate removal. Mischnick *et al* (2013) demonstrated the robustness of the process whilst studying the substituent distribution in methyl celluloses. When the procedure was repeated as part of the current research for the analysis of EPSs, the acid catalysed acetylation introduced a number of small new impurity peaks that interfered with the detection of trace levels of neutral monosaccharides and as such was considered to be unsuitable for linkage analysis of complex mixtures of polysaccharides. The difficulty in performing methylation analysis had prompted Sims *et al*(1996)²⁷⁹ to publish a technical note outlining the precise procedures, which need to be adopted if accurate results are to be obtained using classical methods.

In the last couple of decades a number of new instrumental techniques have been reported for performing linkage analysis, with the most popular being derivatisation with aminobenzoic acid and analysis of the chromophorically labelled sugars by electrospray

ionization-LC-MS²⁸⁰ Whilst the procedures are less time consuming than is the case with GC-MS methods they require access to LC-MS instrumentation.

As was stated in the introduction, in the past couple of decades there has been a large increase in the number of publications where researchers have used HPAEC-PAD for the direct detection and identification of underivatised monosaccharides and oligosaccharides. The use of HPAEC-PAD for the determination of monosaccharide composition of polysaccharides is now routine and after an acid hydrolysis step (which normally takes two hours to complete) samples can be directly analysed with run times of less than an hour. The separation of over a hundred different neutral monosaccharides by anion exchange chromatography have been described²⁸¹. To date only very limited work has been undertaken to determine if HPAEC-PAD can be used to undertake linkage analysis. It was postulated that one possible method for completing linkage analysis by HPAEC-PAD would be to methylate the polysaccharide and then hydrolyse the methylated polysaccharide to generate methylated monomers and to attempt to separate the methylated monomers using HPAEC-PAD. The technique would require the preparation of a standard set of variously methylated monomers whose retention times could be used for comparison. There are very few references to the use of HPAEC-PAD for the analysis of methylated monosaccharides dating back to Koizumi *et al*(1992)²⁸² who prepared a set of mono-methyl D-glucoses substituted at various positions and reported their retention times. Addition of a methyl group reduces the retention time compared to that of the parent monosaccharide and the authors reported similar retention times for the different mono-substituted glucoses. In contrast, in previous studies at the University of Huddersfield HPAEC-PAD analysis has been used to explore the distribution pattern of methyl glucoses generated by acid hydrolysis of partially methylated celluloses. The aim of the work, which was performed by a project student under my supervision in our research team, was to determine if the excipients used in the formulation of drug substances could be determined by studying the pattern of methyl glucoses generated from various formulations of the active excipients. These provisional studies suggested that the different classes of substituted methyl glucoses, mono, di and tri-substituted glucoses, could be separated by HPAEC-PAD.

This chapter describes the work that was undertaken to determine if HPAEC-PAD analysis can be used for linkage analysis. A programme of research was undertaken to prepare and

separate a range of methylated glucoses as standards for use in HPAEC-analysis. Various procedures have been reported to produce partially methylated sugars, which were subsequently reduced and acetylated for use as standards in linkage analysis by GC-MS. In the current work it was decided to use commercially available partially methylated β -cyclodextrin as a source of methyl glucoses from which a specific set of different isomers of, mono, di and tri-substituted glucoses could be recovered. These were chosen as they had been previously used in undergraduate projects and the presence of the 1,4-linkage also restricted the expected number of methyl glucoses to eight compounds which included: unsubstituted glucose; the monosubstituted 2-methyl, 3-methyl and 6-methyl glucoses; the disubstituted 2,3-dimethyl, 2,6-dimethyl and 3,6-dimethyl glucoses; and the trisubstituted 2,3,6-trimethyl glucose.

4.2. Monomer Analysis of Methylcyclodextrin and Separation of its Individual Sugar Units through a Carbon-Silica Column.

Methylcyclodextrin (3mg) was hydrolysed, reduced and acetylated as described in section 2.8.4 and was analysed by the GC-MS. After the hydrolysis step, the sample was also analysed through the HPAEC-PAD.

In an attempt to separate the individual monomer units, a large-scale hydrolysis step was carried out where the methylated β -cyclodextrin (1 g) was reacted with TFA (2 M). A rotary evaporator was used to evaporate the solution to dryness at 70°C. Methanol (2×50 ml) was added and the solution evaporated to dryness in order to remove the TFA and the dried residue was dissolved in UPW (2 ml) and transferred into a carbon-silica column for separation. The carbon-silica column was prepared by mixing carbon (25 g) and silica (25 g) in UPW (200 ml).

The dissolved hydrolysed methyl- β -cyclodextrin (1 g, 2 ml) was transferred onto the carbon-silica column and methanol was used at different concentrations with UPW as the mobile phase to elute the column. The mobile solvents used to separate the fractions were UPW (100% of 200 ml) for fraction 1, 5% methanol (200 ml) for fraction 2, 10% methanol (200 ml) for fraction 3, 20% methanol (200 ml) for fraction 4, 30% methanol (200 ml) for fraction 5, 40% methanol (200 ml) for fraction 6, 50% methanol (200 ml) for fraction 7, 60% methanol (200 ml) for fraction 8, 70% methanol (200 ml) for fraction 9, 80% methanol (200 ml) for

fraction 10, 90% methanol (200 ml) for fraction 11 and 100% methanol (200 ml) for fraction 12.

All these fractions were collected dried using the rotary evaporator and the residues dissolved in D₂O and the ¹H-NMR recorded on the Bruker DPX400 400.13 MHz NMR spectrometer. Small portions of these fractions (100 μl) were diluted with UPW (2 ml) and then analysed by HPAEC-PAD.

4.3. Results

In the first instance, experiments were undertaken to determine the distribution of methyl groups in the partially methylated cyclodextrin and methylcellulose. After acid hydrolysis to generate methyl glucoses (see experimental section), the residues were dissolved in UPW and approximately half of the sample was analysed by HPAEC-PAD (*Fig 4.1*).

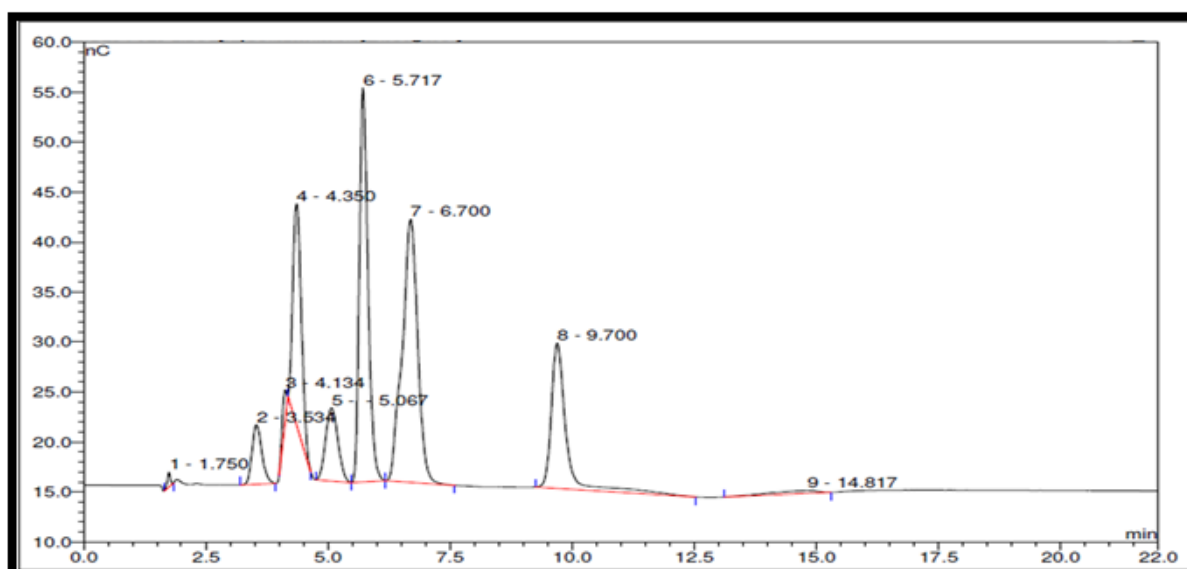


Figure 4.1. HPAEC-PAD Traces of Methyl-β-Cyclodextrin after Hydrolysis

During hydrolysis, the glycosidic bonds of the methyl-β-cyclodextrin are broken down to generate monomer units. A total of 6 peaks (*Fig 4.1*) were observed when the sample was analysed with the HPAEC-PAD but peaks 4 and 7 are seen to have a hump implying they are 2 peaks each which couldn't be separated. So, when we consider these 2 joined peaks the total number of peaks is 8 as expected. The final peak eluting from the column had the same retention time as that of glucose and this confirmed what Koizumi *et al* (1992)²⁸² had found that the addition of methyl group reduces the acidity (increase in pKa) of the monosaccharide and in doing so reduces the retention time of the analyte. Since the HPAEC-

PAD chromatograph couldn't be used to identify which peak represented which of the various substituted glucoses that were present in the individual peaks, the other half of the sample was reduced, acetylated and then analysed by GC-MS (*Fig 4.2*) and the mass spectra obtained for the different peaks were used to determine the substitution pattern.

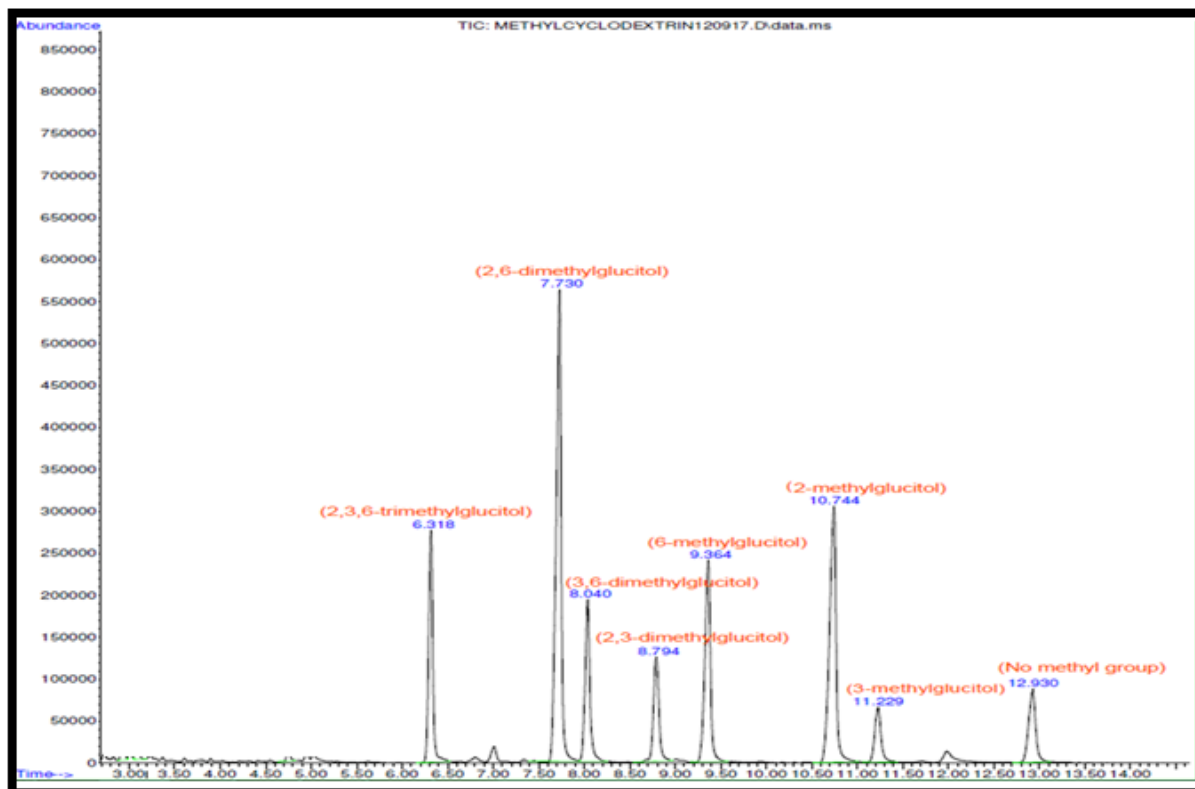


Figure 4.2. Gas Chromatogram of Methyl- β -cyclodextrin from GC-MS

Again, as expected, the GC-trace for the permethylated alditol acetates generated from methyl- β -cyclodextrin contained eight peaks and the identity of each was determined by inspection of the fragmentation patterns (*Fig 4.3*). It is clear that whilst all of the expected derivatives are present there is considerable variation in the relative amounts of each: some are present in only small amounts e.g. 3-methyl glucose, whilst others are present in large amounts (2,6-dimethyl glucose) considering their relative abundance and peak height (*Fig 4.2*).

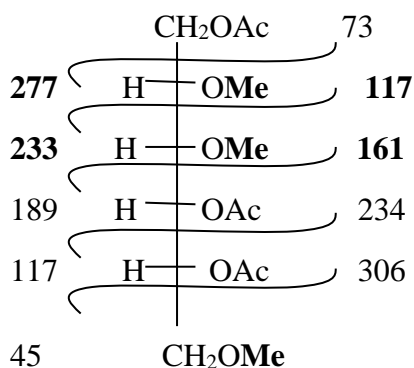


Fig. a. 2,3,6-tri-methylglucitol acetate

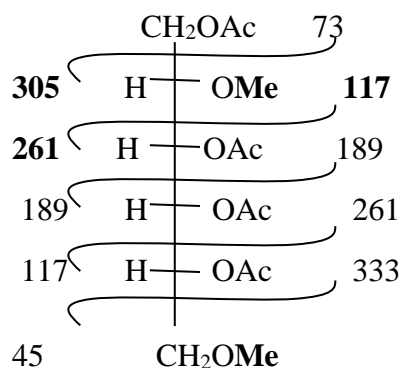


Fig. b. 2,6-di-methylglucitol acetate

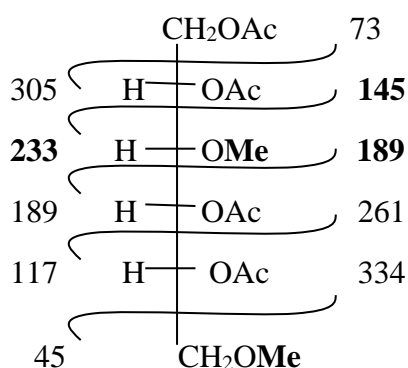


Fig. c. 3,6-di-methylglucitol acetate

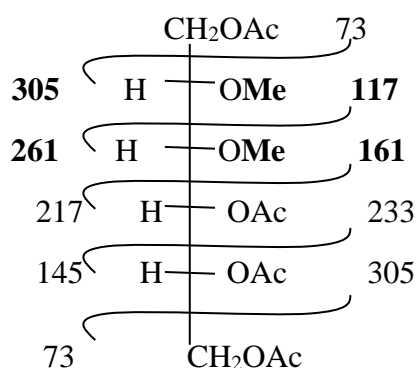


Fig. d. 2,3-di-methylglucitol acetate

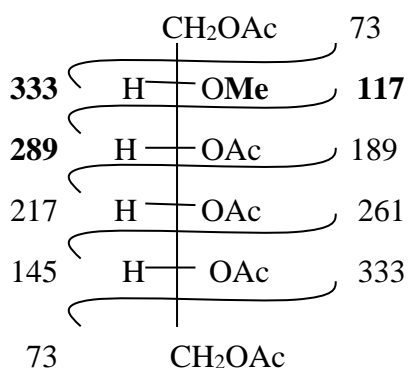


Fig. e. 2-methylglucitol acetate

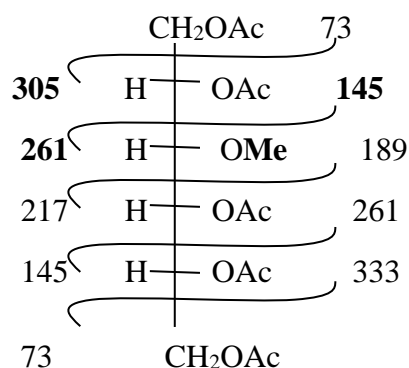


Fig. f. 3-methylglucitol acetate

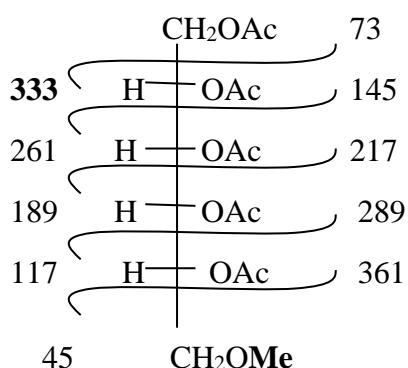


Fig. g. 6-methylglucitol acetate

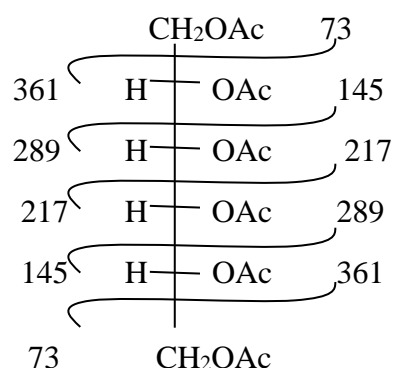


Fig. h. No-Methyl (Glucitol acetate)

Figure 4.3. Fragmentation Patterns of the 8 Peaks Analysed in Methyl- β -cyclodextrin

With knowledge that all eight substitution patterns were present in the partially methylated cyclodextrin, the next step was to perform a large-scale hydrolysis reaction, and an attempt was made to separate each of variously substituted methyl glucoses by passing the reaction mixture through a preparative carbon-celite column (as described in the experimental section) and eluting with increasing percentages of ethanol in combination with UPW. In the first instance the different fractions collected were dried, dissolved in D₂O and their NMRs obtained (Fig 4.4 and Fig 4.5) for 100% water and from 5% methanol to 100% methanol. Subsequently, the samples were analysed by HPAEC.

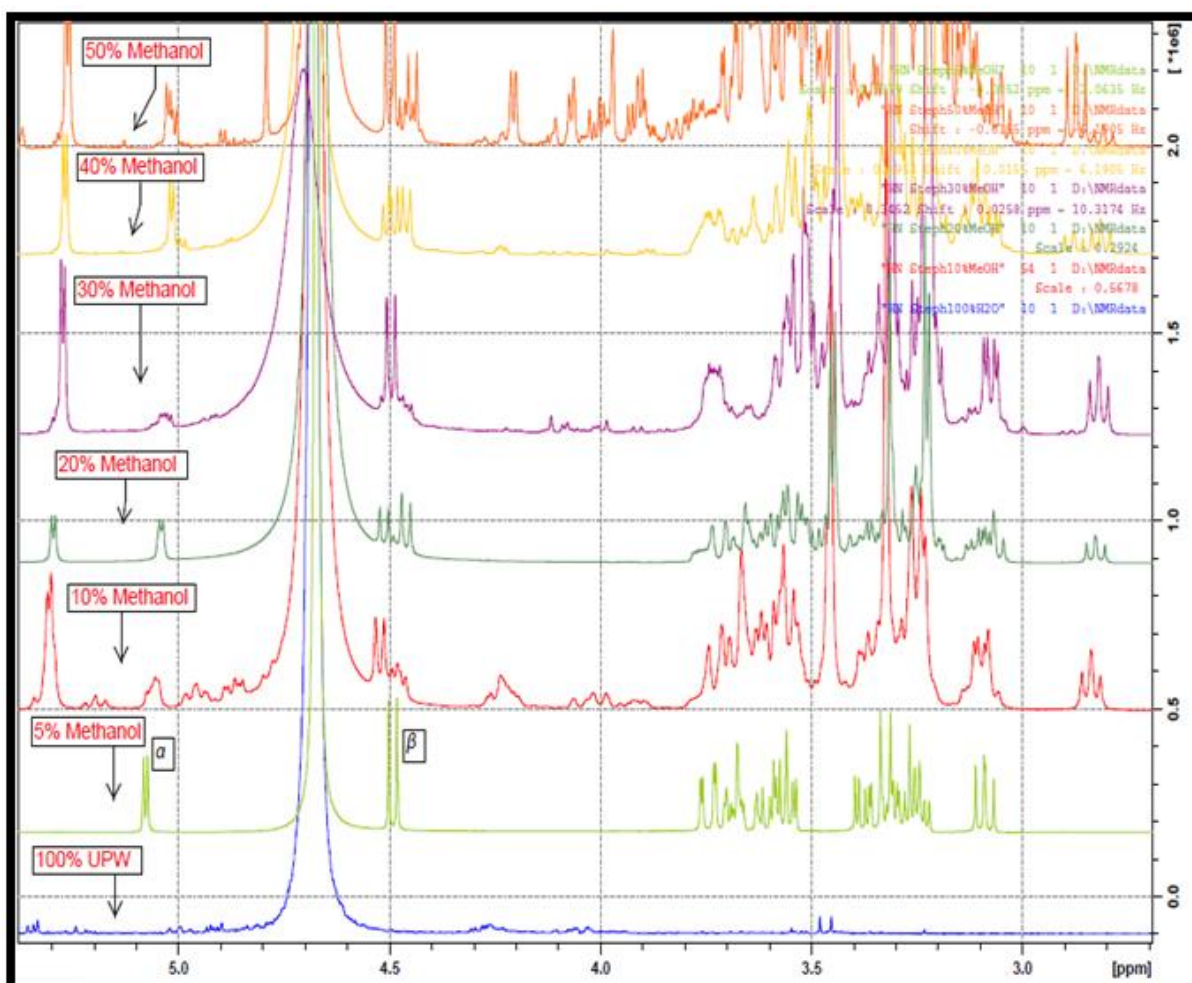


Figure 4.4. ¹H-NMR Spectra of the Fractions obtained from 100% H₂O, 5% to 50% Methanol.

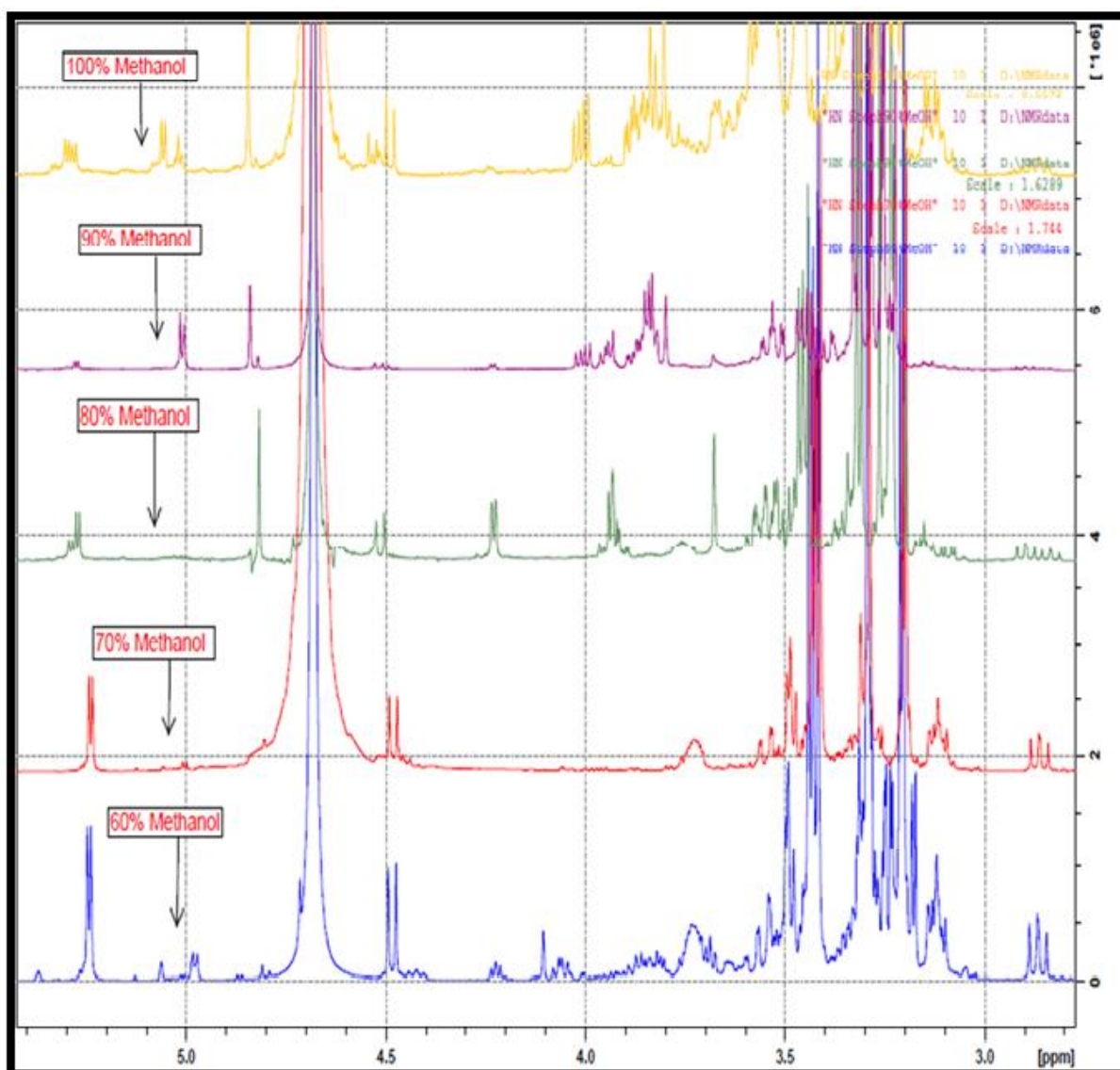


Figure 4.5. ^1H -NMR Spectra of the Fractions obtained from 60% to 100% Methanol

Fraction 1 which eluted with 100% UPW (200 ml), showed no signal on the NMR but when analysed on HPAEC-PAD, a single peak was observed (*Fig 4.6*) and this was identified as glucose. For fraction 2 which eluted with 5% methanol, the anomeric region on *Fig 4.4* indicated that the glucose was present as the two peaks signified that it was the α and β for the glucose molecule. The HPAEC-PAD analysis of this fraction 2 further confirmed that it was the glucose that was collected (*Fig 4.7*).

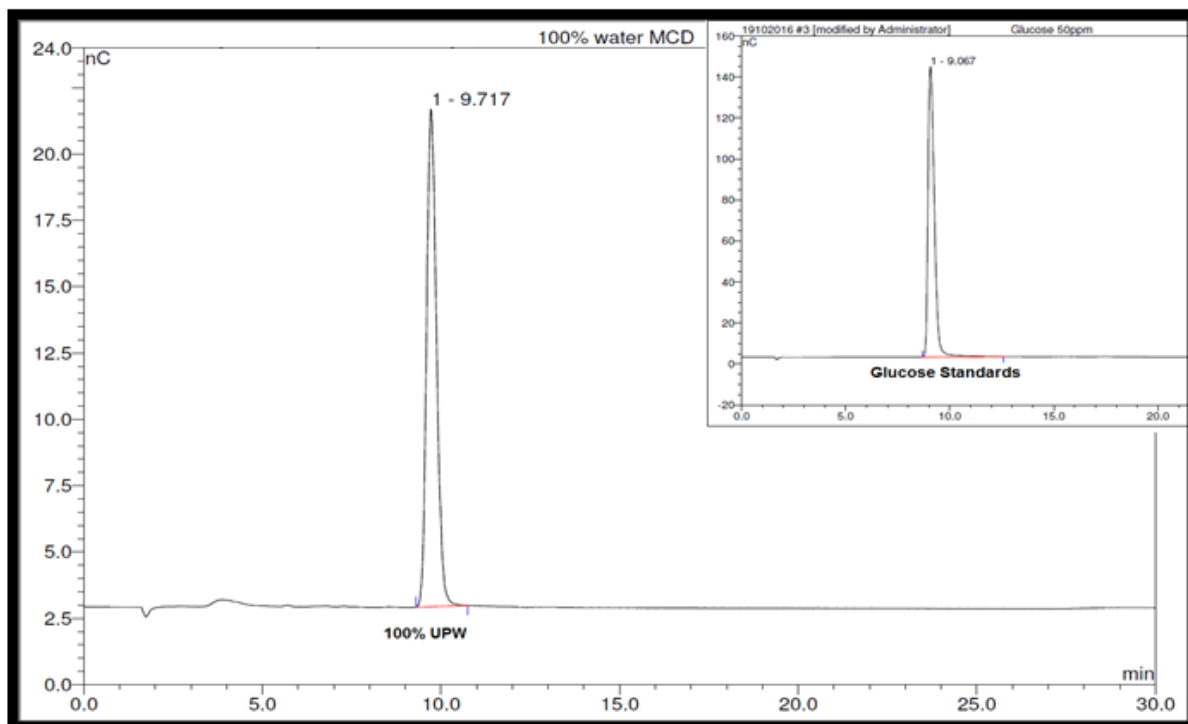


Figure 4.6. HPAEC-PAD Traces for Fraction 1 (100% UPW)

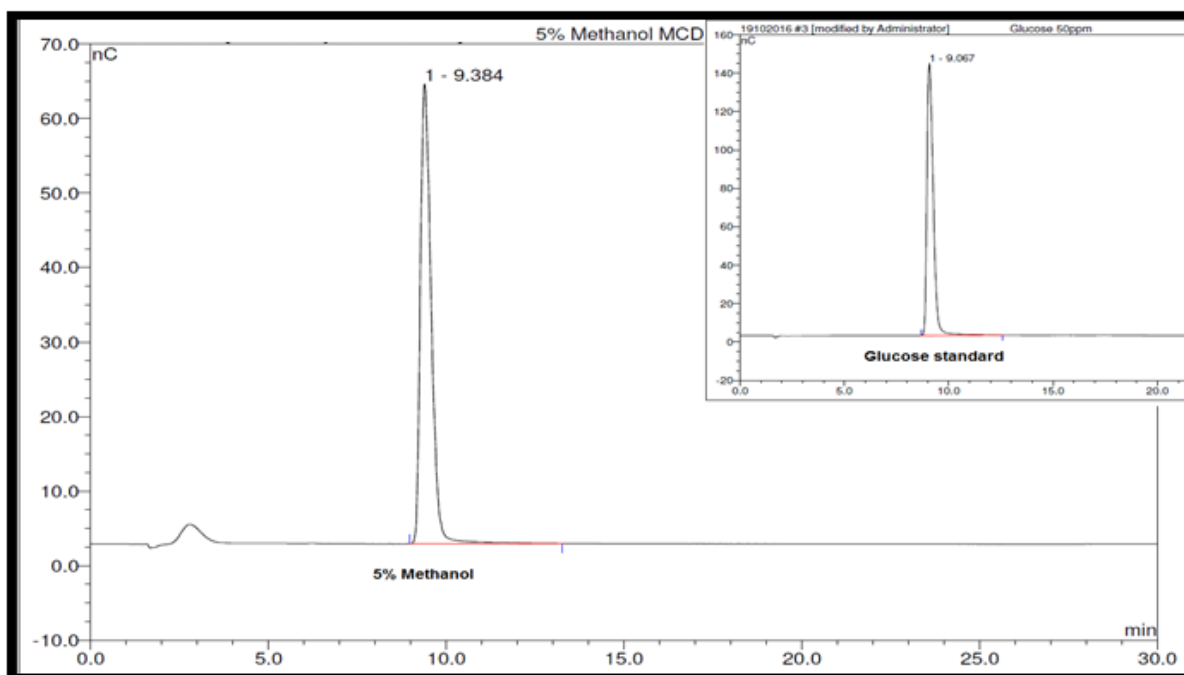


Figure 4.7. HPAEC-PAD Traces for Fraction 2 (5% Methanol)

The HPAEC-PAD results of fraction 3 (10% methanol) (*Fig 4.8*) showed that three peaks were present including glucose and what were suspected to be the mono-substituted sugar units. Comparison of the peak area and height on the HPAEC-PAD traces of 5% and 10% (*Fig 4.7*

and Fig 4.8 respectively) indicated that the level of glucose was decreasing. The glucose level is also seen to drop by comparing the glucose peaks on the $^1\text{H-NMR}$ spectra (Fig 4.4). From inspection of the GC-MS analysis that was performed on the crude material, the sample is expected to contain approximately a 5:3:1 ratio of the 2-mono, 6-mono and the 3-mono glucoses. The material in the 10% fraction was converted to the PMAAs and was analysed by GC-MS which suggests that 2-mono glucose was present in the largest amount and this would suggest that this is the second from last peak to elute from the HPAEC-PAD (RT=7.3 min peak: Fig 4.8). The second peak (RT= 6.2 min peak: Fig 4.8) is therefore likely to be the 6-mono glucose derivative. The elution order on the HPAEC follows the elution order in the GC-MS both of which are the reverse order to which peaks elute from the carbon-celite column.

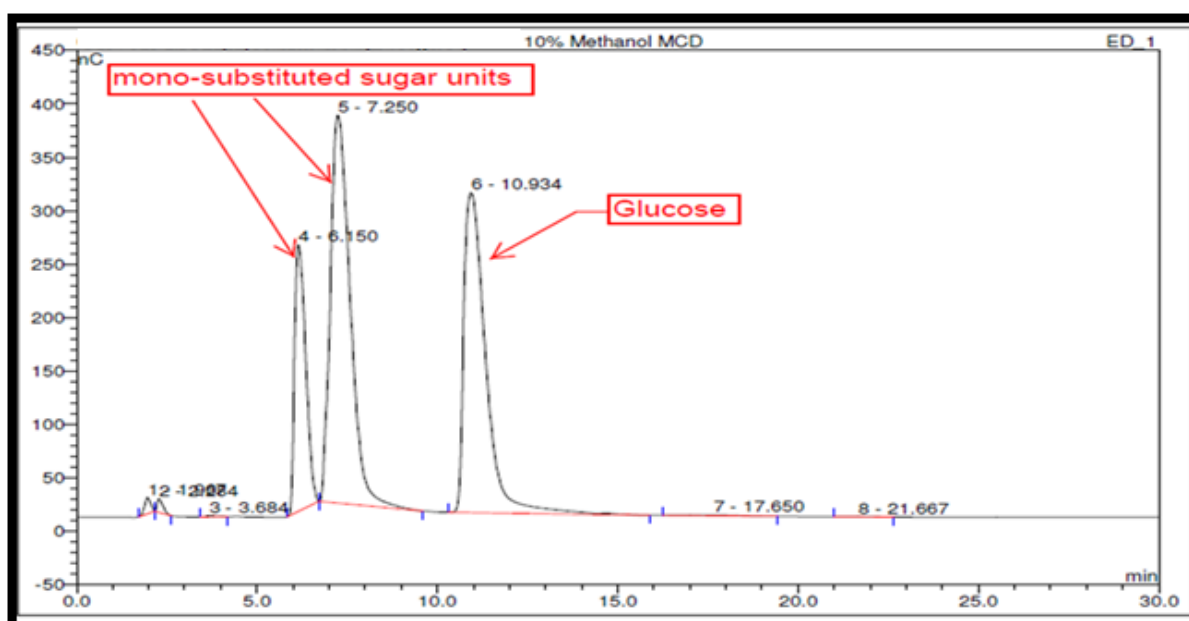


Figure 4.8. HPAEC-PAD Traces for Fraction 3 (10% Methanol)

For the 20% methanol fraction (Fraction 4), the glucose disappears leaving the mono-substituted sugar units, which can be seen, on the HPAEC-PAD chromatogram (Fig 4.9). Whilst the NMR spectra (Fig 4.4) has no peak in the anomeric regions corresponding to glucose but it does have two clearly defined α -anomers and there are also three β -anomeric protons (in an approximate ratio of 2.5:1:3.3), and the latter result suggests that all three mono substituted glucoses are present and that two of the molecules co-elute in the HPAEC-PAD analysis.

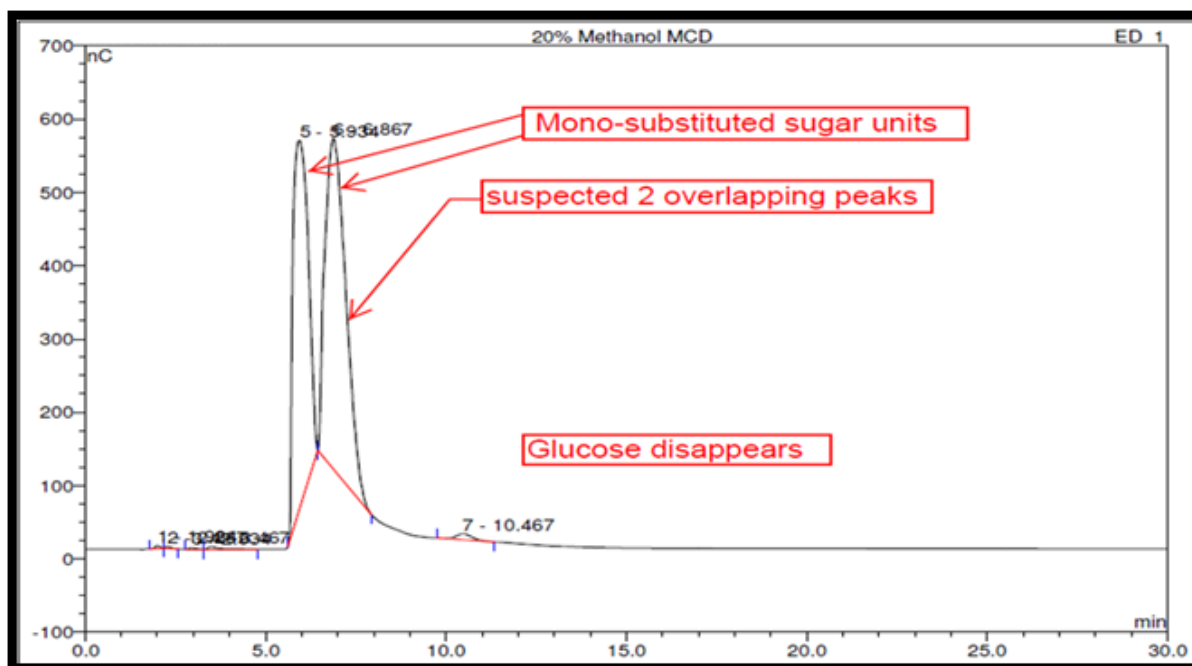


Figure 4.9. HPAEC-PAD Traces for Fraction 4 (20% Methanol)

In the 30% methanol fraction (Fraction 5), a di-substituted sugar is visible as well as small amounts of the mono-substituted sugar units and surprisingly, a late eluting peak is visible which indicates a potential small amount of glucose. There is a decrease in the concentration of the two mono-substituted sugar units in this fraction (*Fig 4.10*). On the $^1\text{H-NMR}$ spectrum of 30% methanol (*Fig 4.4*), a major peak is seen which belongs probably to the di-substituted sugar unit but this is accompanied by minor peaks which are likely to be from mono-substituted sugar units.

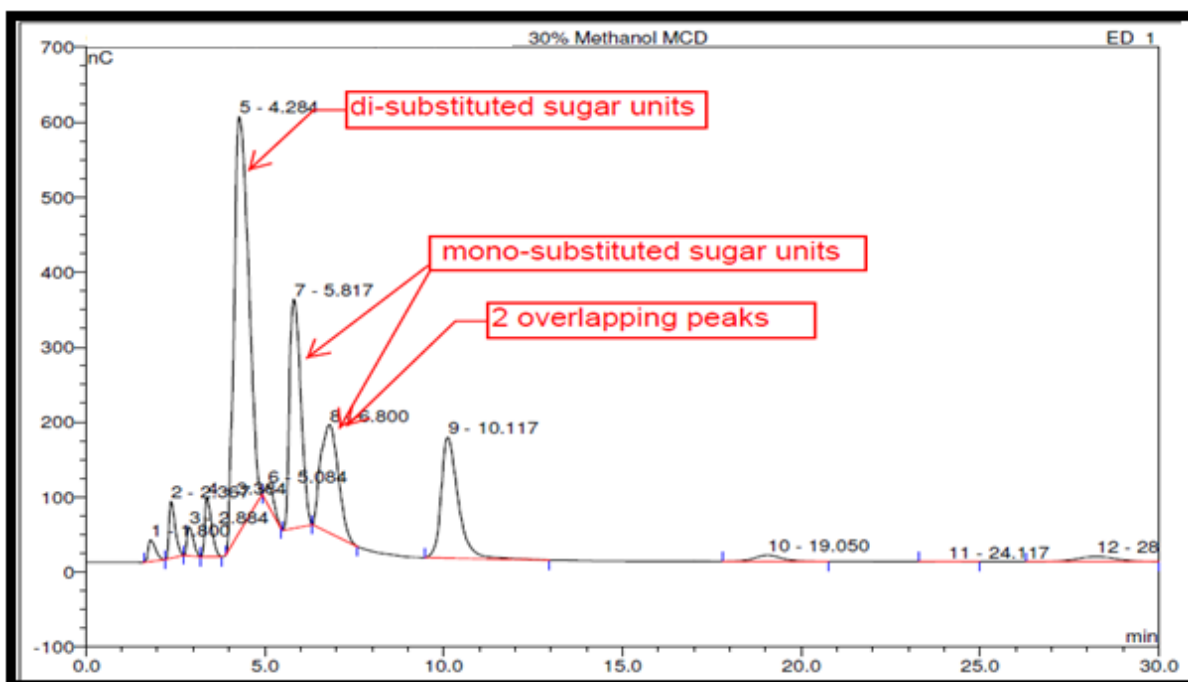


Figure 4.10. HPAEC-PAD Traces for Fraction 5 (30% Methanol)

For the 40% methanol fraction (Fraction 6), the HPAEC-PAD chromatogram (*Fig 4.11*) suggests that dimethyl substituted glucose units have been isolated in this fraction. In the original GC-MS trace (*Fig. 4.2*) of the crude partially methylated cyclodextrin three disubstituted monomers were visible including the 2,3-dimethyl (RT= 8.8 mins) the 3,6-dimethyl (RT= 8.0 mins) and the 2,6-dimethyl (RT= 7.7 mins) and in an approximate ratio of 4.3:1.4:1. The $^1\text{H-NMR}$ spectrum (*Fig 4.12*) has two significant α -anomeric resonances and 3 β -anomeric resonances and the latter result is consistent with 3 disubstituted sugar units eluting within this fraction. The chromatogram also contains a number of minor peaks which suggests that low levels of the mono substituted glucose derivatives were also present.

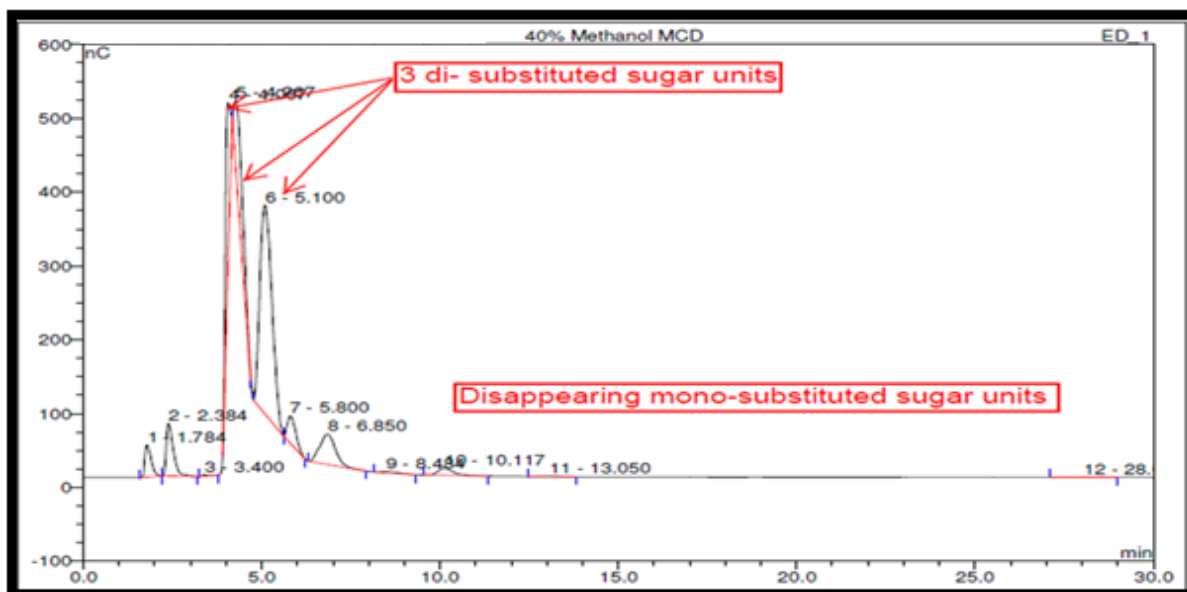


Figure 4.11. HPAEC-PAD Traces for Fraction 6 (40% Methanol)

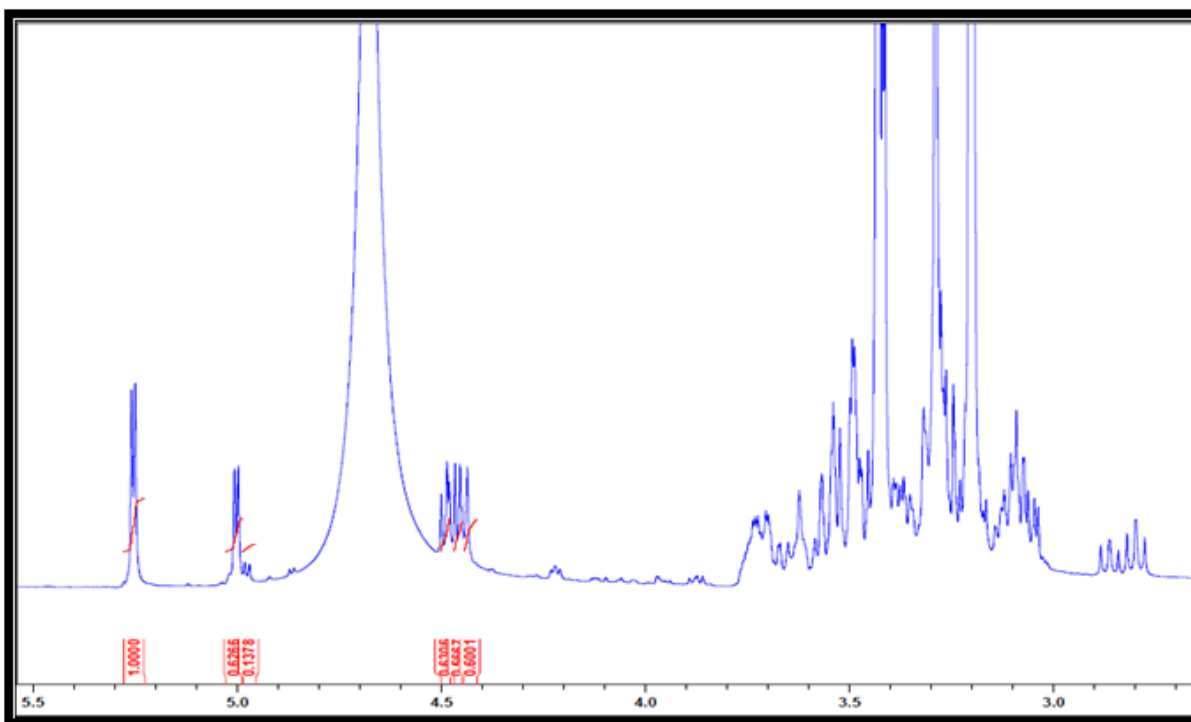


Figure 4.12. ¹H-NMR Spectrum for Fraction 6 (40% Methanol)

To confirm if all three of the di-substituted glucoses were present a number of additional spectra were recorded including a number of ^{13}C -spectra such as the ^{13}C DEPT 135 and 90 spectra. In the DEPT 90 spectra, for the anomeric region, the first 3 signals (95.8, 95.7 & 95.6 ppm) are for the anomeric carbons for the monosaccharides in the α -anomers whilst the remaining three signals (91.9, 89.24 & 89.18) are the corresponding β -anomers which suggests that at least three sets of glucose derivatives were present. In the chemical shift range 80-86 ppm there are 8 signals which range between 80 ppm to 86 ppm and this is the typical location expected of ring methyne carbons that have a methoxy group attached (*Fig 4.13*) and these will correspond to carbons 2 and 3 (underlined) in the following di substituted systems:

α -2,3; β -2,3; α -3,6; β -3,6; α -2,6 and β -2,6

A further 12 signals are observed in the region between 68 ppm and 77 ppm and these are from the non-methylated ring methyne carbons 4 and 5 in the three α -anomers and carbons 4 and 5 in the three β -anomers.

On the DEPT 135, the negative signals identify the CH_2 groups, where at around 70 ppm 4 peaks arise as a result of the two di-methylated sugar units occurring in their α and β forms (i.e. the 2,6 and the 3,6 di-methylated monomers) in which the methylene units carry a methoxy group. The CH_2 signal around 60 ppm indicates a pair of di-methylated sugar monomers, α and β forms anomers, in which the methylene carbon is not a recipient of a methoxyl group i.e. in the 2,3-dimethylated monomer (*Fig 4.13*).

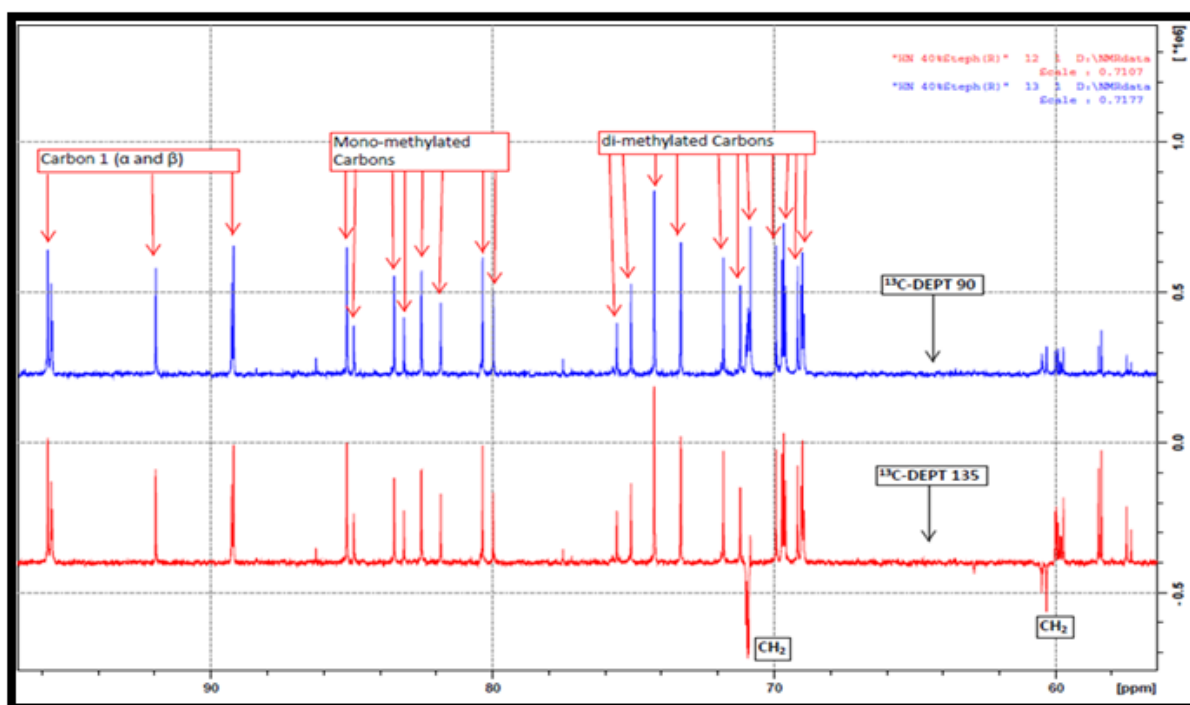


Figure 4.13. ^{13}C DEPT 90 and 135 for the 40% Methanol fraction

The fractions 50%, 60%, 70%, 80%, 90% and 100% showed more complex HPAEC-PAD chromatograms and ^1H -NMR spectra indicate a mixture of the tri-methylated sugar unit and other materials which may have not been hydrolysed. Hence making it difficult to identify in which fraction the tri-methylated sugar unit eluted.

In order to establish if the first major peak eluting from the HPAEC-PAD system was the trimethyl substituted glucose derivative, a second preparative column was run and smaller fractions were collected. One of the difficulties encountered with the recording of spectra for the late running fractions in the first column arose from poor solubility of the products. For the second column several NMR were recorded in deuteriomethanol. The NMR spectrum recorded for the final fraction (*Fig 4.14*), collected with 100% methanol, showed that a mixture of alpha and beta-anomers of the trimethyl glucose derivative had been isolated.

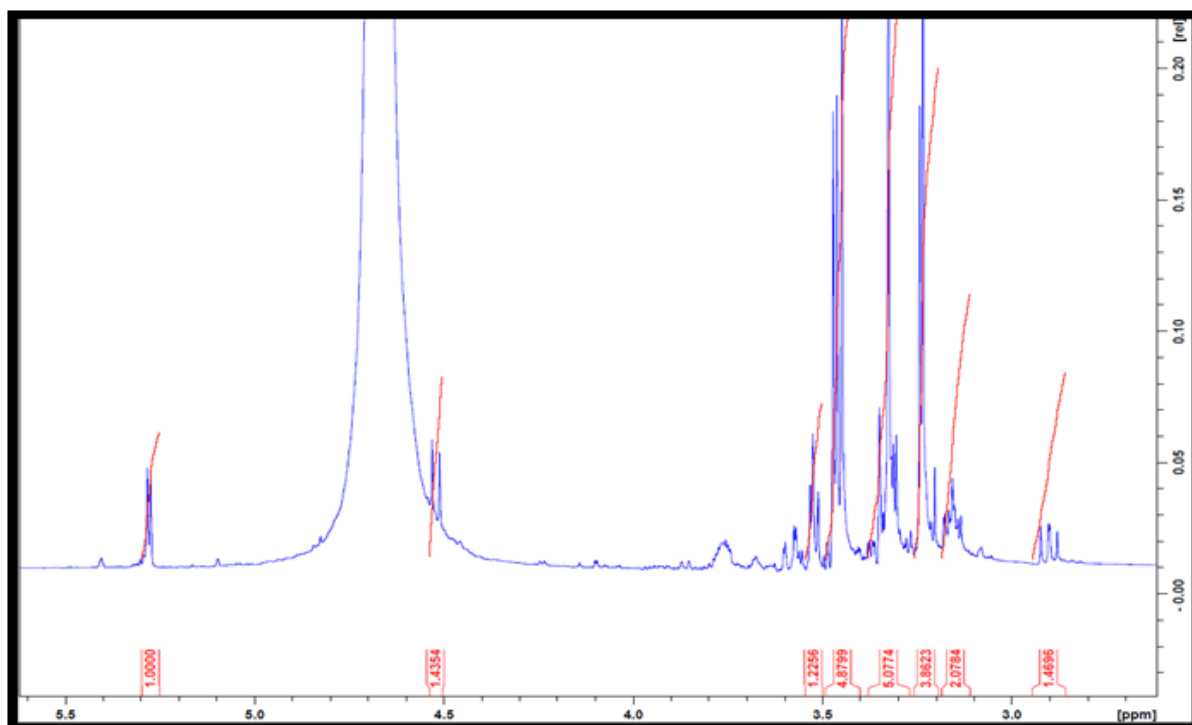


Figure 4.14. ^1H -NMR Spectrum for Fraction of 100% Methanol of the Second Run.

In the NMR the anomeric resonances appear at 5.27 ppm (α -H1) and 4.51 ppm (β -H1) and there are two sets of three methoxyl groups (a large set at 3.47, 3.33 & 3.24 ppm and a smaller set at 3.47, 3.46 and 3.24 ppm; *Fig 4.15*) which identify that this fraction contains the trimethyl substituted glucose. Finally, the fraction was passed through the HPAEC–PAD and the largest peak was observed at 3.7 mins.

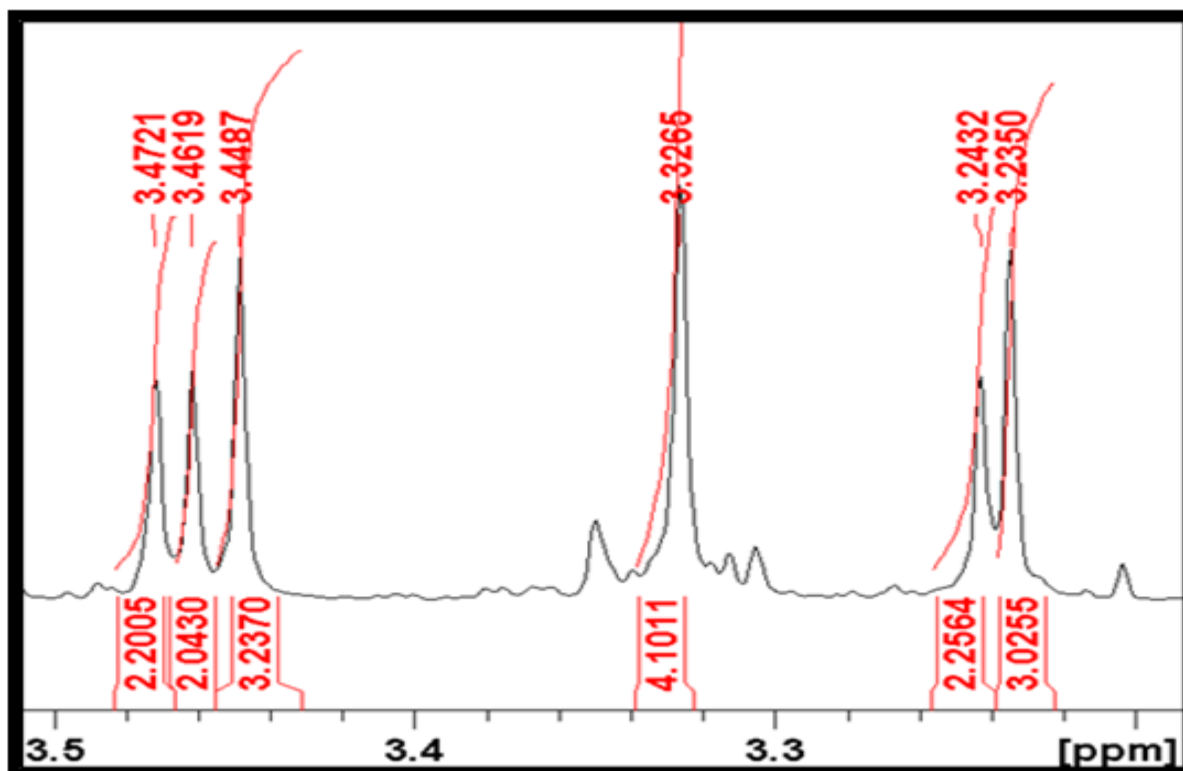


Figure 4.15. ¹H-NMR Indicating the Two Sets of Three Methoxy Groups

4.4. Conclusion

From analysis of the results generated from the early fractions, it is clear that both the HPAEC-PAD analytical chromatography system and the preparative carbon celite column have been able to separate the methylated glucoses based on the degree of substitution: with glucose, the mono-substituted, the disubstituted and the tri-substituted glucoses eluting at different times. The order of elution from the HPAEC-PAD system is clearly dictated by the number of methyl groups present. When the mobile phase was 10 mM NaOH and using a flow rate of 0.5 mL min⁻¹ the trisubstituted glucose eluted first at 3.53 mins, the disubstituted glucoses elute between 4.1 and 5.1 mins, the monosubstituted glucoses elute between 5.7 and 6.7 mins and finally glucose eluted at 9.7 mins. The very similar retention times of the isomeric mono-methylated and the similar retention times of the di-methylated monosaccharides combined with the failure to isolate clean standards from the preparative column suggested that it was highly unlikely that a method for undertaking linkage analysis using HPAEC-PAD is likely to succeed using existing instrumentation and columns. As such, this area of work was not pursued further. Attempts to develop this method was to be used to cut down the amount of time that will be spent for the linkage analysis of the EPSs for the other strains of probiotic

bacterial of interest (*Bifidobacteria breve* 7017). With the difficulties and shortcomings encountered in developing this linkage analysis using the HPAEC-PAD, we had to go back to using the lengthy classical linkage method for the next strain of interest which will be seen in the next chapter (chapter 5).

Chapter 5

5. Production and Isolation of Polysaccharides that are Excreted or Presented at the Cell Surface of *B. breve* 7017.

As was stated in the introduction, one genus of bacteria that includes a range of species that have potential as probiotics is Bifidobacteria. In the early stages of life, large populations of Bifidobacteria colonise the human gastrointestinal tract and there is evidence to suggest that their presence is linked to the development of a healthy immune system ^{283, 284}. As humans grow older the proportion of Bifidobacteria in the gut decreases as other species of bacterial colonise the gastrointestinal tract and a more mature gut microflora is established. In a healthy gut microflora, a large number of species of bacteria co-exist and many of these species support their host by assisting with the absorption of nutrients and with the maintenance of an environment where pathogenic strains of bacteria are unable to flourish. Unfortunately, under the influence of a variety of different factors, the balance of the gut microflora can be disturbed, and this can lead to a variety of illnesses and diseases. It has also been reported that a number of these diseases can to a varying extent be alleviated by administering Bifidobacteria. The presence of specific strains of Bifidobacteria in the gut microbiota has been linked to a range of health benefits ^{111, 112, 285}. These have included providing protection against pathogenic organisms; modulation of immune response ^{9, 12, 113}, strengthening intestinal epithelial barrier function ²⁸⁶, relieving disorders of GI-tract ²⁸⁷⁻²⁸⁹ and reducing the levels of cholesterol ²⁹⁰⁻²⁹³. In research directed at determining the mechanism of this biological activity, researchers have identified a number of potential effector molecules including proteins, small peptides and cell surface polysaccharides including exopolysaccharides (EPSs) ^{114, 294}. It is the polysaccharides that are secreted as exopolysaccharides or presented at the cell surface (capsular polysaccharides) of probiotic organisms, which is of interest in the current research as stated earlier.

A number of comparative genomic studies on Bifidobacteria have been undertaken and these routinely identify that organisms have ability to synthesise a range of polysaccharides including EPS and capsular materials. Despite knowing that the different strains have the genetic machinery to be able to synthesise polysaccharides very little is known about their structures and this is the focus of the work presented in this chapter where an attempt has

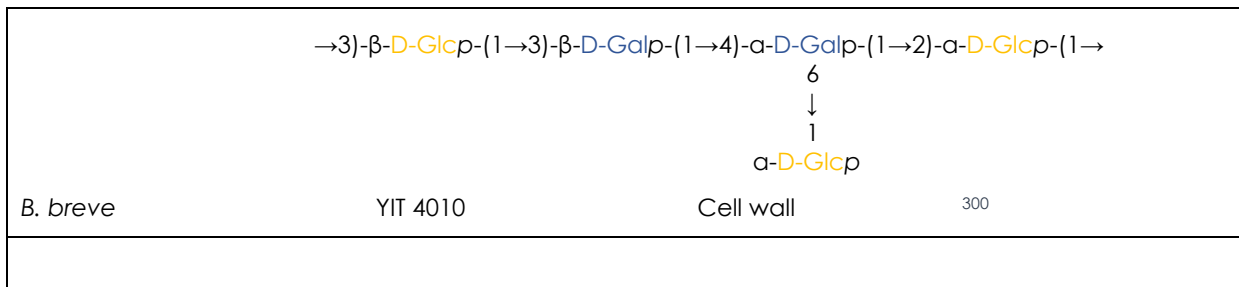
been made to isolate and determine the structures of polysaccharides prepared by a number of different strains of *Bifidobacteria breve*.

At the time of writing this thesis, structures for EPSs from five strains of Bifidobacteria had been reported (table 5.1): three from *Bifidobacterium longum* ²⁹⁵⁻²⁹⁷ and two from *Bifidobacterium animalis* ^{119, 298}. At the same time, the structures or partial structures of nine Bifidobacteria cell-wall polysaccharides have been published ^{13, 110, 299-305}. Finally, the structures of two teichoic acids recovered from Bifidobacteria have also been reported ³⁰⁶.

Table 5.1: The EPS Structures from *Bifidobacteria species*

Species	Strain	EPS location	References.
<i>B. animalis ssp. lactis</i>	RH	Cell wall	298
$\begin{array}{c} \alpha\text{-D-Galp} \\ \\ 1 \\ \downarrow \\ 3 \\ \rightarrow 4\text{-}\alpha\text{-D-Glcp}\text{-}(1\rightarrow 4)\text{-}\alpha\text{-D-Manf}\text{-}(1\rightarrow 4)\text{-}\alpha\text{-L-Rha}\text{-}(1\rightarrow 4)\text{-}\alpha\text{-D-Manf}\text{-}(1\rightarrow 4)\text{-}\alpha\text{-D-Galf}\text{-}(1\rightarrow \end{array}$			
<i>B. longum</i>	JBL05	Extracellular	295
$\begin{array}{c} \beta\text{-D-Glcp} \\ \\ 1 \\ \downarrow \\ 6 \\ \rightarrow 4\text{-}\alpha\text{-D-Galp}\text{-}(1\rightarrow 4)\text{-}\alpha\text{-D-Galp}\text{-}(1\rightarrow 4)\text{-}\alpha\text{-D-Glcp}\text{-}(1\rightarrow 3)\text{-}\alpha\text{-D-Galp}\text{-}(1\rightarrow 3)\text{-}\alpha\text{-L-Rhap}\text{-}(1\rightarrow \\ \\ 4 \\ \downarrow \\ 1 \\ \beta\text{-D-Galp} \end{array}$			
<i>B. longum</i>	BIM B-476-D	Extracellular	305
$\begin{array}{c} \rightarrow 4\text{-}\beta\text{-D-Galp}\text{-}(1\rightarrow 3)\text{-}\beta\text{-D-Galf}\text{-}(1\rightarrow 3)\text{-}\alpha\text{-D-Glcp}\text{-}(1\rightarrow 2)\text{-}\beta\text{-D-Galf}\text{-}(1\rightarrow 6)\text{-}\alpha\text{-D-Sugp}\text{-}1\text{-P}\text{-}(0\rightarrow \\ \\ -1)\text{-Rib-ol-5-P}\text{-}(0\rightarrow \\ \quad \\ 2 \quad 3 \\ \uparrow \quad \uparrow \\ \alpha\text{-D-Glcp} \quad \alpha\text{-D-Glcp} \\ \\ -3)\text{-Gro-1-P}\text{-}(0\rightarrow \\ \\ 2 \\ \uparrow \\ 1 \end{array}$ <p style="text-align: right;">Sug = GlcNAC or Glc (~4.5:1)</p>			
<i>B. longum</i>	YIT 4028	Cell wall	303
$\begin{array}{c} \rightarrow 2\text{-}\alpha\text{-L-Rhap}\text{-}(1\rightarrow 3)\text{-}\alpha\text{-D-Galp}\text{-}(1\rightarrow 2)\text{-}\alpha\text{-L-Rhap}\text{-}(1\rightarrow 3)\text{-}\alpha\text{-D-Galp}\text{-}(1\rightarrow \\ \\ 6 \\ \downarrow \\ 1 \\ \alpha\text{-D-Galp} \end{array}$			
Species	Strain	EPS location	References

			$\begin{array}{c} \beta\text{-Glc} \\ \\ 1 \\ \downarrow \\ 3 \\ \rightarrow 2)\text{-}\alpha\text{-6dTal}\text{-}(1\rightarrow 3)\text{-}\beta\text{-6dTal}\text{-}(1\rightarrow 3)\text{-}\beta\text{-6dTal}\text{-}(1\rightarrow 3)\text{-}\beta\text{-6dTal}\text{-}(1\rightarrow 2)\text{-}\alpha\text{-6dTal}\text{-}(1\rightarrow 2)\text{-}\alpha\text{-6dTal}\text{-}(1\rightarrow \end{array}$		
<i>B. adolescentis</i>	YIT 4011	Cell wall	302		
			$\begin{array}{c} \rightarrow 4)\text{-}\beta\text{-D-Galf}\text{-}(1\rightarrow 5)\text{-}\beta\text{-D-Galf}\text{-}(1\rightarrow \\ \\ 6 \\ \downarrow \\ 1 \\ \alpha\text{-D-Galp} \end{array}$		
<i>B. catenulatum</i>	YIT 4016	Cell wall	301		
			$\begin{array}{c} \rightarrow 6)\text{-}\alpha\text{-D-Glcp}\text{-}(1\rightarrow 3)\text{-}\beta\text{-D-Galf}\text{-}(1\rightarrow 3)\text{-}\alpha\text{-D-Glcp}\text{-}(1\rightarrow 2)\text{-}\beta\text{-D-Galf}\text{-}(1\rightarrow 3)\text{-}\alpha\text{-L-Galp}\text{-}(1\rightarrow 3)\text{-}\alpha\text{-D-Glcp}\text{-}(1\rightarrow \\ \\ 6 \\ \downarrow \\ 1 \\ \alpha\text{-D-Glcp} \end{array}$		
<i>B. bifidum</i>	BIM B-465	Cell wall	110		
			$\begin{array}{c} \text{H}[-5\text{-}\beta\text{-D-Galf}1]_n\text{-}[1\rightarrow 3)\text{-}\alpha\text{-D-Glcp}]_m\text{-}(1\rightarrow 6)\text{-}\beta\text{-D-Galp}\text{-}(1\rightarrow 3)\text{acyl}_2\text{ glycerol} \\ \\ \text{O} \\ \text{O} = \text{P} - \text{O-1-glycerol-3-Ala,H} \\ \\ \text{O}^- \end{array}$		
<i>B. bifidum pennsylvanicum</i> subsp.	BIM B-465	Cell wall (Lipoteichoic acid)	110		
			$3)\text{-}\beta\text{-D-Galf}\text{-}(1\rightarrow 3)\text{-}\alpha\text{-D-Galp}(1\rightarrow$		
<i>B. infantis</i>	ATCC 15697	Cell wall	304		
			$\begin{array}{c} \text{A-D-Galf}\text{-}(1\rightarrow 2)\text{-}\alpha\text{-L-Rhap} \\ \\ 1 \\ \downarrow \\ 2 \\ \rightarrow 4)\text{-}\beta\text{-D-Glcp}\text{-}(1\rightarrow 3)\text{-}\alpha\text{-L-Rhap}\text{-}(1\rightarrow 4)\text{-}\beta\text{-D-Galp}(1\rightarrow \end{array}$		
<i>B. animalis</i> ssp. <i>lactis</i>	IPLA-R1-(A1dOxR)	Extracellular	119		



There are a number of reasons why so few polysaccharides have been isolated from Bifidobacteria and their structures characterised but the two biggest obstacles are; Firstly, the vast majority of the strains are strict anaerobes and, as such, they are considered as being difficult to grow. Secondly, the different strains only produce very small amounts of complex mixtures of polysaccharides (combined yields are typically less than 50 mg/L). Because small amounts of polysaccharides are produced, it is important to ensure that extraneous material, which can interfere with polysaccharide production, should not be added to the fermentation as media components. As was stated in the previous chapter, standard media, which support the growth of Bifidobacteria, (MRSc and BIM), contain polysaccharides that can interfere with the analysis of EPS and CPS. In previous work in our group, a new growth medium (HBM) which is suitable for studying Bifidobacteria was developed²²⁶. Despite the availability of HBM, the task of isolating and characterising polysaccharides remains a difficult task and this is because complex mixtures of different polysaccharides are generated.

In order to increase the number of known structures we undertook a programme of research in which a number of different strains of *Bifidobacteria breve* were grown in HBM media supplemented with different sugars (glucose, galactose and lactose) and attempts were made to isolate polysaccharides that were actively excreted by the bacteria into the fermentation media (EPS found in the supernatant). In addition, we also investigated if it was possible to extract cell wall associated polysaccharides i.e. material remaining associated with the cell biomass and if these could be purified and characterised. Whilst most of the work focused on the strain *B. breve* JCM 7017, polysaccharides were also isolated from *B. breve* JCM 7019, *B. breve* JCM 2258 and an EPS (-ve) mutant of *B. breve* 7017 which was supplied by Douwe Van Sinderen's group at University College Cork.

5.1. Identifying Optimum Conditions for the Growth of *B. breve* JCM7017 in HBM Media.

In the first experiments, the growth of *B. breve* JCM7017 in HBM (the broth with no EPS-equivalence as described in section 2.5.1) was monitored over an extended period to determine if the strain would grow, to measure the length of the induction period and to determine when maximum growth was being achieved. After the fermentation was started, small aliquots of the fermentation media were removed at 2 h intervals and the optical density measured to allow the construction of a growth curve (Fig 5.1).

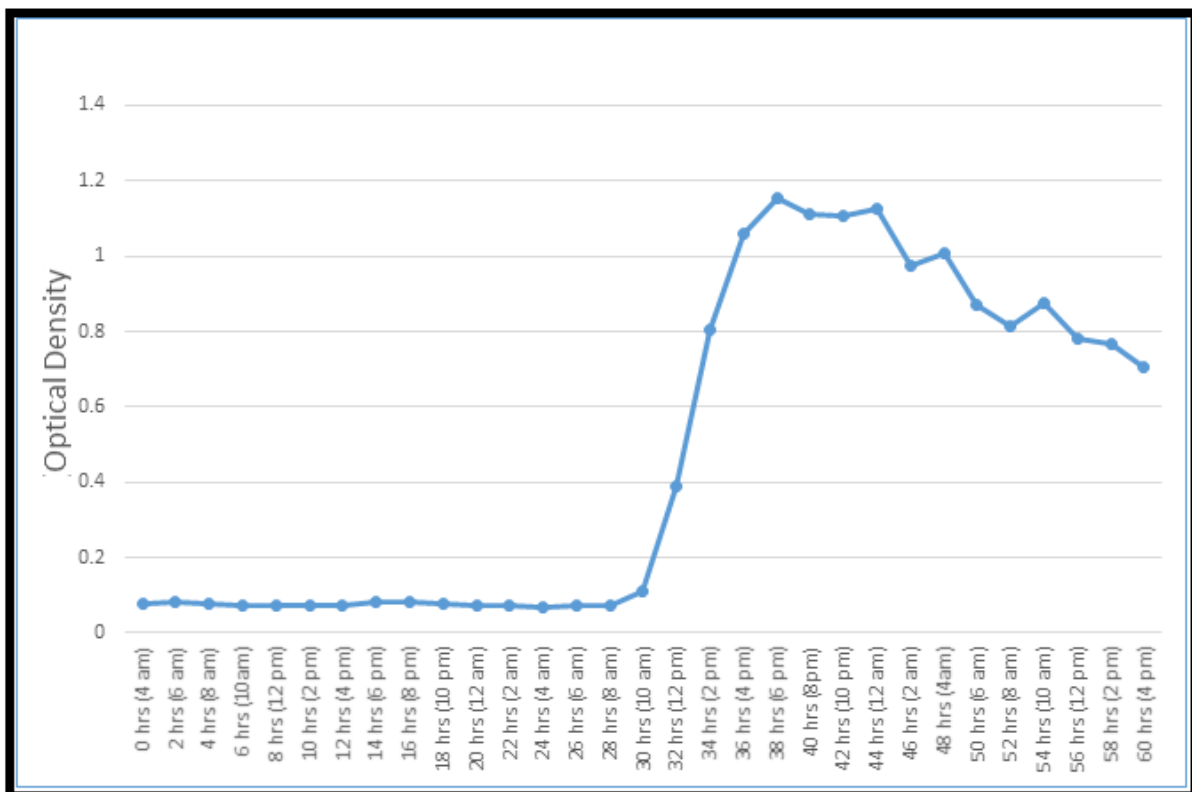


Figure 5.1. Growth Curve of *B. breve* 7017 at a 2h Interval Period with wavelength of 490nm

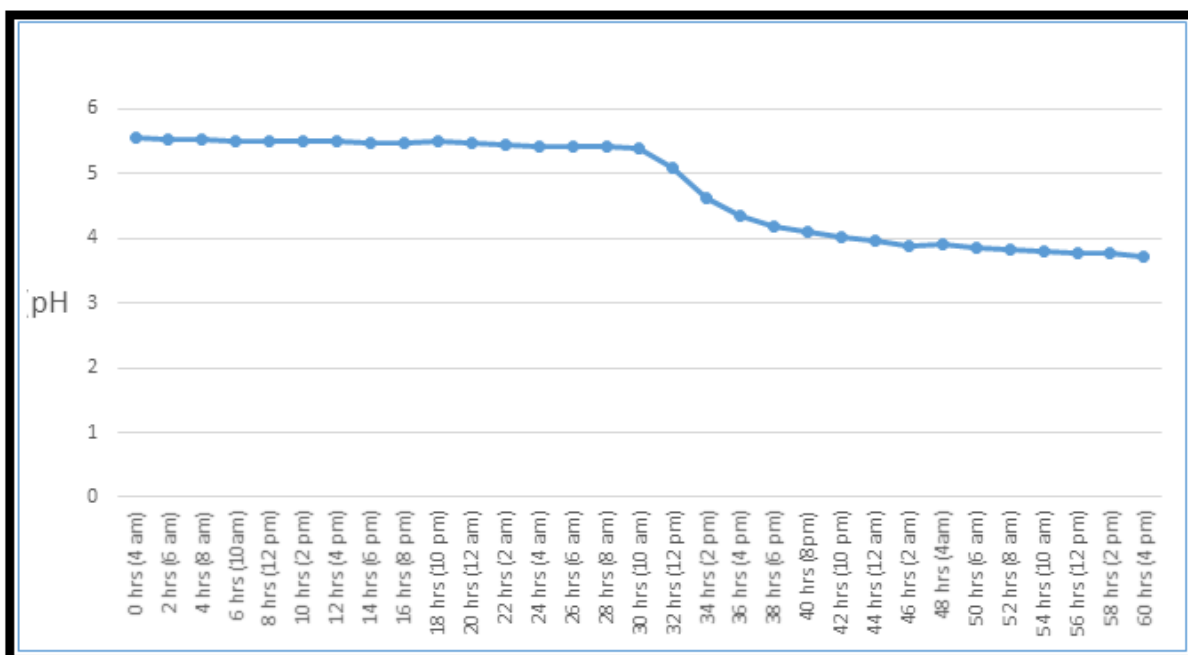


Figure 5.2. Graph of HBM Broth pH Recorded Containing the *B. breve* 7017 at same time during Growth Curve.

Analysis of the growth curve indicated that *B. breve* 7017 was able to grow in HBM media supplemented with glucose but only after a long induction period of approximately twelve hours. After the induction period, strong exponential growth was observed which typically lasted for twelve hours before the fermentation entered the stationary phase. After 48 h, the optical density started to fall-off suggesting that the system had entered the death phase. In subsequent experiments, fermentations were performed for between 48 and 72 hours. The pH of the HBM broth containing the bacteria was also recorded which indicated that as soon as the optical density started increasing, the pH started dropping (*Fig 5.2*) supporting the fact that acid (lactate) was produced as has been seen in the heterolactic and homolactic pathways. At the end of the fermentations, the fermentation broth was processed using a minimal extraction protocol and the four polysaccharide fractions were collected (S1, S2, C1 and C2) as described in the experimental sections 2.7.1.1 and 2.7.1.2. In separate experiments two fermentations were undertaken, in which the sugar used to supplement the HBM media was changed from glucose to galactose or to lactose and the yield of polysaccharide collected in each fraction was determined. The yields for the different fractions are presented in the table (table 5.2) and it is clear whilst the strain was able to use galactose and lactose as a

carbon feed, there was no significant change in the yields of the individual fractions so glucose was used as a carbon feed in all the subsequent fermentations.

Table 5.2: Amount of EPS and CPS for *B. breve* JCM7017

Carbon sources	S1	S2	C1	C2
Glucose	< 5 mg/L	34.8 mg/L	22.4 mg/L	10 mg/L
Galactose	< 5 mg/L	33.9 mg/L	20.1 mg/L	12.4 mg/L
Lactose	< 5 mg/L	35.8 mg/L	24.0 mg/L	15.0 mg/L
¹³ C-Glucose	8 mg/L	37.0 mg/L	26.7 mg/L	17.4 mg/L

We purchased the same bacterial strain from the Japanese culture of microorganisms (JCM) and after the production and isolation of the EPS and CPS as described in section 2.7, it was then compared to that supplied by our collaborators from University College Cork. Knowing that these two strains are the same species, the ¹H-NMR for the S1s & C1s as well as S2 and C2 obtained should be the same. The EPS (S2s) of these strains (batches I and II) confirms that they are of the same structures through having same ¹H-NMR with same signal appearances as well as similar signals for the small impurities too (Fig 5.3). In addition, various batches (four) for the Cork and JCM strains were cultured and their yields noted as well (table 5.3).

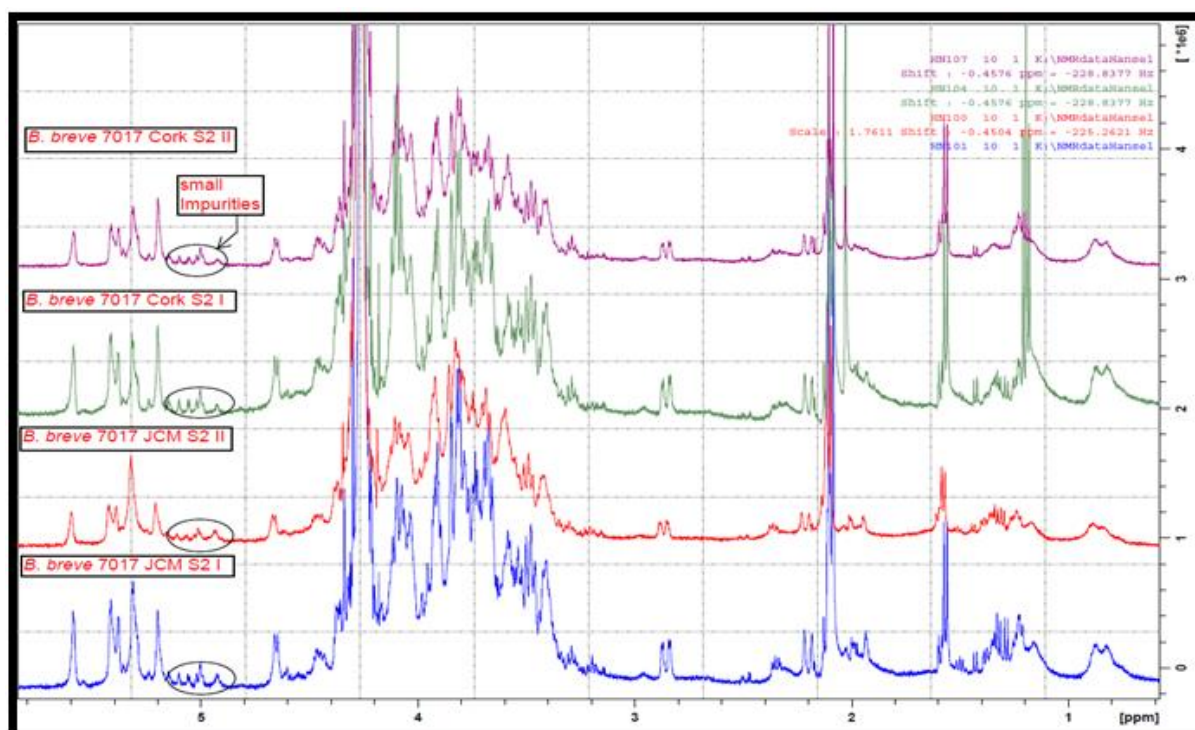


Figure 5.3. ¹H-NMR Spectra for S2s of JCM Strains and Cork Strains of *B. breve* 7017

Table 5.3: EPS yields of *B. breve* 7017 Cultured in HBM Broth

Strains	Batches (HBM broth)	S1	S2	C1 Sonicated	C2 Sonicated
JCM	1	<5 mg/L	30.6 mg/L	22.4 mg/L	10 mg/L
	2	<5 mg/L	32.9 mg/L	178 mg/L	19 mg/L
	3	-----	34.8 mg/L	-----	15.8 mg/L
	4	<5 mg/L	28.5 mg/L	174 mg/L	10 mg/L
CORK	1	18.6 mg/L	30.4 mg/L	-----	26.4 mg/L
	2	-----	38.2 mg/L	230 mg/L	22.1 mg/L
	3	<5 mg/L	30.7 mg/L	-----	32.1 mg/L
	4	<5 mg/L	30.0 mg/L	136 mg/L	20.2 mg/L

The yields for the S1s and C1s were rarely obtained but when the cells are sonicated large amounts of the C1s are produced. The amount of S2 collected ranges from between 20 mg/L to 40 mg/L. Sonication (with an amplitude of 50) is done in order to release the tightly bound CPS but when the ¹H-NMR was ran for these sonicated CPS they showed no presence of the CPS which might imply, the sonication process ends up lysing the cells to release its contents which overshadows any CPS that might be present (Fig 5.5).

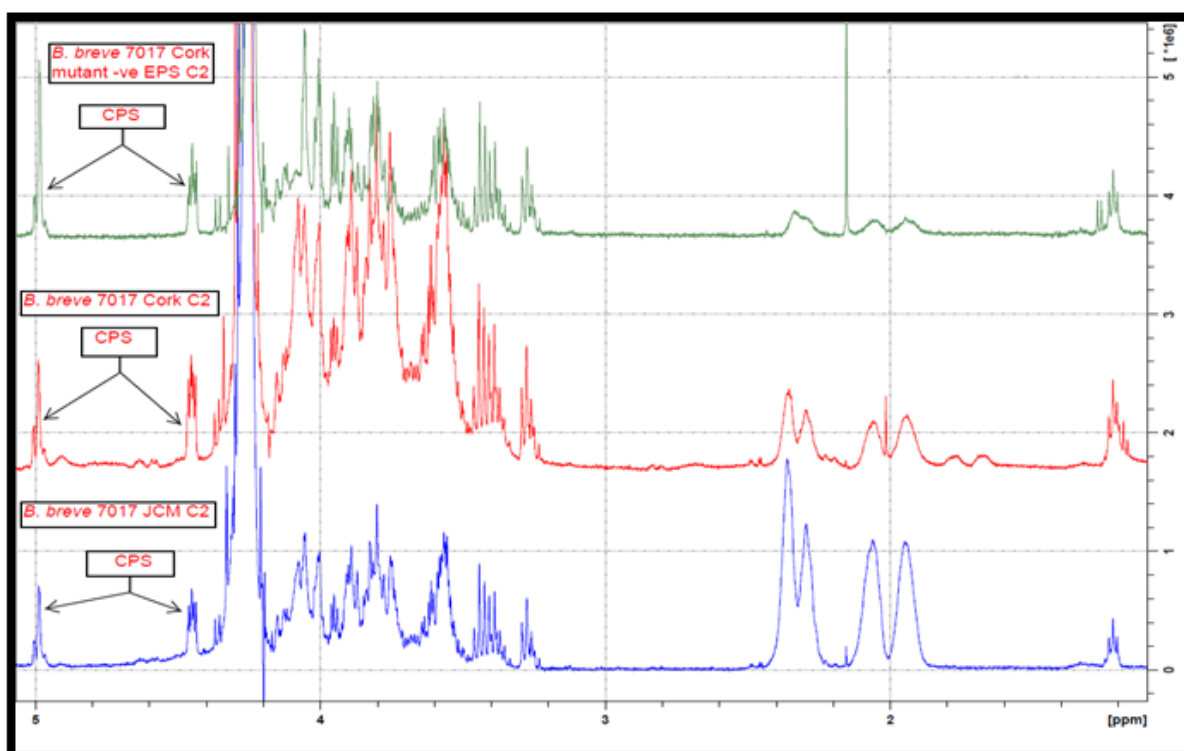


Figure 5.4. ¹H-NMR Spectra for the C2s for *B. breve* 7017 (JCM, Cork and Mutant –ve EPS strains)

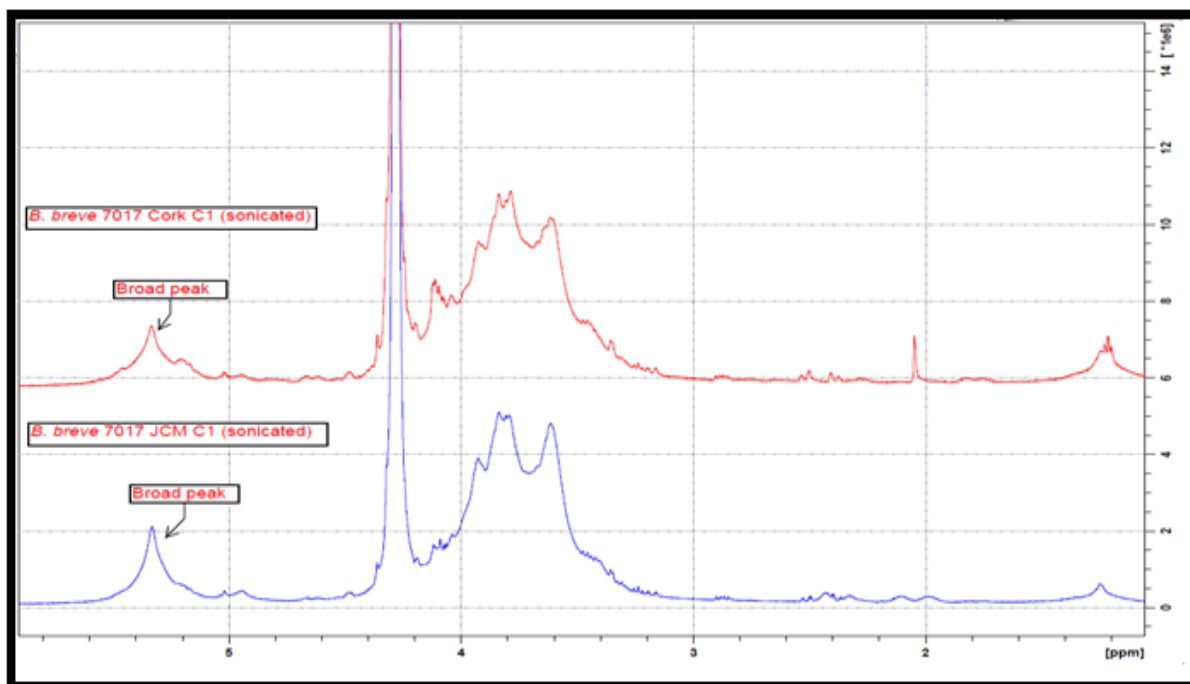


Figure 5.5. ^1H -NMR Spectra for the C1s for *B. breve* 7017 obtained after Sonication.

The C1 sonicated spectra have just the broad peaks (*Fig 5.5*) whereas the C2 from the normal treatment with NaOH (1 M) has the CPS (*Fig 5.4*). This confirms that the cell is lysed by sonication which breaks open the cell wall and its content are mixed up with any CPS present forming a mass of solids. This C1 and C2 will be further characterised in section 5.1.5.

In addition to the various strains being studied was the *B. breve* 7017 mutant type (which had the gene responsible for EPS production deleted) supplied by Prof Douwe Van Sinderen from UCC. After the production and isolation of the material these bacteria produced, their proton NMRs were recorded (*Fig 5.6*). The proton NMRs from the various batches of the mutant type confirmed the fact that the EPS gene was indeed deleted as the spectrum didn't indicate the presence of any EPS. It was noticed that the cells of this mutant type generated CPS (*Fig 5.4*) when treated with NaOH (1M).

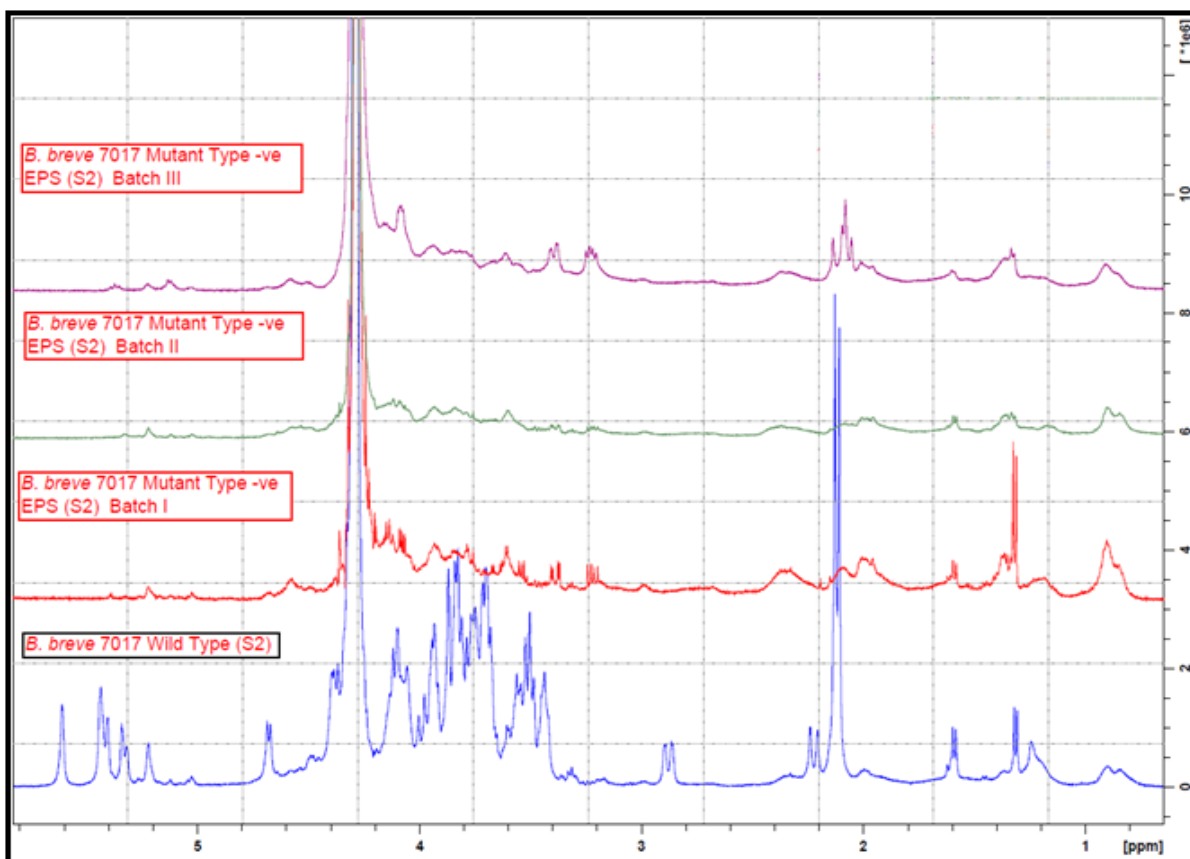


Figure 5.6. $^1\text{H-NMR}$ Spectra for the S2s (EPS) of *B. breve* 7017 Mutant Type compared with the Wild Type Strain.

5.1.1. Analysis of Polysaccharides Present in the S1-fraction; Attempted Recovery of Exopolysaccharides.

In the typical procedures that are reported in the literature for the isolation of exopolysaccharides, solutions of a DNase, RNase and a protease are added to the supernatant in order to remove nucleic acid and protein derived biomacromolecules. In previous studies at the University of Huddersfield, it has been demonstrated that a large proportion of the polysaccharides are lost during these steps. In order to determine the precise nature of all the material present in the supernatant, in early experiments, these steps were removed and all high molecular weight biomacromolecules were isolated and $^1\text{H-NMR}$ spectra were recorded shortly after samples had been isolated.

In total approximately twenty small scale (500 mL) batch fermentations were performed and from each of these S1 fractions were collected. To a first approximation the $^1\text{H-NMR}$ spectra recorded for the S1 and S2-fractions were very similar. The sample recovered in the S1-fractions had one large resonance in the anomeric region at 5.3 ppm (*Fig 5.7*) indicating that

a homoglycan had been recovered and the spectra was identical to that of a ^1H -spectrum recorded for a solution of starch under identical conditions (Fig 5.7). It should be noted that the quality of the spectrum suggests that the polysaccharide is the main component of the material recovered in the S1-fractions. Whilst there is some evidence for proteins being present; small broad methyl and methylene resonances are visible below 2.5 ppm and the presence of these small amounts of protein did not significantly interfere with the characterisation of the S1-material. To confirm that a bacterial glycogen was being recovered in the S1-fractions monomer and linkage analysis was performed on the polysaccharide.

The purity of the polysaccharide (S1) was first examined using size exclusion chromatography and monitoring the elution of peaks using a multi-angle light scattering detector in combination with a concentration dependent differential refractometer and a UV-detector. The sample eluted as a single narrow peak (Fig 5.8) which had a weight average molecular mass of $17.24 \times 10^6 \text{ gmol}^{-1}$ (indicating it to be a HMw) and the sample had a polydispersity of 1.53 suggesting its narrow distribution of molecular masses. No peaks were visible in the UV-trace indicating that if any proteins, they were below detection limit and no nucleic acid contaminants.

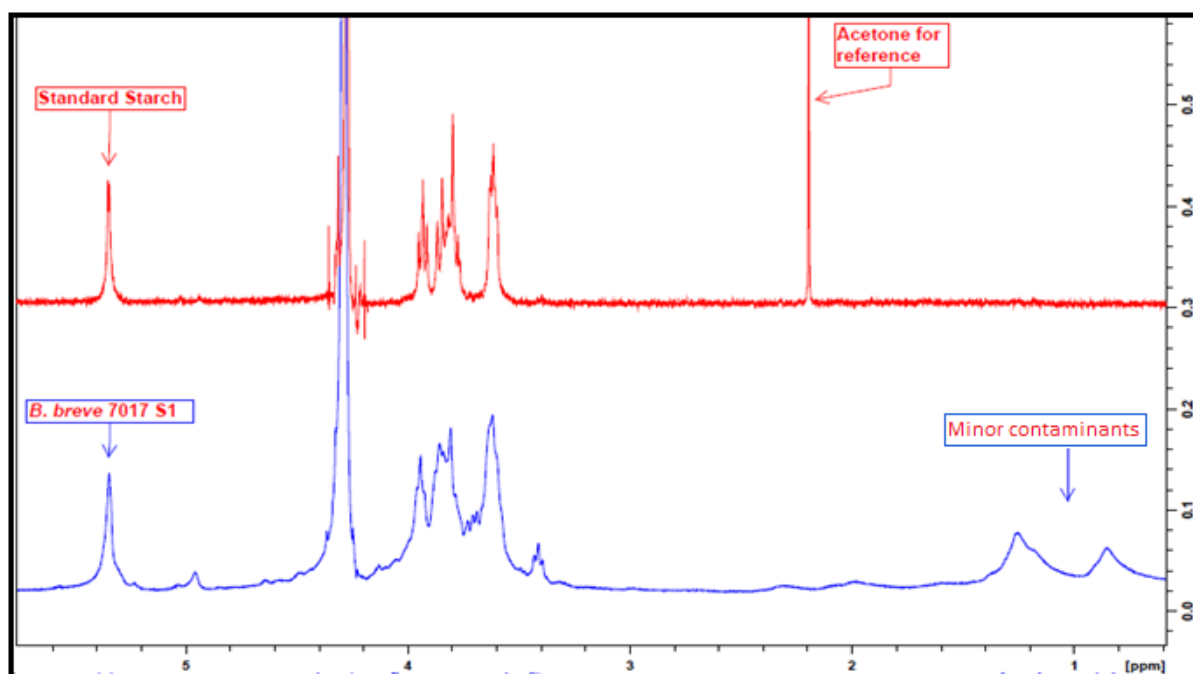


Figure 5.7. ^1H -NMR Spectra for the S1 for *B. breve* 7017 (in blue) compared with that of a Standard Starch (in red)

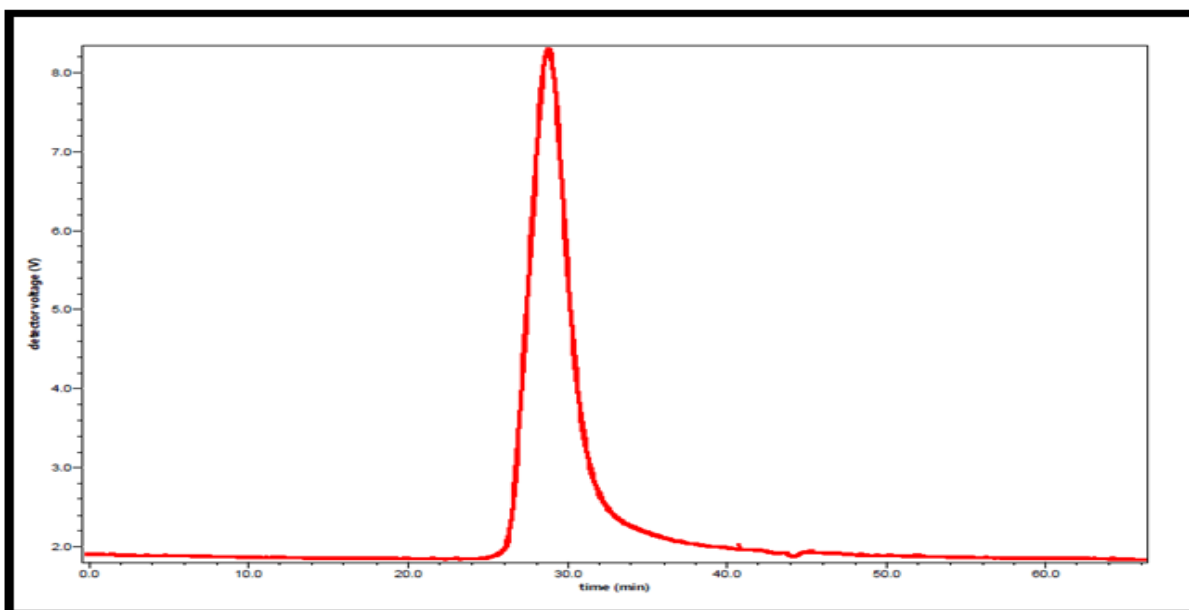


Figure 5.8. SEC-MALLS trace of S1 from *B. breve* 7017 (Light scattering)

The results for the monomer analysis of S1 from *B. breve* 7017, performed by HPAEC then overlaid with galactose and glucose standards (Fig 5.9) and by GC-MS methods with results overlaid with a glucose standard (Fig 5.10), confirmed that glucose was the only monosaccharide present in the **S1**-fraction and the linkage analysis confirmed that the majority of the glucose were 1,4-linked (Fig 5.11)

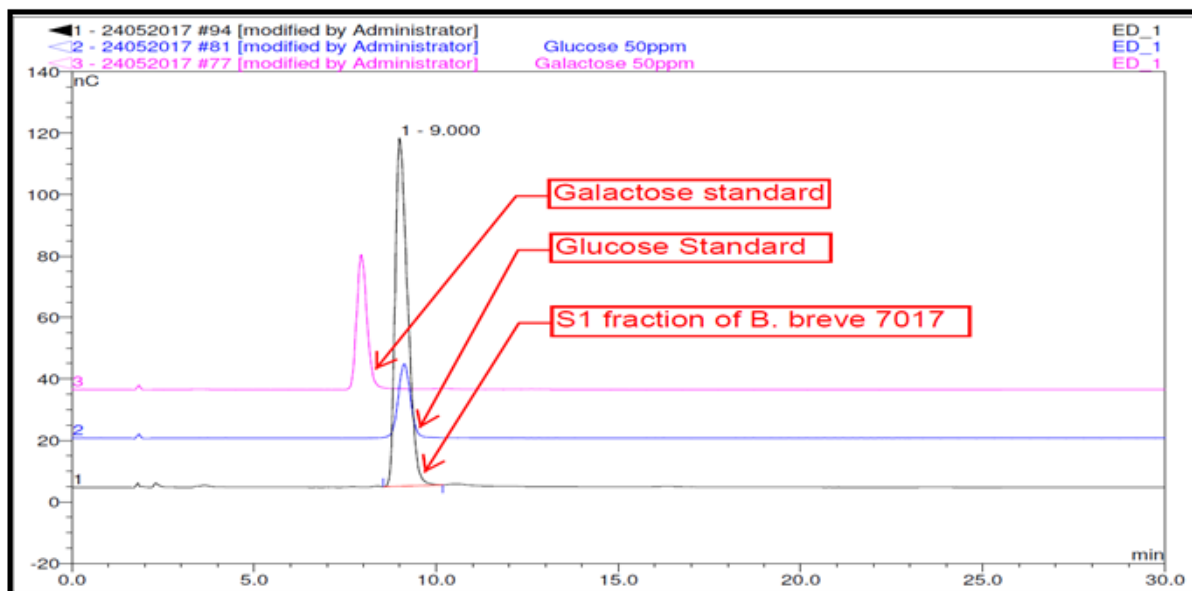


Figure 5.9. HPAEC-PAD Chromatogram of the Polysaccharide (S1 fraction) from *B. breve* 7017 overlaid with glucose and galactose standards.

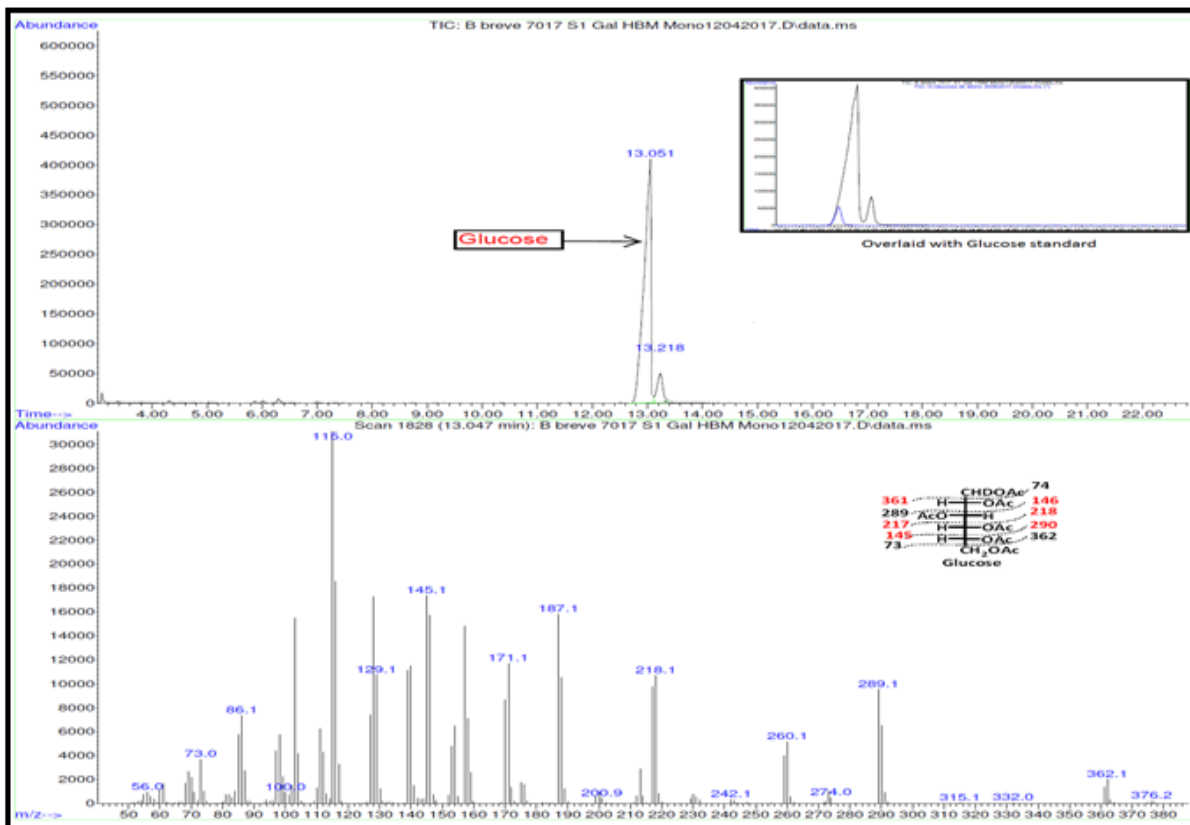


Figure 5.10. Chromatogram and Mass Spectrometer for the Alditol Acetates of the Sugars obtained from the GCMS for Monomer Analysis of *B. breve* 7017.

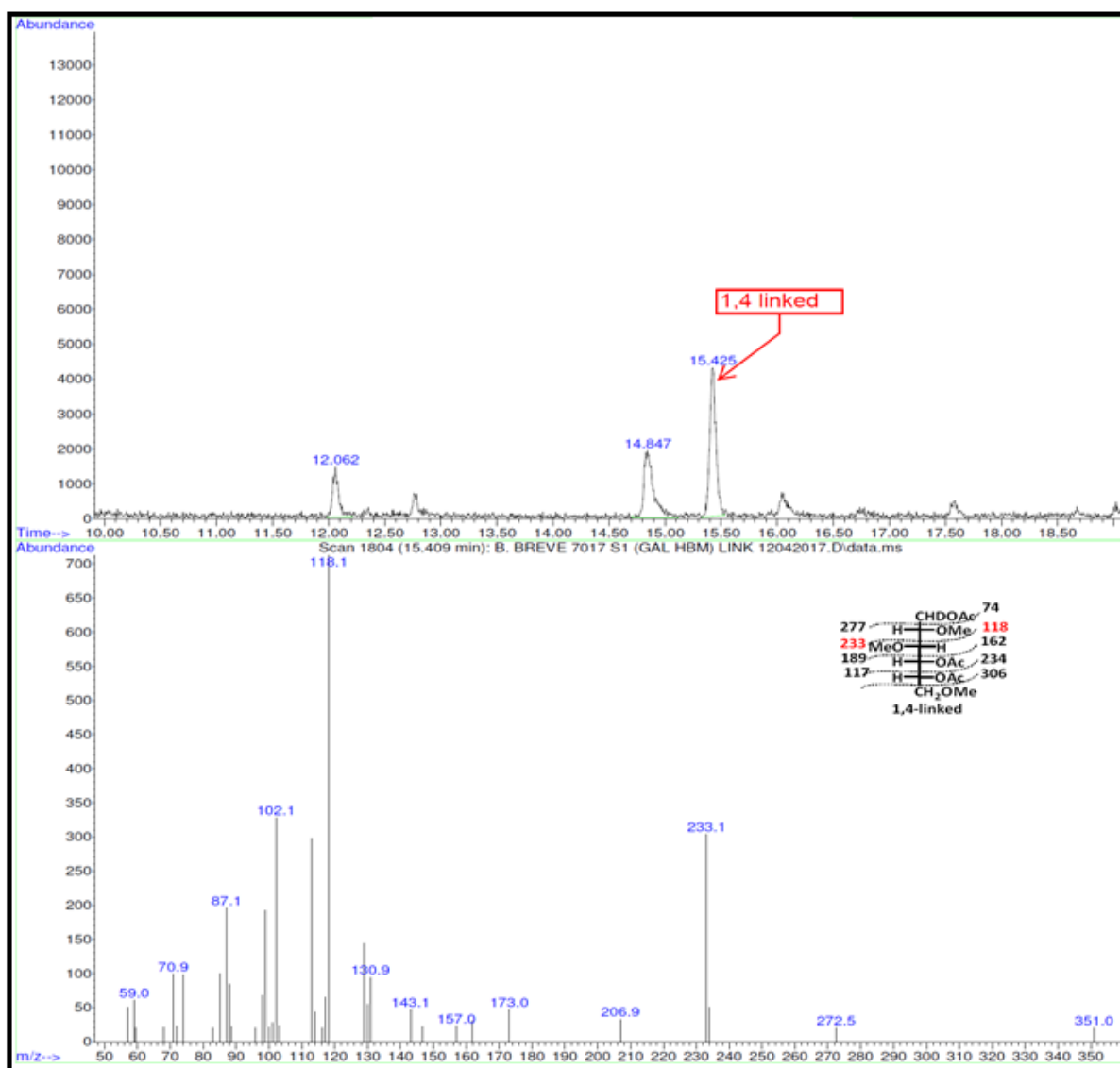


Figure 5.11. Chromatogram and Mass Spectrometer for the Methylated Alditol Acetates of the Sugars obtained from the GCMS for Linkage Analysis of *B. breve* 7017 (S1).

From the linkage results, the location of the anomeric proton at 5.38 ppm and the lack of any significant $^3J_{H1-H2}$ coupling confirmed that the glucose monomers were α -(1,4)-linked and that the homoglycan was indeed a bacterial glyco-gen.

Whilst several authors (Goh *et al* (2014) and Rios-Covian *et al* (2016))^{307, 308} have reported the recovery of bacterial glycogens from a range of bacteria it is unlikely that glyco-gen, an energy rich polysaccharide, would be actively secreted by a bacterium. It is more likely that the glyco-gen is normally present in the cytoplasm and it is only being released at the end of the fermentations when cell lysis occurs.

5.1.2. Analysis of Polysaccharides Present in the S2-fraction; Attempted Recovery of Exopolysaccharides

NMR spectra were recorded for the polysaccharide recovered in the S2-fractions. Spectra that were recorded immediately after the samples had been prepared showed several unusual features and these are best illustrated with reference to the ^1H -NMR spectra recorded for JCM Batch 1 (Fig 5.12)

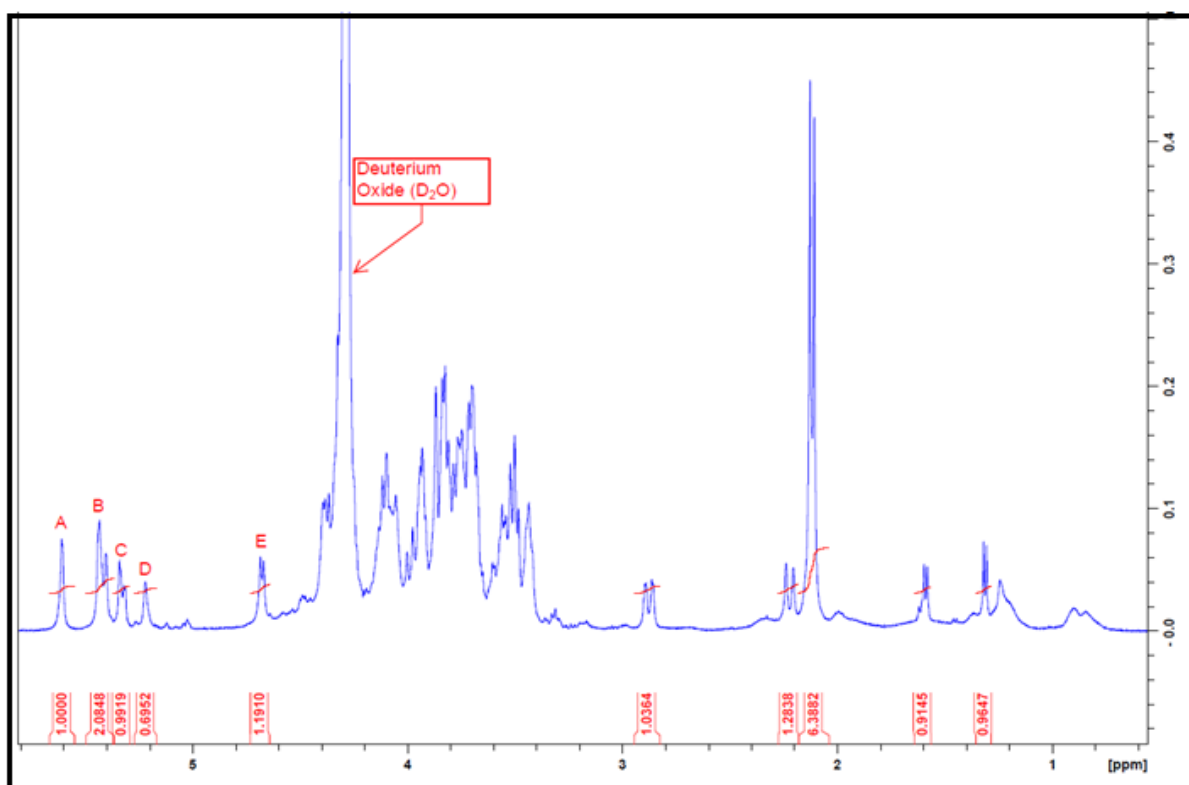


Figure 5.12. ^1H -NMR Spectra for the S2 of *B. breve* 7017

In the anomeric region (4.3-5.8 ppm), several different proton resonances were visible. The spectrum also contained signals at high-field including: doublets at 2.88 ppm and 2.22 ppm both of which integrated to one proton, two large signals with a combined integral of six at 2.13 and 2.11 ppm which are likely to be from acetyl-groups, a doublet centred at 1.59 ppm with an integral close to one and a second doublet at 1.31 also with an integral close to one and these are likely to be methyl-proton resonances of alanine and lactate respectively. In order to gain more insight into the identity of the material in the S2-fraction a ^1H - ^{13}C -HSQC spectrum was recorded (Fig 5.13); it must be noted at this point that the NMR spectra are all recorded at 70 °C and this specific spectrum was run after the sample had been held in the

probe of the spectrometer at 70 °C for a period of approximately four hours (whilst a number of homonuclear 2D-spectra were being recorded).

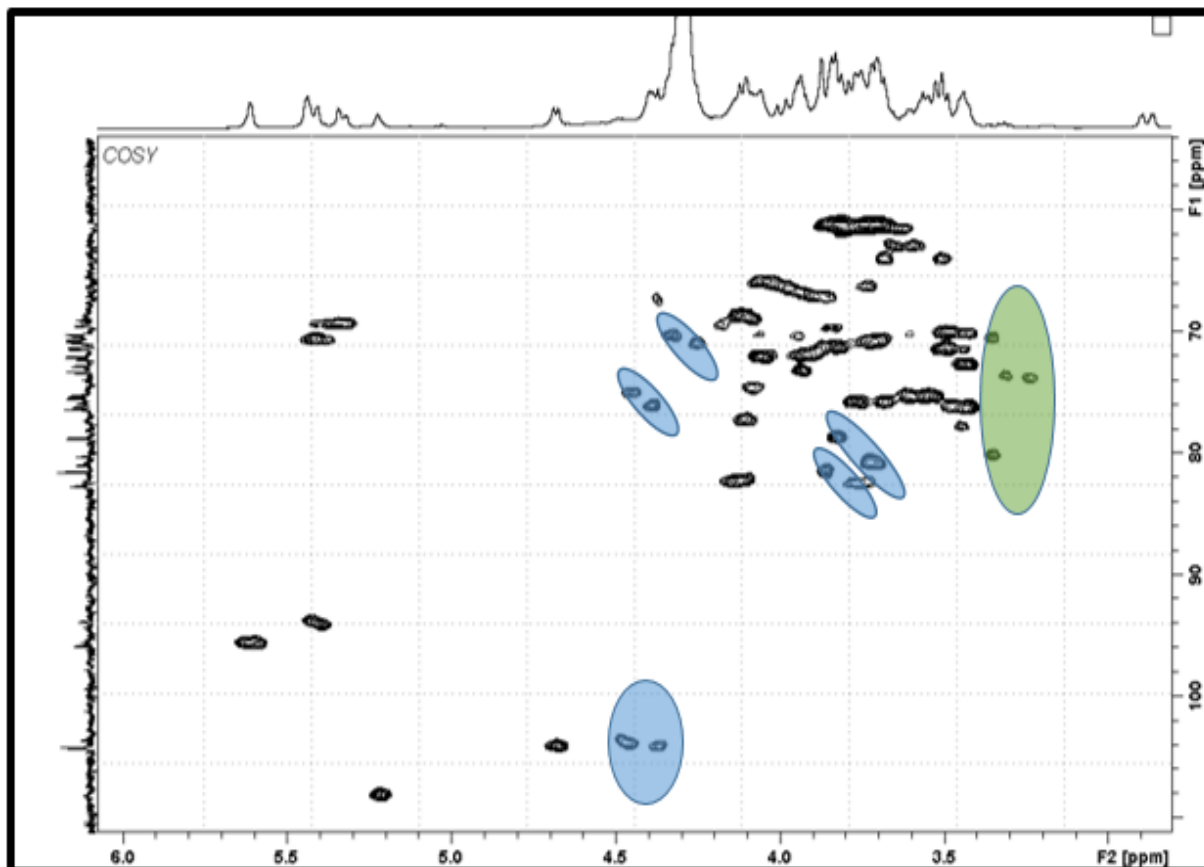


Figure 5.13. ^1H - ^{13}C -HSQC Spectrum for S2 fraction of *B. breve* 7017

The most striking feature of the HSQC spectrum is that after approximately four hours of heating it is clear that additional signals have appeared that were not in the original proton spectrum (see signals highlighted in green) and a number of signals appear in pairs (e.g. see signals highlighted in blue in the spectrum). It was clear that the spectra were changing over time. To understand what was happening, several proton spectra and HSQC spectra were recorded for two different batches of **S2**-fractions with spectra being recorded every four weeks for 12 weeks. The same observations were made for each of the batches and the spectra for each batch changed with time. Whilst the changes are visible on the proton spectrum (*Fig. 5.14*) it was easier to see the full extent of the changes by inspecting a specific set of HSQC spectra (*Fig 5.15*).

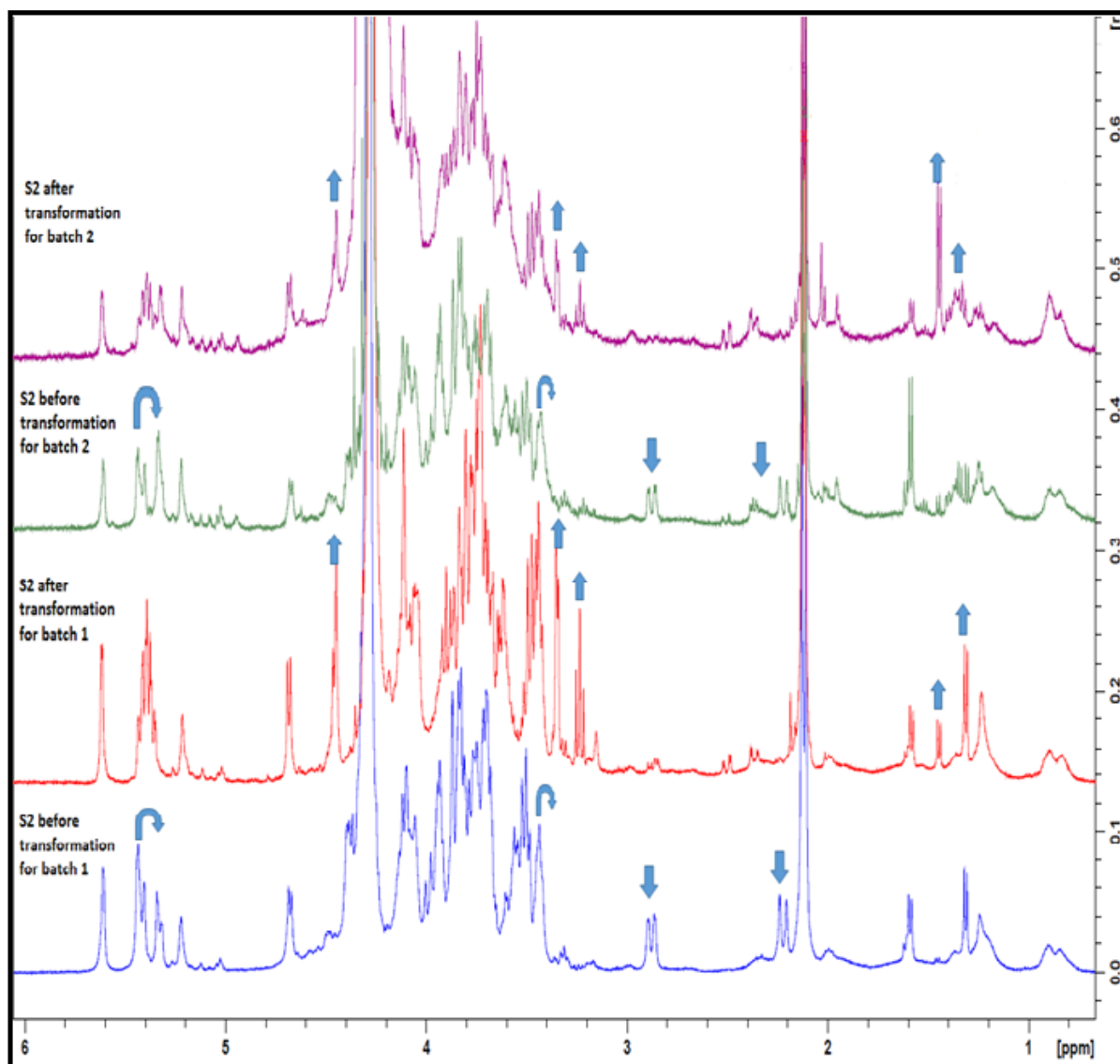


Figure 5.14. ^1H -NMR Spectra for the S2s of *B. breve* 7017 for Batches 1 and 2 at the end of 12 weeks of their Transformation

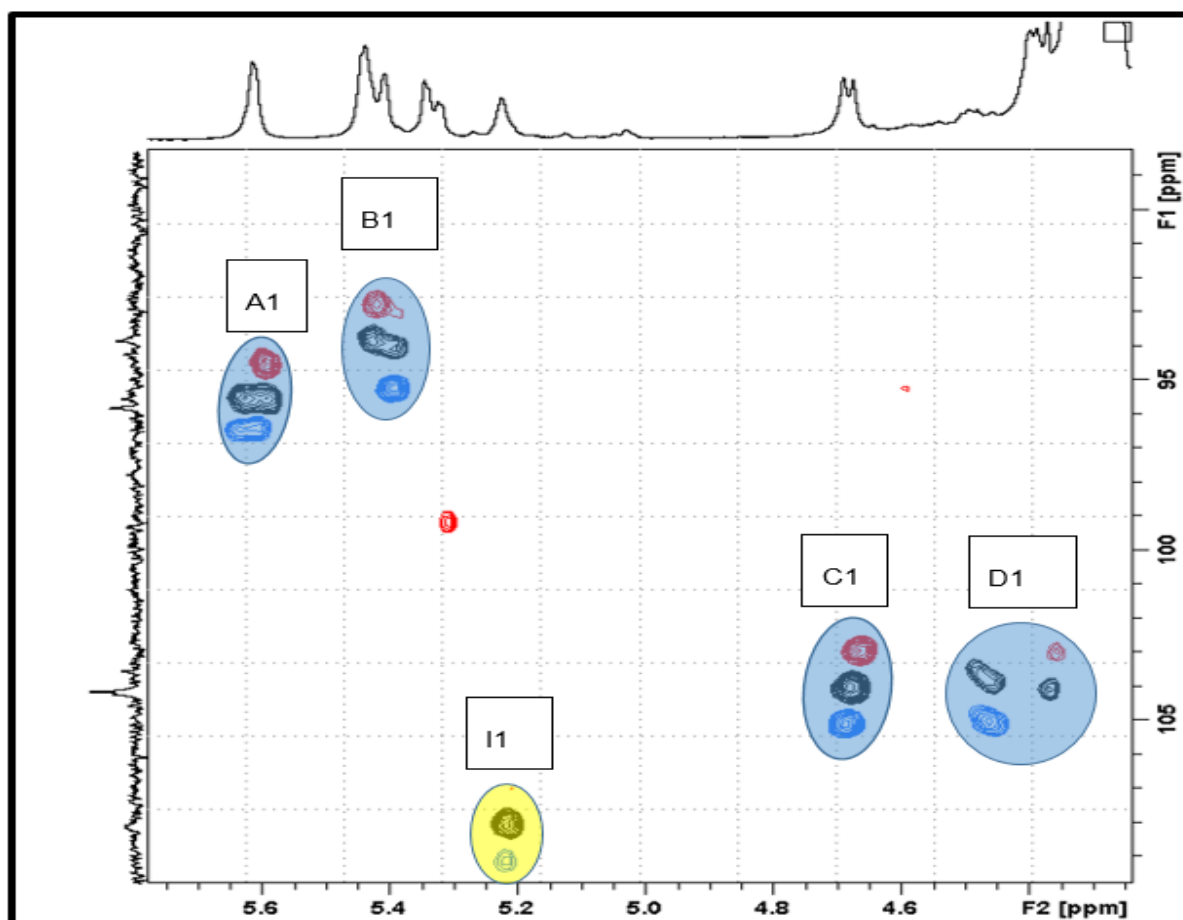


Figure 5.15. The group of ^1H - ^{13}C -HSQC Spectra for S2 fraction of *B. breve* 7017 indicating its Changes from when Freshly Extracted until Final Transformational Change after 12 weeks.

The group of HSQC spectra displayed (*Fig. 5.15*) include a spectrum recorded after four hours of heating at $70\text{ }^\circ\text{C}$ (black), a spectrum recorded after the sample had been in solution at room temperature for two months (blue) and one recorded immediately after the sample has been isolated and placed in the NMR probe at $70\text{ }^\circ\text{C}$ (red). The red contours (which have been displaced to higher field on the F1-axis to increase their visibility) represent the starting point, the black contours represent partial conversion to a new product and the blue contours (which have been displaced to lower field on the F1-axis to increase their visibility) represent full conversion to the final product.

In the anomeric region of the HSQC spectra there are five unique sets of signals, the first is a singlet resonance which starts out at 5.59 ppm (red contour) in the product this resonance shifts down-field very slightly to 5.62 ppm (blue contours) and in the intermediate state a double contour is visible representing both the starting polymer and the product. The next

anomeric resonance is also a singlet which is initially located at 5.43 ppm (red contour) and shifts up-field to 5.39 ppm in the product (blue contour) and, again, overlapping contours are observed for the intermediate phase. The next set of anomeric resonances is at 5.24 ppm highlighted in yellow and these are from an impurity which can be seen to appear in several of the **S2**-fractions. Different fractions contain different amounts of the impurity and it was absent in batch HN172 (*Fig. 5.16*). There is no change in position of the impurity signal as seen in *Fig. 5.15*.

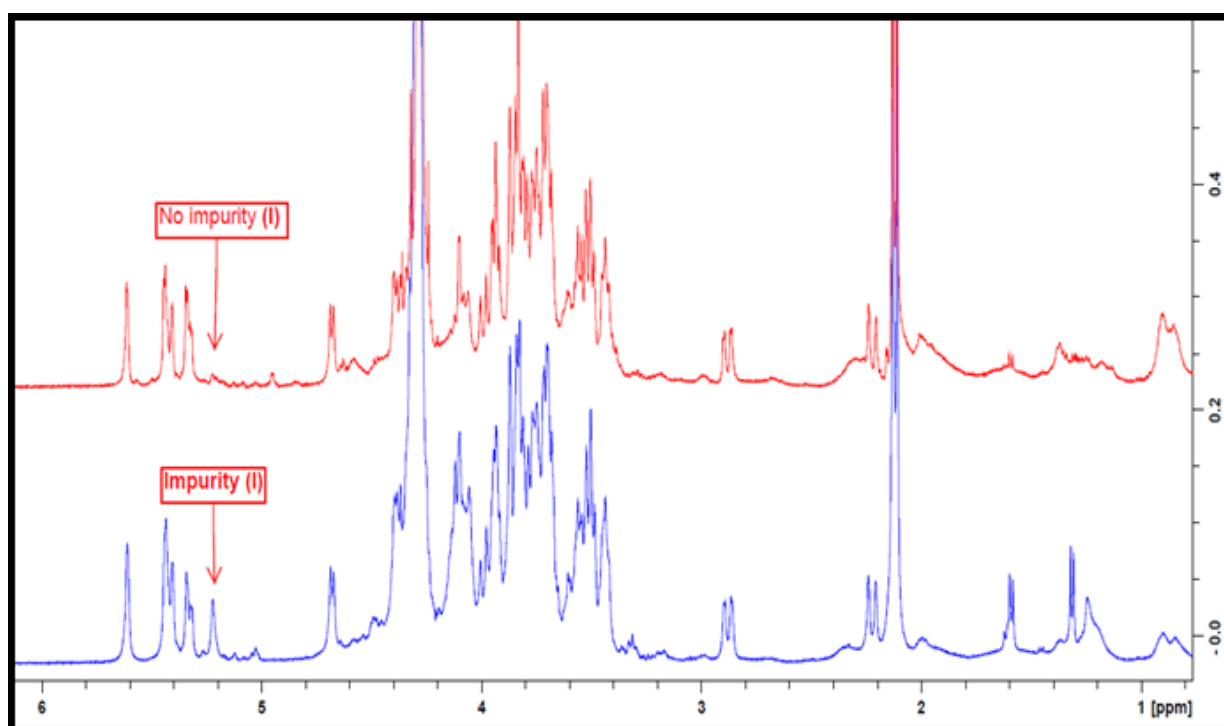


Figure 5.16. ^1H -NMR Spectra for the S2s of *B. breve* 7017 for a Batch with the Impurity and Another Batch with Complete Absence of the Impurity.

The third anomeric signal is a doublet (*Fig. 5.15*), located at 4.67 ppm in the starting material and this shifts a very small distance down-field to 4.69 ppm in the product. The final anomeric signal is the one which moves the most, it starts as a shoulder on the HOD resonance at 4.37 ppm (red contour) and is shifted downfield to 4.47 ppm (blue contour) in the product; in the intermediate spectra two separate contours are observed for the starting material and product (black contours). A similar pattern of shifts is observed for many of the ring protons and a number of these have been highlighted in the expanded version of the HSQC spectrum shown below (*Fig. 5.17*). By tracking the three sets of signals (red top, black middle and blue bottom) the change in position of a significant number of the ring protons can be identified.

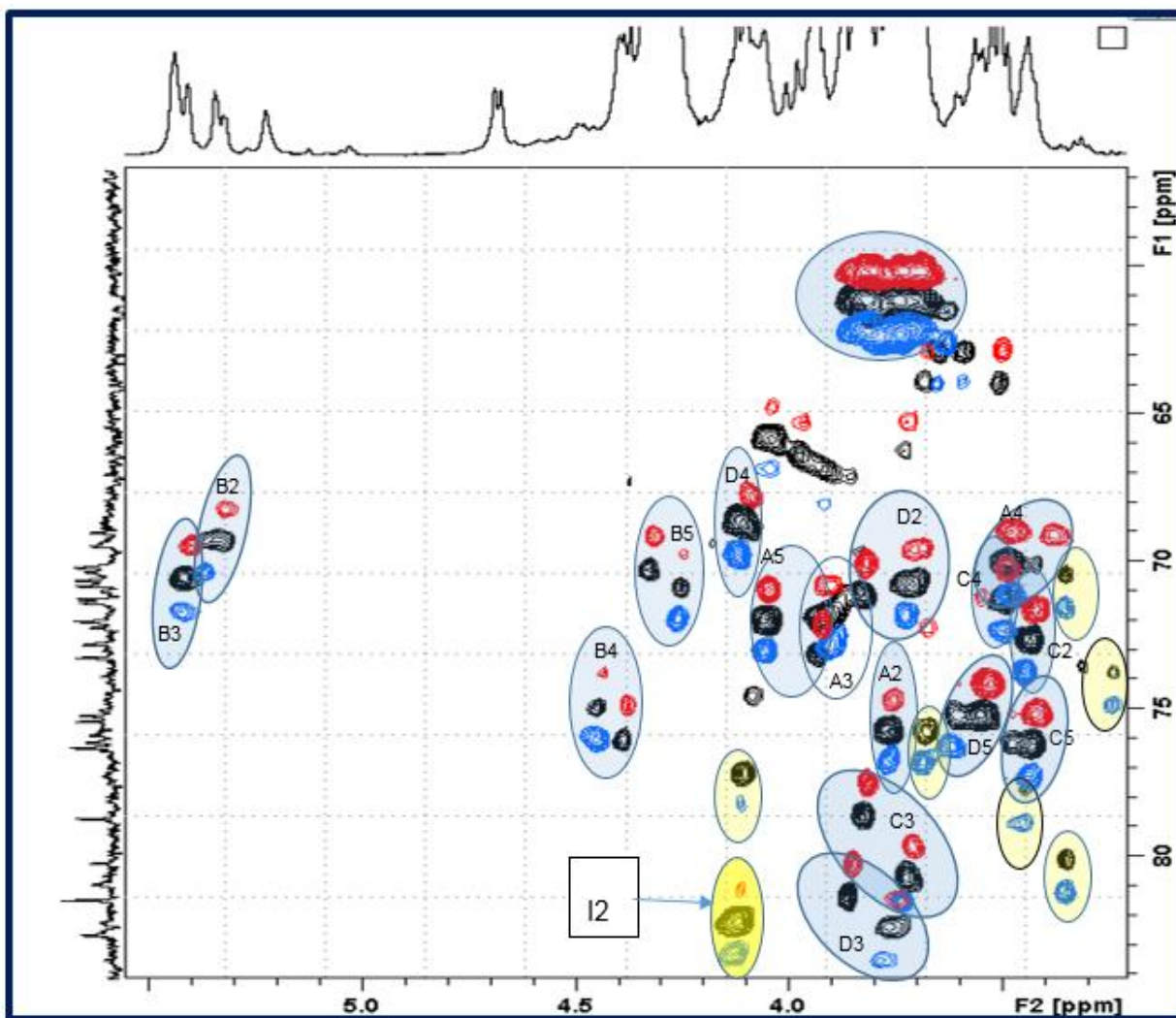


Figure 5.17. The Expanded Version of the ^1H - ^{13}C -HSQC Spectra for S2 fraction of *B. breve* 7017 indicating its Changes in the Ring Protons from when Freshly Extracted until Final Transformational Change after 12 weeks

A couple of features of the HSQC spectrum should be noted: firstly, there are two proton resonances which appear in the anomeric proton region (5.43 ppm and 5.35 ppm) that are not attached to anomeric carbons (typical shifts >90 ppm), and they have carbon shifts typical of ring protons (<80 ppm). It is likely that these two protons are attached to carbons carrying the two acetyl-groups. The second feature of note is that there are pairs of blue and black contours (highlighted in pale yellow ovals) where there are no obvious local red contours which suggests that these signals have migrated some distance in formation of the final product.

5.1.3. Identification of the Resonance Position of the Protons and Carbons of the Monosaccharides (A to D) of the Repeat Unit.

The location of the ring protons and carbons for monosaccharides was determined from examination of a series of 2D-NMR spectra. The 2D-spectra recorded included heteronuclear COSY, TOCSY, NOESY spectra, also heteronuclear HSQC, HMBC, and a HSQC-TOCSY spectrum. In the first instance, the location of the adjacent ring protons (H2) was determined from examination of a ^1H - ^1H -COSY spectrum (Fig. 5.18).

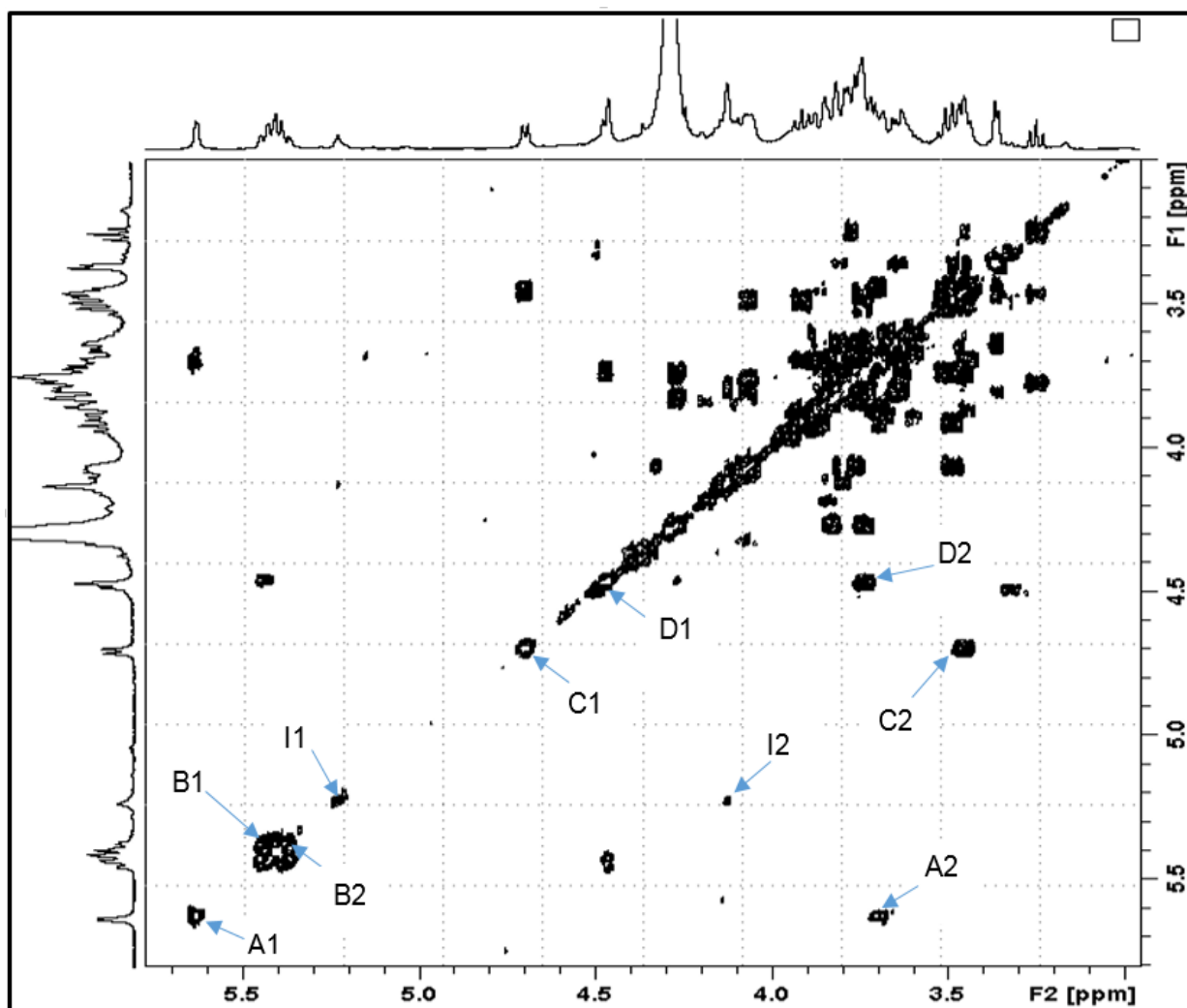


Figure 5.18. ^1H - ^1H -COSY Spectrum for S2 of *B. breve* 7017 after 12 Weeks of Transformation

The position of several other ring protons (H2-H4/5) was then determined from inspection of a TOCSY spectrum (Fig 5.19)

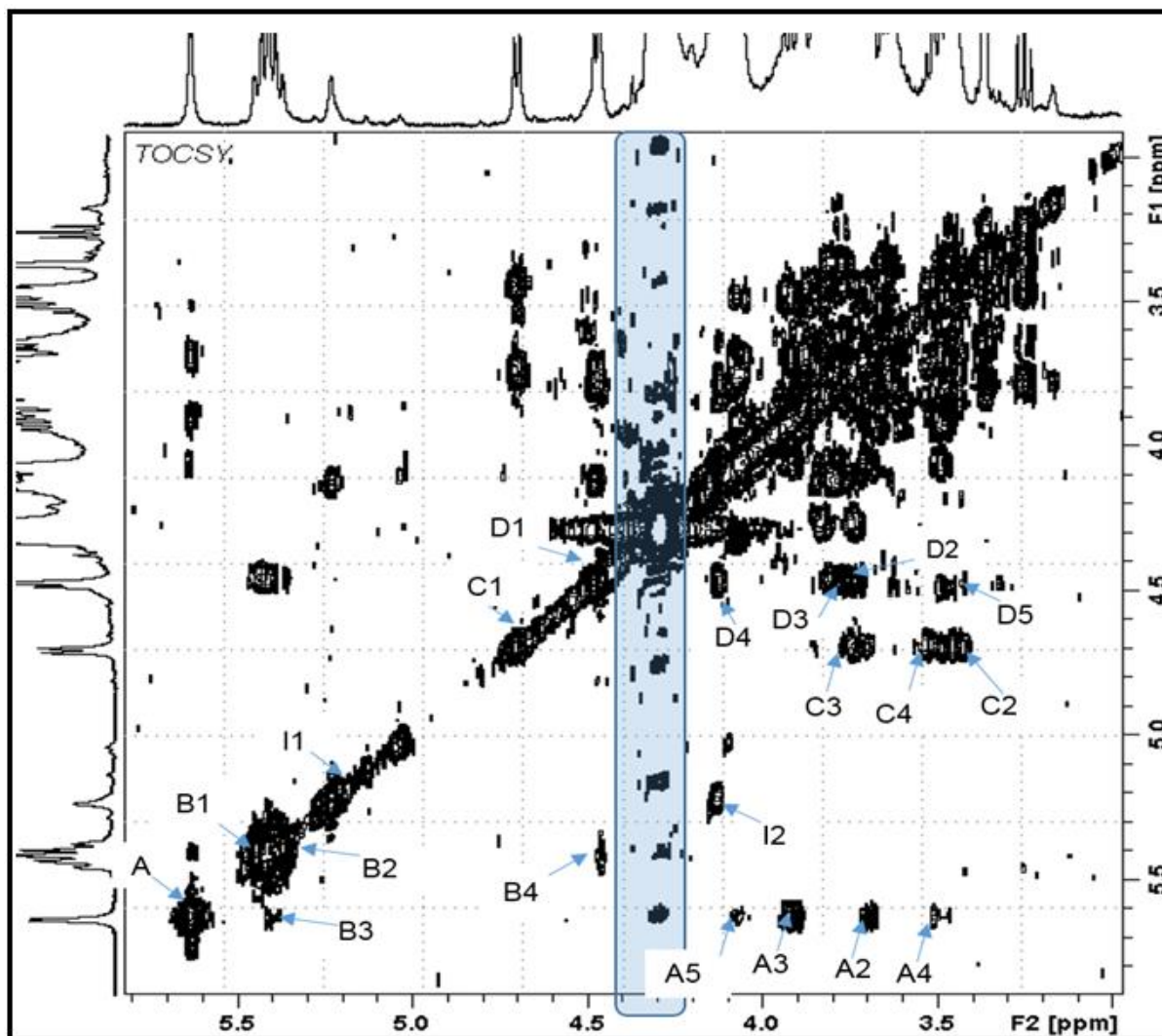


Figure 5.19. ^1H - ^1H -TOCSY Spectrum for S2 of *B. breve* 7017 after 12 Weeks of Transformation

The observation of four unique anomeric signals (labelled **A to D** in order of decreasing chemical shift of their proton resonances), suggests the repeat unit of the polysaccharide contains four monosaccharides (Fig. 5.20) and there is also evidence for other structural components which are not cyclic sugars as will be discussed in the following section.

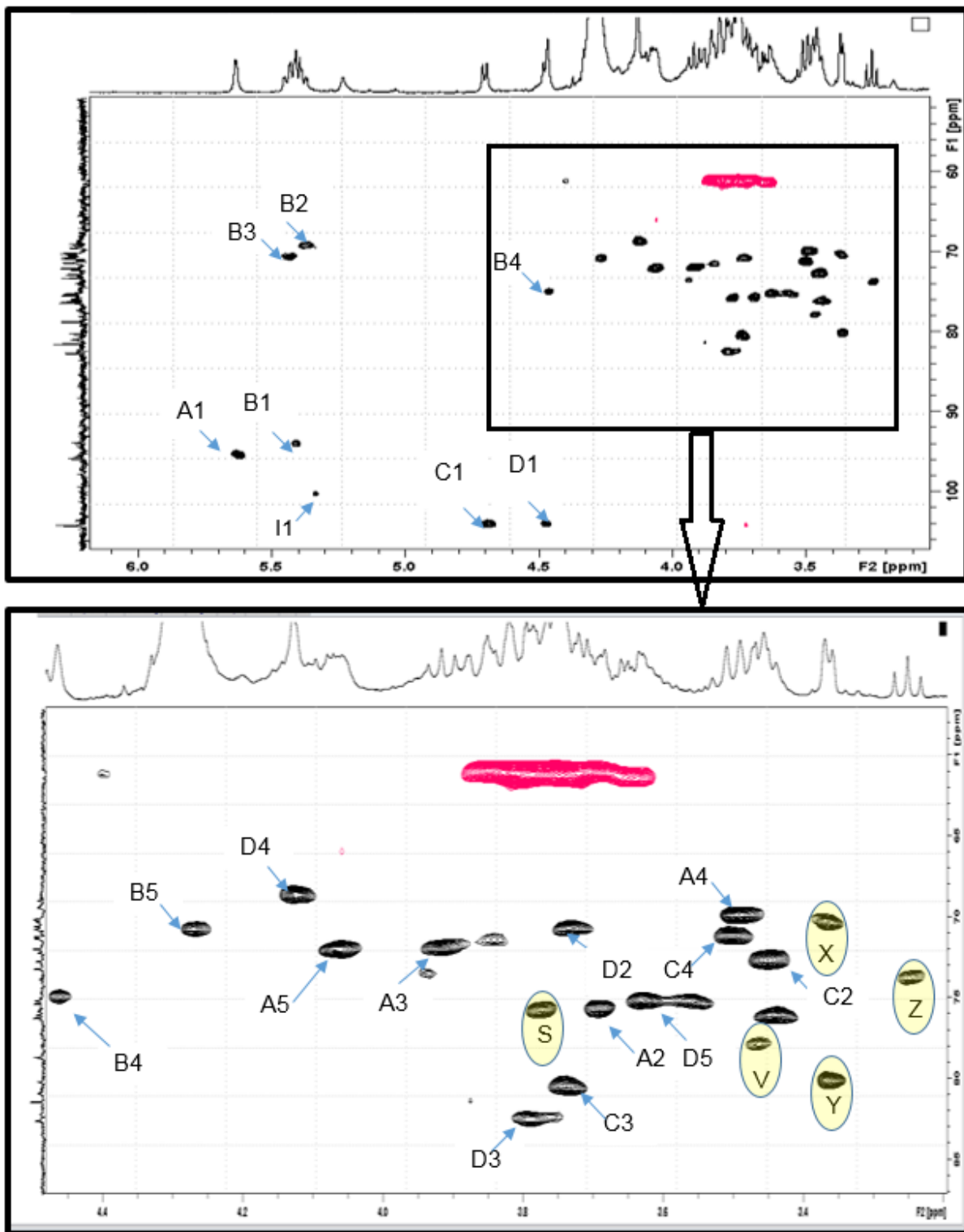


Figure 5.20. ^1H - ^{13}C -HSQC Spectra for S2 fraction of *B. breve* 7017 indicating the 4 Unique Anomeric Protons of the 4 Monosaccharides (top spectra) and their Ring Protons (bottom expanded spectrum).

Unfortunately, it wasn't possible to locate the H5 & C5s for residues **B** and **C** from the TOCSY spectrum. The location of the C6 methylene protons and carbons on the edited HSQC spectrum all occur in a highly congested region of the spectra (Fig. 5.20, Red contours) but significantly, the carbon resonances all have shifts lower than 65 ppm which suggests that the polysaccharide does not contain any 1,6-linked sugars. The latter result means that any long-range couplings observed on a HMBC spectrum from the methylene carbon region is likely to identify the location of hydrogens attached to carbons within the same ring system. On the HMBC spectrum (Fig 5.21) a long-range scalar coupling starting from one of the methylenes is visible starting from the contour centred at 4.27 ppm on the F2-axis & 61 ppm on the F1-axis to one of the methyne carbons at 77.2 ppm on the F1-axis. The methyne carbon resonance corresponds to **B4** and the proton resonance is therefore almost certainly **B5**. The observation of a strong through space interaction on the NOESY spectrum gives further support to this assignment.

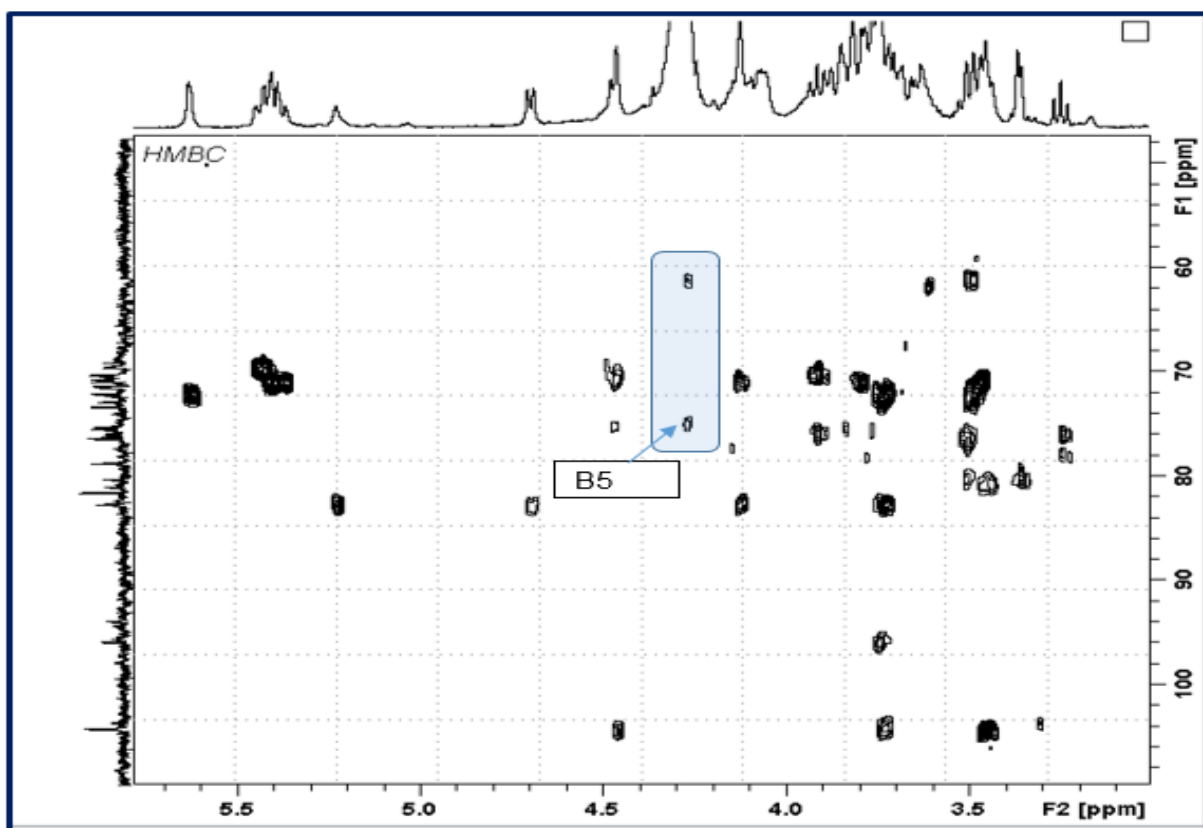


Figure 5.21. ^1H ^{13}C -HMBC Spectra for S2 fraction of *B. breve* 7017 indicating the Methyne Carbons for B4 and B5.

The location of the final methyne signal, C5, was found using a combination of a HSQC spectrum and a HSQC-TOCSY spectrum (Fig. 5.22). The relay of the scalar coupling from the anomeric C1 proton (4.70 ppm) gives rise to three significant contours and one minor contour on the F1-axis. Fortunately, by following the scalar coupling for the minor contour (75.1 ppm) three additional contours (highlighted in yellow circles) were visible on the F2-axis including one corresponding to C3, one corresponding to C4 and one corresponding to an as yet unassigned significant contour and which is present on both spectra and this therefore can only be C5 i.e. the proton resonance for C5 and C2 occur at identical positions.

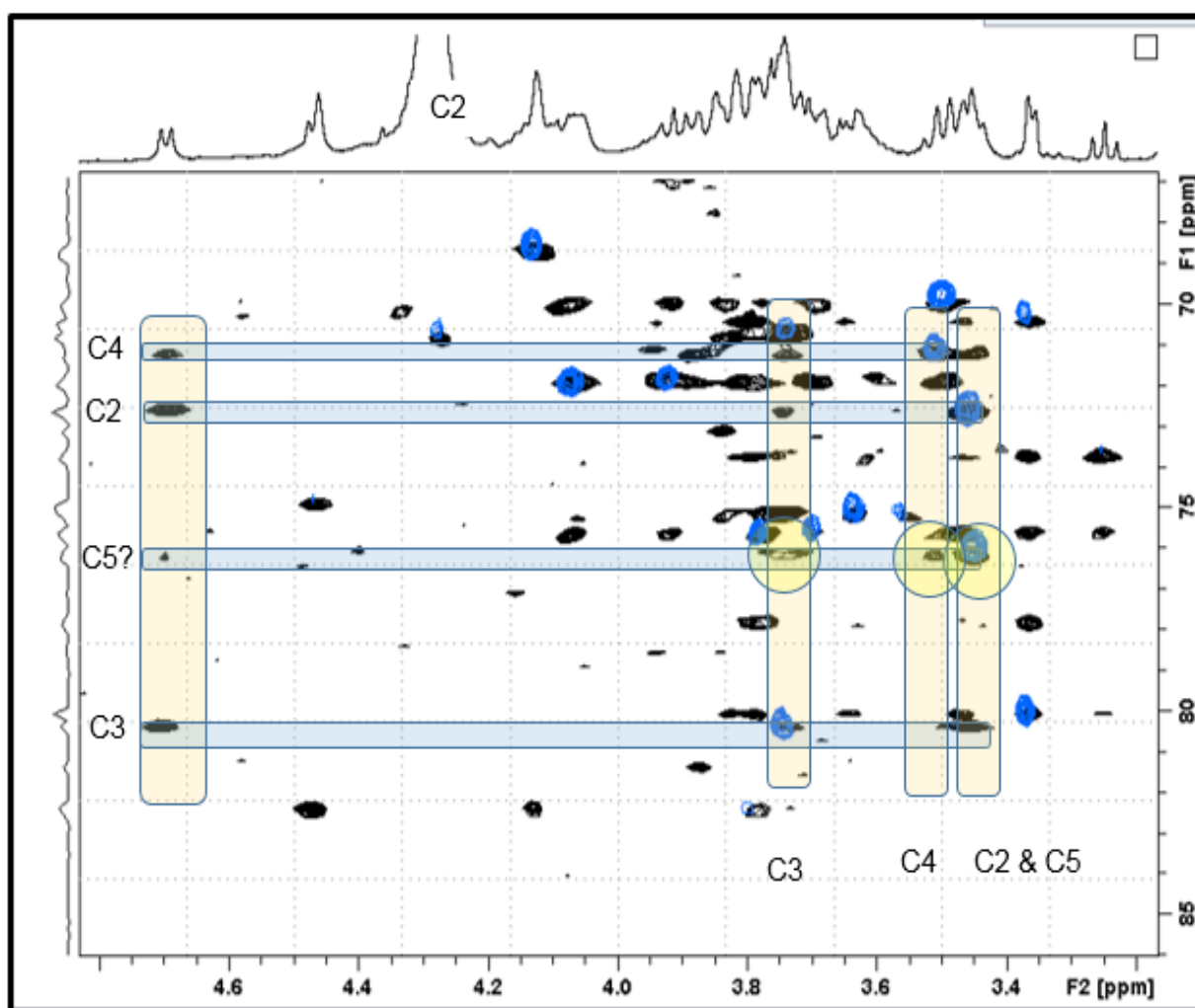


Figure 5.22. Combined ^1H - ^{13}C -HSQC Spectrum and a ^1H - ^{13}C -HSQC-TOCSY Spectrum for S2 Fraction of *B. breve* 7017 indicating the Final Methyne Signal for C5.

Finally, because of the substantial congestion surrounding the methylene signals, no attempt was made to identify the locations of the individual C6 and H6's. The resonance positions for the hydrogens and carbons in the four monosaccharides are listed in the Table (Table 5.4).

Table 5.4: Resonance Positions for the Hydrogens and Carbons

Monosaccharide	1	2	3	4	5	6	
A $^1J_{C-H} = 173 \text{ Hz}$	5.63 95.2	3.70 75.7	3.91 71.8	3.49 70.0	4.07 71.9	3.6-3.9 60-63	α -D-Glucose
B $^1J_{C-H} = 176 \text{ Hz}$	5.41 94.1	5.38 69.3	5.43 70.6	4.46 74.9	4.27 70.8	3.6-3.9 60-63	α -D-Galactose
C $^1J_{C-H} = 150 \text{ Hz}$	4.70 104.0	3.46 72.7	3.75 80.4	3.51 71.3	3.45 76.2	3.6-3.9 60-63	β -D-Glucose
D $^1J_{C-H} = 155 \text{ Hz}$	4.48 103.9	3.74 70.8	3.80 82.5	4.13 68.7	3.63 75.2	3.6-3.9 60-63	β -D-Galactose

The position of ring carbon resonances can usually be taken as indicative of the glycosidic linkages present in the repeat unit; carbons forming part of a glycosidic linkage are normally shifted to low field (>75 ppm). Looking at the data presented in Table 5.4, residues **C** and **D** are 1,3-linked sugars with **C3** at 80.4 ppm and **D3** at 82.5 ppm respectively. In a similar manner, residue **A** must be a 1,2-linked sugar with **A2** at 75.7 ppm. The chemical shift data for residue **B** is not as clear cut, given that both the 2- and 3- positions of the residue **B** are occupied by acetyl groups and that for the aged samples the chemical shifts for carbon six is typical for a glucose residue that does not have a glycosidic bonds at this position, then the only position where residue **B** would be able to form a link is at position four. It is difficult to decide what the chemical shift for **B4** in residue **B** signifies about whether a linkage is present at this position. The chemical shift for the **B4** resonance at 74.9 ppm is shifted slightly down-field (compared to 70.2 ppm in unsubstituted methyl α -D-galactose) but it is not shifted to the higher values normally associated with a single α -1,4-linked galactose (the shift reported in the literature is 79.3 ppm) but the value is close to that reported for 3,4-linked galactoses (75.1 and 76.6 ppm). The linkage analysis however suggests that there are two 1,3-linked sugars, a 1,2-linked sugar and a 1,4-linked sugar. As the only sugar with a carbon at position-4 that is shifted down-field, it is not unreasonable to suggest that **B** is the 1,4-linked sugar.

5.1.3.1. Identification of the Monosaccharides and their Anomeric Configuration in S2-fraction of *B. breve* 7017

The results of the monomer analysis suggested that the polysaccharide was composed of equal amounts of galactose and glucose. The location of the hydrogen at position 4 resonance can be used to differentiate between these two monosaccharides: for a galactopyranose sugar H4 resonates at chemical shift above 4 ppm whilst for a glucose residue the chemical shift of H4 is significantly below 4 ppm. This would suggest that residues **A** (**A4** at 3.49 ppm) and residue **C** (**C4**-residue at 3.51ppm) all highlighted in yellow in table 4.3 are the glucose residues whilst residues **B** (**B4**-residue at 4.46ppm) and residue **D** (**D4**-residue at 4.13ppm) all highlighted in grey are the galactose residues. The anomeric configuration of the monosaccharides was determined from examination of a coupled HSQC spectrum (Fig 5.23) shown by measurement of the $^1J_{C-H}$ coupling constant: values greater than 170 Hz identify alpha-linked sugars and values less than 170 Hz correspond to β -linked sugars. Residues **A** ($^1J_{C-H} = 173$ Hz) and **B** ($^1J_{C-H} = 176$ Hz) have α -linkages whilst residues **C** ($^1J_{C-H} = 165$ Hz) and **D** ($^1J_{C-H} = 164$ Hz) have β -linkages.

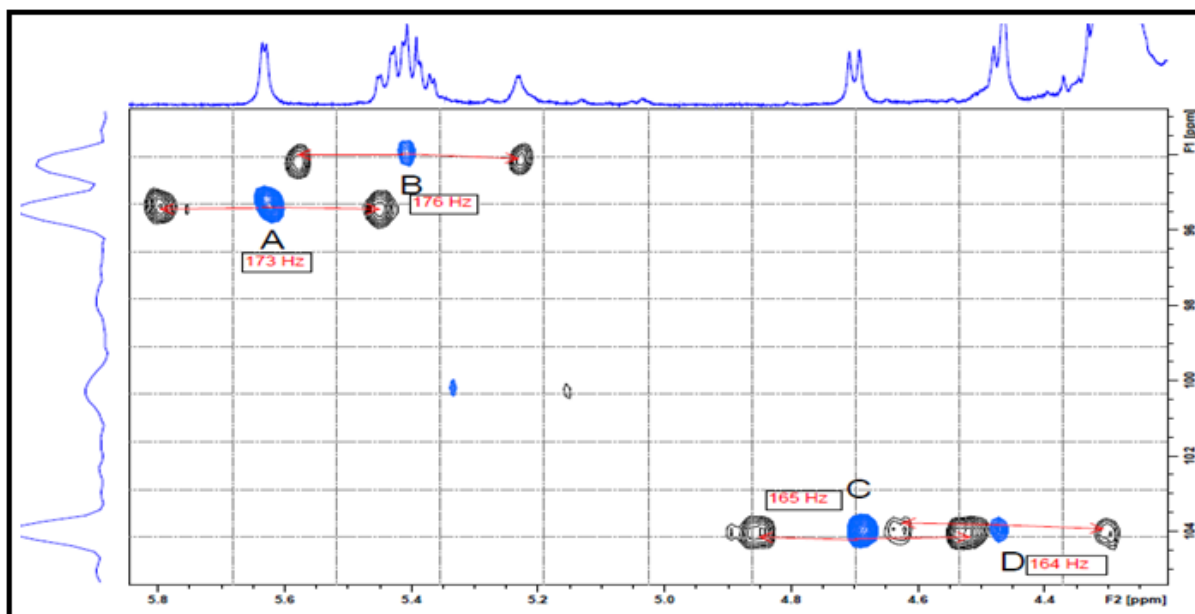


Figure 5.23. The coupled ^1H - ^{13}C -HSQC Spectrum Overlaid with ^1H - ^{13}C -HSQC Decoupled Spectrum S2 for *B. breve* 7017

After the extraction of this EPS (S2), its purity was first examined using size exclusion chromatography and monitoring the elution of peaks using a multi-angle light scattering detector in combination with a concentration dependent differential refractometer and a UV-

detector following the procedure as described in section 2.8.6. A single broad peak was eluted for the light scattering (Fig 5.24) which had a weight average molecular mass of $1.241 \times 10^6 \text{ gmol}^{-1}$ (indicating it to be a HMw) and the sample had a polydispersity of 1.55 suggesting its distribution to be that of a narrow molecular mass. A small hump is noticeable on this single broad peak suggesting that it could be a mixture of a HMw and MMw. No peaks were visible in the UV-trace indicating that if any proteins, they were below detection limit and no nucleic acid contaminants.

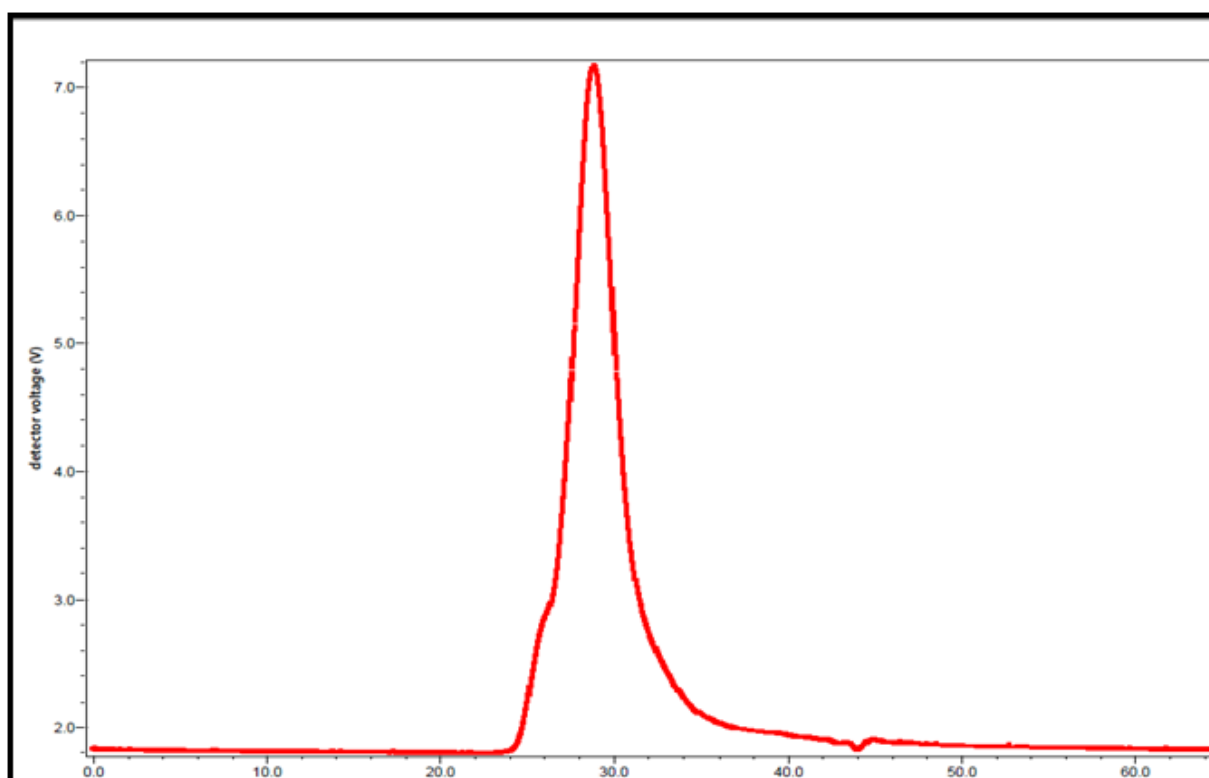


Figure 5.24. SEC-MALLS Trace of S2 from *B. breve* 7017 (Light Scattering)

The suggested components (galactose and glucose) of the S2 fraction were further confirmed by carryout some wet chemistry monomer analysis as described in the experimental section 2.8.4. After hydrolysis the HPAEC-PAD results identified the two main peaks which were then confirmed with standards to be the galactose and glucose (Fig 5.25).

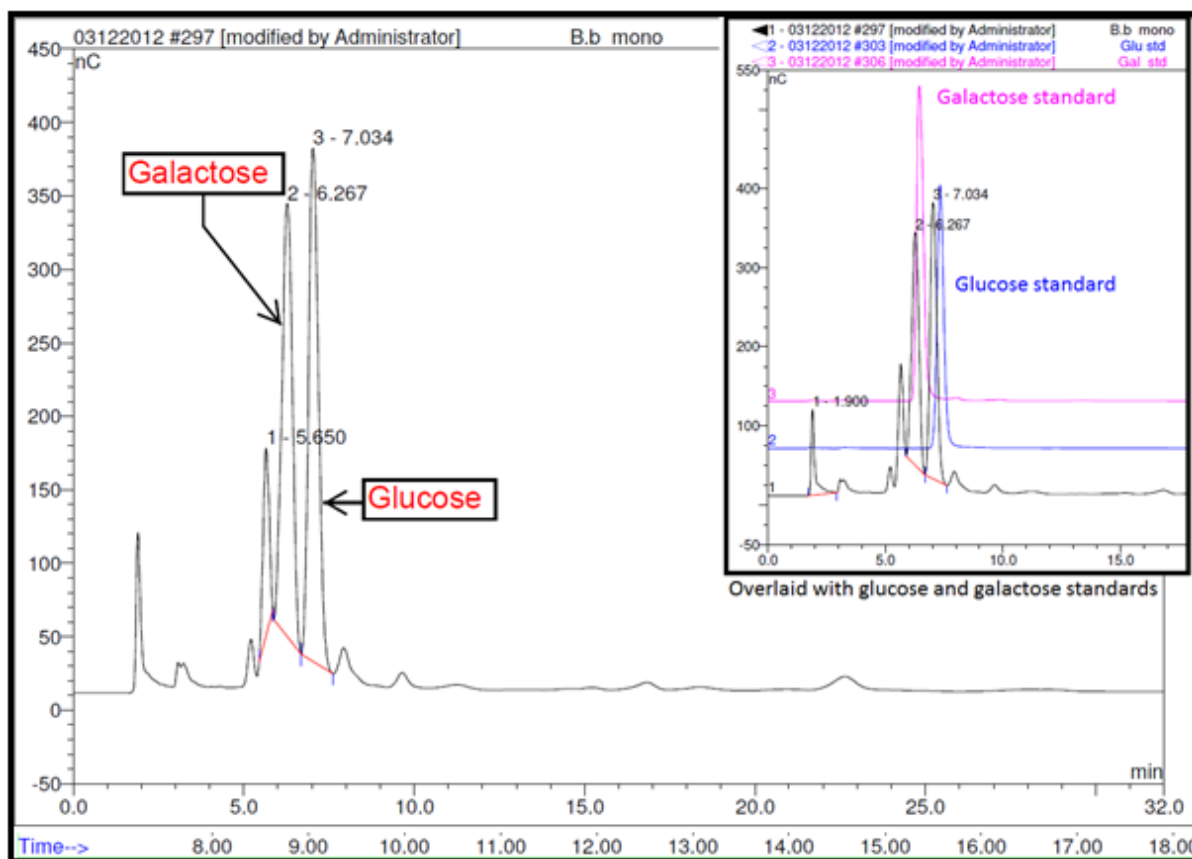


Figure 5.25. HPAEC-PAD Chromatogram of the Polysaccharide (S2 fraction) from *B. breve*

7017

After hydrolysis, the remainder of the sample was then reduced and acetylated to give the alditol acetates of these two identified sugars, which was then recorded on the GC-MS to specifically identify them showing their mass spectra (*Fig 4.19*). It should be noted that the glucose and galactose molecule all have same mass spectra. The chromatogram of the S2 sample was then overlaid with those of the standard glucose and galactose to confirm their identity (*Fig 5.26*).

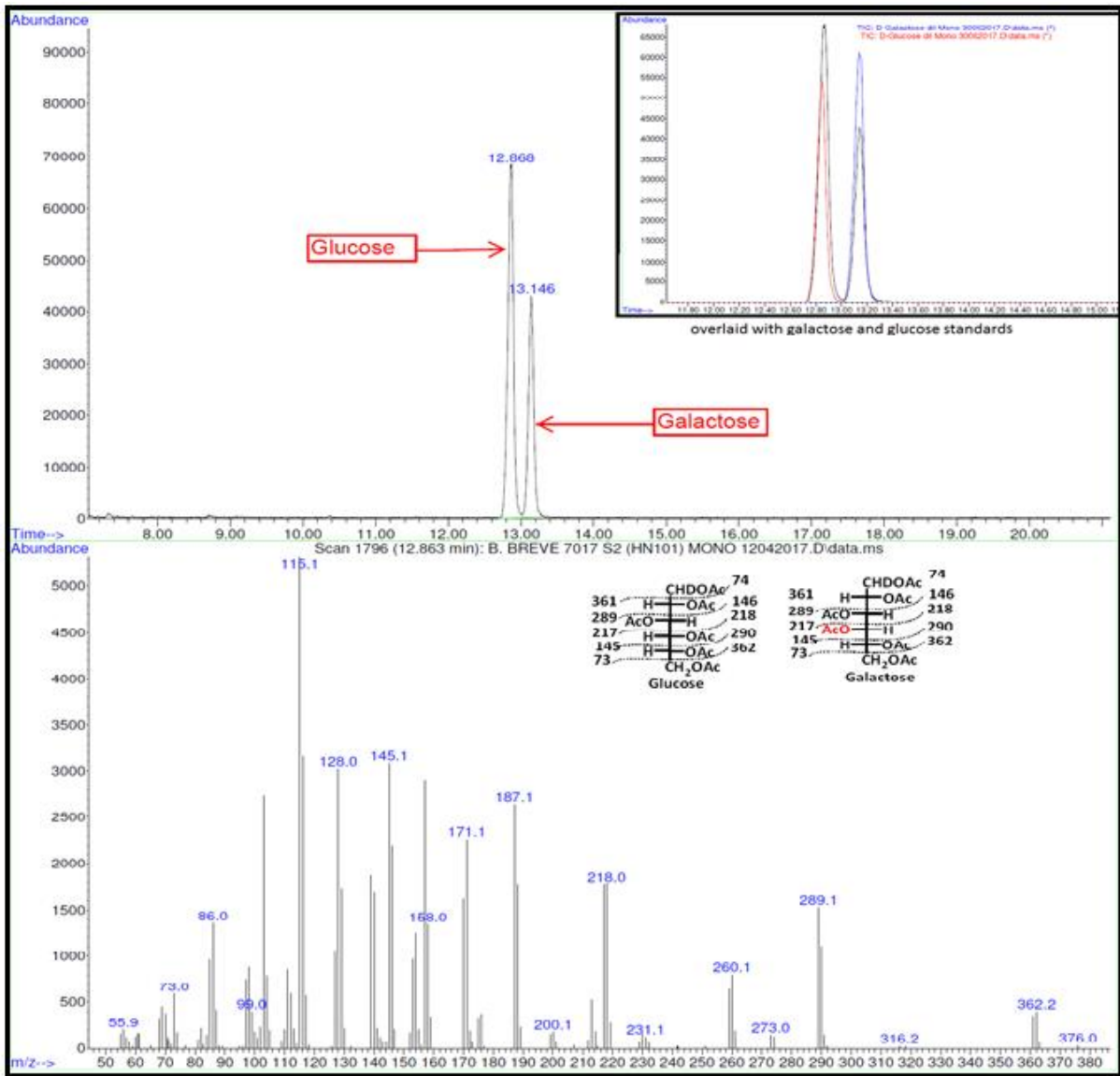


Figure 5.26. Chromatogram and Mass Spectrometer for the Alditol Acetates of the Sugars obtained from the GCMS for Monomer Analysis of *B. breve* 7017.

The absolute configuration of these monomers was determined to be D-glucose and D-galactose (Fig 5.27) after carrying out the procedures described in section 2.8.7.

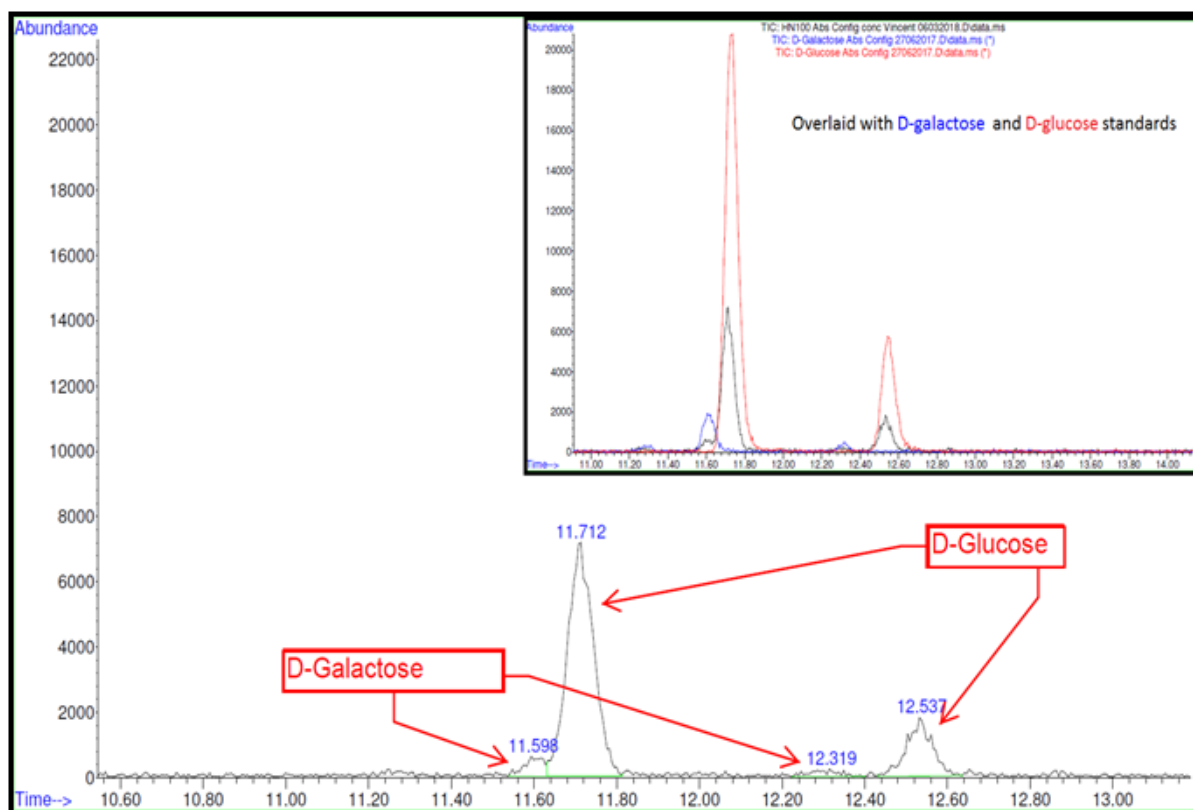


Figure 5.27. Chromatogram of the Absolute Configuration of S2 from *B. breve* 7017

When the chromatogram of the absolute configuration of the S2 was overlaid with those of D-glucose and D-galactose standards, the peaks fitted perfectly confirming the D-glucose to be the higher peaks and D-galactose to be the lower peaks. This was further confirmed by comparing their mass spectra with those of the instrument's standard saved library.

5.1.3.2. Determination of the Linkage Pattern in the S2-fraction of *B. Breve* 7017

Following the procedures for the linkage analysis as described in section 2.8.5, the methylated alditol acetates were obtained from the GC-MS (Fig 5.28) indicating the various linkages that occur in this polysaccharide.

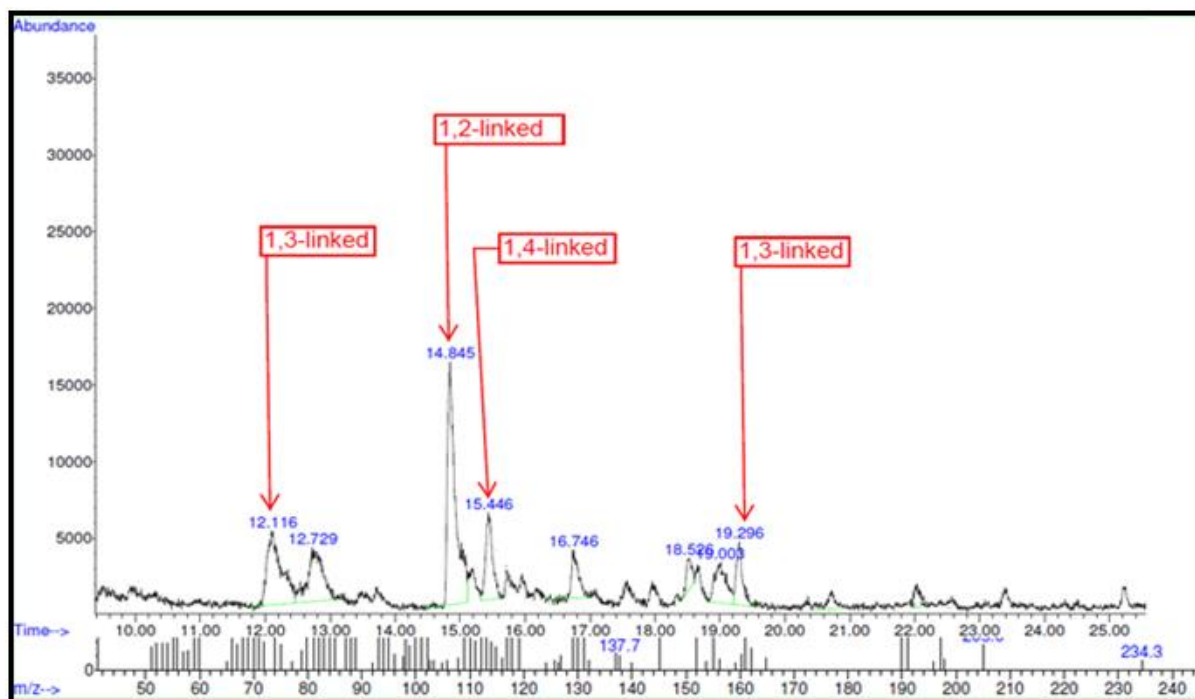


Figure 5.28. Chromatogram and Mass Spectrometer for the Methylated Alditol Acetates of the Sugars obtained from the GCMS for Linkage Analysis of S2 from *B. breve* 7017.

Seeing that the anomeric region on the proton NMR indicates four anomeric protons signals then implies that there are four major peaks for the linkage analysis. The main linkages existing in this S2 polysaccharides are the 1,3-linkage (Fig 5.29 and Fig 5.30), 1,2-linkage (Fig 5.31) and 1,4-linkage (Fig 5.32) which will be further confirmed with NMR results that follows.

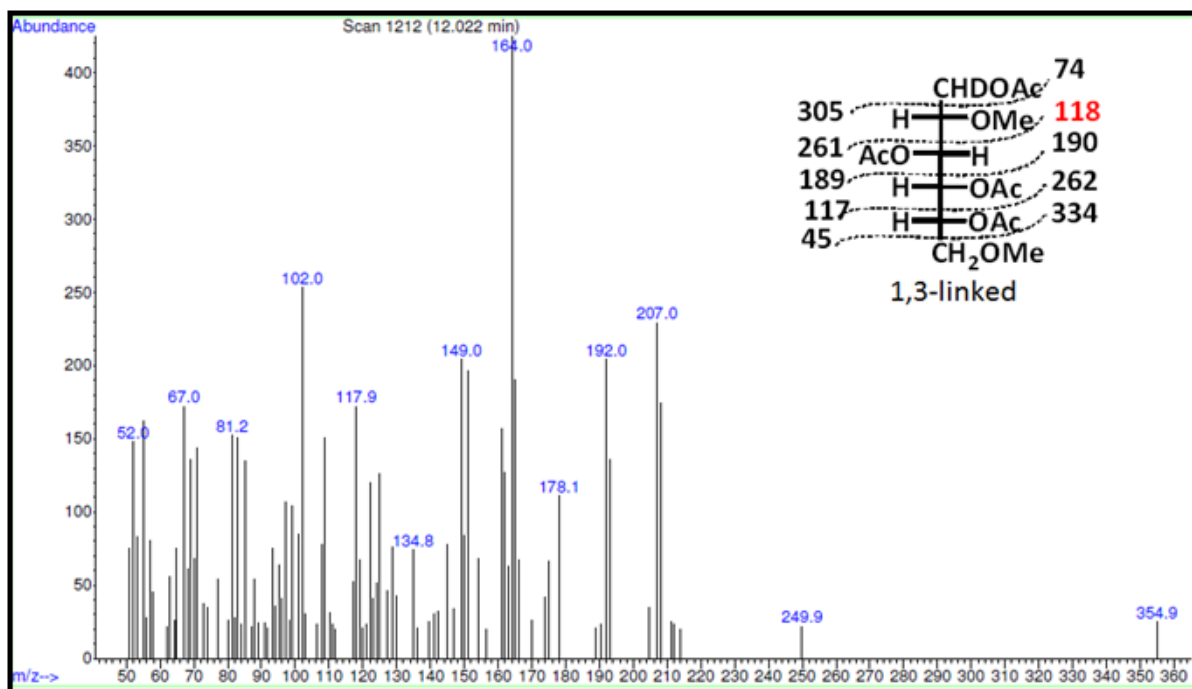


Figure 5.29. MS of the 1,3-linkedglucosyl unit at 12.022 mins

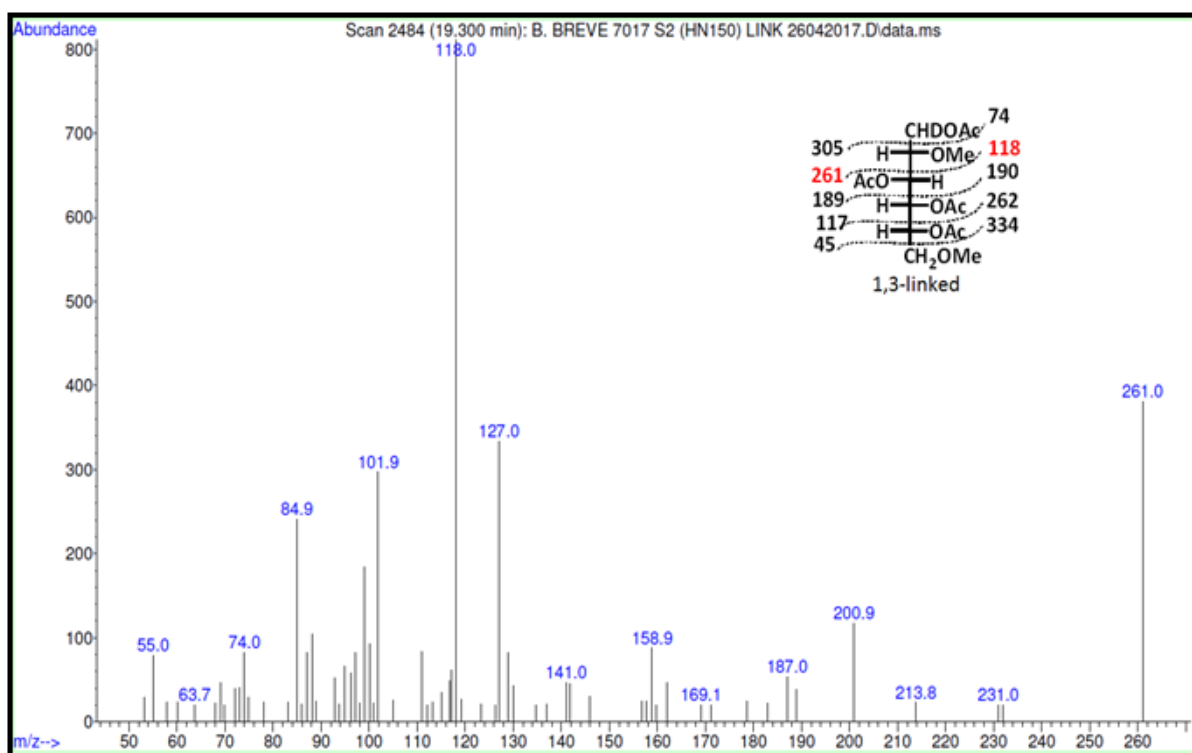


Figure 5.30. MS of the 1,3-linkedglucosyl unit at 19.300 mins

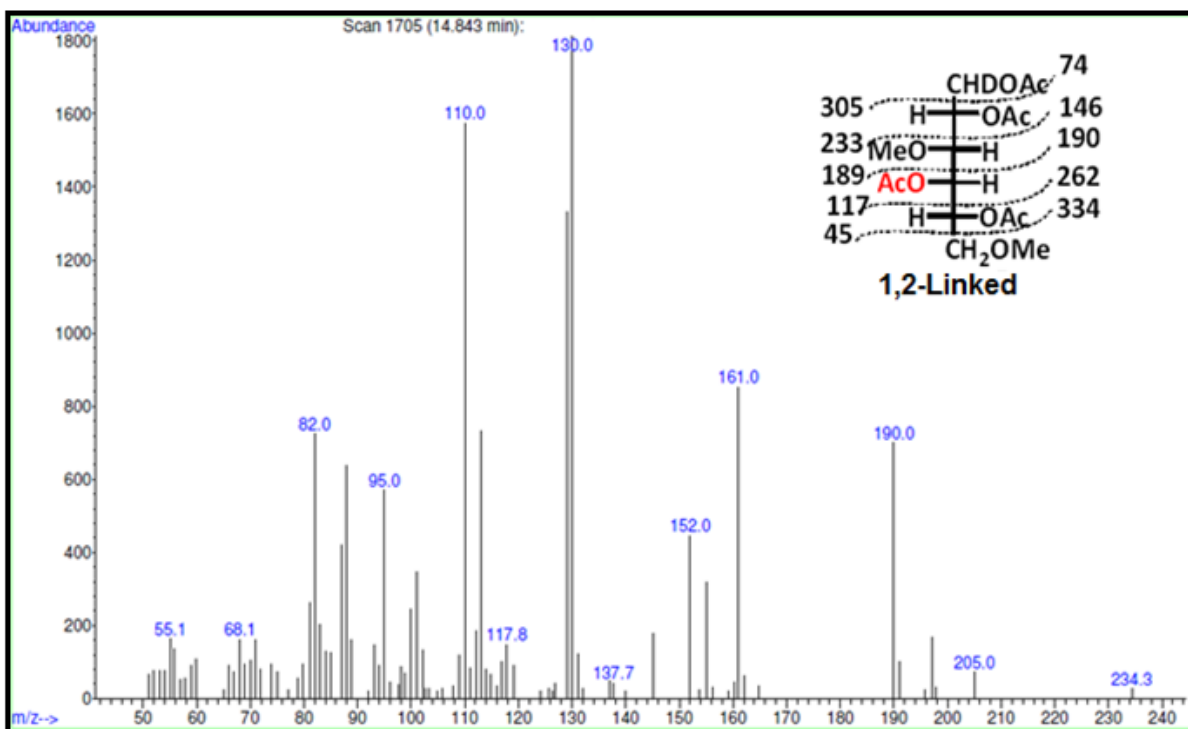


Figure 5.31. MS of the 1,3-linkedglucosyl unit at 14.843 mins

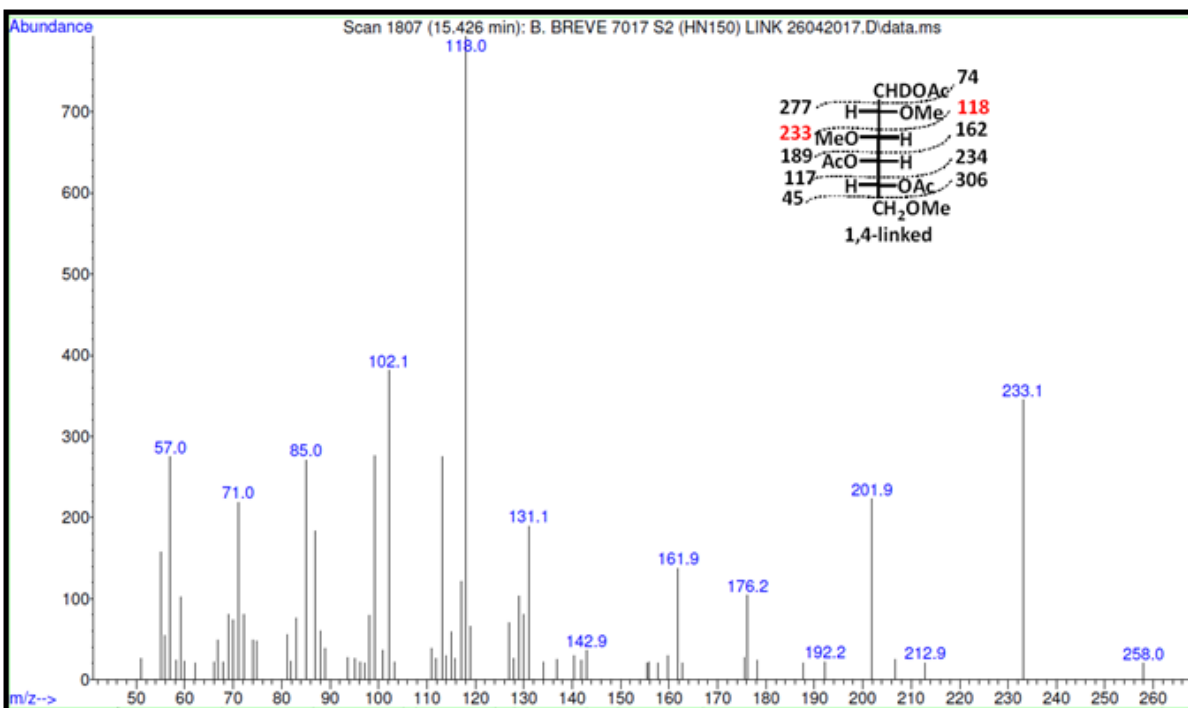


Figure 5.32. MS of the 1,3-linkedglucosyl unit at 15.426 mins

The NOESY and HMBC spectra can also be used to determine the sequence of the monosaccharides in the repeat unit. On the NOESY spectrum inter-residues NOES (highlighted in green, Fig 5.33) were observed between: **A** H1 and **C** H3 identifying a 1,3-link between the two sugars; **B** H1 and both **A** H1 and **A** H2 a 1,1-linkage is ruled out by the previous assignment of a glycosidic link from **A** to the 3-position of **C** and the fact that this would correspond to a change in direction of the chain, it is therefore likely that there is a 1,2-link from **B** to **A**; the final inter-residue NOE is between **C** H1 and **D** H3 identifying a 1,3-linkage from **C** to **D**.

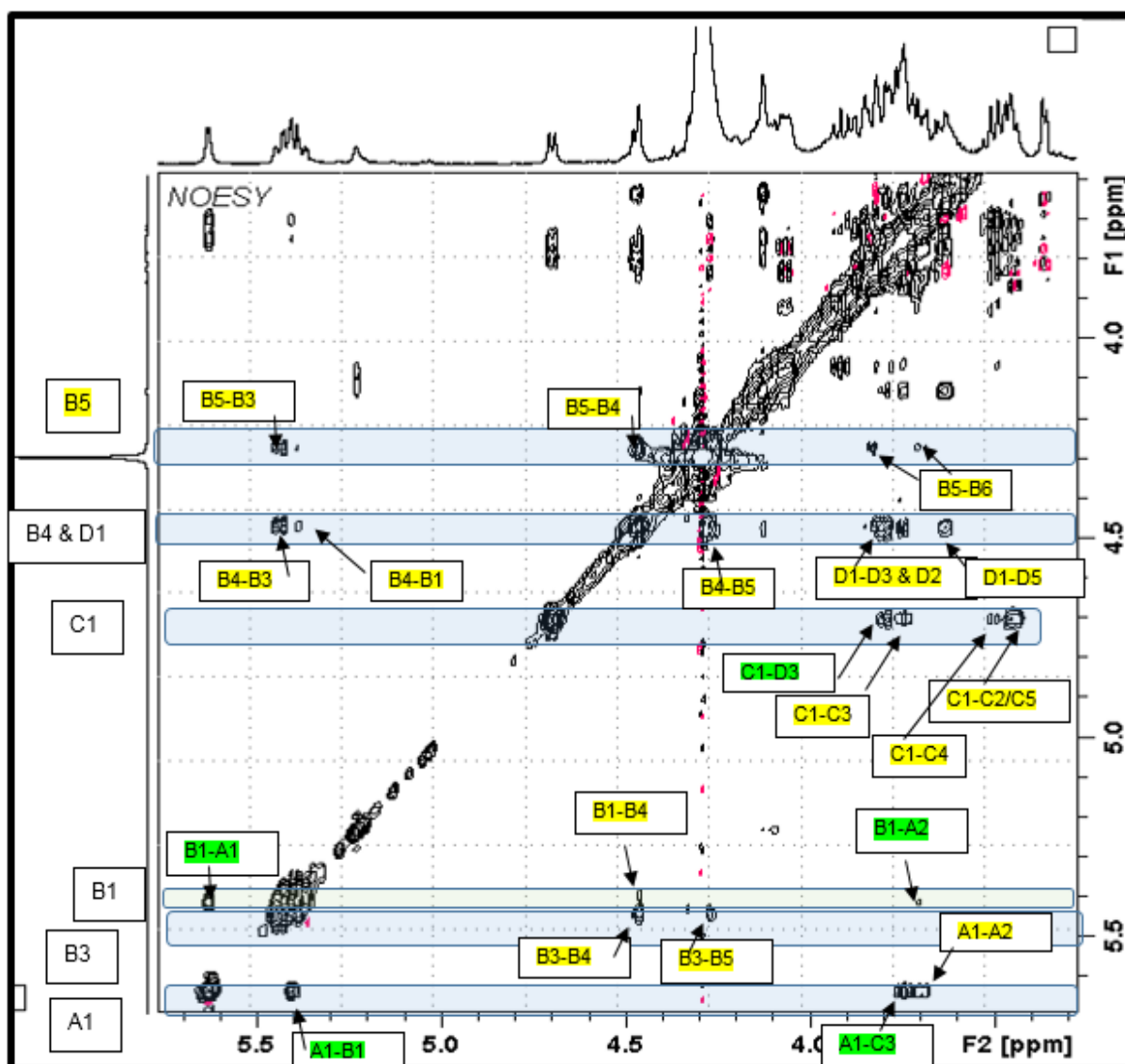


Figure 5.33. ^1H - ^1H -ROESY Spectrum Showing the Inter-residue NOES identifying the Linkage in the Repeating Unit of *B. breve* 7017.

More information about the linkages present in the repeat unit were obtained from inspection of the anomeric carbon region of a combination of the HMBC and HSQC spectrum

(Fig. 5.34). Scalar coupling between the **A1** carbon and the **C3** hydrogen confirm the presence of a glycosidic link between **A1** and **C3** and the scalar coupling between the **D3** carbon and the **C1** proton confirms the presence of a glycosidic link between **C1** and **D3**.

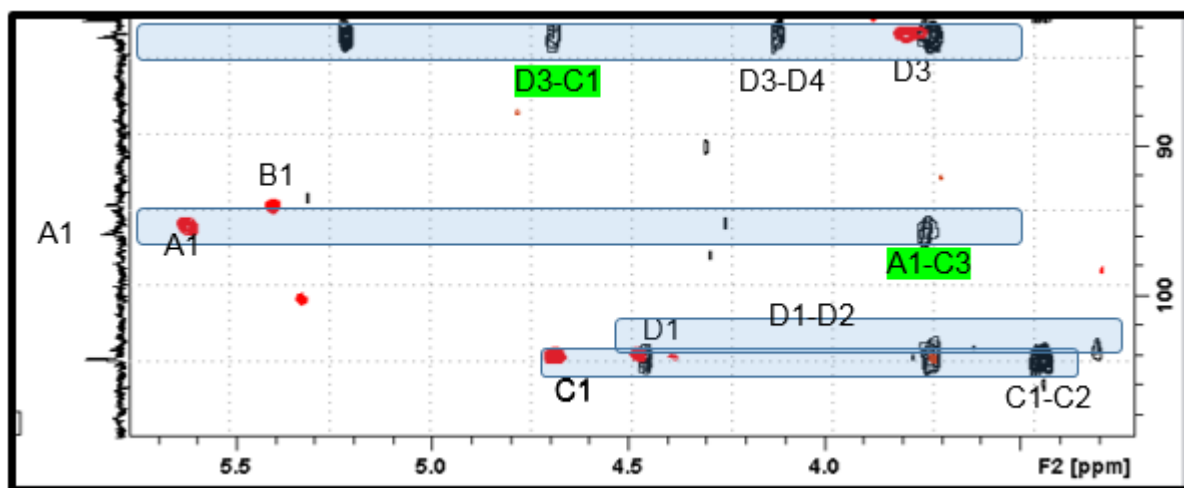
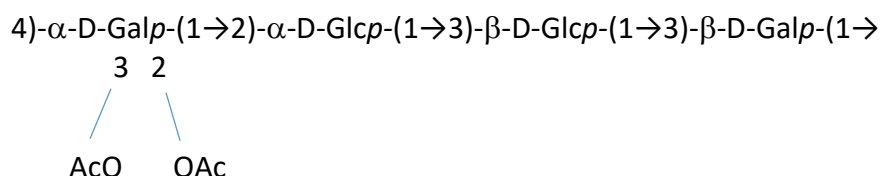


Figure 5.34. Combined ^1H -HMBC Spectrum and a ^1H - ^{13}C -HSQC Spectrum giving more Information for the Linkages.

The linkage data extracted from the HMBC and NOESY spectra suggest that the monosaccharides present in the backbone of the repeat structure have the following sequence:



Unfortunately, the resonances for both H4 in **B** and H1 in **D** occur at the same frequency, so it was not possible to detect either a direct NOE between the two protons or scalar coupling on the HMBC spectrum.

5.1.3.3. Identifying other Components present in the S2-fraction of *B. Breve* 7017

Further inspection of the 2D-homonuclear spectra show that several resonances are not involved in splitting patterns linked to anomeric protons: these have been labelled on the HSQC spectrum (Z, X, Y and S, Fig. 5.20). These four signals belong to methyne groups and, from inspection of expansions of a combination of the COSY and TOCSY spectra, the spin systems also incorporate additional methylene protons (Fig 5.35; R and U). A number of these resonances were not visible in the NMRs spectra recorded immediately after the samples had

been prepared and it was thought that these are potentially being associated with a decoration, which is joined to the repeating unit by a labile bond. In order to assess whether this was the case, one batch of the S2-fraction (HN0176) was left in solution until no further changes in the spectra were observed at which point the sample was dialysed and new sets of spectra were recorded for the high molecular weight material remaining in the dialysis bag and for the low molecular weight material in the dialysate.

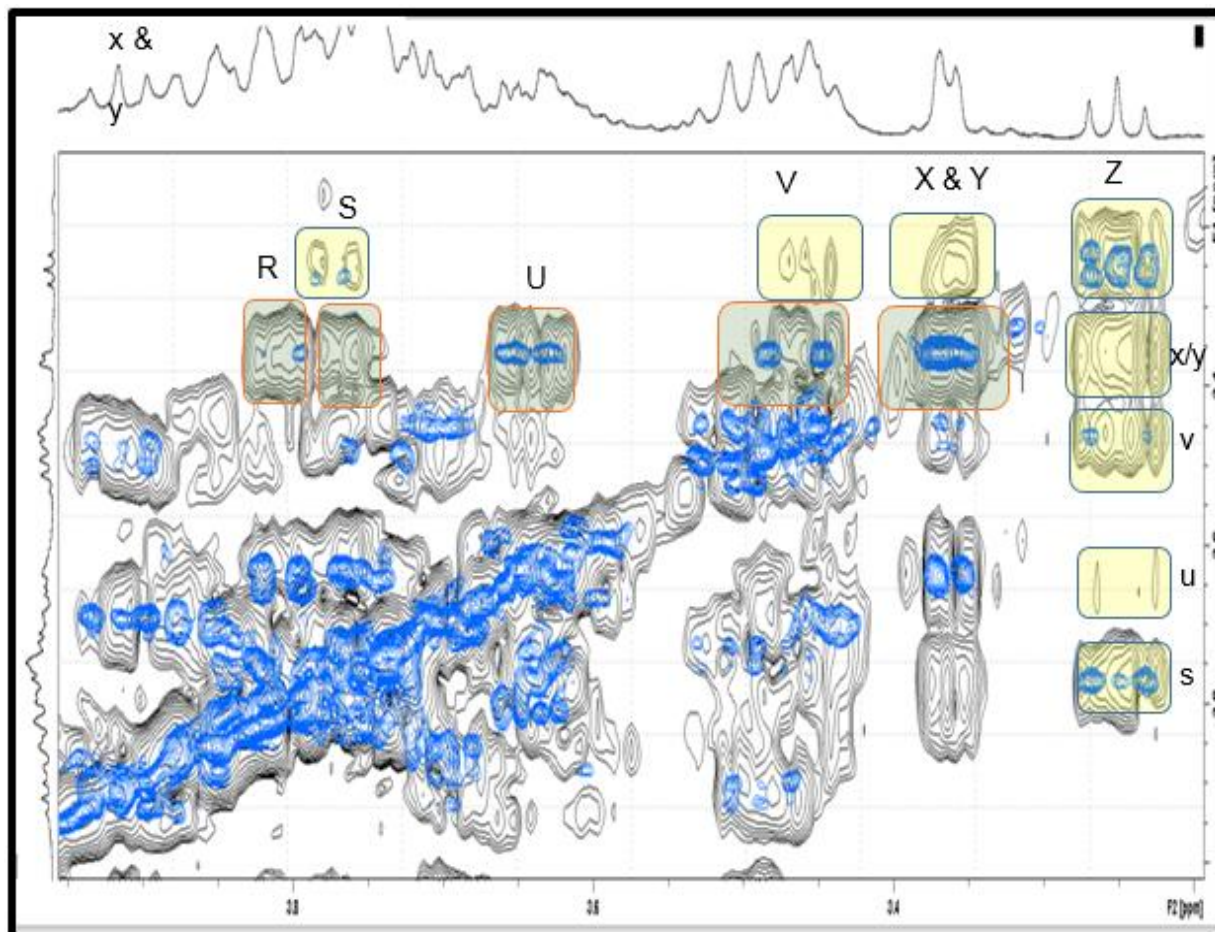


Figure 5.35. Expanded Combined ^1H - COSY Spectrum and ^1H - TOCSY Spectrum indicating the Four Methyne Group Signals (Z, X, Y and S) and the Additional Methylene Proton Signals (R and U).

5.1.3.4. Analysis of the NMR Spectra Recorded for Material in the Dialysate

A very small amount of material was recovered after the dialysate has been freeze-dried (>2 mg) and this was dissolved in D_2O and a proton NMR was recorded. Whilst the signals in the spectrum were not very strong it is clear that the decoration present in the repeating unit had been isolated and the resonances corresponded to the signals in the original sample that were

not linked to anomeric protons i.e. Z, X, Y, U, S and R (Fig 5.36) along with those from lactic acid; it should be noted that no anomeric signals were visible in the spectrum.

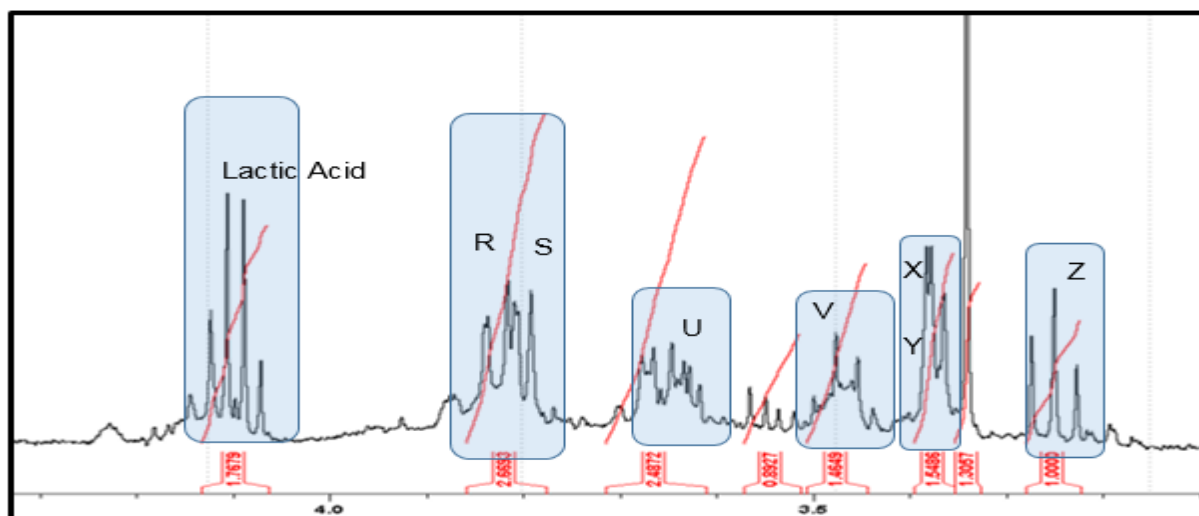


Figure 5.36. ^1H -NMR Spectrum of the Signals not Linked to the Anomeric Protons including the Lactic Acid (The Dialysate)

To gain further insight about the identity of this material a series of 2D-NMR spectra were recorded. On an edited HSQC spectrum (Fig 5.37) six unique methyne signals (black contours) were visible, the signal at 3.97 ppm which is encircled was from lactic acid and the five remaining signals corresponded to Z (f2-3.13 ppm & f1-72.95 ppm) X (f2-3.24 ppm & f1-69.5 ppm) Y (f2-3.25 ppm & f1-79.5 ppm) V (f2-3.34 ppm & f1-77.1 ppm) & S (f2- 3.67 ppm & f1-74.9 ppm).

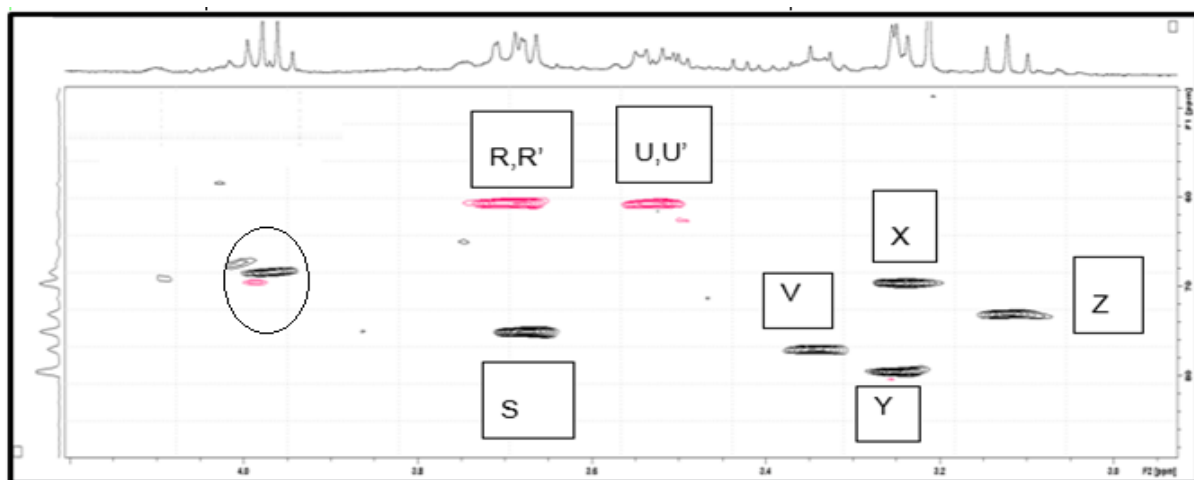


Figure 5.37. The Edited ^1H - ^{13}C -HSQC Spectrum indicating the Six Unique Methyne Signals of the Dialysate of *B. breve* 7017.

Finally, two methylene resonances were present (red contours) these correspond to the **R** and **U** resonances in the original proton S2 HSQC spectrum and, after subtracting one for the **S**-proton, these signals integrate to approximately four protons. On close inspection of an expanded proton spectrum, the **R** signal appears to be two halves of two overlapping AB spin systems this would suggest that each of the methylene contours signals is in fact one proton from each of two separate methylene groups i.e. one methylene group CH_RH_U and the second being $\text{CH}_{R'}\text{H}_{U'}$ with identical carbon chemical shifts and very similar proton shifts for the R,R' and U,U' pairs.

The latter result suggests that the two methylenes are in similar magnetic environments and this suggests that two similar terminal hydroxymethyls are present. The absence of any obvious anomeric protons would suggest that if the decoration is a monosaccharide it is not an aldose. Several short-range scalar couplings between different proton resonances were identified from inspection of the COSY spectrum (Fig 5.38) and additional long-range coupling from inspection of the TOCSY spectrum (Fig 5.39).

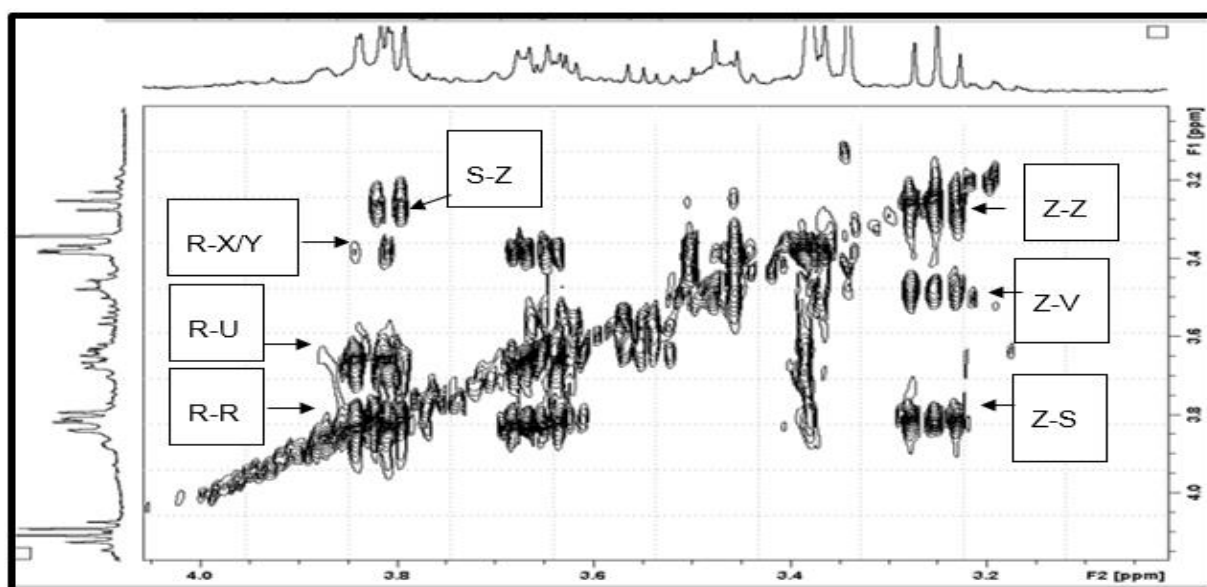


Figure 5.38. ^1H - ^1H -COSY Spectrum of the *B. breve* 7017 S2 Dialysate indicating Short Range Scalar Couplings between the Different Protons.

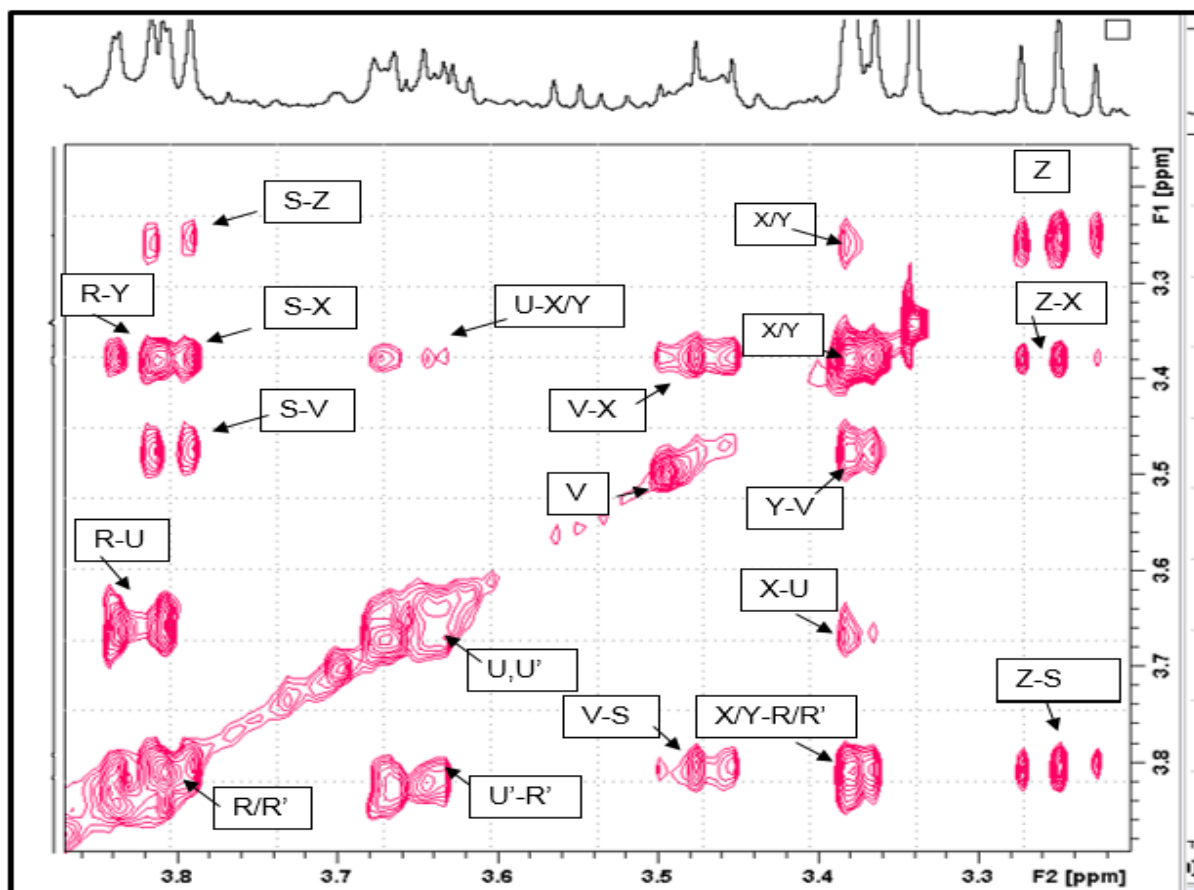


Figure 5.39. ^1H - ^1H -TOCSY Spectrum of the *B. breve* 7017 S2 Dialysate indicating the Additional Long Range Coupling between the Different Proton Resonances.

The scalar couplings starting from proton **Z** are consistent with the unknown molecule having a carbon skeleton with a minimum of 4-contiguous methyne carbons with **V** and **S** as immediate neighbours and either **X** as the next nearest neighbour. The observation of a cross peak between **V** and either **X** on the COSY spectrum and the absence of a similar cross peak between **S** and either **X** or **Y** suggests that either **X** or **Y** is a neighbour of **V** (Fig 5.40). Again, looking at the COSY spectrum, other than the direct couple with **Z** the only other cross peaks visible to **S** is potentially one to HU' .

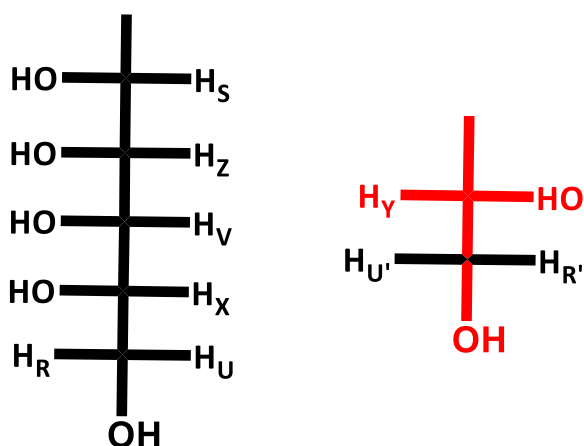


Figure 5.40. Fischer Projection indicating Positions of the Various Signals.

On the COSY spectrum (Fig 5.38) there is evidence that the methylene protons **R & R'** are coupled to their methylene partner **U & U'** respectively and both have a short-range coupling to either **X** or **Y** (unfortunately it was not possible to distinguish between X and Y on the COSY). The NMR data is consistent with two structural fragments being present but because of the limited amount of sample available our attempts to record a HMBC spectrum which would have been able to probe if the fragments were part of larger systems, including quaternary carbons, wasn't possible (see section on future work).

5.1.4. Characterisation of the Polysaccharide Material Associated with the Cells: the **C1** and **C2**-fractions.

For the *B. breve* 7017 strain, the highest yield of polysaccharides was recovered from the cells when they were left stirring overnight in an aqueous alkaline solution (NaOH, 1M). After centrifugation, polysaccharides were precipitated from the supernatant on the addition of ethanol. NMR spectra recorded for the precipitated materials suggested that complex mixtures of polysaccharides were being recovered as will be discussed in the sections that follows. As was the case with the **S**-fractions discussed previously, it was possible to partially fractionate and separate two polysaccharides by gradually increasing the percentage of ethanol that was being added to the supernatant. Again, addition of one volume of chilled ethanol precipitated a glycogen-rich fraction labelled **C1**. Whilst, addition of a second volume of ethanol released a small amount of a second polysaccharide, labelled as fraction **C2**.

5.1.5. Characterisation of the Polysaccharides Present in the C1-fraction from *B. Breve* 7017.

5.1.5.1. Monomers, Linkage, Absolute Configuration and SEC-MALLS Analysis of the C1 fraction from *B. breve* 7017.

Monomer analysis identified that glucose was the only monosaccharide present (*Fig 5.41*) in the C1-fraction (>95%) and, after conversion to its (S)-2-methylpropyl glycoside using Gerwig's *et al.* (1978)²⁰⁹ method, the glucose was shown to have D-absolute configuration (*Fig 5.42*). The polysaccharide was subjected to linkage analysis, which included preparation of methylated alditol acetates. As was the case for the S1-fraction, the C1-fraction gave a large peak for 2,3,6-trimethyl-1,4,5-tri-O-acetylhexitol which suggests that the polysaccharide is a 1,4-linked glucan (*Fig 5.43*). A second smaller peak was also present, and the MS confirmed that this was 2,3-dimethyl-1, 4, 5, 6-tetra-O-acetylhexitol whose presence is consistent with a small amount of a 1,4,6-linked hexose as a branching point. These results suggested that the C1-fraction is either glycogen adhering to the cells or another possibility is that the material was simply starch which was being added as one of the media components. To rule out the latter possibility, the fermentation was repeated but using D-glucose-1-¹³C as a carbon feed. When monomer analysis was performed, C-1-deuterioalditol acetates were recovered and this confirmed that the glucan was being produced *in situ*.

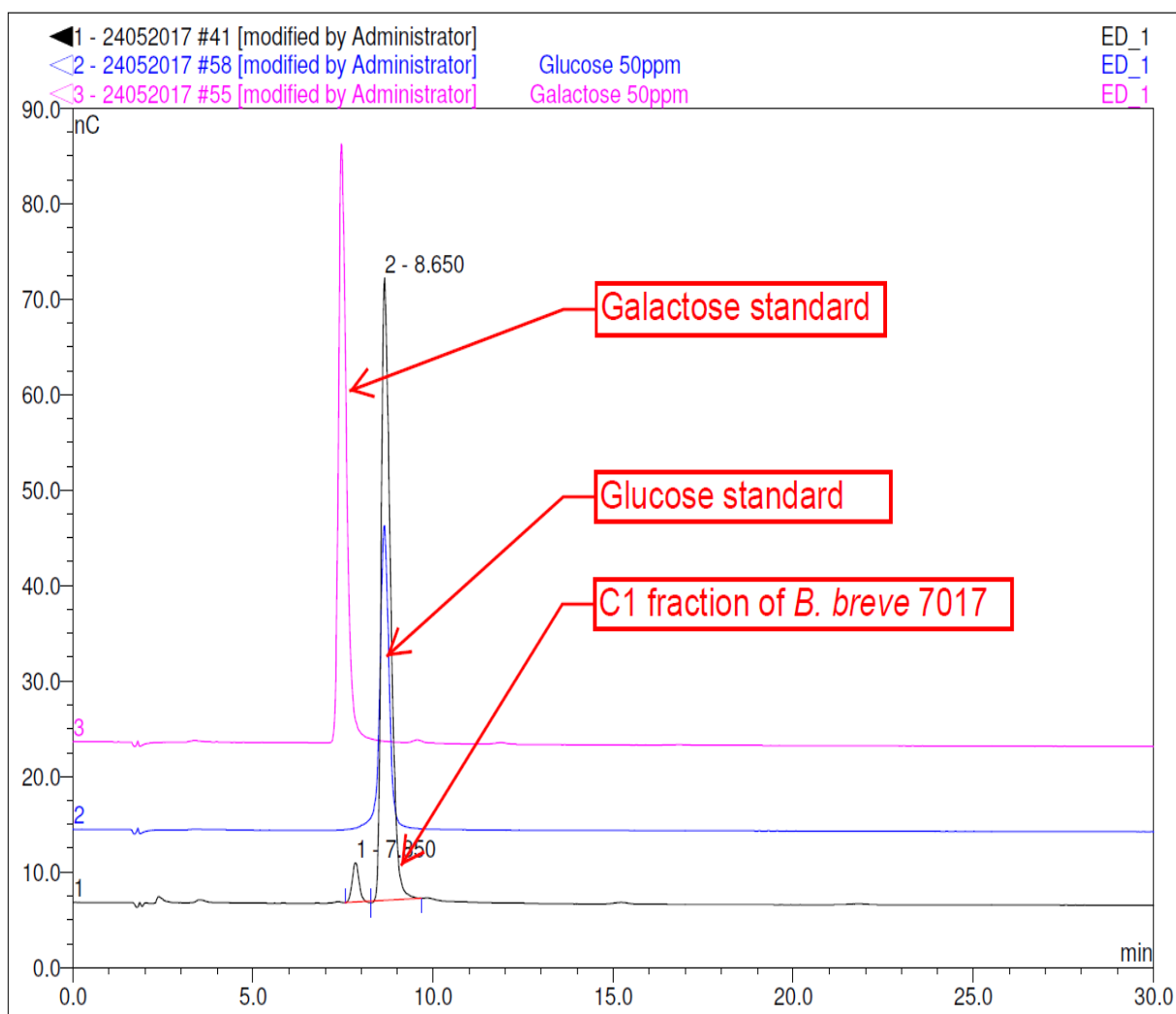


Figure 5.41. HPAEC-PAD Chromatography of C1 from *B. Breve* 7017 Overlaid with Glucose and Galactose Standards

The overlay showed the peak for the C1 fraction to fit perfectly with that of the glucose standard confirming that the polymer chain is made up of entirely a glucose repeat unit.

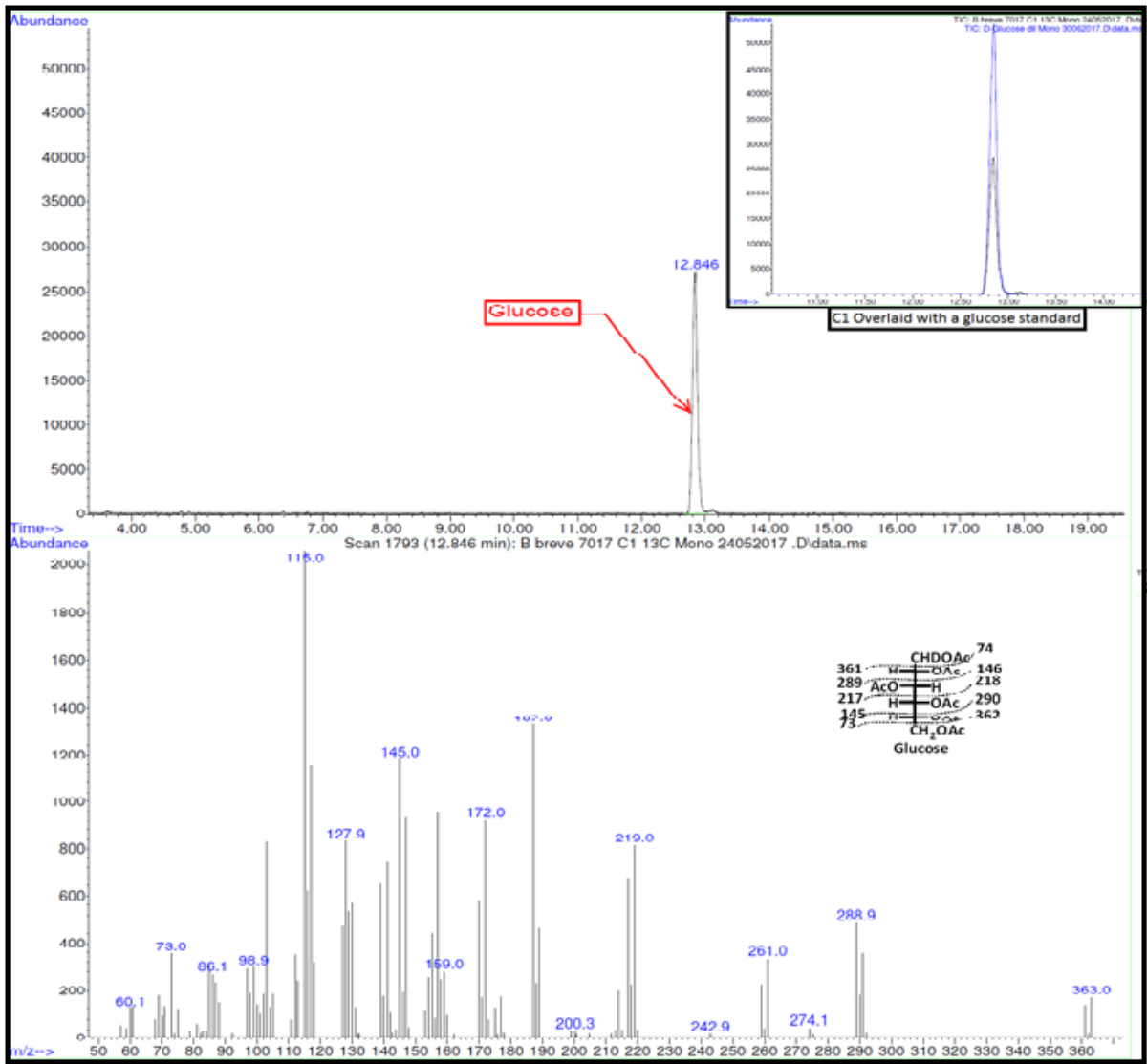


Figure 5.42. Chromatogram for the Alditol Acetates from C1 of *B. breve* 7017 and its Mass Spectrometer.

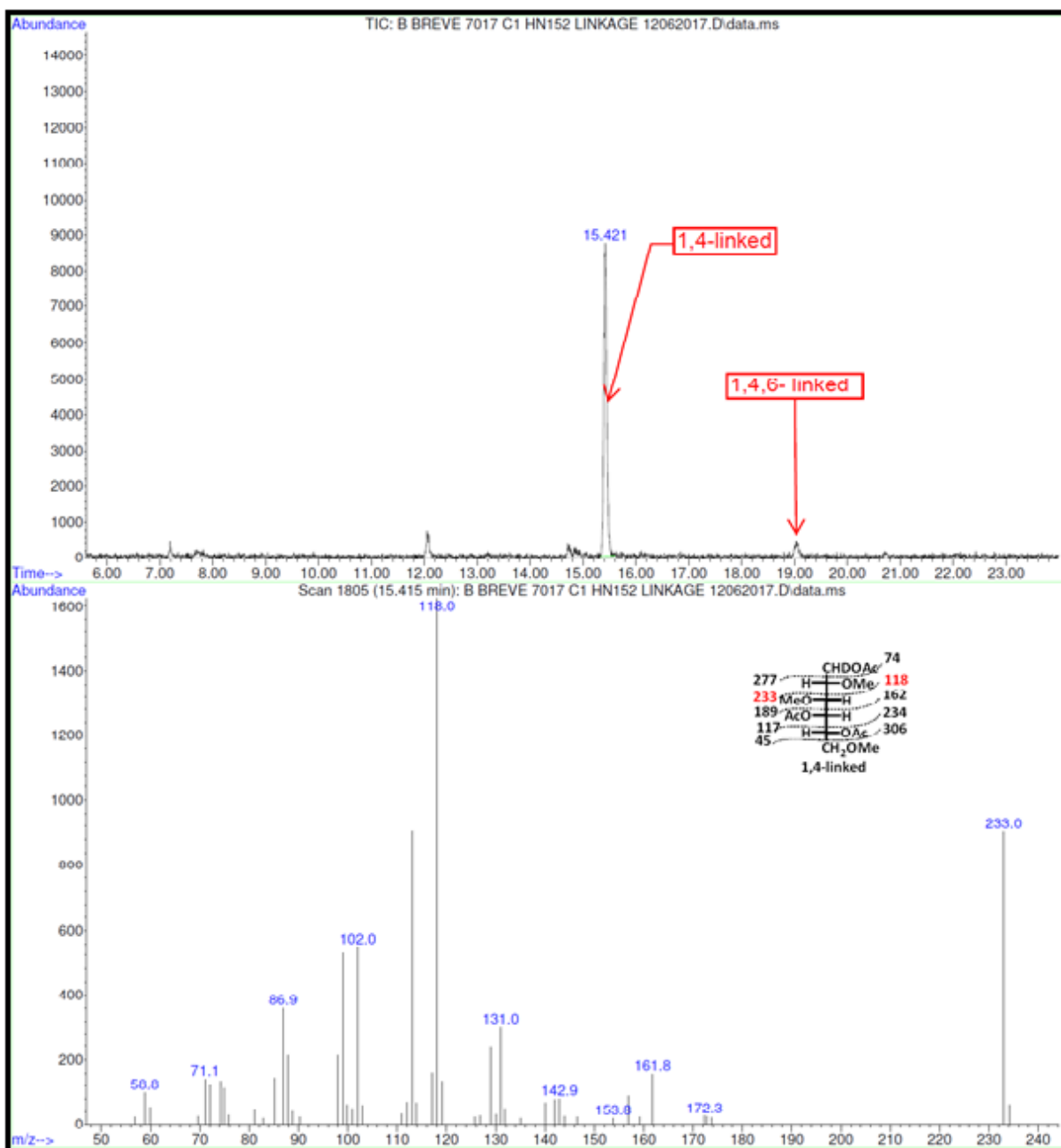


Figure 5.43. Chromatogram for the Methylated Alditol Acetates of the Sugars obtained from the GCMS for Linkage Analysis of C1 from *B. breve* 7017

As for the tiny peak at 19.02 minutes the mass spectrometer (*Fig 5.44*) confirms that it is a 1,4,6-link branch to parent molecule.

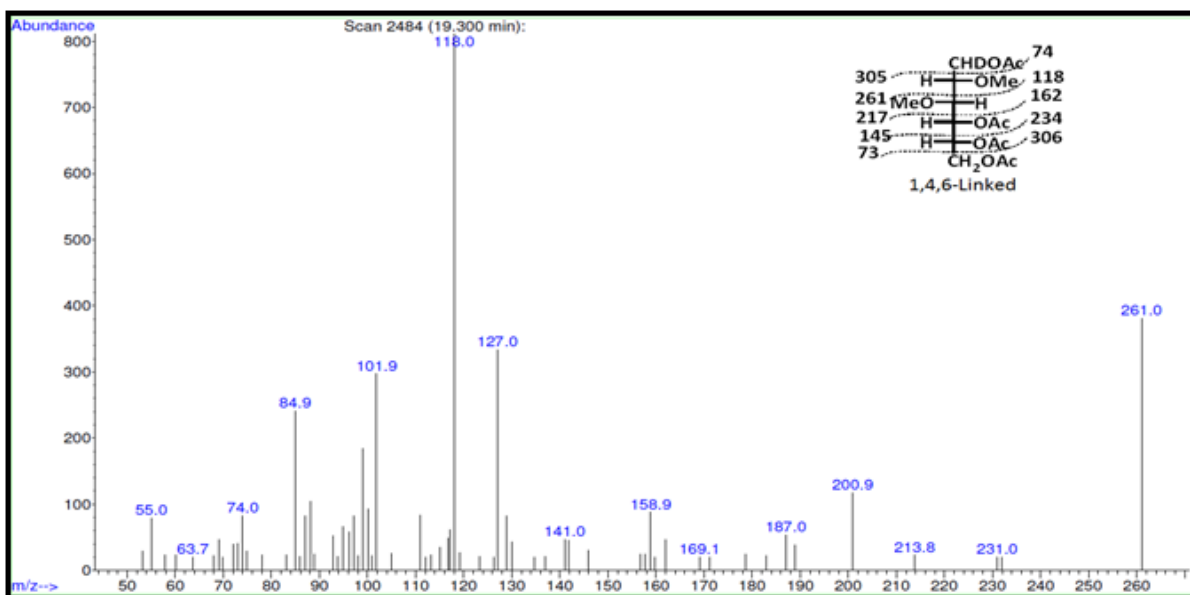


Figure 5.44. The Mass Spec for the 1,4,6-link which is Branched in the Main C1 Polymeric Chain

The absolute configuration for this main sugar was determined to be D-glucose and after carrying out some wet chemistry, the absolute configuration of the C1 was then compared with those of the standards (Fig 5.45) where it matches that of D-glucose. This was further confirmed by matching the mass spec of the peaks with that of the saved library references in the instrument for sugar standards.

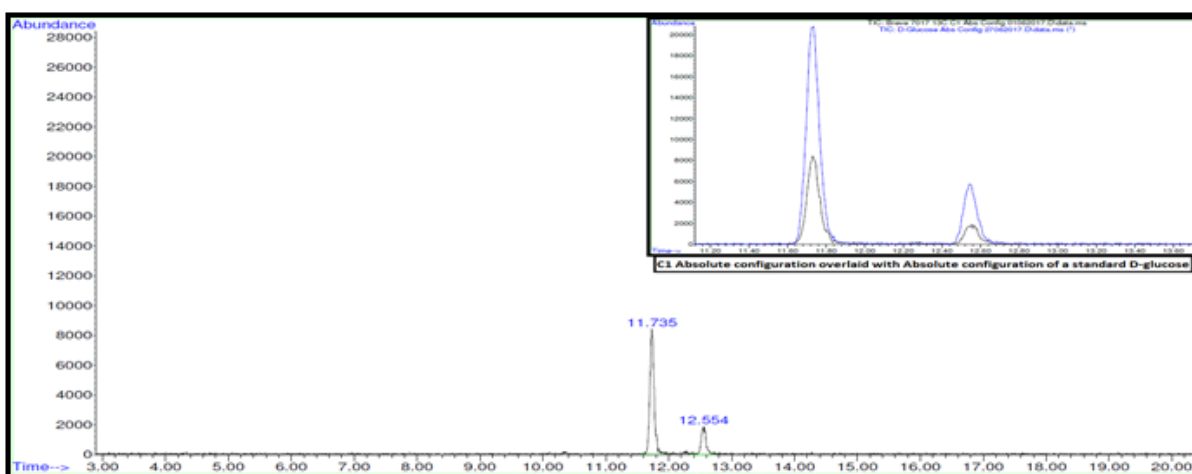


Figure 5.45. Chromatogram and MS of the Absolute Configuration of C1 from *B. breve* 7017 and also an Overlaid Chromatogram with a Standard D-glucose (top-right)

The proton NMR spectrum of the C1-fraction was recorded for two different batches of material and the spectra compared to the NMR recorded for a starch standard (Fig 5.46).

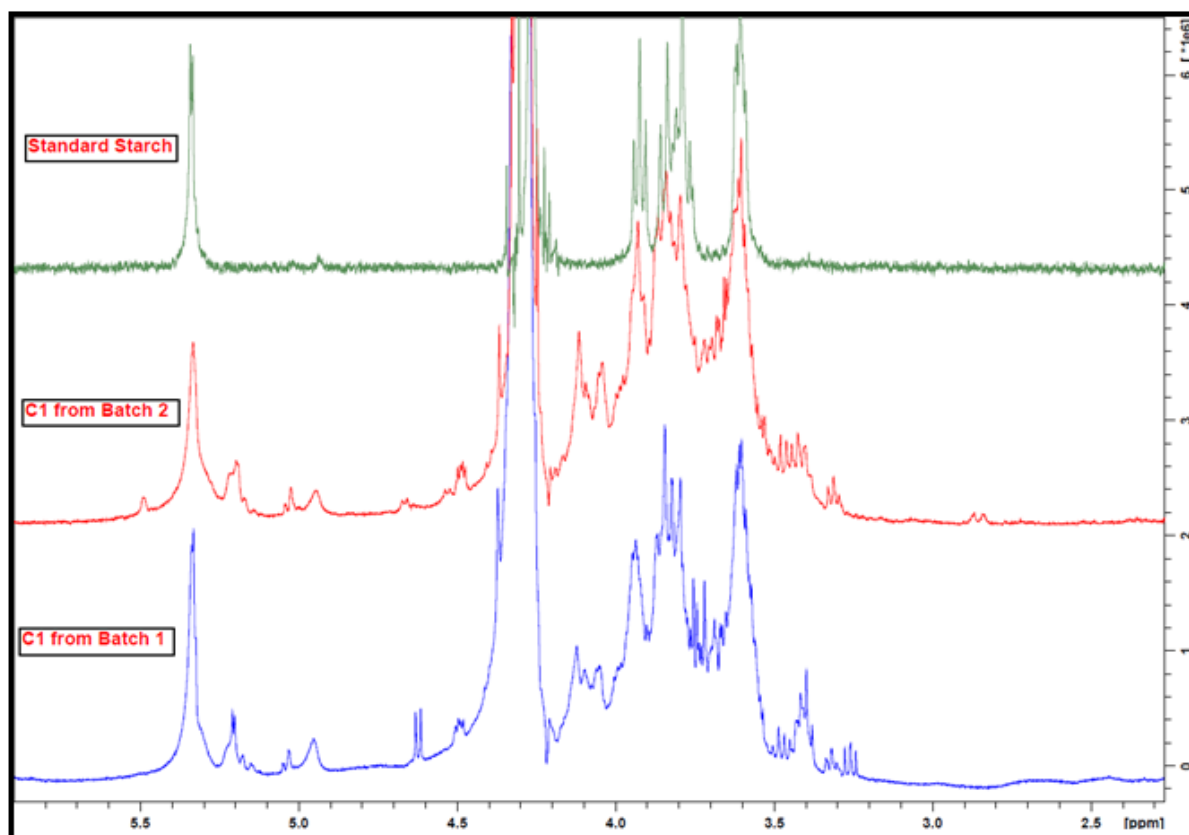


Figure 5.46. ¹H-NMR for the C1 from *B. breve* 7017 of Two Different Batches Compared with that of a Standard Starch.

It is clear that the main peaks present in the **C1**-fractions are the same as those in the starch spectrum (and the same as those observed for the **S1**-fractions). A number of additional small peaks were visible in the NMR spectrum and many are also observed for the **C2**-fraction (which will be seen in the sections that follows) suggesting that the fractionation process has not completely separated the different polysaccharides.

The purity and the molecular mass of the **C1**-samples was determined using SEC-MALLS coupled to refractive index (RI) and UV-detectors. A very broad peak corresponding to a medium molecular weight material eluted between 25-35 minutes (Fig. 5.47), a similar broad peak was observed in the refractive index trace and the asymmetric profile suggests that two different populations of material were present (Fig 5.48).

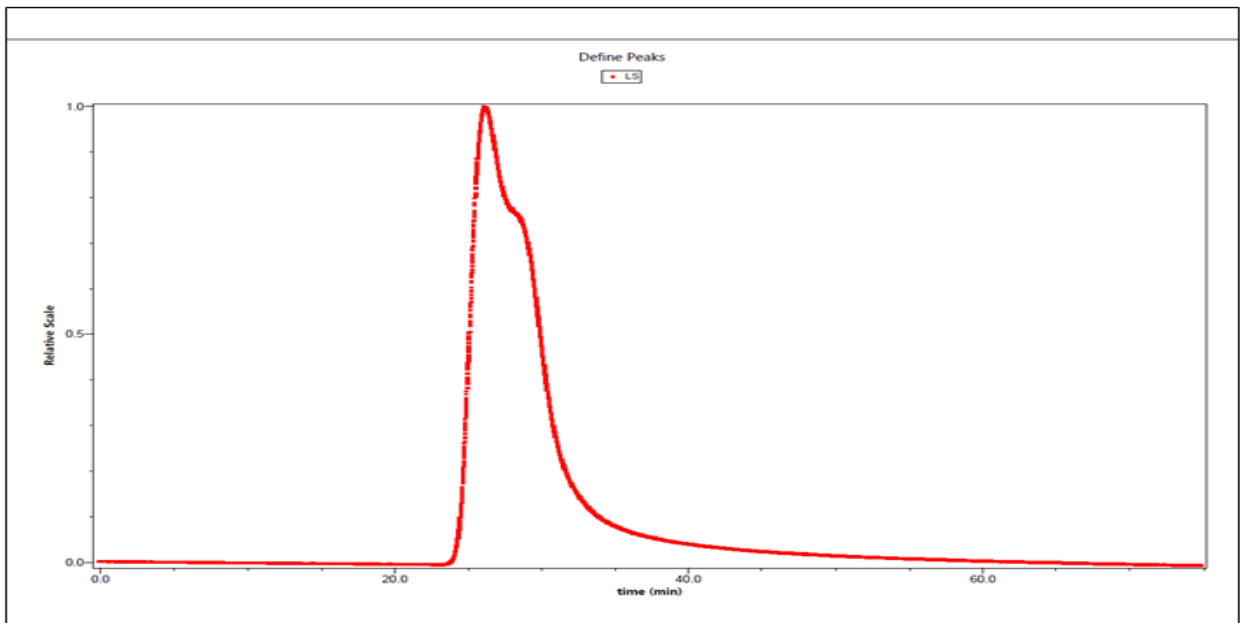


Figure 5.47. Light Scattering of the C1 from *B. breve* 7017

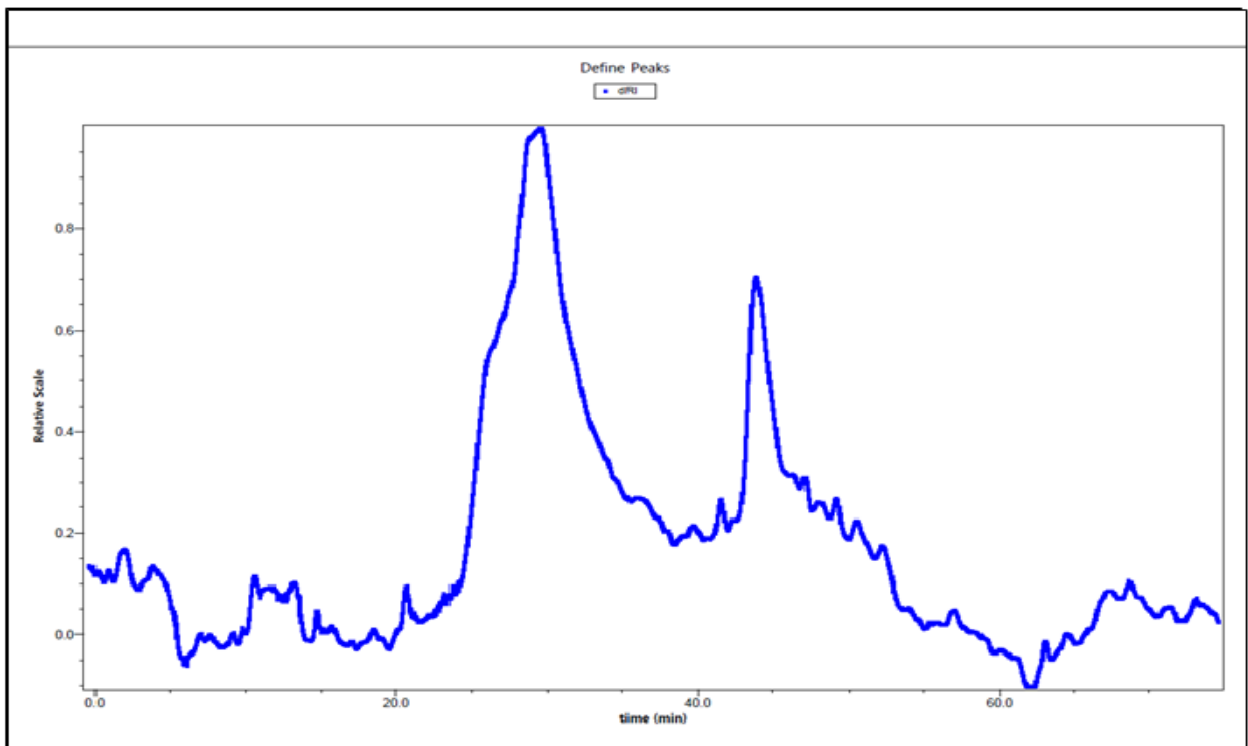


Figure 5.48. Refractive Index of the C1 from *B. breve* 7017

The weight average mass of the combined polysaccharide peaks was measured as 1.0×10^5 g/mol. The refractive index trace also contains a late eluting peak and it is likely that this is a small amount of protein that is present in the sample.

5.1.6. Characterisation of the Polysaccharides Present in the C2-fraction from *B. breve* 7017.

5.1.6.1. SEC-MALLS, Monomers, linkage and Absolute Configuration Analysis for the C2 from *B. breve* 7017

A number of different batches C2-fractions were collected, the amount of material was small (typically 20-25 mg from a 1L fermentation). Again, the composition of the material was examined using SEC-MALLS. Unfortunately, the light scattering detector did not show any significant peaks and only low molecular weight materials (50-5 kDa) were present. A late running peak was visible in both the RI and UV traces, which suggested that a mixture of polysaccharides and proteins was being recovered (Fig 5.49 and Fig 5.50). In the RI trace three distinct closely eluting peaks were visible (Fig 5.49); the final peak has a significant UV chromophore (Fig 5.50) and this is likely to be protein.

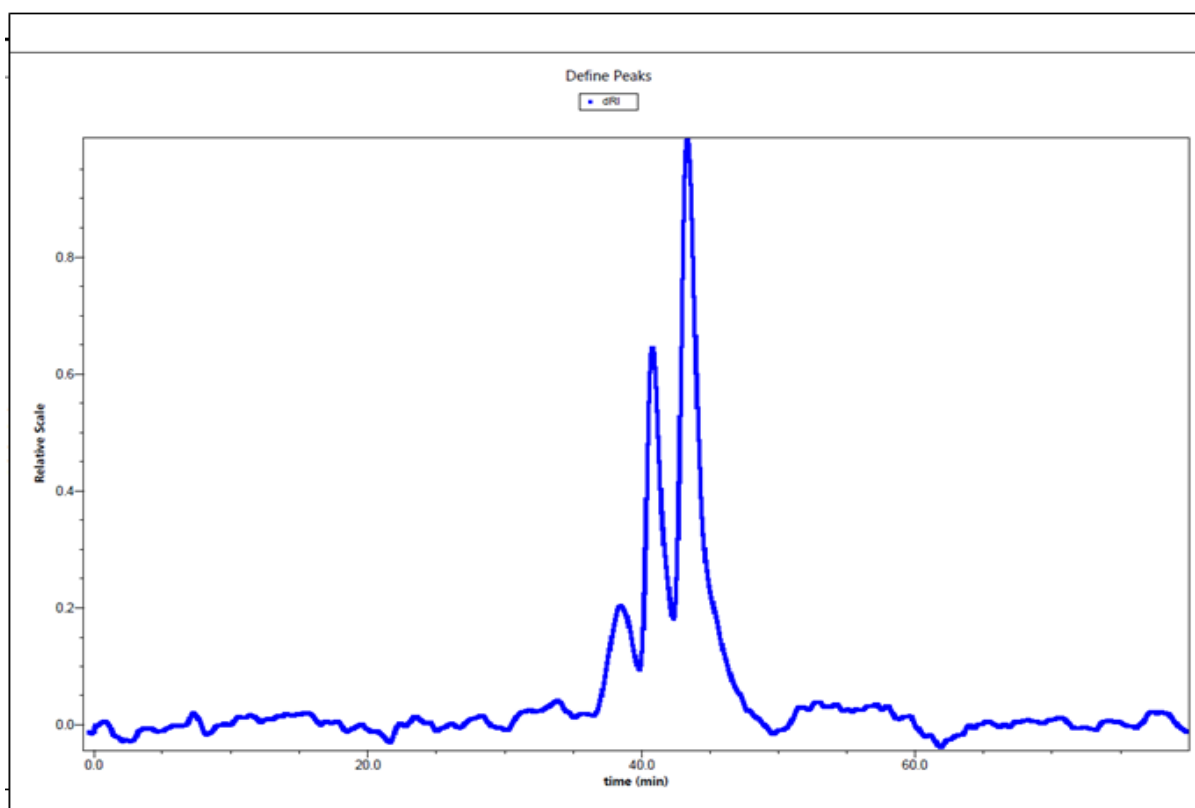


Figure 5.49. Refractive Index of C2 from *B. breve* 7017.

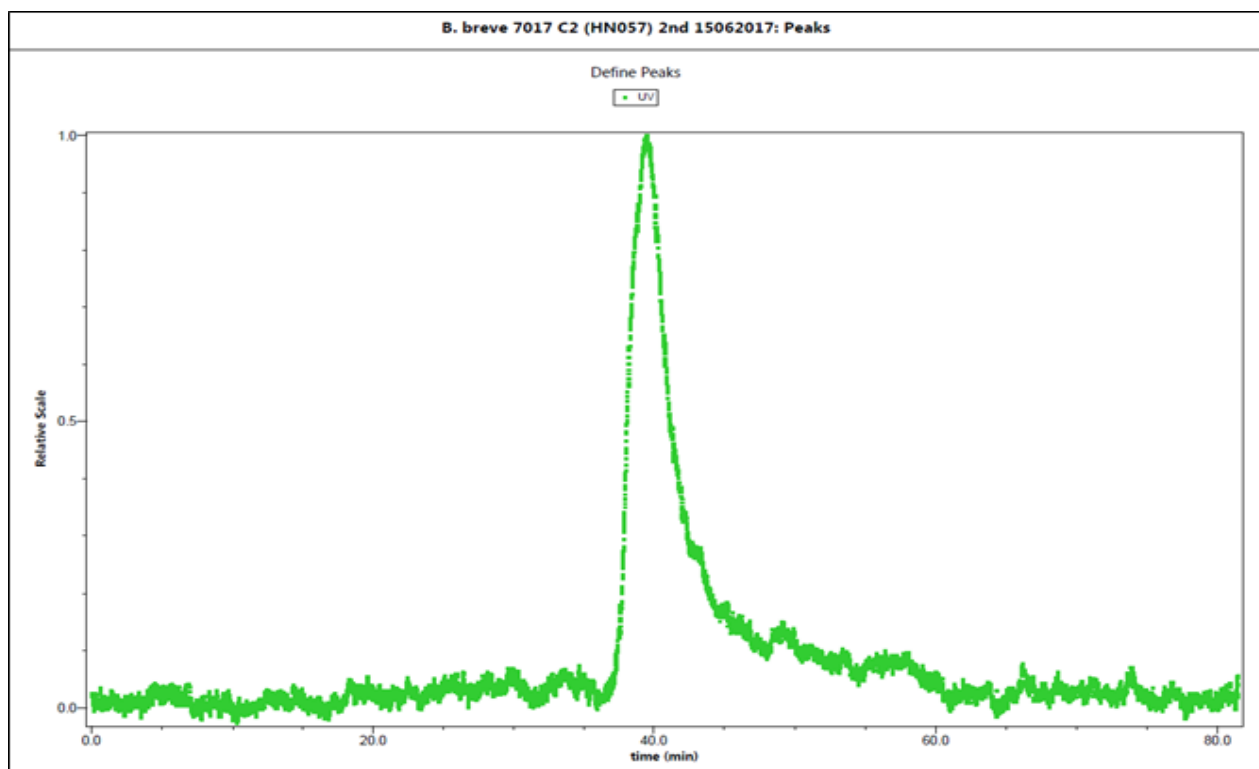


Figure 5.50. The UV of C2 from *B. breve* 7017

The other two peaks do not absorb UV and do not scatter light to any appreciable extent and are therefore likely to be low molecular weight polysaccharides.

$^1\text{H-NMR}$ spectra were recorded for the **C2**-fractions and the spectra (*Fig 5.51*) contain two sets of anomeric signals: at 5.1-5.0 ppm & at 4.55-4.45 ppm. The same $^1\text{H-NMR}$ anomeric profile was recorded for the **C2**-fractions recovered from the other *B. breve* strains and the *B. breve* 7107 EPS (-ve) mutant.

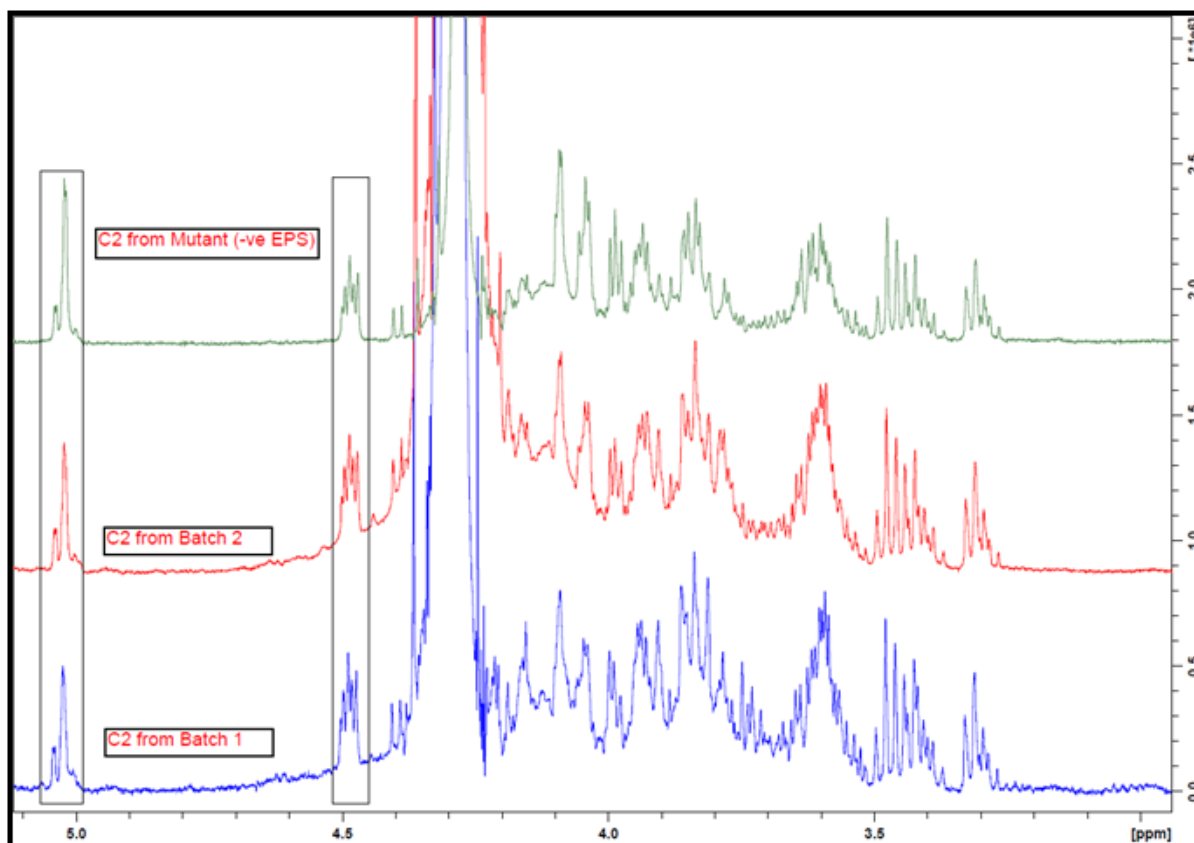


Figure 5.51. ^1H -NMR Spectra for the C2s from *B. breve* 7017 Wild Type (batches 1&2) and Mutant Type (-ve EPS)

In the different **C2**-fractions generated in this work, the relative integral areas for these two sets of protons differed from one batch to the next and, when taken into consideration in combination with the SEC-MALLS data, the results suggest that two different low molecular weight polysaccharides were being produced. A number of attempts were made to separate the different polysaccharides using preparative size exclusion chromatography and also using anion exchange chromatography but without success, so the components were analysed as a mixture.

Monosaccharide analysis identified that the **C2**-fractions contained galactose and glucose as confirmed by the HPAEC-PAD chromatography (*Fig 5.52*) and GC-MS (*Fig. 5.53*), however the ratio between the two varied between 1:1.05 and 1:2.0 for the different **C2**-fractions. The latter result is likely to be due to the fact that a small amount of glycogen is present and this has caused increased glucose levels in these fractions.

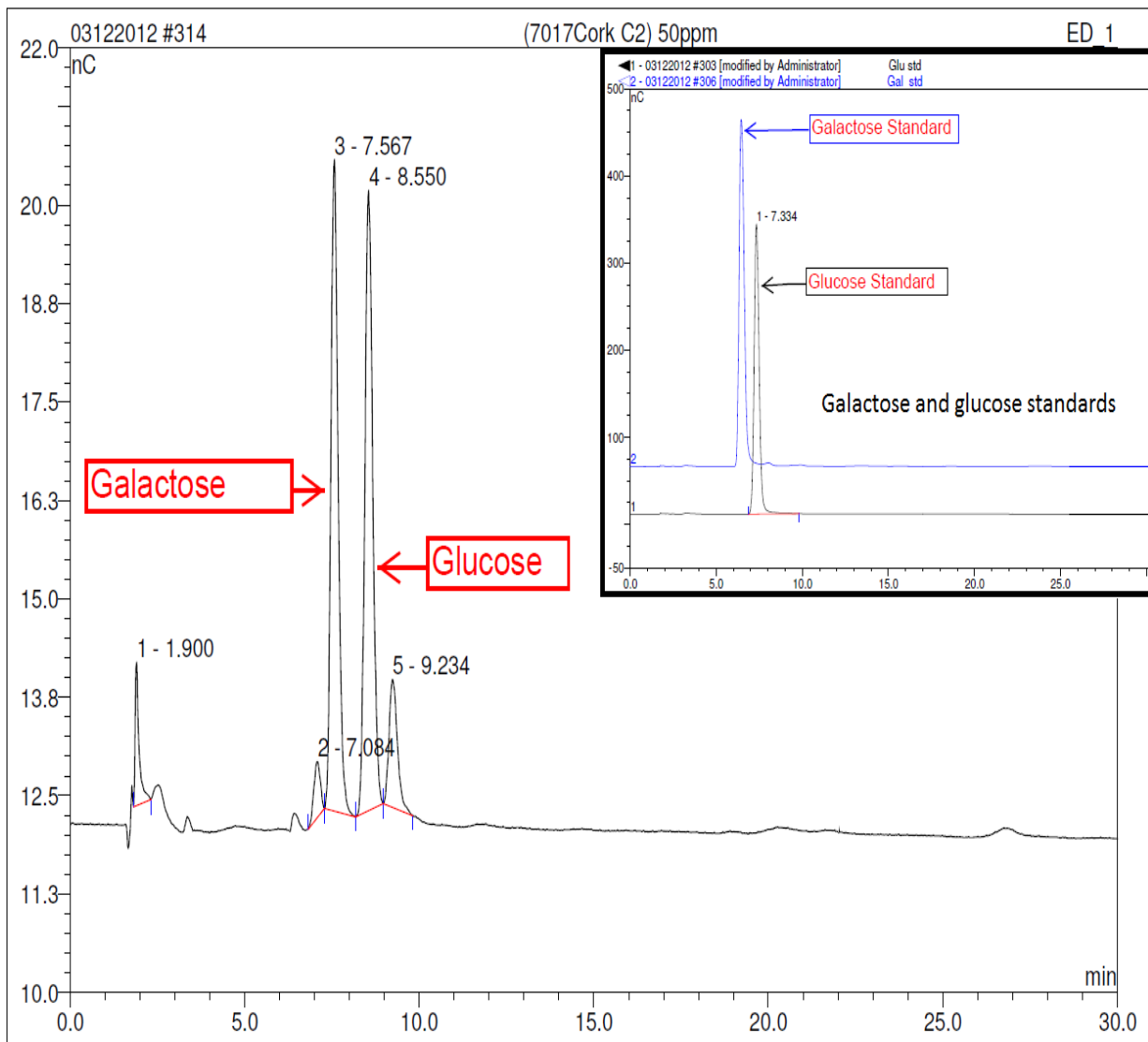


Figure 5.52. HPAEC-PAD Chromatography of C2 from *B. breve* 7017

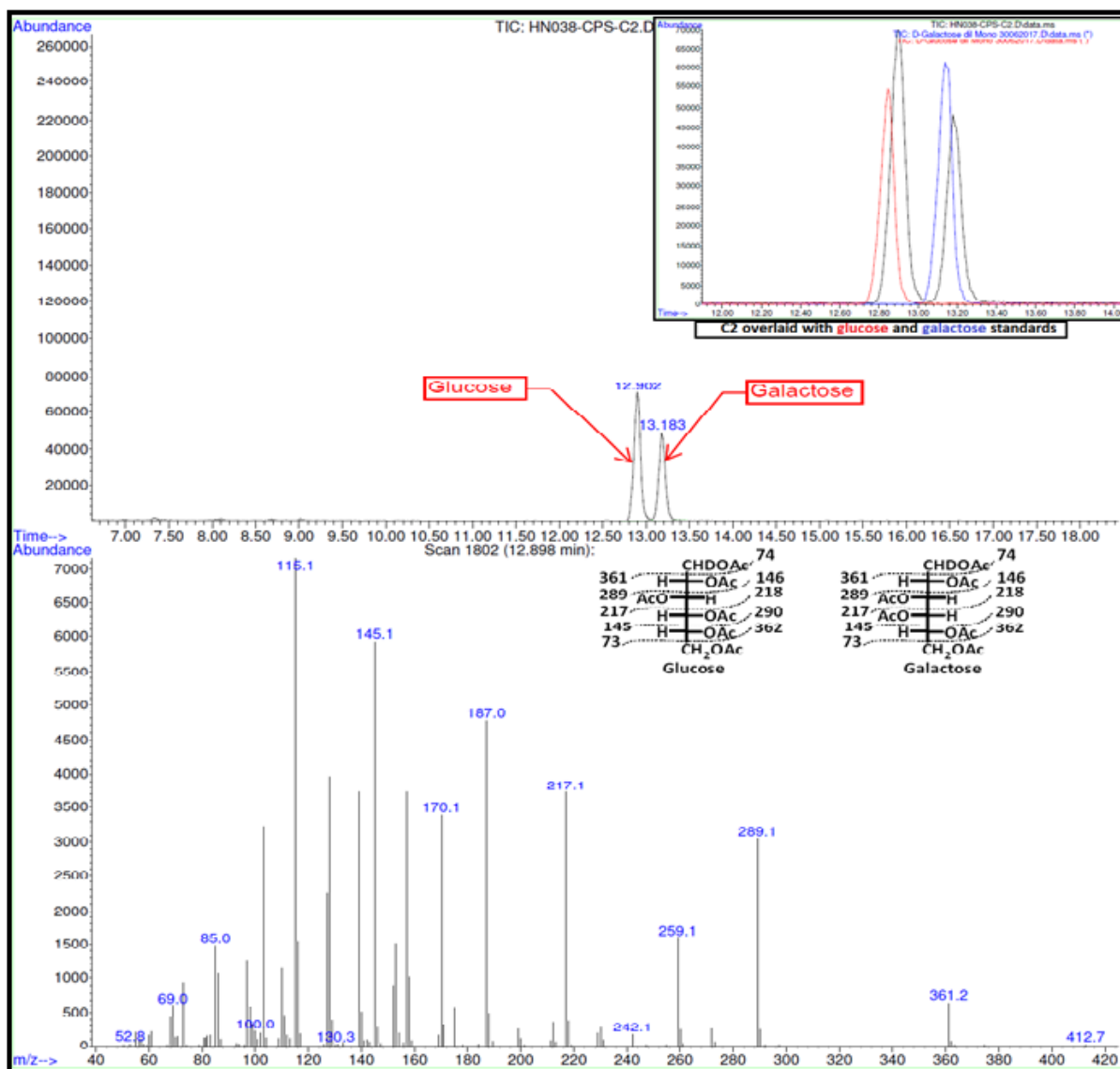


Figure 5.53. Chromatogram and Mass Spec for the Alditol Acetates of the Sugars obtained from the Monomer Analysis of C2 from *B. breve* 7017.

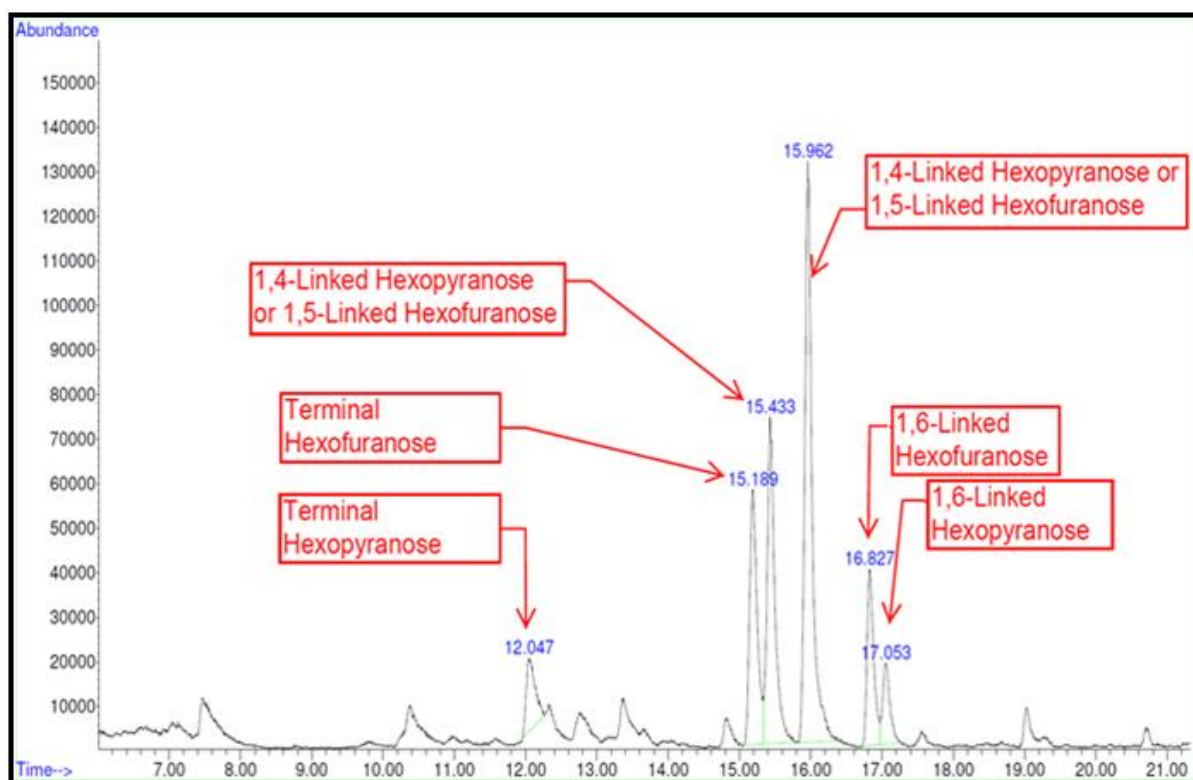


Figure 5.56. Chromatogram for the Methylated Alditol Acetates of the Sugars obtained from the Linkage Analysis of C2 from *B. breve* 7017.

Linkage analysis (Fig 5.56) identified the presence of six methylated alditol acetates including: a small peak for 1,5-di-*O*-acetyl-2,3,4,6-tetra-*O*-methylhexitol derived from a terminal hexopyranose (Fig 5.57); a peak for 1,4-di-*O*-acetyl-2,3,5,6-tetra-*O*-methylhexitol derived from a terminal hexofuranose (Fig 5.58); a peak for 1,4,5-tri-*O*-acetyl-2,3,6-tri-*O*-methylhexitol, which is from either a 1,4-linked-hexopyranose or a 1,5-linked-hexofuranose (Fig 5.59); a second peak for 1,4,5-tri-*O*-acetyl-2,3,6-tri-*O*-methylhexitol which is large and also consistent with either a 1,4-linked-hexopyranose or a 1,5-linked-hexofuranose (Fig 5.60); a peak for a 1,4,6-tri-*O*-acetyl-2,3,4-tri-*O*-methylhexitol which is from a 1,6-linked-hexofuranose (Fig 5.61) and finally a peak for 1,5,6-tri-*O*-acetyl-2,3,5-tri-*O*-methylhexitol which is derived from a 1,6-linked-hexopyranose (Fig 5.62). Despite the observation of small amounts of terminal sugars, no branching points were detected in the linkage analysis which suggests that only linear polysaccharide chains are present. The mass specs of these six methylated alditol acetates are as follows;

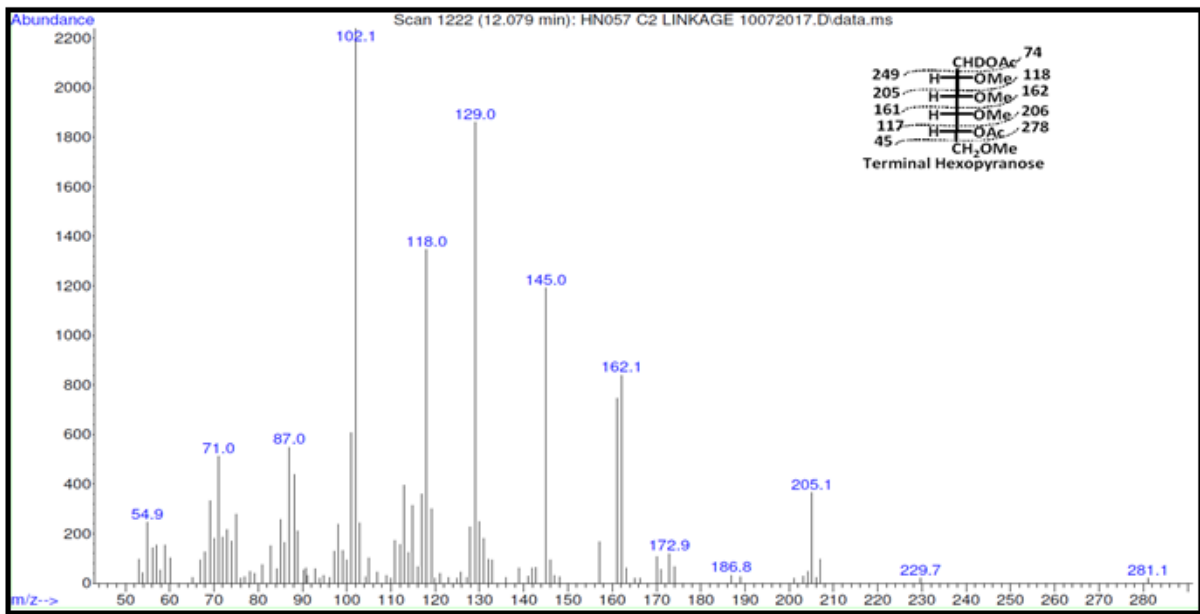


Figure 5.57. Mass Spec for 1,5-di-*O*-acetyl-2,3,4,6-tetra-*O*-methylhexitol (Terminal Hexopyranose)

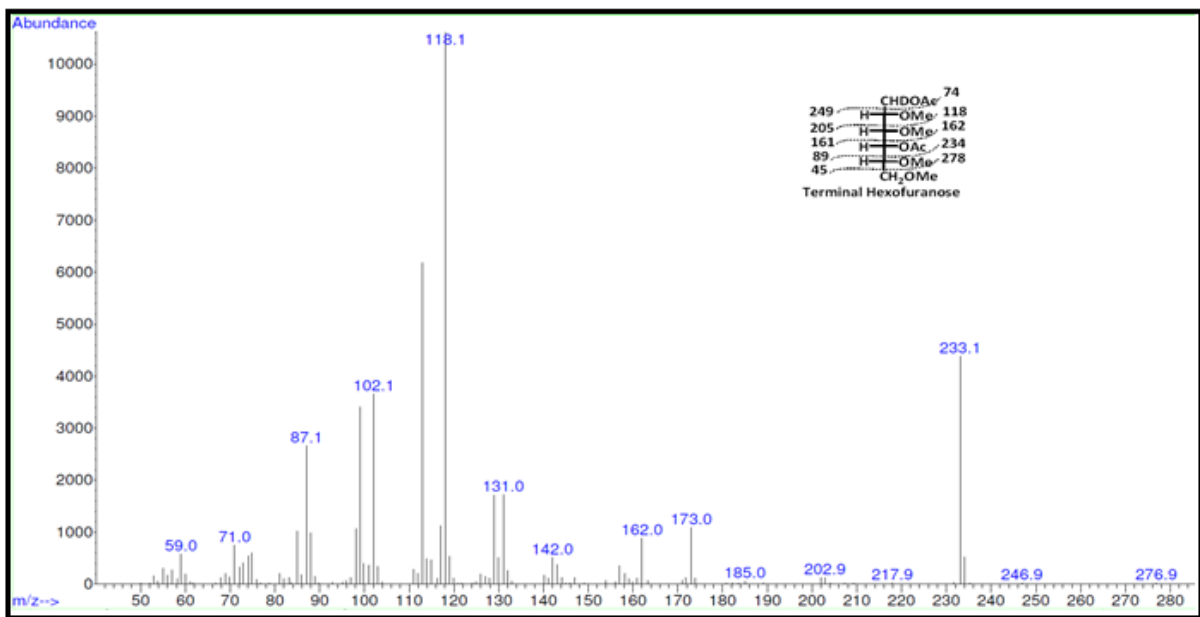


Figure 5.58. Mass Spec for 1,4-di-*O*-acetyl-2,3,5,6-tetra-*O*-methylhexitol (Terminal Hexofuranose)

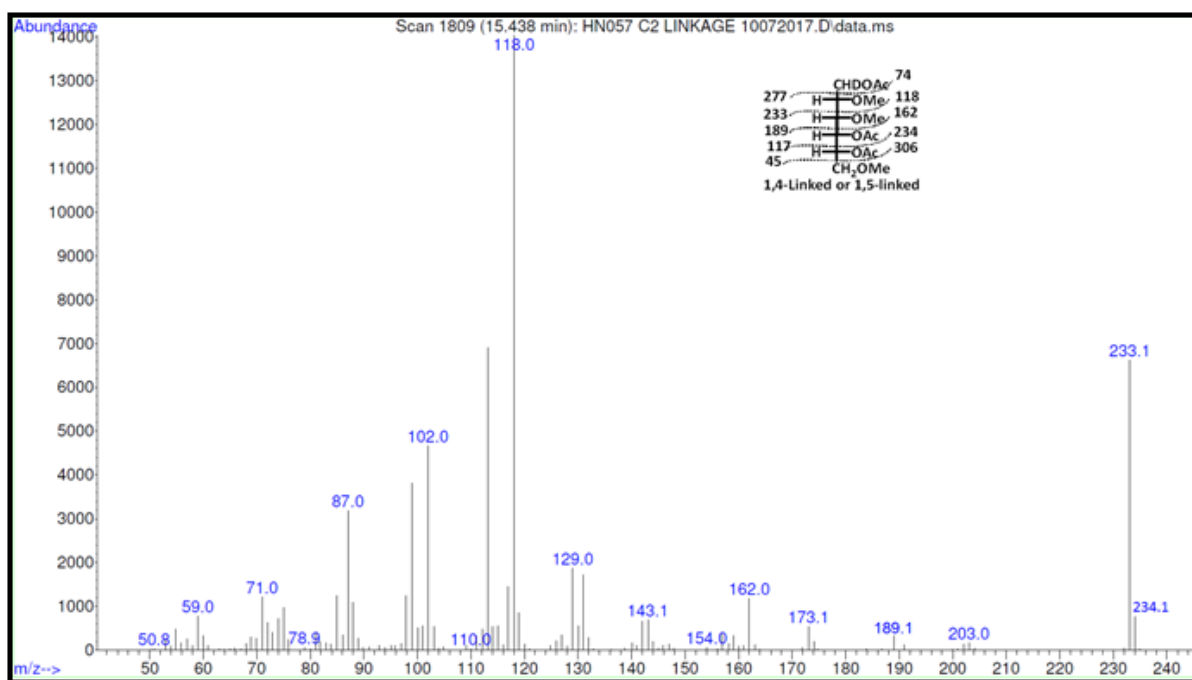


Figure 5.59. Mass Spec for 1,4,5-tri-*O*-acetyl-2,3,6-tri-*O*-methylhexitol (1,4-linked-Hexopyranose or a 1,5-linked-hexofuranose)

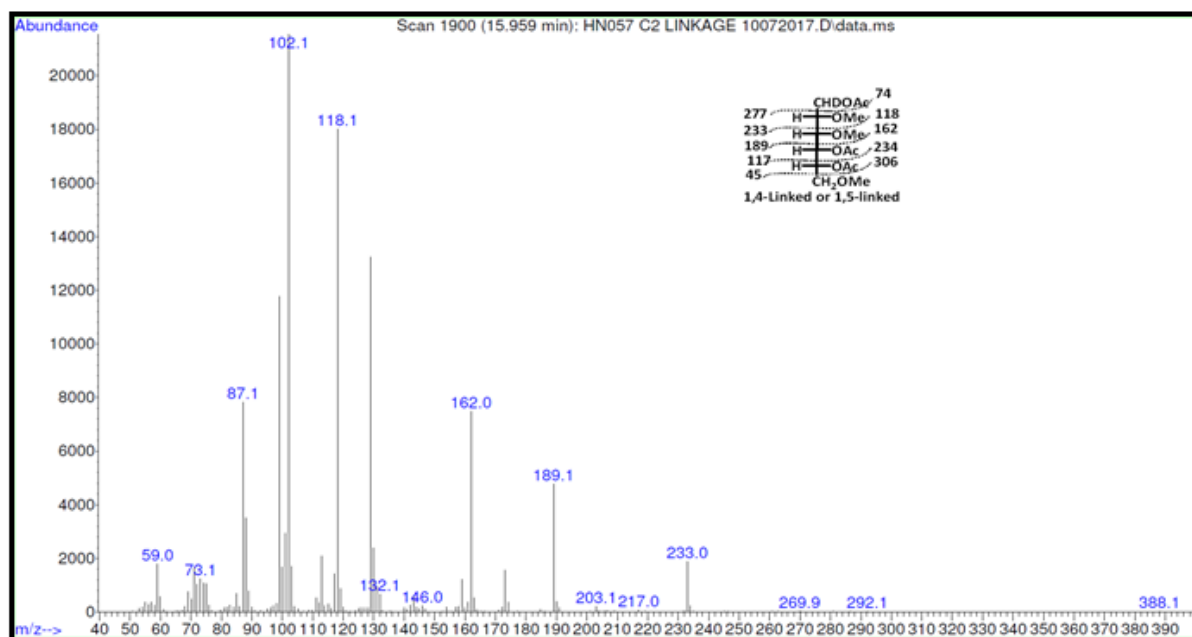


Figure 5.60. Mass Spec for the second 1,4,5-tri-*O*-acetyl-2,3,6-tri-*O*-methylhexitol (1,4-linked-hexopyranose or a 1,5-linked-hexofuranose)

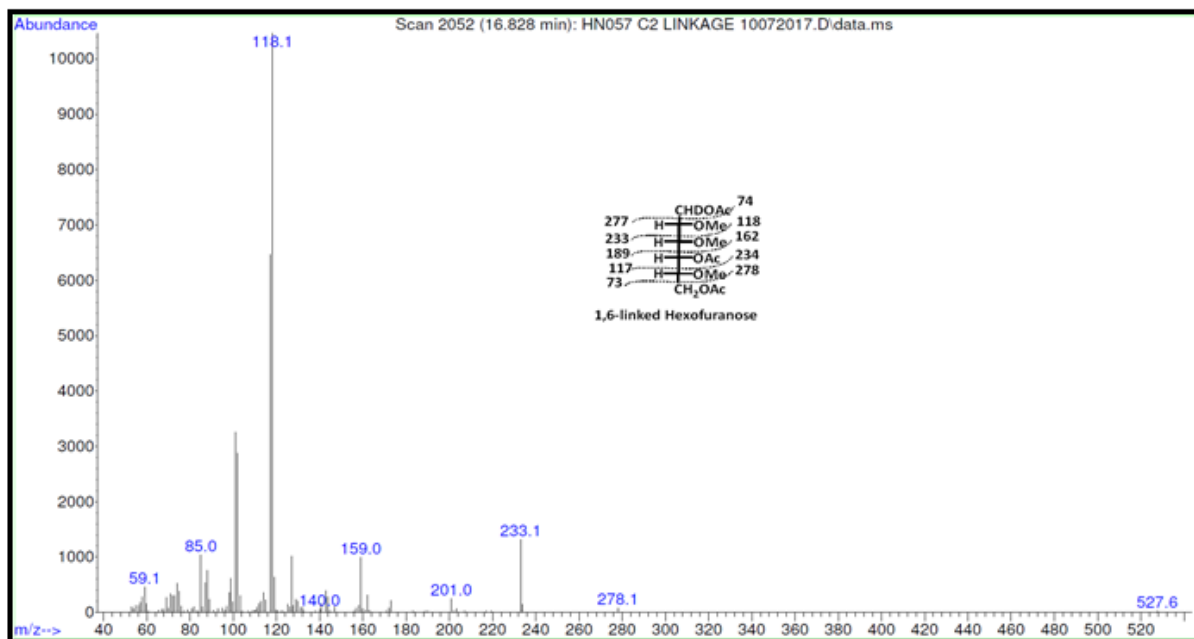


Figure 5.61. Mass Spec for 1,5,6-tri-*O*-acetyl-2,3,4-tri-*O*-methylhexitol (1,6-linked-hexofuranose)

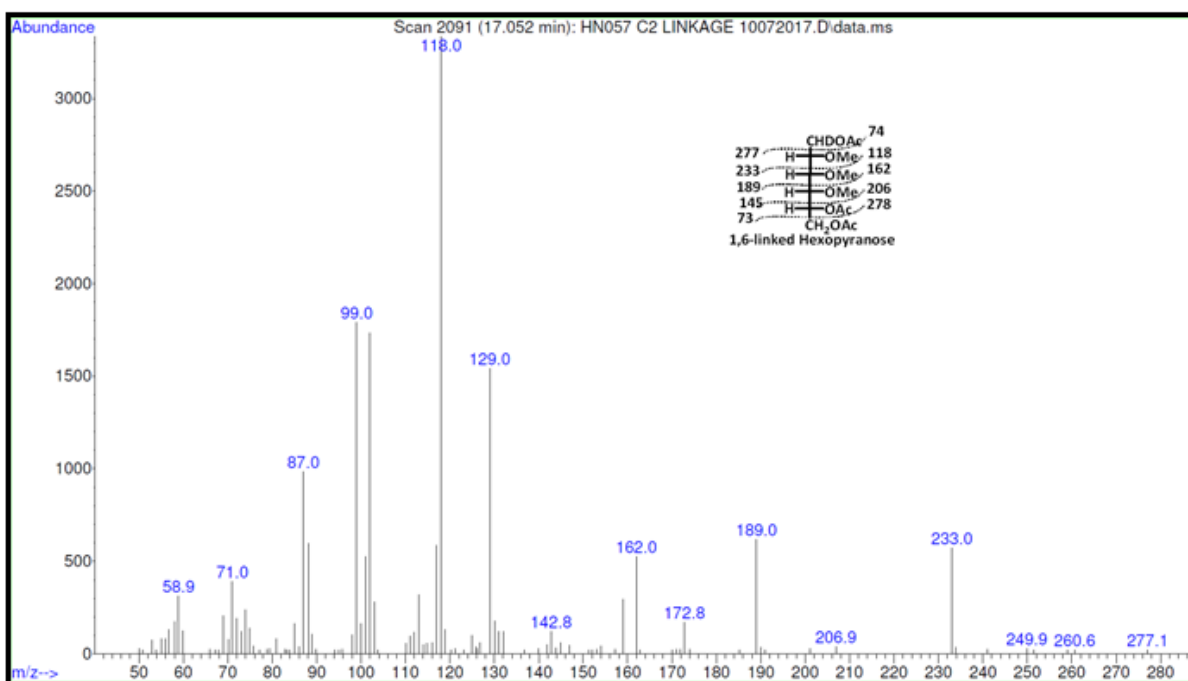


Figure 5.62. Mass Spec for 1,4,6-tri-*O*-acetyl-2,3,5-tri-*O*-methylhexitol (1,6-linked-hexopyranose)

Absolute configuration analysis confirmed that the polysaccharides were composed of D-galactose and D-glucose (Fig 5.63).

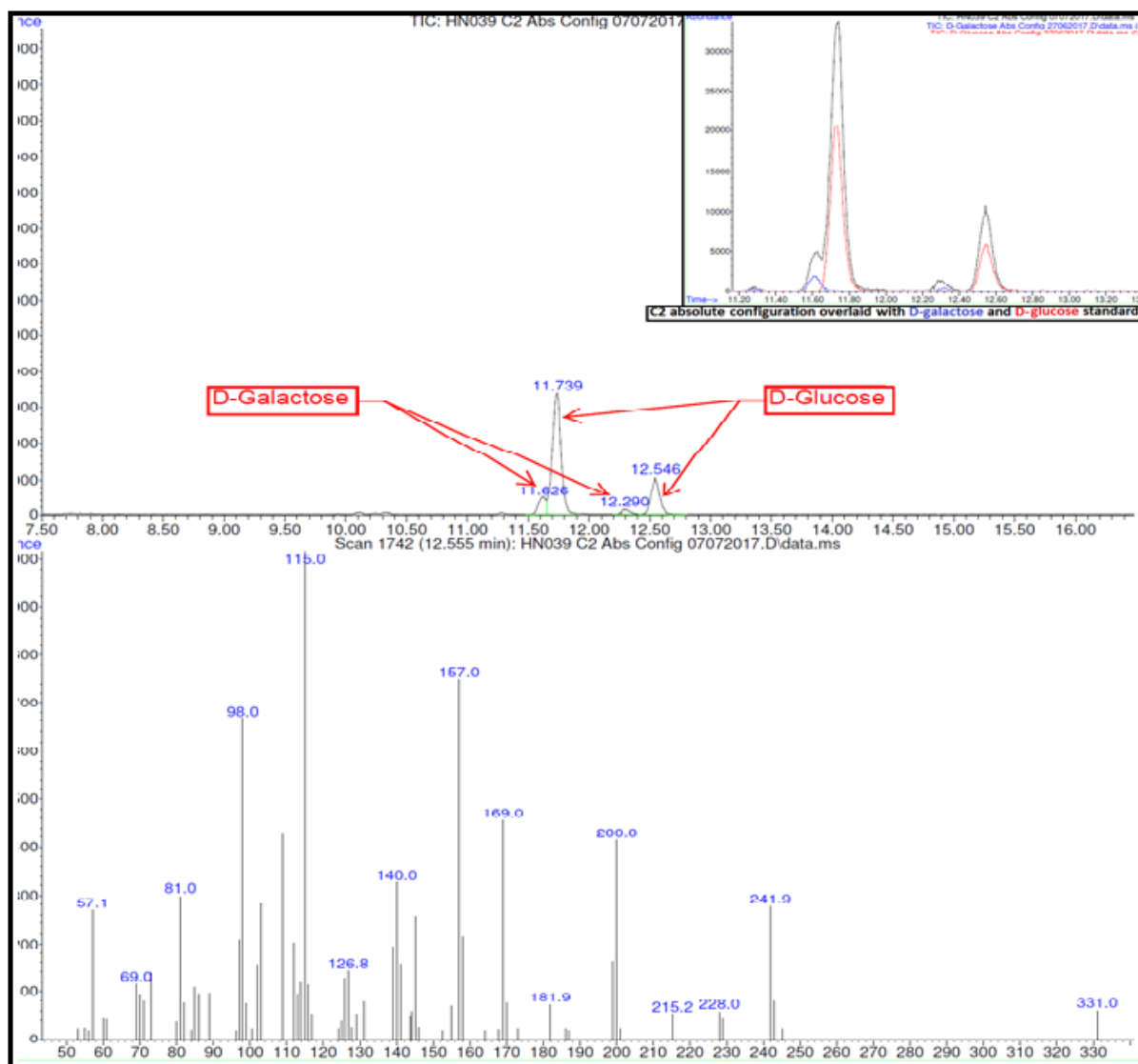


Figure 5.63. Chromatogram and MS of the Absolute Configuration of C1 from *B. breve* 7017 and an Overlaid Chromatogram with a standard D-glucose (top-right)

5.1.6.2. Use of 1D- and 2D-NMR to Determine the Structures of the Polysaccharides present in the C2-fraction from *B. breve* 7017.

A series of 2D-NMR spectra were recorded for the C2-fractions so as to uncover more information about the structure of the recovered material (the same set of spectra as were recorded for the S2-fractions-see discussion above). On the ^1H - ^{13}C HSQC spectrum (Fig 5.64) the anomeric proton signal observed at 5.06 ppm is attached to a carbon resonating at 108 ppm, which is characteristic of a β -hexofuranose. A second set of anomeric proton resonances

appeared as a series of overlapping doublets centred at 4.5 ppm (Fig 5.64 F2-axis, 4.55-4.45 ppm).

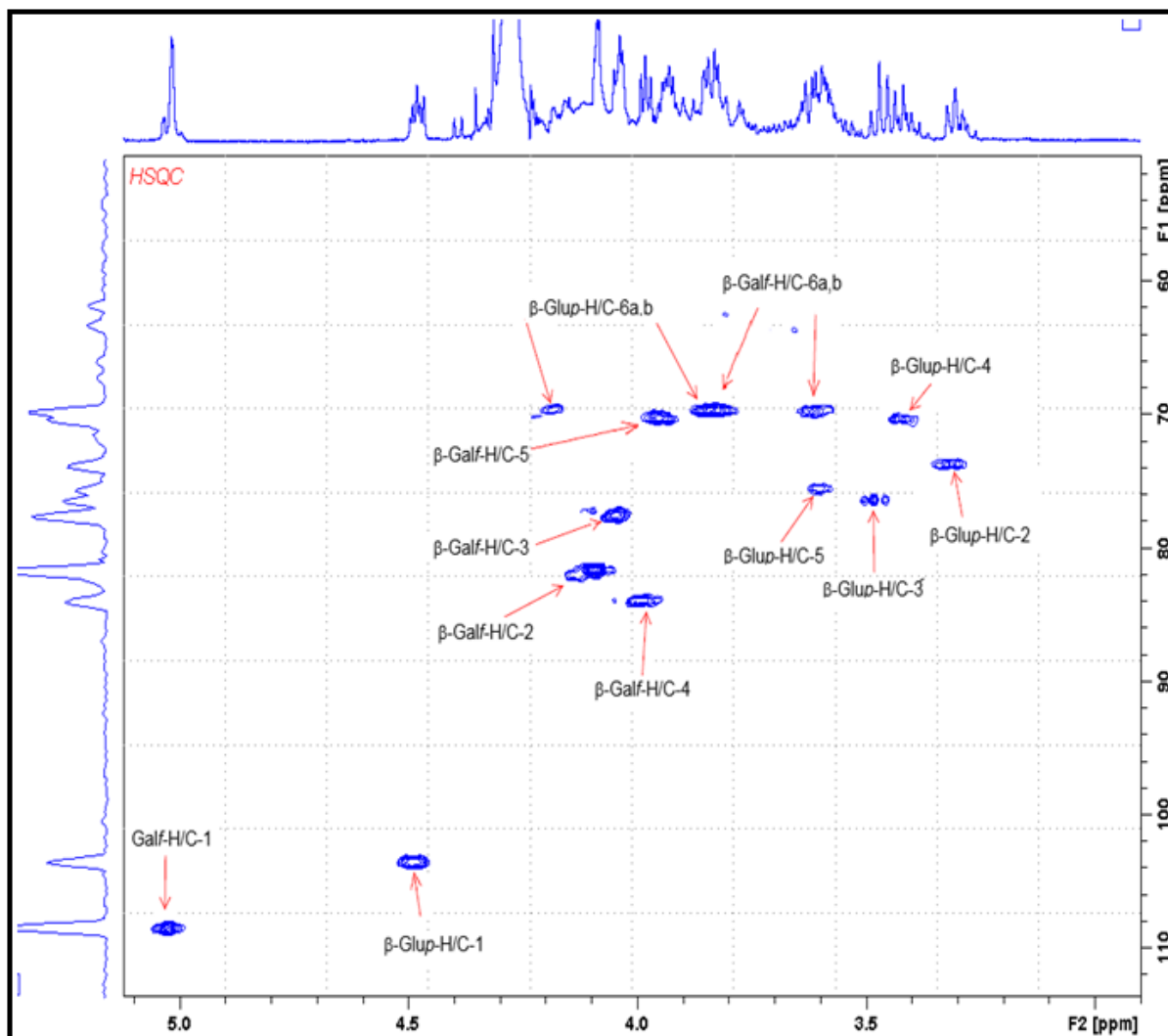


Figure 5.64. ^1H - ^{13}C HSQC Spectrum for C2 of *B. breve* 7017

As was the case for the **S2**-fractions, the location of H1 through to H6 for these two sets of splitting patterns was determined using a COSY (Fig 5.65) and TOCSY spectra (Fig 5.66): the chemical shifts are listed in Table 5.5 and the identity of the hydrogens for the most prominent resonances are highlighted on the HSQC spectrum (Fig 5.64).

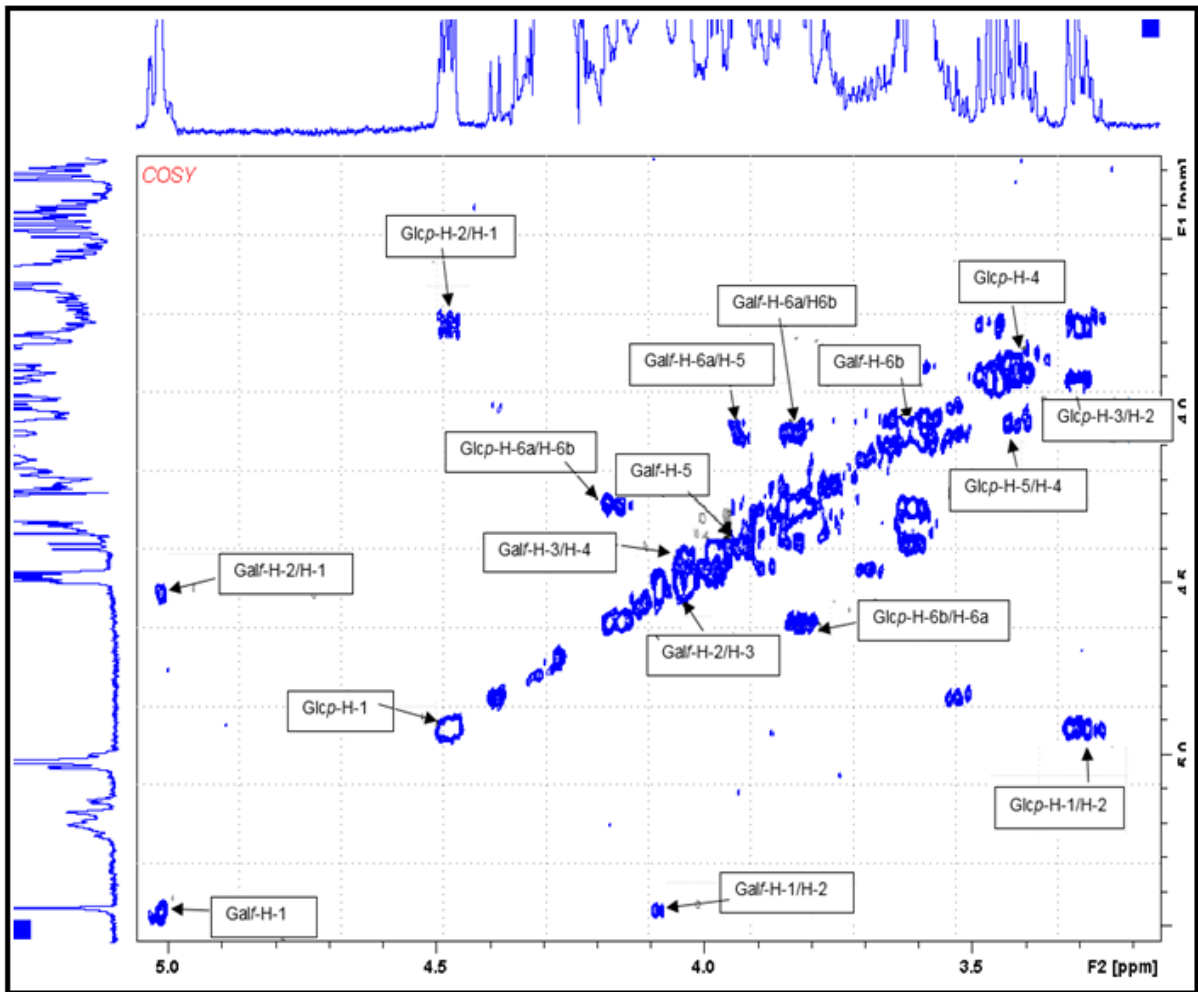


Figure 5.65. ¹H-¹H-COSY Spectrum for C2 of *B. breve* 7017

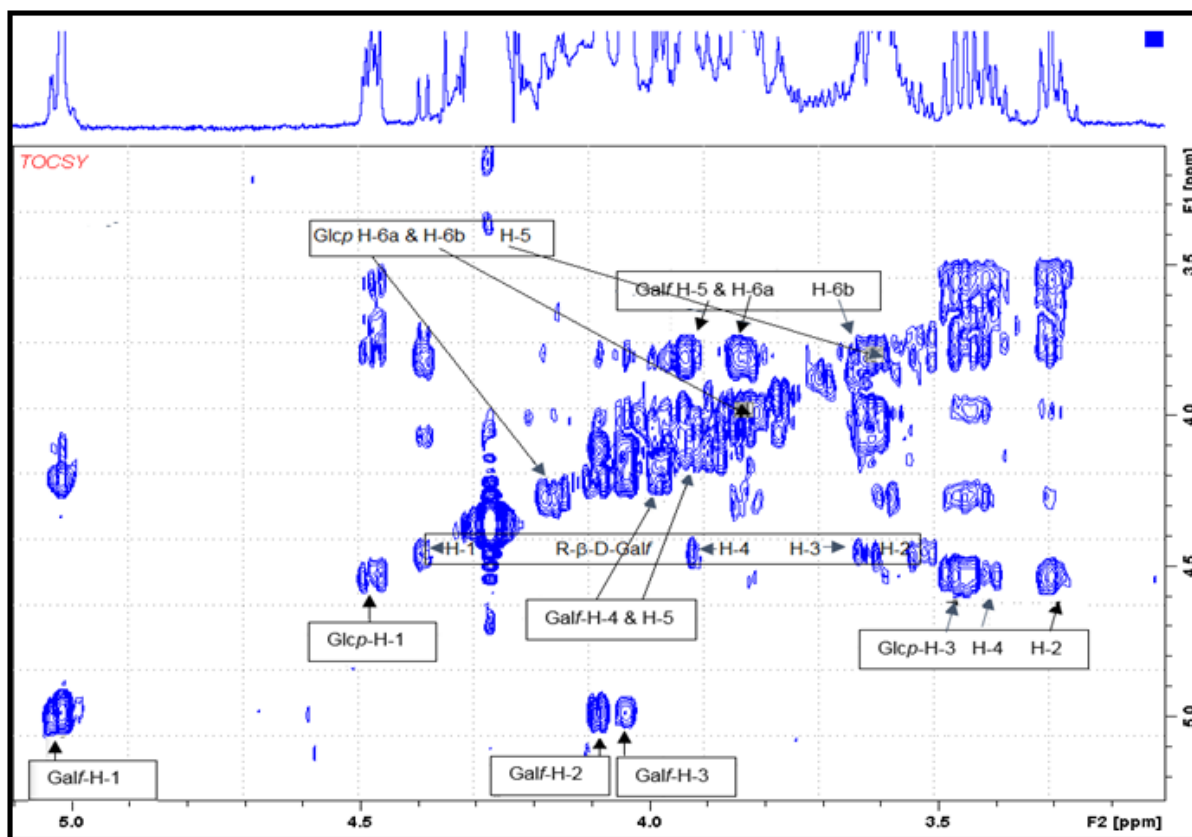


Figure 5.66. ^1H - ^1H -TOCSY Spectrum for C2 of *B. breve* 7017

The location of the corresponding carbons, C-1 to C-6, was identified from inspection of a combination of a HSQC spectrum (Fig 5.48) and a HSQC-TOCSY spectrum.

Table 5.5: Chemical Shifts of Monosaccharide Resonances

Chemical shifts of monosaccharide resonances (ppm)						
Residue	C-1 H-1	C-2 H-2	C-3 H-3	C-4 H-4	C-5 H-5	C-6 H-6
-6- β -D-Galp-1	108.4 5.04	81.5 4.11	77.4 4.06	83.8 4.00	70.1 3.90	69.7 3.85 & 3.62
Reference -6- β -D-Galp-1	109.0 5.05	82.1 4.12	78.0 4.07	84.5 4.01	70.8 3.97	70.2 3.86 & 3.65
-6- β -D-Glcp-1	103.4 4.49	73.5 3.32	76.2 3.48	70.3 3.44	75.4 3.61	69.4 4.19 & 3.86
Reference -6- β -D-Glcp-1	104.2	74.2	76.8	70.6	76.1	70.0
R- β -D-Galp-1- Gro	103.6 4.40	71.7 3.54	69.7 3.63	70.4 3.94	ND ND	ND ND

For the hexofuranose, the chemical shifts for each of the carbons and hydrogens are very close to those that have previously been reported for a β -D-(1 \rightarrow 6)-galactofuranan³⁰⁹. For the second set of resonances, the chemical shifts for each of the carbons are very close to those that have previously been reported for a β -D-(1 \rightarrow 6)-glucan³¹⁰.

5.2. Discussion

The common procedures employed in extracting the EPS and CPS are time consuming and usually recover a mixture of very small complex amounts of polysaccharides⁴⁹. Leivers *et al* (2011)¹¹⁹ confirmed this where they reported low yields of polysaccharides recovered from *Bifidobacterium animalis* subsp. *lactis* IPLA-R1 with their NMR spectra and SEC-MALLS traces indicating the recovered polysaccharide to be a mixture. The original aim of this work was to isolate and characterise the EPS produced by *B. breve* 7017 and the isolation procedures have been adapted from those normally used to extract EPS material from broth fermentations or from cultures grown on plates. In the original experiments performed with *B. animalis* by Alhudhud *et al* (2014)²²⁶, at the end of a batch fermentation the broth was centrifuged and attempts were made to isolate EPS from the supernatant, unfortunately, this resulted in the recovery²²⁶ of small amounts of complex mixtures of polysaccharides.

The fractionation of bacterial polysaccharides by selective precipitation of components with ethanol has previously been reported³¹¹ and the application of the technique, in the studies described above, gave four different fractions **S1**, **S2**, **C1** and **C2** which were amenable to analysis. The various NMR spectra recorded for both the **S1** and **C1**-fractions confirmed that the material was a bacterial glycogen with a medium molecular weight. Whilst the scientific literature contains a significant number of references to bacteria that can produce glycogen³¹², this is the first report of the isolation of a soluble glycogen from a bifidobacteria. Previous reports of bacterial glycogen, including an insoluble glycogen-like material isolated from *B. bifidum* ssp. *Pennsylvanicum*³¹³, have been identified to be an intracellular storage polysaccharide and therefore the presence of glycogen in the supernatant of this present research is likely to be as a result of a significant amount of cell lysis occurring either in the fermentation or during the extraction process.

5.2.1. The Identity of the Material Extracted from the Cells from *B. breve* 7017.

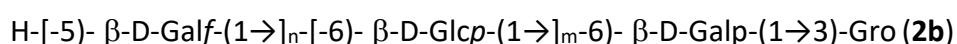
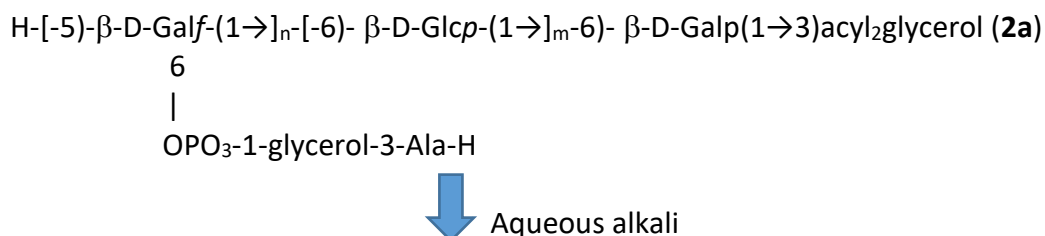
Analysis of the NMR of the **C2**-fraction identified the presence of two homoglycans: a β -D-(1 \rightarrow 6)-galactofuranan and a β -D-(1 \rightarrow 6)-glucan. One feature of the NMR spectra recorded for

all **C2**-fractions that remains to be explained is why a series of overlapping doublets are observed for the anomeric proton of the β -glucan. Variable decoration of the backbone would account for the multiple doublets, but this possibility can be ruled out by the linkage analysis which excludes any branching and by our failure to observe substituents, esters or ethers etc., in the NMR. In the linkage analysis, the majority of the peaks (eluting in the order :1, 2, 5 and 6 of Fig 5.56) are consistent with the mixture being composed of a β -D-(1 \rightarrow 6)-galactofuranan and a β -D-(1 \rightarrow 6)-glucan. The ratio of the peak areas for the terminal hexopyranose (peak 1) with that for the 1,6-linked hexopyranose (peak 6) (Fig 5.56) suggests that the β -D-(1 \rightarrow 6)-glucan has a low molecular weight (this assumes that the small amount of residual glycogen (responsible for peak 4) has a high molecular weight similar to that observed in the **C1**-fraction). In contrast, the ratio of the peak areas for the terminal hexofuranose (peak 2) with that for the 1,6-linked hexofuranose (peak 5) suggests that the (1 \rightarrow 6)-galactofuranan has a higher molecular weight. If the β -D-(1 \rightarrow 6)-glucan does have a relatively low DP then this might explain why overlapping doublets are observed for the anomeric proton resonances: the proximity to the reducing and non-reducing termini determining the absolute chemical shifts of the anomeric protons. Finally, it should be noted that the third peak observed in the monomer analysis did not correlate with either of the structures deduced from the NMR spectra and it's not clear why this is present.

A second question which needs addressing is why neutral low molecular weight polysaccharides should be found associated with the cells and are not released as EPSs. The fact that the *B. breve* 7017 EPS (-ve) mutant which lacks the gene coding for the priming glycosyl transferase which is needed for EPS synthesis is capable of producing the same material suggests that the polysaccharides are not EPSs that are tightly associated with the cell surface and are being retained with the cells after centrifugation. An indication about where the polysaccharides may come from can be found in work published by Den Camp *et al* (1984)^{314, 315} who reported that *B. bifidum* produces an intimate mixture of two lipoteichoic acids: one with a β -D-(1 \rightarrow 5)-galactofuranan backbone (**1a**) and the second with a β -D-(1 \rightarrow 6)-glucan backbone (**1b**).



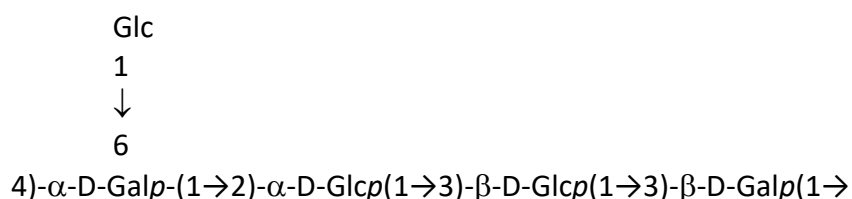
However, in later work, Fischer *et al* (1987)^{316, 317} suggested that *B. bifidum* actually produces a single lipoteichoic-acid-like macromolecule (**2a**) which in solution with aqueous alkali undergoes hydrolysis to generate the linear two block polysaccharide (**2b**).



The highly alkaline pH used in the extraction experiments reported here would be expected to rapidly hydrolyse phosphate linkages and to remove lipid fatty acids. It is possible that the low molecular weight polysaccharides isolated in the **C2**-fraction may originally have been present as fragments of either a lipoteichoic-acid-like molecule or as two lipoteichoic acids which have been released during the extraction procedure. If this was the case, then the NMR spectra would be expected to include signals derived from either glycerol or a 1,6-linked-galactopyranosylglycerol located at the reducing terminus. On closer inspection of the proton spectrum there is an additional low intensity anomeric resonance at 4.40 ppm which is potentially a reducing end 6-linked hexose in the β -configuration³¹⁸. Using a combination of the COSY and TOCSY spectra it was possible to track the scalar coupling but only from H-1 through to H-4 (typical of a galactose residue); the corresponding carbons were obtained from the HSQC spectrum. The position of these C-1 & H-1 resonances perfectly match those published for 1-*O*- β -galactopyranosylglycerol³¹⁹. Unfortunately, because of signal crowding in the 3.5-3.9 ppm region it wasn't possible to locate any low intensity glycerol proton resonances. Despite many attempts, the low amount of available material and the quality of the spectra means that it wasn't possible to establish by NMR any link between the glucan and galactofuranan fragments. The most convincing evidence for the presence of two separate low molecular weight polysaccharides is the observation of separate peaks in the SEC-MALLS chromatographs.

5.2.2. Identity of the Material Excreted into the Media by *B. Breve* 7017

As was stated above, the material in the **S1**-fractions is clearly a soluble bacterial glycogen and it is likely that this has been released during lysis of cells during the fermentation. In contrast, the material in the **S2**-fractions has all the characteristics of an EPS and it is found only in the supernatant and has a high molecular weight. The repeat unit structure is very similar to that of cell wall material isolated from the cell walls of *B. breve* YIT4010 which has the same linear chain but without the acetyl groups but which also has a glucose residue bonded to the 6-position of the 1,4-linked galactose³²⁰:



In their publication, the team from Yakult reported the anomeric proton for the terminal glucose in the side chain as having a resonance at 4.98 ppm and the anomeric carbon at 98.5 ppm, this signal was not visible in any of the batches of S2-fractions³²⁰.

When the carbohydrate content of S2 (for *B. breve* 7017 JCM batch 2) was measured using the Dubois test, the amount of carbohydrate calculated was 453.87 $\mu\text{g}/\text{mL}$ which was below expectation hence confirming the works of Tuiner *et al* (1999)²⁵⁹ who had reported low carbohydrate content from a purified exopolysaccharide isolate from *Lactococcus lactis* subsp *cremoris*.

5.3. Conclusion

In this research, the outcome from the common extraction of EPS from various strains of *Bifidobacteria species* results in multiple polysaccharide recovery. It has been demonstrated that the *B. breve* strains are capable of producing multiple polysaccharides. The chromatographic and NMR spectroscopic method used here confirmed the isolated polysaccharides to be a complex mixture of materials. This complexity was confirmed from the different results obtained analysing the S1, S2, C1 and C2. The isolation of bacterial glycogen in both the C1 and S1 fractions suggests that there is considerable lysis during the thirty-six hours fermentation which resulted to producing a bacterial glycogen. The β -glucan and β -galactofuranan found in the C2-fractions are likely to be derived from the hydrolysis of phosphate linkages in cell wall associated lipoteichoic acids which is catalysed by the sodium

hydroxide used in the extraction process and these material are likely close in structure to the polysaccharides that have previously been recovered from *B. bifidum* subspecies *pennsylvanicum* reported by Fischer *et al* (1987)²⁹⁹. In this work, isolating the three homoglycans brings about the importance of identifying the different components which are found in the glycan mixture known to be responsible for their biological activity. Finally, the S2-material is a novel exopolysaccharide, which is decorated with acetyl groups and a labile C7-fragment.

Chapter 6

6. Overall Conclusion and Future Work

For all the probiotic bacteria under study, their isolated EPSs and CPS were analysed using both NMR and wet chemical analysis.

In this study, culturing the *L. paracasei* DG in both the MRS and HBM broths was suitable for the production and extraction of its pure surface polysaccharides (CPS and EPS) as has been with other species. These extracted surface polysaccharides were seen to have the same ¹H-NMR profiles but only differed in the lactic acid signal that was present on the EPS profile which didn't affect the determination of the structure since it was removed by the purification process (dialysis). After purification, the chromatographic methods and NMR spectroscopy used to characterise the repeating units of this surface polysaccharides of *L. paracasei* DG showed the structure to be novel when compared with those previously studied of the *Lactobacillus casei* group. The CPS and EPS for the *L. paracasei* DG were similar in structure and was seen to be a novel rich rhamnose heteropolysaccharide made up of six monosaccharides in their repeat units which were rhamnose, galactose and *N*-acetylgalactosamine in the ratio 4:1:1. In addition, this structure published here is also seen to differ from other characterised EPS structures from a range of LAB. With the presence of the rhamnose unit being the polymeric backbone of most of these probiotic bacteria, its high content in the EPS of *L. paracasei* DG (as seen in the ratio 4:1:1) makes it unique when compared with LAB already reported. In collaboration with our research partners from Italy, the EPS and CPS of the *L. paracasei* DG displayed immuno-stimulatory properties making it a potential novel molecule suitable for pharmaceutical and nutraceutical applications.

Choosing the *Lactobacillus salivarius* CCUG44481 to work on was ideal as it was of a bird origin found to produce significantly higher levels of EPS as compared to other strains of LAB and not much has been explored and characterised of this strain²²⁷. The chromatographic methods revealed glucose to be the main molecule forming the backbone of the structure with the linkage analysis confirming the presence of a terminal hexose, 1,3-linked hexose, 1,6-linked hexose and a 1,3,6-linked hexose. The NMR spectroscopy results further shows the profile of the EPS extracted from the *L. salivarius* CCUG44481 to be similar to that of a standard commercial dextran but with a much more highly branched structure with a 1,6-

linked hexose forming the main backbone. The chromatographic and NMR spectroscopic methods used for the analysis of the EPS from the *L. salivarius* CCUG44481 was seen to be a highly branched dextran with a backbone of a repeating unit of α -(1,6)-linked glucose having multiple branches of 1,3-linked glucoses. The highly branched nature of this EPS was unique accounting for its dramatic higher producing levels making it a novel structure when compared with the other reported strains. This highly branched dextran EPS of the *L. salivarius* CCUG44481 gives it a novel structure which has been reported by Raftis *et al* (2011)²²⁷ in their research work not to be well characterised in comparison to the other *Lactobacillus species* studied.

HPAEC-PAD analysis of substances has been seen to be relatively quicker involving just one step (acid hydrolysis) which in conjunction with preparative carbon-celite column was used to attempt separate the commercially available methylated glucose units. After passing the hydrolysed methylated glucose units through the preparative column, the various fractions obtained from the different percentages of methanol were analysed through HPAEC-PAD which gave partial results with some peaks not clearly distinguished from others as a result of overlapping. In this research, seeing how time consuming the linkage analysis was, we made attempts into developing a faster method using the HPAEC-PAD which looked promising but still had some shortcomings and due time constraints we had to continue with our old method which is usually cumbersome, lengthy but accurate. Attempting to use this promising method was a novel technique brought in to cut down on the length of time used for the linkage analysis derivatisation process.

In this study, the isolation of the surface polysaccharides of *B. breve* 7017 was achieved by partially fractionating them through the precipitation steps with increasing volumes of ethanol (1 and 2 volumes). The addition of these 1 and 2 volumes precipitated the S1, C1 and S2, C2 respectively. When the polysaccharides of the *B. breve* 7017 were analysed, the S1 and C1 fractions were seen to indicate a bacterial glycogen that was being isolated. It was noticed that the S2 fractions changed with time and this was confirmed to be as a result of slow loss of the ribitol-like moiety due to prolonged storage. This S2 was made up of a glucose and galactose residues linked which also had another glucose residue linked to the 6-position of the 1,4-linked galactose decorated with acetyl groups and a labile C7-fragment making it a

novel structure. The C2 for the *B. breve* 7017 was also identified to have 2 homoglycans (a β -D-(1,6)-galactofuranan and a β -D-(1,6)-glucan) which were likely to be derived from hydrolysis of phosphate linkages in cell wall associated lipoteichoic acids. The chromatographic and NMR spectroscopic methods used for the characterisation of this EPS and CPS (S1, S2, and C1, C2 respectively) revealed them to have different structures which was evident just from looking at their $^1\text{H-NMR}$ profile. The results reported here indicated a mixture three homoglycans was isolated which has not been reported before making it a novel finding. As for future work, further work should still be carried out to study the biological activity of these different fractions (S1, S2, C1 and C2)

At the end of this work, the issue encountered was that very little amount of the polysaccharides (EPS and CPS) isolated from the various cultures was recovered. Moreover, in the case where the ultrasonic disruption was used in an attempt to release more of the attached EPS, the presence of significant amount of proteins suggests that the cells had been ruptured. In future if ultrasonic disruption is still considered, a much lower amplitude should be used so as to avoid lysing the cells. That notwithstanding, another simple approach that could be used in the future in order to increase the chances of recovering more polysaccharides without rupturing or lysing the cells is by using a fermenting chamber with constant stirring rather than the static fermentation employed. Stirring and agitation of the broth may well lead to increased polysaccharide production and the shear forces may physically remove material bound to cells. Another thing could be to use a much lower concentration of the NaOH when extracting the CPS since it was noticed that some proteins were still detectable after extracting with NaOH (2M).

From the results gathered in the various extractions performed in this study, the polysaccharides isolated from the second addition of chilled absolute ethanol were more useful in that they provided material of a reasonable purity that could be used in characterisation studies. Therefore, in future more focus should be on the fractions recovered from addition of the second volume of chilled ethanol. It will also be interesting to see what can be extracted if an additional third volume of absolute ethanol were to be added.

After the collection of the EPSs from the various bacteria, an attempt was made to calculate its carbohydrate content using the Dubois method, which indicated that the EPS is not made

of entirely the carbohydrates and other non-carbohydrates contents are present. Whilst the presence of these biomacromolecules didn't influence the characterisation studies they would interfere in the measurement of their biological and chemical properties. Future work could involve carrying out the Bradford protein assay test for protein determination and use of spectrophotometric methods for determining the nucleic acid content of samples. Since the crude polysaccharides extracted were not made up entirely of carbohydrates, a size exclusion column should be used in future in order to try and separate any impurities as well as any proteins or nucleic acids present to obtain pure polysaccharide.

It will be necessary to check for the biological activity of these polysaccharides by investigating their interaction with human immune cells and this work is currently being explored by postdoctoral research fellows at the University of Huddersfield. At the same time, it would be interesting to explore the antioxidant activities and free radical scavenging activity of the extracted polysaccharides. The proposed methods that could be used are in vitro experiments: testing for the superoxide radical scavenging, testing the scavenging activity of the 1,1-diphenyl-2-picrylhydrazyl (DPPH) as well as using ascorbic acid-Cu(2+)-cytochrome c system to test the hydroxyl radical scavenging activities.

In the future, another analysis that could help with characterising the bacterial polysaccharide is performing Smith degradation. During this process, the polysaccharide is degraded selectively to either a smaller repeat unit of the polysaccharide (oligosaccharide) and then the deduction of structural information is easily obtained.

Seeing that the linkage analysis using HPAEC-PAD was difficult to perform and was time consuming, some modifications could be made and a different approach used. This could involve the development of more discriminating stationary phases or columns with longer dimensions working with higher pressures, which may make it possible to separate the isomeric methyl glucoses more easily.

References

1. F. Guarner and G. Schaafsma, *International journal of food microbiology*, 1998, **39**, 237-238.
2. C. Hill, F. Guarner, G. Reid, G. R. Gibson, D. J. Merenstein, B. Pot, L. Morelli, R. B. Canani, H. J. Flint and S. Salminen, *Nature reviews Gastroenterology & hepatology*, 2014, **11**, 506-514.
3. P. Singleton, *Bacteria in biology, biotechnology and medicine*, John Wiley & Sons, Chichester 2004.
4. C. L. Sears, *Anaerobe*, 2005, **11**, 247-251.
5. P. W. O'Toole, J. R. Marchesi and C. Hill, *Nature microbiology*, 2017, **2**, 17057.
6. R. Fuller, *J. Appl. Bacteriol*, 1989, **66**, 365-378.
7. E. P. o. B. Hazards, *EFSA Journal*, 2015, **13**, 4138.
8. M. De Vrese and J. Schrezenmeir, in *Food biotechnology*, Springer, 2008, pp. 1-66.
9. C. Hidalgo-Cantabrana, P. López, M. Gueimonde, G. Clara, A. Suárez, A. Margolles and P. Ruas-Madiedo, *Probiotics and antimicrobial proteins*, 2012, **4**, 227-237.
10. M. Nagaoka, S. Hashimoto, T. Watanabe T. Yokorura and Y. Mori, *Biological and Pharmaceutical Bulletin*, 1994, **17**, 1012-1017.
11. R. Rosania, F. Giorgio, M. Principi, A. Amoroso, R. Monno, A. Di Leo and E. Ierardi, *Current clinical pharmacology*, 2013, **8**, 169-172.
12. P. Lopez, D. C. Monteserin, M. Gueimonde, G. Clara, A. Margolles, A. Suarez and P. Ruas-Madiedo, *Food Research International*, 2012, **46**, 99-107.
13. Y. Uemura and M. Matsumoto, *Glycoconjugate journal*, 2014, **31**, 555-561.
14. K. L. Lindhorst, *Essentials of Carbohydrate Chemistry and Biochemistry*, Darmstadt Germany, 2007.
15. G. D. McGinnis and C. J. Biermann, *Analysis of Carbohydrates by GLC and MS*, CRC Press, Florida, USA, 1989.
16. D. L. Nelson, M. M. Cox and A. L. Lehninger, *Lehninger principles of biochemistry*, W.H. Freeman, New York, 7th edn., 2017.
17. P. Collins and R. Ferrier, *Monosaccharides: their chemistry and their roles in natural products*, John Wiley and Sons Inc., New York, 1995.
18. J. Cummings and A. Stephen, *European journal of clinical nutrition*, 2007, **61**, S5.
19. FAO, *Carbohydrates in human nutrition. Food and Agriculture Organization of the United Nations*, FAO Food and Nutrition, Rome, 1998.
20. J. Cummings, M. Roberfroid, H. Andersson, C. Barth, A. Ferro-Luzzi, Y. Ghos, M. Gibney, K. Hermansen, W. James and O. Korver, *European Journal of Clinical Nutrition*, 1997, **51**, 417-423.
21. V. A. Yaylayan, S. Harty-Majors and A. A. Ismail, *Carbohydrate Research*, 1999, **318**, 20-25.
22. N. J. Campbell, *Biology*, New York, Forth edn., 1996.
23. J. M. Berg, J. L. Tymoczko and L. Stryer, *Biochemistry*, W. H. Freeman, New York, 6th edn., 2007.
24. D. Voet, J. G. Voet and C. W. Pratt, *Principles of biochemistry*, Wiley, Hoboken, N.J, 4th, International student version. edn., 2013.
25. I. Sutherland, *Advances in microbial physiology*, 1982, **23**, 79-150.
26. F. Freitas, V. D. Alves, C. A. Torres, M. Cruz, I. Sousa, M. J. Melo, A. M. Ramos and M. A. Reis, *Carbohydrate polymers*, 2011, **83**, 159-165.
27. C. Mathews, K. van Holde and K. Ahern, *Bioquímica*, Addison Wesley, 3rd edn, 2002.
28. M. Miljković, in *Carbohydrates*, Springer, 2010, pp. 27-56.
29. R. V. Stick and S. J. Williams, *Carbohydrates: the essential molecules of life*, Elsevier, Amsterdam;London;, 2nd edn., 2009.
30. R. L. Davidson, *Handbook of water-soluble gums and resins*, McGraw-Hill, New York;London;, 1980.
31. P.E. Jansson, L. Kenne and B. Lindberg, *Carbohydrate Research*, 1975, **45**, 275-282.

32. L. De Vuyst and B. Degeest, *FEMS microbiology reviews*, 1999, **23**, 153-177.
33. J. P. Kamerling and G. J. Boons, *Comprehensive glycoscience: from chemistry to systems biology*, Elsevier, 2007.
34. J. K. Fredrickson, J. M. Zachara, D. L. Balkwill, D. Kennedy, S.-m. W. Li, H. M. Kostandarithes, M. J. Daly, M. F. Romine and F. J. Brockman, *Applied and Environmental Microbiology*, 2004, **70**, 4230-4241.
35. B. Alberts, *Essential cell biology*, Garland Science, Taylor and Francis group, New York, 4th edn., 2014.
36. W. B. Whitman, D. C. Coleman and W. J. Wiebe, *Proceedings of the National Academy of Sciences*, 1998, **95**, 6578-6583.
37. J.-M. Ghuysen and R. Hackenbeck, *Bacterial cell wall*, Amsterdam : Elsevier, 1994.
38. S. M. Shaban, A. Fouda, M. Elmorsi, T. Fayed and O. Azazy, *Journal of Molecular Liquids*, 2016, **216**, 284-292.
39. S. Baron, *Epidemiology--Medical Microbiology*, Texas -Galveston, 4th edn, 1996.
40. R. Garimella, J. L. Halye, W. Harrison, P. E. Klebba and C. V. Rice, *Biochemistry*, 2009, **48**, 9242-9249.
41. K. Knox and A. Wicken, *Bacteriological reviews*, 1973, **37**, 215.
42. M. Caroff, D. Karibian, J.-M. Cavaillon and N. Haeffner-Cavaillon, *Microbes and infection*, 2002, **4**, 915-926.
43. C. Erridge, E. Bennett-Guerrero and I. R. Poxton, *Microbes and infection*, 2002, **4**, 837-851.
44. M. G. Rittig, A. Kaufmann, A. Robins, B. Shaw, H. Sprenger, D. Gemsa, V. Foulongne, B. Rouot and J. Dornand, *Journal of leukocyte biology*, 2003, **74**, 1045-1055.
45. H. Tsujimoto, N. Gotoh and T. Nishino, *Journal of Infection and Chemotherapy*, 1999, **5**, 196-200.
46. C. Hershberger and S. Binkley, *Journal of Biological Chemistry*, 1968, **243**, 1578-1584.
47. E. M. Chastain and S. D. Miller, *Immunological reviews*, 2012, **245**, 227-238.
48. G. J. Tortora, B. R. Funke and C. L. Case, *Microbiology: an introduction*, Pearson, Boston;London;, 11th edn., 2013.
49. P. Ruas-Madiedo and C. De Los Reyes-Gavilán, *Journal of Dairy Science*, 2005, **88**, 843-856.
50. J. Monod, *Annual Reviews in Microbiology*, 1949, **3**, 371-394.
51. M. T. Madigan, J. M. Martinko, K. S. Bender, D. H. Buckley, D. A. Stahl and T. D. Brock, *Brock biology of microorganisms*, Pearson, Boston, 14 edn., 2015.
52. A. N. Glazer and H. Nikaido, *Microbial biotechnology: fundamentals of applied microbiology*, Cambridge University Press, 2nd edn, 2007.
53. I. Sutherland, *Surface carbohydrates of the prokaryotic cell*, 1977, **1**, 27-96.
54. A. J. Anderson, G. W. Haywood and E. A. Dawes, *International journal of biological macromolecules*, 1990, **12**, 102-105.
55. B. Rehm and S. Valla, *Applied microbiology and biotechnology*, 1997, **48**, 281-288.
56. I. Dogsa, M. Kriechbaum, D. Stopar and P. Laggner, *Biophysical journal*, 2005, **89**, 2711-2720.
57. U. U. Nwodo, E. Green and A. I. Okoh, *International Journal of Molecular Sciences*, 2012, **13**, 14002-14015.
58. I. Sutherland, *Advances in microbial physiology*, 1972, **8**, 143-213.
59. I. W. Sutherland, *Annual Reviews in Microbiology*, 1985, **39**, 243-270.
60. C. M. Taylor and I. S. Roberts, in *Concepts in Bacterial Virulence*, Karger Publishers, 2005, vol. 12, pp. 55-66.
61. T. R. Neu and J. R. Lawrence, *FEMS Microbiology Ecology*, 1997, **24**, 11-25.
62. I. W. Sutherland, *International review of cytology*, 1988, **113**, 187-231.
63. M. T. Madigan and T. D. Brock, *Brock biology of microorganisms*, Pearson, Boston,;London;, 13th edn., 2012.
64. A. Laws, Y. Gu and V. Marshall, *Biotechnology advances*, 2001, **19**, 597-625.

65. M. R. Prado, L. M. Blandón, L. P. Vandenberghe, C. Rodrigues, G. R. Castro, V. Thomaz-Soccol and C. R. J. F. i. m. Soccol, 2015, **6**, 1177.
66. G. Tortora, B. Funke and C. J. M. A. i. Case, 2013, 483-485.
67. H. Yoshioka, K.-i. Iseki and K. J. P. Fujita, 1983, **72**, 317-321.
68. S. J. I. j. o. e. r. Fijan and p. health, 2014, **11**, 4745-4767.
69. F. P. Douillard, A. Ribbera, H. M. Järvinen, R. Kant, T. E. Pietilä, C. Randazzo, L. Paulin, P. K. Laine, C. Caggia and I. von Ossowski, *Applied and environmental microbiology*, 2013, **79**, 1923-1933.
70. W. Holzapfel and B. Wood, *The genera of lactic acid bacteria London Blackie Academic & Professional*, ISBN 0-7514-0215-X, 1998.
71. S. Salminen and A. Von Wright, *Lactic acid bacteria: microbiological and functional aspects*, CRC Press, 2004.
72. H. Cai, B. T. Rodriguez, W. Zhang, J. R. Broadbent and J. L. Steele, *Microbiology*, 2007, **153**, 2655-2665.
73. J. Marchand and Y. Vandenplas, *European journal of gastroenterology & hepatology*, 2000, **12**, 1077-1088.
74. V. Azaïs-Braesco, J. Bresson, F. Guarner and G. Corthier, *British Journal of Nutrition*, 2010, **103**, 1079-1081.
75. M. Rogosa, R. Wiseman, J. A. Mitchell, M. Disraely and A. J. J. o. B. Beaman, 1953, **65**, 681.
76. P. Casey, G. Casey, G. Gardiner, M. Tangney, C. Stanton, R. Ross, C. Hill and G. J. L. i. a. m. Fitzgerald, 2004, **39**, 431-438.
77. H. T. A. Hilmi, A. Surakka, J. Apajalahti and P. E. J. A. E. M. Saris, 2007, **73**, 7867-7873.
78. R. Martín, E. Jiménez, M. Olivares, M. Marín, L. Fernández, J. Xaus and J. J. I. j. o. f. m. Rodríguez, 2006, **112**, 35-43.
79. M. Ortiz-Lucas, A. Tobias, J. Sebastián and P. Saz, *Rev Esp Enferm Dig*, 2013, **105(1)**, 19-36.
80. A. A. Niccoli, A. L. Artesi, F. Candio, S. Ceccarelli, R. Cozzali, L. Ferraro, D. Fiumana, M. Mencacci, M. Morlupo and P. J. J. o. c. g. Pazzelli, 2014, **48**, S34-S36.
81. B. Neville and P. J. F. M. O'Toole, 2010, **5**, 759-774.
82. R. D'Incà, M. Barollo, M. Scarpa, A. R. Grillo, P. Brun, M. G. Vettorato, I. Castagliuolo and G. C. Sturniolo, *Digestive diseases and sciences*, 2011, **56**, 1178-1187.
83. A. Tursi, G. Brandimarte, G. M. Giorgetti and M. E. Modeo, *Medical Science Monitor*, 2004, **10**, CR662-CR666.
84. C. Ferrario, V. Taverniti, C. Milani, W. Fiore, M. Laureati, I. De Noni, M. Stuknyte, B. Chouaia, P. Riso and S. Guglielmetti, *The Journal of nutrition*, 2014, **144**, 1787-1796.
85. S. Guglielmetti and V. Taverniti, *Genes & nutrition*, 2011, **6**, 261.
86. P. Ruas-Madiedo, M. Gueimonde, C. De Los Reyes-Gavilan and S. Salminen, *Journal of dairy science*, 2006, **89**, 2355-2358.
87. H.-C. Flemming and J. Wingender, *Nature Reviews Microbiology*, 2010, **8**, 623-633.
88. B. Vu, M. Chen, R. J. Crawford and E. P. Ivanova, *Molecules*, 2009, **14**, 2535-2554.
89. D. Commane, R. Hughes, C. Shortt and I. Rowland, *Mutation Research/Fundamental and Molecular Mechanisms of Mutagenesis*, 2005, **591**, 276-289.
90. M. Du Toit, C. Franz, L. Dicks, U. Schillinger, P. Haberer, B. Warlies, F. Ahrens and W. Holzapfel, *International journal of food microbiology*, 1998, **40**, 93-104.
91. H. Nakajima, Y. Suzuki and T. HIROTA, *Journal of food science*, 1992, **57**, 1327-1329.
92. A. Hosono, J. Lee, A. Ametani, M. Natsume, M. Hirayama, T. Adachi and S. Kaminogawa, *Bioscience, biotechnology, and biochemistry*, 1997, **61**, 312-316.
93. H. Kitazawa, T. Yamaguchi, M. Miura, T. Saito and T. Itoh, *Journal of dairy science*, 1993, **76**, 1514-1519.
94. M. Maeno, N. Yamamoto and T. Takano, *Journal of Dairy Science*, 1996, **79**, 1316-1321.
95. S. F. Solga, *Medical hypotheses*, 2003, **61**, 307-313.
96. M. Cross, L. Stevenson and H. Gill, *International immunopharmacology*, 2001, **1**, 891-901.

97. K. Merk, C. Borelli and H. C. Korting, *International journal of medical microbiology*, 2005, **295**, 9-18.
98. K. Ludbrook, C. Russell and R. Greig, *Journal of food science*, 1997, **62**, 597-600.
99. S.-Q. Liu, *International journal of food microbiology*, 2003, **83**, 115-131.
100. V. M. Marshall and H. Rawson, *International journal of food science & technology*, 1999, **34**, 137-143.
101. S. Kontusaari and R. Forsén, *Journal of dairy science*, 1988, **71**, 3197-3202.
102. A. Williams, J. Noble and J. Banks, *International Dairy Journal*, 2001, **11**, 203-215.
103. S. Awad, A. Hassan and K. Muthukumarappan, *Journal of Dairy Science*, 2005, **88**, 4204-4213.
104. B. Biavati, M. Vescovo, S. Torriani and V. Bottazzi, *Annals of microbiology*, 2000, **50**, 117-132.
105. A. Zinedine and M. Faid, *World Journal of Dairy & Food Sciences*, 2007, **2**, 28-34.
106. P. Ruas-Madiedo, N. Salazar and C. G. de los Reyes-Gavilán, in *Microbial Glycobiology*, 2010, DOI: 10.1016/B978-0-12-374546-0.00045-6, pp. 885-902.
107. B. Mayo and D. Van Sinderen, *Bifidobacteria: genomics and molecular aspects*, Horizon Scientific Press, Poole, 2010.
108. L. Masco, G. Huys, E. De Brandt, R. Temmerman and J. Swings, *International Journal of Food Microbiology*, 2005, **102**, 221-230.
109. F. Bottacini, M. Ventura, D. Van Sinderen and M. O. C. Motherway, *Microbial cell factories*, 2014, **13**, S4.
110. E. L. Zdorovenko, V. V. Kachala, A. V. Sidarenka, A. V. Izhik, E. P. Kisileva, A. S. Shashkov, G. I. Novik and Y. A. Knirel, *Carbohydrate research*, 2009, **344**, 2417-2420.
111. S. Arbolea, C. Watkins, C. Stanton and R. P. Ross, *Frontiers in microbiology*, 2016, **7**, 1204.
112. R. Tojo, A. Suárez, M. G. Clemente, C. G. de los Reyes-Gavilán, A. Margolles, M. Gueimonde and P. Ruas-Madiedo, *World journal of gastroenterology: WJG*, 2014, **20**, 15163.
113. S. Fanning, L. J. Hall, M. Cronin, A. Zomer, J. MacSharry, D. Goulding, M. O. C. Motherway, F. Shanahan, K. Nally and G. Dougan, *Proceedings of the National Academy of Sciences*, 2012, **109**, 2108-2113.
114. C. Hidalgo-Cantabrana, B. Sánchez, C. Milani, M. Ventura, A. Margolles and P. Ruas-Madiedo, *Applied and Environmental Microbiology*, 2014, **80**, 9-18.
115. B. Ebel, F. Martin, L. Le, P. Gervais and R. Cachon, *Journal of dairy science*, 2011, **94**, 2185-2191.
116. T. Odamaki, J. Xiao, S. Yonezawa, T. Yaeshima and K. Iwatsuki, *Journal of dairy science*, 2011, **94**, 1112-1121.
117. B. Biavati and P. Mattarelli, in *The prokaryotes*, Springer, 2006, pp. 322-382.
118. V. Scardovi, *Ann Microbiol Enzymol*, 1965, **15**, 19-24.
119. S. Leivers, C. Hidalgo-Cantabrana, G. Robinson, A. Margolles, P. Ruas-Madiedo and A. P. Laws, *Carbohydrate research*, 2011, **346**, 2710-2717.
120. M. Adams and P. Marteau, *International journal of food microbiology*, 1995, **27**, 263-264.
121. N. Ishibashi and S. Yamazaki, *The American journal of clinical nutrition*, 2001, **73**, 465s-470s.
122. K. Kailasapathy and J. Chin, *Immunology and cell Biology*, 2000, **78**, 80-88.
123. M. C. Collado, M. Gueimonde, M. Hernandez, Y. Sanz and S. Salminen, *Journal of food protection*, 2005, **68**, 2672-2678.
124. J. M. Saavedra, N. A. Bauman, J. Perman, R. Yolken and I. Oung, *The lancet*, 1994, **344**, 1046-1049.
125. T. Jiang, A. Mustapha and D. A. Savaiano, *Journal of Dairy Science*, 1996, **79**, 750-757.
126. V. Lievin, I. Peiffer, S. Hudault, F. Rochat, D. Brassart, J. Neeser and A. Servin, *Gut*, 2000, **47**, 646-652.
127. C. Moubareck, F. Gavini, L. Vaugien, M. Butel and F. Doucet-Populaire, *Journal of Antimicrobial Chemotherapy*, 2005, **55**, 38-44.
128. G. E. Hatcher and R. S. Lambrecht, *Journal of Dairy Science*, 1993, **76**, 2485-2492.

129. K. Sekine, E. Watanabe-Sekine, T. Toida, T. Kasashima, T. Kataoka and Y. Hashimoto, *Immunopharmacology and immunotoxicology*, 1994, **16**, 589-609.
130. T. Takahashi, T. Oka, H. Iwana, T. Kuwata and Y. Yamamoto, *Bioscience, biotechnology, and biochemistry*, 1993, **57**, 1557-1560.
131. J. Singh, A. Rivenson, M. Tomita, S. Shimamura, N. Ishibashi and B. S. Reddy, *Carcinogenesis*, 1997, **18**, 833-841.
132. Y. Deguchi, T. Morishita and M. Mutai, *Agricultural and Biological Chemistry*, 1985, **49**, 13-19.
133. F. Joint, *London, Ontario, Canada*, 2002, **30**.
134. A. P. Laws and V. M. Marshall, *International Dairy Journal*, 2001, **11**, 709-721.
135. J. Schmid, V. Sieber and B. Rehm, *Frontiers in microbiology*, 2015, **6**, 496.
136. H. L. Tytgat and S. Lebeer, *Microbiology and Molecular Biology Reviews*, 2014, **78**, 372-417.
137. B. H. Rehm, *Microbial production of biopolymers and polymer precursors: applications and perspectives*, Caister Academic Press, Norfolk, 2009.
138. M. Ullrich, *Bacterial polysaccharides: current innovations and future trends*, Caister Academic Press, Bremen, 2009.
139. A. A. Zeidan, V. K. Poulsen, T. Janzen, P. Buldo, P. M. Derkx, G. Øregaard and A. R. Neves, *FEMS microbiology reviews*, 2017, **41**, S168-S200.
140. P. Postma, J. Lengeler and G. Jacobson, *Microbiological reviews*, 1993, **57**, 543-594.
141. D. V. F. De Vuyst L, *From Chemistry to Systems Biology*, Oxford: Elsevier, 2007, **2**, 477-519.
142. A. R. Neves, W. A. Pool, J. Kok, O. P. Kuipers and H. Santos, *FEMS microbiology reviews*, 2005, **29**, 531-554.
143. A. D. Welman and I. S. Maddox, *Trends in biotechnology*, 2003, **21**, 269-274.
144. A. R. Neves, W. A. Pool, R. Castro, A. Mingote, F. Santos, J. Kok, O. P. Kuipers and H. Santos, *Journal of Biological Chemistry*, 2006, **281**, 36864-36873.
145. P. Ryan, R. Ross, G. Fitzgerald, N. Caplice and C. Stanton, *Food & function*, 2015, **6**, 679-693.
146. M. I. Torino, G. F. de Valdez and F. Mozzi, *Frontiers in microbiology*, 2015, **6**, 834.
147. S. Galle and E. K. Arendt, *Critical reviews in food science and nutrition*, 2014, **54**, 891-901.
148. S. A. van Hijum, S. Kralj, L. K. Ozimek, L. Dijkhuizen and I. G. van Geel-Schutten, *Microbiology and Molecular Biology Reviews*, 2006, **70**, 157-176.
149. S. T. Islam and J. S. Lam, *Canadian journal of microbiology*, 2014, **60**, 697-716.
150. W. Li, J. Ji, X. Chen, M. Jiang, X. Rui and M. Dong, *Carbohydrate polymers*, 2014, **102**, 351-359.
151. D. A. Patten, S. Leivers, M. J. Chadha, M. Maqsood, P. N. Humphreys, A. P. Laws and A. Collett, *Carbohydrate research*, 2014, **384**, 119-127.
152. K. Zhou, Y. Zeng, M. Yang, S. Chen, L. He, X. Ao, L. Zou and S. Liu, *Carbohydrate polymers*, 2016, **144**, 205-214.
153. C. Grangeasse, *Trends in microbiology*, 2016, **24**, 713-724.
154. J. Nourikyan, M. Kjos, C. Mercy, C. Cluzel, C. Morlot, M.-F. Noirot-Gros, S. Guiral, J.-P. Lavergne, J. W. Veening and C. Grangeasse, *PLoS genetics*, 2015, **11**, e1005518.
155. A. D. Cefalo, J. R. Broadbent and D. L. Welker, *Canadian journal of microbiology*, 2011, **57**, 1002-1015.
156. C. Suzuki, M. Kobayashi and H. Kimoto-Nira, *Bioscience, biotechnology, and biochemistry*, 2013, **77**, 2013-2018.
157. E. R. Vedamuthu and J. M. Neville, *Applied and Environmental Microbiology*, 1986, **51**, 677-682.
158. L. Cuthbertson, I. L. Mainprize, J. H. Naismith and C. J. M. M. B. R. Whitfield, *Microbiol Mol Biol Rev*, 2009, **73**, 155-177.

159. J. G. Leid, C. J. Willson, M. E. Shirliff, D. J. Hassett, M. R. Parsek and A. K. J. T. J. o. I. Jeffers, *J Immunol*, 2005, **175**, 7512-7518.
160. C. Vuong, S. Kocianova, J. M. Voyich, Y. Yao, E. R. Fischer, F. R. DeLeo and M. J. J. o. B. C. Otto, *Journal of Biological Chemistry*, 2005, **280**, 12064-12064.
161. M. Crouzet, C. Le Senechal, V. S. Brözel, P. Costaglioli, C. Barthe, M. Bonneu, B. Garbay and S. J. B. m. Vilain, 2014, **14**, 253.
162. P. Landini, D. Antoniani, J. G. Burgess, R. J. A. m. Nijland and biotechnology, 2010, **86**, 813-823.
163. Z. Lewandowski, D. Caldwell, D. Korber and H. J. A. R. M. Lappin-Scott, 1995, **49**, 711-745.
164. N. Høiby, T. Bjarnsholt, M. Givskov, S. Molin and O. J. I. j. o. a. a. Ciofu, 2010, **35**, 322-332.
165. R. M. Donlan and J. W. J. C. m. r. Costerton, 2002, **15**, 167-193.
166. B. H. J. N. R. M. Rehm, 2010, **8**, 578.
167. W. H. Van Casteren, P. de Waard, C. Dijkema, H. A. Schols and A. G. J. C. r. Voragen, 2000, **327**, 411-422.
168. Y. Yamamoto, T. Nunome, R. Yamauchi, K. Kato and Y. Sone, *Carbohydrate Research*, 1995, **275**, 319-332.
169. A. Ouwehand, E. Isolauri, P. Kirjavainen, S. Ölkö and S. J. L. i. A. M. Salminen, 2000, **30**, 10-13.
170. P. Duboc and B. Mollet, *International Dairy Journal*, 2001, **11**, 759-768.
171. L. De Vuyst, F. De Vin, F. Vaningelgem and B. Degeest, *International Dairy Journal*, 2001, **11**, 687-707.
172. F. Levander, M. Svensson and P. Rådström, *BMC microbiology*, 2001, **1**, 23.
173. S. Shimamura, F. Abe, N. Ishibashi, H. Miyakawa, T. Yaeshima, T. Araya and M. Tomita, *Journal of Dairy Science*, 1992, **75**, 3296-3306.
174. S. Petry, S. Furlan, M.-J. Crepeau, J. Cerning and M. Desmazeaud, *Applied and environmental microbiology*, 2000, **66**, 3427-3431.
175. G. Grobben, J. Sikkema, M. Smith and J. d. Bont, *Journal of Applied Microbiology*, 1995, **79**, 103-107.
176. P. Pham, I. Dupont, D. Roy, G. Lapointe and J. Cerning, *Applied and environmental microbiology*, 2000, **66**, 2302-2310.
177. E. Knoshaug, J. Ahlgren and J. Trempey, *Journal of Dairy Science*, 2000, **83**, 633-640.
178. J. Cerning, C. Bouillanne, M. Desmazeaud and M. Landon, *Biotechnology Letters*, 1986, **8**, 625-628.
179. M. Garcia-Garibay and V. Marshall, *Journal of Applied Microbiology*, 1991, **70**, 325-328.
180. L. De Vuyst, F. Vanderveken, S. Van de Ven and B. Degeest, *Journal of Applied Microbiology*, 1998, **84**, 1059-1068.
181. J. Lemoine, F. Chirat, J.-M. Wieruszkeski, G. Strecker, N. Favre and J.-R. Neeser, *Applied and Environmental Microbiology*, 1997, **63**, 3512-3518.
182. J. Antón, I. Meseguer and F. Rodriguez-Valera, *Applied and environmental microbiology*, 1988, **54**, 2381-2386.
183. J. Cerning, C. Bouillanne, M. Desmazeaud and M. Landon, *Biotechnology Letters*, 1988, **10**, 255-260.
184. L. P. Harding, V. M. Marshall, M. Elvin, Y. Gu and A. P. Laws, *Carbohydrate research*, 2003, **338**, 61-67.
185. M. Dubois, K. A. Gilles, J. K. Hamilton, P. t. Rebers and F. Smith, *Analytical chemistry*, 1956, **28**, 350-356.
186. J. N. BeMiller, in *Food analysis*, Springer, Boston, 2010, pp. 147-177.
187. Y. Brummer, S. W. J. F. c. c. Cui, physical properties and applications, *Understanding carbohydrate analysis*, CRC Press, Florida, 2005, pp. 67-84.
188. S. W. Gunner, J. N. Jones and M. Perry, *Canadian Journal of Chemistry*, 1961, **39**, 1892-1899.

189. P. Albersheim, D. J. Nevins, P. D. English and A. Karr, *Carbohydrate Research*, 1967, **5**, 340-345.
190. J. Blake and G. Richards, *Carbohydrate Research*, 1970, **14**, 375-387.
191. G. G. Dutton, in *Advances in carbohydrate chemistry and biochemistry*, Elsevier, 1973, vol. 28, pp. 11-160.
192. R. Whiton, P. Lau, S. Morgan, J. Gilbert and A. Fox, *Journal of Chromatography A*, 1985, **347**, 109-120.
193. D. Fengel and G. Wegener, in *Hydrolysis of Cellulose: Mechanisms of Enzymatic and Acid Catalysis*, AMERICAN CHEMICAL SOCIETY, 1979, vol. 181, ch. 7, pp. 145-158.
194. C. J. Biermann and G. D. McGinnis, *Analysis of Carbohydrates by GLC and MS*, CRC press, Florida, USA, 1988.
195. R. D. Rocklin and C. A. Pohl, *Journal of Liquid Chromatography*, 1983, **6**, 1577-1590.
196. Y. C. Lee, *Analytical biochemistry*, 1990, **189**, 151-162.
197. T. R. Cataldi, C. Campa and G. E. De Benedetto, *Fresenius' journal of analytical chemistry*, 2000, **368**, 739-758.
198. J. J. T. F. S. Rohrer, Technical Note, 2012, **20**, pp. 1-12.
199. H. A. Currie and C. C. Perry, *Journal of Chromatography A*, 2006, **1128**, 90-96.
200. M. T. Madigan, J. M. Martinko and J. Parker, *Brock biology of microorganisms*, Pearson, USA, 2017, pp. 35-78.
201. J. H. Xie, M.-Y. Shen, S.-P. Nie, X. Liu, H. Zhang and M.-Y. J. C. p. Xie, 2013, **98**, 976-981.
202. K. Stellner, H. Saito and S.-I. Hakomori, *Archives of Biochemistry and Biophysics*, 1973, **155**, 464-472.
203. T. Purdie and J. C. Irvine, *Journal of the Chemical Society, Transactions*, 1904, **85**, 1049-1070.
204. W. S. Denham and H. Woodhouse, *Journal of the Chemical Society, Transactions*, 1913, **103**, 1735-1742.
205. W. N. Haworth, *Journal of the Chemical Society, Transactions*, 1915, **107**, 8-16.
206. S.-I. Hakomori, *The Journal of Biochemistry*, 1964, **55**, 205-208.
207. C. J. Biermann and G. D. McGinnis, *Analysis of carbohydrates by GLC and MS*, CRC Press, Boca Raton, Fla, 1989.
208. I. Ciucanu and F. J. C. r. Kerek, 1984, **131**, 209-217.
209. G. J. Gerwig, J. P. Kamerling and J. F. Vliegthart, *Carbohydrate Research*, 1978, **62**, 349-357.
210. B. Leeflang, E. Faber, P. Erbel and J. Vliegthart, *Journal of biotechnology*, 2000, **77**, 115-122.
211. B. Bose-Basu, J. Zajicek, G. Bondo, S. Zhao, M. Kubsch, I. Carmichael and A. S. Serianni, *Journal of Magnetic Resonance*, 2000, **144**, 207-216.
212. R. Csuk and B. I. Glänzer, in *Advances in carbohydrate chemistry and biochemistry*, Elsevier, 1988, vol. 46, pp. 73-177.
213. M. Michalik, M. Hein and M. Frank, *Carbohydrate research*, 2000, **327**, 185-218.
214. W. A. Bubb, *Concepts in Magnetic Resonance Part A*, 2003, **19**, 1-19.
215. S. W. Cui, *Food carbohydrates: chemistry, physical properties, and applications*, CRC press, 2005.
216. T. Doco, J.-M. Wieruszkeski, B. Fournet, D. Carcano, P. Ramos and A. Loones, *Carbohydrate research*, 1990, **198**, 313-321.
217. M. Tafazzoli and M. Ghiasi, *Carbohydrate research*, 2007, **342**, 2086-2096.
218. J. Keeler, *Understanding NMR spectroscopy*, John Wiley & Sons, Oxford, 2nd edn, 2011.
219. R. A. de Graaf, in *Magnetic Resonance Spectroscopy*, eds. C. Stagg and D. Rothman, Academic Press, San Diego, 2014, DOI: <https://doi.org/10.1016/B978-0-12-401688-0.00004-5>, pp. 40-48.
220. H. Sato, K. Fukae and Y. Kajihara, *Carbohydrate Research*, 2008, **343**, 1333-1345.

221. H. Friebolin, *Basic one- and two-dimensional NMR spectroscopy*, Wiley-VCH, Weinheim, 5th edn., 2011.
222. P. J. Wyatt, *Analytica chimica acta*, 1993, **272**, 1-40.
223. S. Badel, T. Bernardi and P. Michaud, *Biotechnology advances*, 2011, **29**, 54-66.
224. E. Dertli, I. J. Colquhoun, A. P. Gunning, R. J. Bongaerts, G. Le Gall, B. B. Bonev, M. J. Mayer and A. J. J. o. b. c. Narbad, 2013, **288**, 31938-31951.
225. M.-H. Lin, Y.-L. Yang, Y.-P. Chen, K.-F. Hua, C.-P. Lu, F. Sheu, G.-H. Lin, S.-S. Tsay, S.-M. Liang and S.-H. Wu, *The Journal of biological chemistry*, 2011, **286**, 17736-17745.
226. M. Alhudhud, P. Humphreys and A. Laws, *Journal of microbiological methods*, 2014, **100**, 93-98.
227. E. J. Raftis, E. Salvetti, S. Torriani, G. E. Felis and P. W. O'Toole, *Applied and environmental microbiology*, 2011, **77**, 954-965.
228. C. Gram, *Fortschritte der Medicin*, 1884, **2**, 185-189.
229. R. Ashraf and N. P. Shah, *International Journal of Food Microbiology*, 2011, **149**, 194-208.
230. R. I. Dave and N. P. Shah, *Journal of Dairy Science*, 1996, **79**, 1529-1536.
231. D. Roy, *International Journal of Food Microbiology*, 2001, **69**, 167-182.
232. F. Gancel and G. Novel, *Journal of Dairy Science*, 1994, **77**, 689-695.
233. I. Ciucanu and R. Caprita, *Analytica chimica acta*, 2007, **585**, 81-85.
234. I. Ciucanu and F. Kerek, *Journal of Chromatography A*, 1984, **284**, 179-185.
235. S. Balzaretto, V. Taverniti, S. Guglielmetti, W. Fiore, M. Minuzzo, H. N. Ngo, J. B. Ngere, S. Sadiq, P. N. Humphreys and A. P. Laws, *Applied and environmental microbiology*, 2017, **83**, e02702-02716.
236. H. M. Harris, M. J. Bourin, M. J. Claesson and P. W. O'Toole, *Microbial genomics*, 2017, **3**, 1-16.
237. G. W. Robijn, H. L. Wienk, D. J. van den Berg, H. Haas, J. P. Kamerling and J. F. Vliegthart, *Carbohydrate research*, 1996, **285**, 129-139.
238. .
239. F. Stingle, J.-R. Neeser and B. Mollet, *Journal of bacteriology*, 1996, **178**, 1680-1690.
240. E. J. Faber, M. J. van den Haak, J. P. Kamerling and J. F. Vliegthart, *Carbohydrate research*, 2001, **331**, 173-182.
241. W. A. Bubb, T. Urashima, R. Fujiwara, T. Shinnai and H. Ariga, *Carbohydrate research*, 1997, **301**, 41-50.
242. E. J. Faber, P. Zoon, J. P. Kamerling and J. F. Vliegthart, *Carbohydrate research*, 1998, **310**, 269-276.
243. V. M. Marshall, H. Dunn, M. Elvin, N. McLay, Y. Gu and A. P. Laws, *Carbohydrate research*, 2001, **331**, 413-422.
244. G. W. Robijn, R. G. Gallego, D. J. van den Berg, H. Haas, J. P. Kamerling and J. F. Vliegthart, *Carbohydrate research*, 1996, **288**, 203-218.
245. S. J. Vincent, E. J. Faber, J.-R. Neeser, F. Stingle and J. P. Kamerling, *Glycobiology*, 2001, **11**, 131-139.
246. M. Gruter, B. R. Leeflang, J. Kuiper, J. P. Kamerling and J. F. Vliegthart, *Carbohydrate research*, 1993, **239**, 209-226.
247. L. P. Harding, V. M. Marshall, Y. Hernandez, Y. Gu, M. Maqsood, N. McLay and A. P. Laws, *Carbohydrate research*, 2005, **340**, 1107-1111.
248. C. Vanhaverbeke, C. Bosso, P. Colin-Morel, C. Gey, L. Gamar-Nourani, K. Blondeau, J.-M. Simonet and A. Heyraud, *Carbohydrate research*, 1998, **314**, 211-220.
249. V. K. Bajpai, I. A. Rather, R. Majumder, S. Shukla, A. Aeron, K. Kim, S. C. Kang, R. Dubey, D. Maheshwari and J. Lim, *Bangladesh Journal of Pharmacology*, 2015, **11**, 1-23.
250. G. W. Robijn, D. J. Van den Berg, H. Haas, J. P. Kamerling and J. F. Vliegthart, *Carbohydrate research*, 1995, **276**, 117-136.
251. F. Stingle, J. Lemoine and J.-R. Neeser, *Carbohydrate research*, 1997, **302**, 197-202.

252. Y. Yamamoto, S. Murosaki, R. Yamauchi, K. Kato and Y. Sone, *Carbohydrate research*, 1994, **261**, 67-78.
253. M. Staaf, G. Widmalm and Z. Yang, *Carbohydrate research*, 1996, **291**, 155-164.
254. M. Staaf, Z. Yang and G. Widmalm, *Carbohydrate Research*, 2000, **326**, 113-119.
255. Z. Yang, M. Staaf and G. Widmalm, *Carbohydrate Research*, 2000, **329**, 465-469.
256. W. S. Bahary, M. P. Hogan, M. Jilani and M. P. Aronson, ACS Publications, 1995.
257. A. P. Laws, S. Leivers, M. Chacon-Romero and M. J. Chadha, *International dairy journal*, 2009, **19**, 768-771.
258. R. D'Incà, M. Barollo, M. Scarpa, A. R. Grillo, P. Brun, M. G. Vettorato, I. Castagliuolo, G. C. J. D. d. Sturniolo and sciences, 2011, **56**, 1178-1187.
259. R. Tuinier, P. Zoon, C. Olieman, C. Stuart, G. Fleer and C. De Kruif, *Biopolymers*, 1999, **49**, 1-9.
260. S. Górska, M. Schwarzer, W. Jachymek, D. Srutkova, E. Brzozowska, H. Kozakova and A. J. A. E. M. Gamian, 2014, **80**, 6506-6516.
261. S. Górska-Frączek, C. Sandström, L. Kenne, J. Rybka, M. Strus, P. Heczko and A. J. C. r. Gamian, 2011, **346**, 2926-2932.
262. M. Kojic, M. Vujcic, A. Banina, P. Cocconcelli, J. Cerning and L. J. A. E. M. Topisirovic, 1992, **58**, 4086-4088.
263. C. Landersjö, Z. Yang, E. Huttunen and G. J. B. Widmalm, 2002, **3**, 880-884.
264. G. W. Robijn, H. L. Wienk, D. J. van den Berg, H. Haas, J. P. Kamerling and J. F. J. C. r. Vliegthart, 1996, **285**, 129-139.
265. M.-R. Van Calsteren, P.-R. Corinne, A. Bégin and R. J. B. J. Denis, 2002, **363**, 7-17.
266. C. Vanhaverbeke, C. Bosso, P. Colin-Morel, C. Gey, L. Gamar-Nourani, K. Blondeau, J.-M. Simonet and A. J. C. r. Heyraud, 1998, **314**, 211-220.
267. T. Harutoshi, in *Lactic acid bacteria-R & D for food, health and livestock purposes*, IntechOpen, 2013.
268. R. La Ragione, A. Narbad, M. Gasson and M. J. J. L. i. A. M. Woodward, 2004, **38**, 197-205.
269. J. Delcour, T. Ferain, M. Deghorain, E. Palumbo and P. Hols, in *Lactic acid bacteria: genetics, metabolism and applications*, Springer, 1999, pp. 159-184.
270. A. Jeanes, W. C. Haynes, C. Wilham, J. C. Rankin, E. Melvin, M. J. Austin, J. Cluskey, B. Fisher, H. Tsuchiya and C. J. J. o. t. A. C. S. Rist, 1954, **76**, 5041-5052.
271. G. Lacaze, M. Wick and S. J. F. M. Cappelle, 2007, **24**, 155-160.
272. A. L. Bhavani and J. J. I. J. P. B. S. Nisha, 2010, **1**, 569-573.
273. N. W. H. Cheetham, E. Fiala-Beer and G. J. Walker, *Carbohydrate Polymers*, 1990, **14**, 149-158.
274. K. Bock and C. Pedersen, *Journal of the Chemical Society, Perkin Transactions 2*, 1974, 293-297.
275. R. Dimler, I. Wolff, J. Sloan and C. Rist, *Journal of the American Chemical Society*, 1955, **77**, 6568-6573.
276. J. C. Rankin and A. Jeanes, *Journal of the American Chemical Society*, 1954, **76**, 4435-4441.
277. B. J. Hardy, A. Gutierrez, K. Lesiak, E. Seidl and G. Widmalm, *The Journal of Physical Chemistry*, 1996, **100**, 9187-9192.
278. J. Cuers, M. Rinken, R. Adden and P. Mischnick, *Analytical and bioanalytical chemistry*, 2013, **405**, 9021-9032.
279. I. M. Sims, S. L. Munro, G. Currie, D. Craik and A. Bacic, *Carbohydrate Research*, 1996, **293**, 147-172.
280. Y. Sun and J. Cheng, *Bioresource technology*, 2002, **83**, 1-11.
281. K. A. Garleb, L. D. Bourquin and G. C. Fahey Jr, *Journal of agricultural and food chemistry*, 1989, **37**, 1287-1293.
282. K. Koizumi, Y. Kubota, H. Ozaki, S. Keiko, M. Fukuda and T. Tanimoto, *Journal of Chromatography A*, 1992, **595**, 340-345.

283. K. Kato, T. Odamaki, E. Mitsuyama, H. Sugahara, J.-z. Xiao and R. Osawa, *Current microbiology*, 2017, **74**, 987-995.
284. A. O'Callaghan and D. van Sinderen, *Frontiers in Microbiology*, 2016, **7**, 1-21.
285. K. Orrhage and C. Nord, *Drugs under experimental and clinical research*, 2000, **26**, 95-111.
286. K. R. Hughes, L. C. Harnisch, C. Alcon-Giner, S. Mitra, C. J. Wright, J. Ketskemety, D. Van Sinderen, A. J. M. Watson and L. J. Hall, *Open Biology*, 2017, **7**, 1-11.
287. M. J. Saez-Lara, C. Gomez-Llorente, J. Plaza-Diaz and A. Gil, *BioMed Research International*, 2015, **2015**, 1-15.
288. S. Duranti, F. Gaiani, L. Mancabelli, C. Milani, A. Grandi, A. Bolchi, A. Santoni, G. A. Lugli, C. Ferrario, M. Mangifesta, A. Viappiani, S. Bertoni, V. Vivo, F. Serafini, M. R. Barbaro, A. Fugazza, G. Barbara, L. Gioiosa, P. Palanza, A. M. Cantoni, G. Luigi de'Angelis, E. Barocelli, N. de'Angelis, D. van Sinderen, M. Ventura and F. Turroni, *FEMS Microbiology Ecology*, 2016, **92**, 1-12.
289. P. Ruas-Madiedo, M. Gueimonde, A. Margolles, C. G. De Los Reyes-Gavilán and S. Salminen, *Journal of Food Protection*, 2006, **69**, 2011-2015.
290. A. Bordoni, A. Amaretti, A. Leonardi, E. Boschetti, F. Danesi, D. Matteuzzi, L. Roncaglia, S. Raimondi and M. Rossi, *Applied Microbiology and Biotechnology*, 2013, **97**, 8273-8281.
291. S. H. Choi, M. Y. Lee, D. Y. Jhon, Y. I. Choi and J. J. Lee, *Korean Journal for Food Science of Animal Resources*, 2013, **33**, 701-707.
292. F. Miremedi, M. Ayyash, F. Sherkat and L. Stojanovska, *Journal of Functional Foods*, 2014, **9**, 295-305.
293. O. Öner, B. Aslim and S. B. Aydaş, *Journal of Molecular Microbiology and Biotechnology*, 2014, **24**, 12-18.
294. S. Fanning, L. Hall, M. Cronin, A. Zomer, J. MacSharry, D. Goulding, M. Motherway, F. Shanahan, K. Nally, G. Dougan and D. van Sinderen, *Proc Natl Acad Sci USA*, 2012, **109**, 2108 - 2113.
295. M. Kohno, S. Suzuki, T. Kanaya, T. Yoshino, Y. Matsuura, M. Asada and S. Kitamura, *Carbohydrate Polymers*, 2009, **77**, 351-357.
296. F. Altmann, P. Kosma, A. O'Callaghan, S. Leahy, F. Bottacini, E. Molloy, S. Plattner, E. Schiavi, M. Gleinser, D. Groeger, R. Grant, N. R. Perez, S. Healy, E. Svehla, M. Windwarder, A. Hofinger, M. O. Motherway, C. A. Akdis, J. Xu, J. Roper, D. Van Sinderen and L. O'Mahony, *PLoS ONE*, 2016, **11**.
297. R. Inturri, A. Molinaro, F. Di Lorenzo, G. Blandino, B. Tomasello, C. Hidalgo-Cantabrana, C. De Castro and P. Ruas-Madiedo, *Carbohydrate Polymers*, 2017, **174**, 1172-1180.
298. N. Shang, R. Xu and P. Li, *Carbohydrate polymers*, 2013, **91**, 128-134.
299. W. FISCHER, *The FEBS Journal*, 1987, **165**, 639-646.
300. Y. Habu, M. Nagaoka, T. Yokokura and I. Azuma, *The Journal of Biochemistry*, 1987, **102**, 1423-1432.
301. M. Nagaoka, S. Hashimoto, H. Shibata, I. Kimura, K. Kimura, H. Sawada and T. Yokokura, *Carbohydrate research*, 1996, **281**, 285-291.
302. M. Nagaoka, M. Muto, T. Yokokura and M. Mutai, *The Journal of Biochemistry*, 1988, **103**, 618-621.
303. M. Nagaoka, H. Shibata, I. Kimura, S. Hashimoto, K. Kimura, H. Sawada and T. Yokokura, *Carbohydrate research*, 1995, **274**, 245-249.
304. Y. Tone-Shimokawa, T. Toida and T. Kawashima, *Journal of bacteriology*, 1996, **178**, 317-320.
305. O. A. Valueva, A. S. Shashkov, E. L. Zdorovenko, A. O. Chizhov, E. Kiseleva, G. Novik and Y. A. Knirel, *Carbohydrate research*, 2013, **373**, 22-27.
306. J. Veerkamp, G. Hoelen and H. O. Den Camp, *Biochimica et Biophysica Acta (BBA)-General Subjects*, 1983, **755**, 439-451.
307. Y. J. Goh and T. R. J. M. c. f. Klaenhammer, 2014, **13**, 94.

308. D. Rios-Covian, I. Cuesta, J. R. Alvarez-Buylla, P. Ruas-Madiedo, M. Gueimonde and G. J. B. m. Clara, 2016, **16**, 150.
309. C. Bertin, C. Pau-Roblot, J. Courtois, L. Manso-Silván, F. Thiaucourt, F. Tardy, D. Le Grand, F. Poumarat and P. Gaurivaud, *PLoS one*, 2013, **8**, e68373.
310. H. Saitô, T. Ohki, N. Takasuka and T. Sasaki, *Carbohydrate Research*, 1977, **58**, 293-305.
311. M. T. Dueñas-Chasco, M. A. Rodríguez-Carvajal, P. Tejero-Mateo, J. L. Espartero, A. Irastorza-Iribas and A. M. Gil-Serrano, *Carbohydrate Research*, 1998, **307**, 125-133.
312. J. Shively, *Annual Reviews in Microbiology*, 1974, **28**, 167-188.
313. J. H. Veerkamp, G. E. J. M. Hoelen and H. J. M. Op Den Camp, *BBA - General Subjects*, 1983, **755**, 439-451.
314. H. J. M. O. Op Den Camp, J. H. Veerkamp, A. Oosterhof and H. van Halbeek, *Biochimica et Biophysica Acta (BBA)/Lipids and Lipid Metabolism*, 1984, **795**, 301-313.
315. H. O. Den Camp, J. Veerkamp, A. Oosterhof, H. J. B. e. B. A.-L. Van Halbeek and L. Metabolism, 1984, **795**, 301-313.
316. W. Fischer, *European Journal of Biochemistry*, 1987, **165**, 639-646.
317. W. Fischer, W. Bauer and M. Feigel, *European Journal of Biochemistry*, 1987, **165**, 647-652.
318. K. Bock and C. Pedersen, *Journal of the Chemical Society, Perkin Transactions 2*, 1974, DOI: 10.1039/P29740000293, 293-297.
319. W. Wei, D. Qi, H.-z. Zhao, Z.-x. Lu, F. Lv and X. Bie, *Food chemistry*, 2013, **141**, 3085-3092.
320. Y. Habu, M. Nagaoka, T. Yokokura and I. J. T. J. o. B. Auma, 1987, **102**, 1423-1432.